Identifying the Signaling Molecules Involved in the Early Stage of Epimorphic Regeneration Using Zebrafish (Larva) Tail as a Model System

Hongyu Kang

School of Biosciences
University of Sheffield

2023 September

Contents

Abstract

The mechanism of the epimorphic regeneration of zebrafish tail is unknown. By fully understanding the molecular and cellular basis of the epimorphic regeneration mechanism of the zebrafish tail, it is possible to reverse-engineer it to develop therapies that can be used in mammals or even humans to reduce fibrosis, local inflammation & scar formation, and promote wound healing and regeneration. These therapies may then be utilized in unexpected ways and to varying degrees to facilitate treating a variety of chronic diseases. In the current study, in order to identify the signaling molecules involved in the notochord bead formation that happens in the early stage of zebrafish (larva) tail regeneration, chemical screening was carried out. Pharmacological treatments using either inhibitors or scavengers to down-regulate the candidate signaling molecules with the intention of intervening in the zebrafish (larva) tail regeneration process were performed, and the outcomes of these small molecule chemical treatments on either notochord bead formation or amputation-induced Ca2+ level or H2O2 level or SFK activity were assessed. After testing more than 30 chemicals, I found out that Ca2+, H2O2, SFK, CREB, EGFR, MAPKK, microtubule, MMP, PDE, PI3K, PKA, PKB & PKC are involved in the early stage (i.e., prior to blastema formation) of zebrafish tail regeneration, which can be broken down into 3 parts: (1) H2O2, SFK, EGFR, MMP, PDE, PI3K, PKA & microtubule participate in the notochord bead formation; (2) H2O2 & SFK promote Ca2+ signaling; (3) Ca2+, MAPKK, PKB, PKC & CREB up-regulate H2O2 signaling. In conclusion, I identified a few signaling molecules that might play a role in the early stage of zebrafish tail regeneration. Further investigation is needed to fully elucidate the interaction and signaling transduction networks between these molecules.

Chapter 1 Introduction

1.1 Regeneration

Regeneration

In the fields of biology and medicine, all organisms have the ability to regenerate (Stocum, 2006). Biological regeneration can take place in different species. It can happen in both adult form and larva form. It is observed at different levels, from the cellular level to the tissue/organ levels. Different species have different degrees of regenerative capacity. Generally speaking, lower vertebrates' regenerative capacity is higher than that of higher animals. The lower vertebrates have strong organ/whole body level regeneration ability, while the higher animals have weak organ/whole body level regeneration ability but retain some cell/tissue level regeneration ability. For example, in plants, a whole carrot can be regenerated from a single cell (Steward et al., 1964). In vertebrates, such as planaria and hydra, their whole body can be regenerated from fragments (Goss,1969; Alvarado, 2000). In invertebrates, amphibians and teleost fish can regenerate relatively large and complex structures (e.g., limbs and tails); in mammals, including humans, the regenerative ability is rather limited compared to the forementioned species (Stocum, 2006). In the same individual, there is a difference in regenerative ability between the larva and the adult. In general, the larva's regenerative ability is stronger than that of the adult. Different tissues/organs of the same species might utilize different regeneration mechanisms.

Regeneration at cellular level

For the regeneration that happens at the cellular level, its capacity is rather limited compared to the regeneration that happens at the tissue/organ level. For example, in invertebrates, the protozoan, which is unicellular, is able to regrow into a complete cell (Goss, 1969). This can happen as long as there is some nuclear material left, even if the damage has removed most of the cell (Goss, 1969). One amoeba can regenerate into a complete amoeba, even though there is only 1/80 of it left after the damage (Vorontsova & Liosner, 1960). In vertebrates, both the motor nerve axons and the sensory nerve axons are able to regenerate in vivo (Yannas, 2001). This can happen as long as the endoneurial tubes, which wrap the axons, are unimpaired after damage such as transection or crush (Yannas, 2001).

Regeneration at tissue/organ level

For the regeneration that happens at the tissue/organ level, 3 conditions should be met: (1) Mitotically-competent cells must be present in the damaged tissue/organ; these cells must respond to the new local environment created by damage in a pro-regeneration way through various signaling transduction pathways. (2) Signals that are regeneration-permissive, which means they can be pro-proliferative or pro-differentiative, must be present in this new local environment; (3) Any other factors or signals that are regeneration-inhibitory must be absent from this local environment (Stocum, 2006). They can be suppressed or neutralized (Stocum, 2006). For example, many mammalian tissues/organs such as epithelia (kidney epithelium), blood, blood vessels, pancreas, liver, bone and skeletal muscle, have mitotically competent cells. Therefore, these tissues/organs are able to regenerate through these cells (Stocum, 2006).

Mechanisms of regeneration at tissue/organ level in vertebrates (Compensatory hyperplasia, ASC activation & Dedifferentiation)

For the regeneration that happens at tissue/organ level in vertebrates, it often occur through compensatoty hyperplasia, the activation of ASC or dedifferentiation (Figure 1-1).

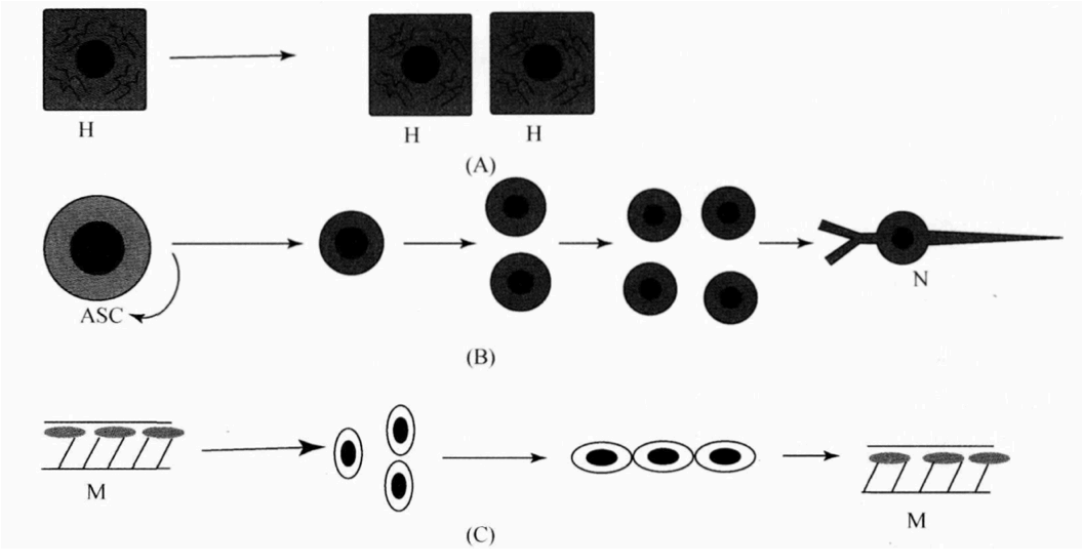

Figure 1-1. Mechanisms of regeneration at tissue/organ level in vertebrates. (A) Compensatory hyperplasia. Liver regeneration serves as a classic example. Following injury, remaining hepatocytes generate new liver cells. H stands for hepatocyte. (B) ASC activation. After damage, these undifferentiated stem cells are activated and produce 2 types of daughter cells (straight arrows & curved arrow). One type of daughter cell divides and differentiates into a specific lineage with a defined function, e.g., neurons (straight arrows), while the other type of daughter cell stays an ASC (curved arrow). N stands for neuron. (C) Dedifferentiation. Myofibers convert their protein molecules into individual stem cell-like entities, which then divide and re-differentiate into new muscle fibers. M stands for myofiber. Adapted from (Stocum, 2006).

Compensatory hyperplasia regenerates new tissue/organ through the proliferation of differentiated cells (Stocum, 2006). The sources of these differentiated cells are the extracellular matrix (ECM) and the syncytial complex (Stocum, 2006). They keep some/all of the differentiated functions while they divide during regeneration (Stocum, 2006). For example, the liver regenerates through compensatory hyperplasia (Michalopoulos & DeFrances, 1997; Trembly & Steer, 1998). After damage, such as partial hepatectomy, both the hepatocytes and the non-parencymal cells (such as Kupffer cells, fenestrated epithelial cells and bile duct epithelial cells) divide to regenerate the new liver; they stop when the original mass is met (Stocum, 2006). During this process, these cells maintain some/all of the differentiated functions, such as glucose regulation, bile secretion, blood protein synthesis and drug metabolism (Stocum, 2006).

Adult stem cells (ASCs) are cells that are not fully differentiated and lineage-restricted and are set aside and reserved during late embryonic/fetal life (Stocum, 2006). These cells can be found in the blood circulation or in some tissues (Stocum, 2006). Apart from being used for regeneration throughout life, they can also be utilized for juvenile growth, which happens after hatching/birth (Fuchs & Segre, 2000; Weissman, 2000). There are a couple of characteristics obtained by ASCs: (1) They are capable of self-renewing through asymmetric cell division. (2) Their developmental potential varies (Stocum, 2006). The degree depends on which tissue they reside in and which developmental stage they are in within a specific lineage (Stocum, 2006). Besides vertebrates, regeneration at the tissue/organ level through the activation of ASCs can also be found in multi-cellular invertebrates, such as planarians, which can regenerate via a kind of ASC called neoblasts (Alvarado, 2000).

De-differentiation means the loss of phenotypic specialization, which is obtained through differentiation (Stocum, 2006). It can turn differentiated cells into stem cells, such as ASCs. These ASCs produced by de-

differentiation then regenerate through proliferation and differentiation (Ferretti & Géraudie, 1998). Although regeneration at the tissue/organ level through de-differentiation is a common mechanism seen in vertebrates, it is relatively more common in lower vertebrates (Stocum, 2006). Lower vertebrates such as fish, lizards, anuran tadpoles and the urodele amphibians (larve and adult) can regenerate through this mechanism (Stocum, 2006). Fish can regenerate fins and barbels (Stocum, 2006). Certain species of lizards can regenerate tails (Stocum, 2006). Tadpoles and amphibians can regenerate tails, limbs, the spinal cord, the lens, the jaws, the intestine and the neural retina (Stocum, 2006). Lower vertebrates such as tadpoles and amphibians can regenerate through compensatory hyperplasia and ASC activation as well, just like higher vertebrates, including mammals (Stocum, 2006). However, the aforementioned complex tissue/organ generated by tadpoles and amphibians through de-differentiation cannot be generated by mammals (Stocum, 2006).

Modes of regeneration (Morphallaxis & Epimorphosis)

2 modes of regeneration, which are morphallaxis and epimorphosis, have been distinguished (Morgan, 1901). The regeneration process of these 2 modes did not involve any types of regeneration-competent cells (Figure 1-2) (Stocum, 2006).

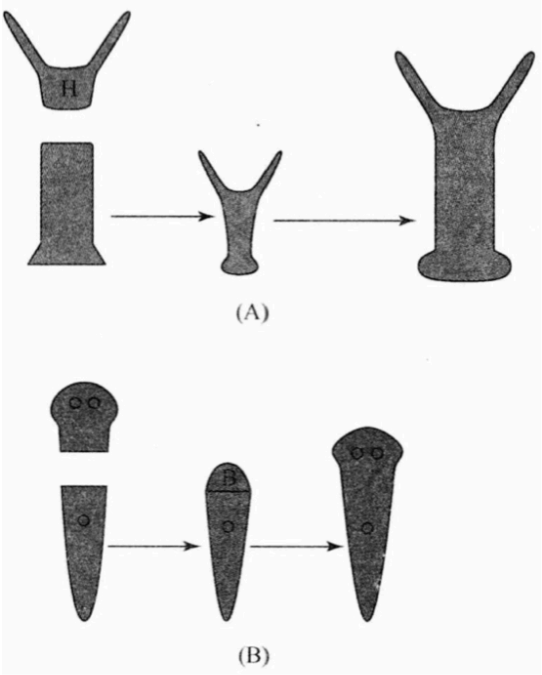

Figure 1-2. Modes of regeneration. (A) Morphallaxis of hydra. Following head amputation, the remaining cells initially form a miniature version of the original hydra (as it existed prior to decapitation), subsequently growing to its original dimensions. H stands for head region. (B) Epimorphosis of planarian. After head amputation, a blastema first develops at the severed end, which then grows into a new head identical to the original in both size and function. This process involves no re-arrangement of the remaining cell or tissue. B stands for blastema. Adapted from (Stocum, 2006).

Morphallaxis is the regeneration process that starts with a re-patterning stage that turns the remaining tissue into a smaller whole with normal proportions, followed by a growth stage that turns the smaller whole into a

bigger whole with the original size (Stocum, 2006). Morphallaxis is often observed in invertebrates, especially in multicellular organisms with simple tissue structures, such as Hydra (Stocum, 2006).

Epimorphosis is the regeneration process that includes one stage, which is the formation of a blastema (Stocum, 2006). The blastema is crucial in epimorphic regeneration as it contains intrinsic morphogenetic information that is needed for the following stage of stem/progenitor cell proliferation and differentiation (Stocum, 2006). The blastema usually arises from epithelial-mesenchymal interactions (Stocum, 2006). Mammals, amphibians, flatworms, and annelid worms are able to regenerate through epimorphic regeneration (Stocum, 2006). Amphibians can regenerate their appendages (such as limbs) and jaws (Stocum, 2006). Mammal structures, such as rabbit ear tissue, deer antlers and fetal digits, can be regenerated through epimorphosis (Stocum, 2006).

Types of regeneration (Physiological regeneration, Hypertrophy & Reparative regeneration)
Physiological regeneration is the replacement of body parts that happens naturally (Carlson, 2007). It can happen in various species at different levels, including the cellular level and the tissue/organ level. Cell turnover of the epidermal cells or epithelial cells in the gut, the replacement of endometrium after menstrual periods and the renewal of blood cells are examples of physiological regeneration that happens at the cellular level in mammals (Carlson, 2007). If physiological regeneration happens at the tissue/organ level in vertebrates, it can happen through the forementioned mechanisms (compensatory hyperplasia, ASC activation & dedifferentiation). Therefore, physiological regeneration refers to a type of regeneration rather than a mechanism of regeneration (Carlson, 2007). These variety of regeneration processes that happen in different species at different levels using different mechanisms have one common feature: the purpose of these processes is the same, which is to maintain the normal physiological cell or tissue equilibrium within the organism's body (Carlson, 2007).

Hypertrophy usually happens at the organ level. After damage or the removal of one member (for organs that come in pairs, such as kidneys) (Addis & Lew, 1940), some organs have the ability to increase their mass (Higgins & Anderson, 1931). To be noted, for the hypertrophy that happens in most internal organs, the key point of the outcome is the functional mass increase rather than the external form restoration (Carlson, 2007).

Reparative regeneration refers to the regeneration process that happens after trauma (Carlson, 2007). It can happen in various species at different levels, including the cellular level and the tissue/organ level. Salamander and newt limb/tail regeneration and planarian entire body reconstitution are examples of reparative regeneration (Carlson, 2007). If reparative regeneration happens at the tissue/organ level in vertebrates, it can happen through the forementioned mechanisms (compensatory hyperplasia, ASC activation & dedifferentiation). Thus, reparative regeneration refers to a type of regeneration rather than a mechanism of regeneration (Carlson, 2007). The variety of regeneration processes that happen in different species at different levels using different mechanisms have one common feature: the purpose of these processes is the same, which is to repair the traumatized part of the organism's body (Carlson, 2007). Reparative regeneration includes cellular regeneration, tissue regeneration, morphallaxis and epimorphosis (Carlson, 2007). Cellular regeneration refers to the reparative regeneration process that happens at the cellular level (Carlson, 2007). The regeneration of protozoa after natural fission or resection and the regeneration of peripheral nerve axons after transection are examples of cellular regeneration (Carlson,

2007). Tissue regeneration refers to the reparative regeneration process that does not include the stage of blastema formation (Carlson, 2007).

Fibrosis & scar formation during wound healing

The process of wound healing is quite often observed in multicellular organisms. Wound healing processes are universally adaptive (Stocum, 2006). It seems like natural selection selected them because they are crucial for the survival of these organisms (Stocum, 2006). However, epimorphic regeneration is less commonly observed. Within each phylum, only a few species are capable of epimorphic regeneration (Stocum, 2006). Many adult tissues have regenerative cells, but when injury happens, for many vertebrate species, their response is the wound healing process, which includes fibrosis and scar formation, rather than epimorphic regeneration (Stocum, 2006). Why? One possible reason is that regeneration takes a longer period of time and therefore requires more energy compared to fibrosis and scar formation in wound healing (Stocum, 2006). The difference is especially large in more complex structures such as appendages (e.g., tails and limbs) (Stocum, 2006). In higher vertebrates, such as mammals, after injury, the damaged tissues/ organs are susceptible to infection caused by microorganisms such as bacteria, and the organism's body is facing the problem of water loss (Stocum, 2006). A rapid closure of the wound by the scar prevents bacterial infection and fluid loss (Stocum, 2006). The fibrosis and scar formation provide a better chance of survival (Stocum, 2006). So epimorphic regeneration is suppressed because it does not have the advantages that wound healing has (Stocum, 2006). This suppression has been reported to be related to immune system maturity in the regeneration process that happens in Xenopus limb and mammalian skin (Harty et al., 2003).

1.2 Zebrafish caudal fin regeneration

Zebrafish caudal fin regeneration stages

Currently, the general process observed in zebrafish caudal fin epimorphic regeneration can be divided into 4 stages (Figure 1-3) (Figure 1-4) (Shi et al., 2015): (1) Wound healing. This event takes place immediately after damage. Immune response to infections is also initiated during this stage. The apical epidermal cap (AEC) is formed in this phase by spreading the lateral epithelial cells, which are non-proliferative, over the wound (Nechiporuk & Keating, 2002). The AEC is fundamental for the subsequent blastema formation (Akimenko et al., 2003). (2) Blastema formation. The blastema is thought to be an accumulated mound of pluripotent mesenchymal precursor cells that have differential and developmental plasticity, meaning they have the ability to differentiate into many types of cells in the regrowing tissues. The cell origin of the blastema is currently unclear and under debate. Cell de-differentiation and proliferation in the mesenchymal tissue located under AEC are often observed in this period as well (Nechiporuk & Keating, 2002). The signals that originated from the wound epidermis are crucial for this stage. The appearance of the blastema is a critical turning point in epimorphic regeneration because this structure is not formed during the human regeneration process, during which a scar is established instead. Based on proliferation rate & msxb (an important blastema marker) expression, blastema can be further divided into proximal blastema & distal blastema (Nechiporuk & Keating, 2002). (3) Blastemal outgrowth. This step is characterized by the dramatic proliferation, migration & differentiation of proximal blastemal cells. These cells have different temporal and spatial profiles as well as a record of their original position, and they use this information to carry out spatiotemporal organization, modify surrounding tissues, and become integrated into the existing structures. These newly proliferated blastemal cells migrate to appropriate locations at appropriate timepoints to restore the structure using fibroblasts & mesenchymal cells. Re-patterning of these new cells is also involved in specifying the final pattern of the regenerate. This stage is tightly regulated by many molecular signaling pathways and associated with massive expression of specific genes. Many conserved signaling pathways, some of which are involved in fin development, also play a role in regeneration. (4) Termination. At the end of this regeneration procedure is the formation of a fully-patterned functional equivalent that recaptures the function and form in a 3D structure. However, the molecular & cellular mechanisms in this phase are still in the dark (Iovine, 2007).

Figure 1-3. Zebrafish fin distribution. 1. Dorsal fin; 2. Pectoral fin; 3. Pelvic fin; 4. Anal fin; 5. Caudal fin. Adapted from (Lin et al., 2022).

Previous studies have reported that the zebrafish caudal fin epimorphic regeneration's time course is approximately 2-3 weeks (adult fish) (Figure 1-5) or 3 days (larva fish) (Tal et al., 2009; Poss et al., 2003).

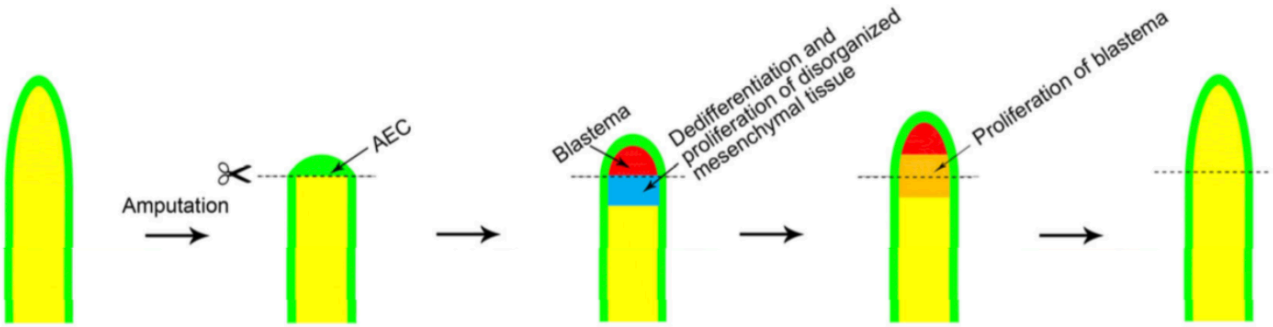

Figure 1-4. A schematic diagram demonstrates the general process of caudal fin regeneration in zebrafish. Following caudal fin amputation, an AEC rapidly forms at the incision site, covering the wound. Subsequently, mesenchymal cells located under the AEC undergo de-differentiation and divide to form a blastema. This blastema then proliferates and differentiates to generate a new fish tail, almost identical in size and function to the original. Adapted from (Shi et al., 2015).

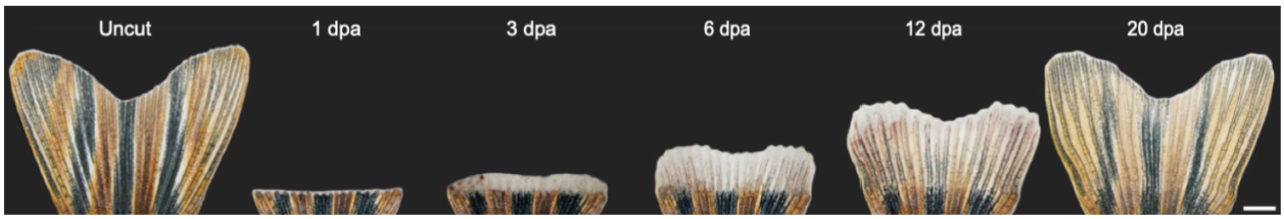

Figure 1-5. Regeneration of adult zebrafish fin. At 1 dpa, the cut surface exhibits a layer of pale white tissue. These consist of epidermal cells and some blastema cells. At 3 dpa, a large expanse of white tissue is present above the incision plane, containing blastema. Although these blastema appear uniform, they can be sub-divided at the molecular and cellular levels. At 6 dpa, the newly grown tissue is largely colored, containing pigment and faintly visible bone, indicating ongoing re-differentiation. A trace of white tissue remains at the fin periphery. At 12 dpa, the regenerated caudal fin has begun to take shape. At 20 dpa, the newly-grown caudal fin has reached the same size as the original fin. A trace of white tissue still remains at the fin margin. Adapted from (Pfefferli & Jaźwińska, 2015).

The known unknowns on zebrafish caudal fin / tail regeneration

Events we do not understand about the epimorphic zebrafish caudal fin / tail regeneration, such as the roles and interactions of numerous molecules (e.g., post-transcriptional regulators & epigenetic regulators) and signaling pathways, the expression patterns of various differentially-expressed genes, source of cells & tissue interactions to ensuring the fin/body scaling by switching between isometric growth and allometric growth to regulate segment number and length, relaying of positional information by regulating the proximal/ distal amputation plane‘s growth rate through molecules' graded expression along the proximo-distal axis, and ray & inter-ray boundary patterning by directing the osteoblast progenitor cells to migrate into 2 different pools, with the considerations of cellular heterogeneity & cellular epistasis, are all under investigation.

Adult VS Larva & Caudal fin fold VS Tail

In the laboratory, both adult & larval zebrafish are utilized, each possessing distinct advantages and disadvantages. I employed larval zebrafish because chemical screening requires a large number of fish to perform caudal fin / tail amputation for repeated regeneration experiments, while raising zebrafish to adulthood requires 2-4 months, and complete caudal fin / tail regeneration takes at least 2 weeks. Caudal fin / tail regeneration in adult & larval zebrafish exhibits similarities. This holds true at both the molecular level (including gene expression) and the cellular level. It has been reported that the process of caudal fin regeneration in adult & larval zebrafish is morphologically similar. Both involve the initial formation of apical wound epithelium, followed by the development of a blastema, which subsequently turns into various cell types (Kawakami et al., 2004). It has also been reported that certain genes are expressed in both adult & larval zebrafish caudal fin fold regeneration (Yoshinari et al., 2008).

In addition, it should be noted that both zebrafish caudal fin regeneration & zebrafish tail regeneration have been studied in the laboratory (Figure 1-6). The main difference between these 2 is that tail regeneration is more complex than caudal fin regeneration because it additionally involves the regeneration of muscle & spine/spinal cord (Figure 1-7)(Figure 1-8) with the regeneration of nerves, bones (excluding spinal bones), blood vessels, skin, connective tissue & pigment cells are required for both caudal fin & tail regeneration. In my current study, I mainly performed tail amputation rather than caudal fin fold amputation. Previous studies in the Roehl lab have reported that the zebrafish tail epimorphic regeneration's time course is approximately 4/5 days (larva fish) (Figure 1-9) (Romero et al., 2018).

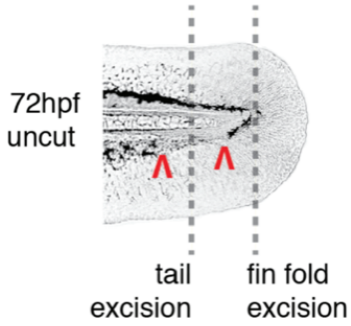

Figure 1-6. Amputation position for zebrafish larva. 2 dotted lines indicate 2 methods: tail excision & fin fold excision. Pigment gap marked by red arrows. Adapted from (Romero et al., 2018).

Figure 1-7. Male zebrafish longitudinal section with H&E staining. 1. Eye; 2. Brain; 3. Gill; 4. Muscle; 5. Pectoral fin; 6. Spine; 7. Caudal fin. Adapted from (Lin et al., 2022).

Figure 1-8. Zebrafish cross section with H&E staining. 1. Spinal cord; 2. Spine; 3. Muscle of the tail; 4. Cloacal orifice. Adapted from (Lin et al., 2022).

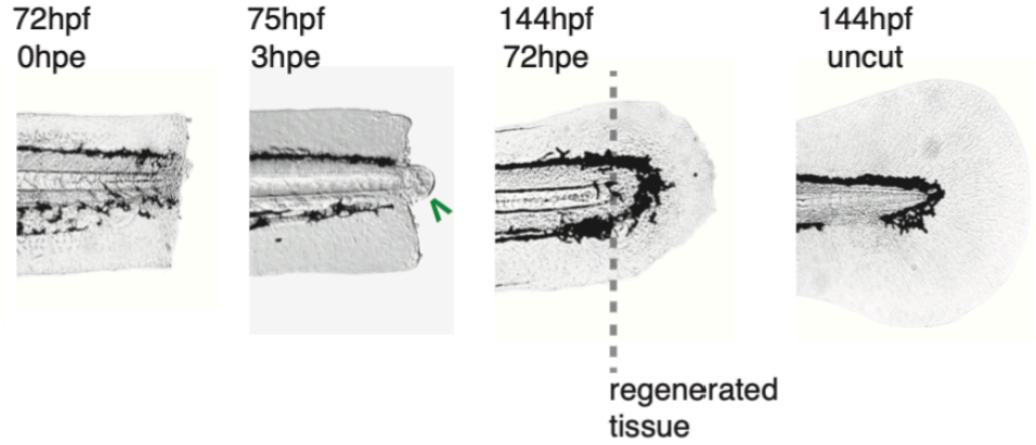

Figure 1-9. Tail regeneration of zebrafish larva when cut between the pigment gap. Notochord bead begins to form at 3 hpa. Tail regeneration is complete after 4/5 days. Notochord bead marked by green arrow. Adapted from (Romero et al., 2018).

1.3 Ca2+

Ca2+ & biological processes related to zebrafish (larva) tail regeneration: a mini review

In this review, I shall outline how Ca2+ (one of the 3 core molecules in my project, with the other 2 being H2O2 & SFK, which are central because they are the ones visualized and quantified) participates in biological processes related to tail regeneration in zebrafish (larva). Given that zebrafish tail regeneration requires the regeneration of muscle, nerve, bone, blood vessels, notochord/spinal cord, skin, connective tissue & pigment cells, and that regeneration sometimes resembles development to some extent, I looked for the following biological processes: (epimorphic) regeneration/morphogenesis of muscle/nerve/bone/blood vessels/notochord/skin, wound healing & inflammation. Numerous literature was found for Ca2+. Due to my limited space, I will only select a few (i.e., embryonic development, skeletal muscular system's regeneration and development & vascular system's development). Therefore, this review is incomplete, as Ca2+ is also involved in other biological processes related to zebrafish tail regeneration.

I shall only sketch out in broad, vague terms: (1) Ca2+ participates in a certain process; (2) during this process, which other (signaling) molecules does Ca2+ interact with. Numerous other molecules are mentioned in the literature; I shall favor selecting those relevant to my project, namely the other 2 core molecules (i.e., H2O2 and SFK), those non-major molecules (i.e., the target molecules of those intervening chemicals) & the protein molecules directly involved in Ca2+ signal transduction [(a) Ca2+ transporters; (b) CaBPs as non-enzyme signaling molecules: CaM, TnC & S100, etc; (c) CaBPs as enzymic signaling molecules: PKC, PLC & PLA2, etc; (d) protein kinases depend on 'Ca2+ and/or CaM': CaMK I, II, III, IV, V, MLCK & PhK, etc]; (3) which cells Ca2+ interacts with during this process. While a lot of cells are cited in the literature, I tend to prioritize those pertinent to my project: cells from muscle/nerve/bone/blood vessels/ notochord/skin, alongside stem cells & immune cells. Details omitted (with possible exceptions) include: (1) pathological processes; (2) which (signaling) molecule is upstream/downstream in the interaction; (3) whether this interplay is inhibitory/activating; (4) for each sub-type of a specific molecule, whether its inhibitory/activating effect is redundant/unique; (5) chemical principles/mechanisms of inter-molecular binding/dissociation, etc.

Ca2+ is involved in embryonic development (reviewed in Paudel et al., 2018; Whitaker, 2005). Ca2+ participates in various stages of embryonic development, including fertilization, oocyte activation, cleavage, blastula, gastrulation & neural induction, across different species. On Ca2+'s role in fertilization & oocyte activation, in all vertebrate oocytes studied up to 2013, an increase in cytoplasmic Ca2+ level was observed during fertilization (Kashir et al., 2013). In humans, zebrafish, Xenopus & mice, inhibiting increases in cytoplasmic Ca2+ level disrupts normal fertilization in different ways (Ferrer-Buitrago et al., 2017). Other molecules such as PLC and STIM1 are also involved in fertilization & oocyte activation. During egg activation, PLC activates STIM1, a channel that allows Ca2+ to flow from intra-cellular calcium stores into the cytoplasm, thereby elevating cytoplasmic Ca2+ concentration (Kashir et al., 2013). In cleavage & blastula, Ca2+ signaling is involved in cell division regulation (Paudel et al., 2018). In zebrafish, Ca2+ waves were observed in the cleavage furrow area (Mizuno et al., 2013). While in Xenopus's late blastula stages, Ca2+ waves were seen at the anterior ectoderm (Leclerc et al., 2000). Other molecules, including STIM1, ORAI1 & microtubules, are also participatory in cleavage & blastula. In zebrafish, Ca2+ signaling located at the cleavage furrow is associated with STIM1 & ORAI1, both of which are Ca2+ channels for SOCE (store-operated Ca2+ entry) (Chan et al., 2015; Chan et al., 2016). Also in zebrafish, Ca2+ waves located at the furrow promote the formation of the furrow microtubule array, which is fundamental for cytokinesis, from

microtubules through remodeling (Chan et al., 2015; Chan et al., 2016). In Xenopus, disrupting Ca2+ activity leads to microtubule misalignment and the subsequent failure of gastrulation (Hara et al., 2013). In the gastrulation stage, Ca2+ signaling is responsible for the regulation of massive tissue movement (Webb & Miller, 2006). In zebrafish & Xenopus's mid/late-blastula and early gastrula stage, Ca2+ signal's frequency and amplitude dramatically decrease (Chen et al., 2017; Ma et al., 2008). Other molecules such as SERCA, VOC & P2Y11 (a purinergic receptor) are also shown to be associated with gastrulation. In zebrafish's gastrulation stage, diminishment of Ca2+ signaling, using a SERCA blocker, utterly impaired normal fish development, leading to tail defects and cyclopia (Creton, 2004). In Xenopus, jeopardizing Ca2+ signaling using inhibitors for L-type VOC & P2Y11 severely decreases the migration speed and protrusion activity of cells (Hayashi et al., 2018; Shindo et al., 2010). As for neural induction, except for Ca2+, other molecules such as BMP (Cho et al., 2014), VOC (Leclerc et al., 2000), TRP, IP3R & RyR also play a role (Paudel et al., 2018).

Ca2+ also takes part in the skeletal muscular system's regeneration & development (reviewed in Al-Shanti & Stewart, 2009; Paudel et al., 2018; Sinha et al., 2022; Tu et al., 2016). Ca2+ participates in different stages of regeneration and development of the muscular system (skeletal) across various species. On Ca2+'s role in the skeletal muscular system's regeneration, in Xenopus laevis's tail regeneration, Ca2+ is involved in muscle satellite cell activation and proliferation (Tu & Borodinsky, 2014). In humans, Ca2+ engages in myoblast differentiation (Antigny et al., 2014). Other molecules, including IP3R, TRPC, calcineurin & calpain (a Ca2+-dependent phosphatase), are also involved in the regeneration process. In humans, IP3R, as a Ca2+ transporter, participates in the differentiation of myoblast (Antigny et al., 2014). In mice, another Ca2+ transporter, TRPC, engages in muscle satellite cell activation (Liu & Schneider, 2014). In rodent legs, calcineurin, as a down-stream effector of Ca2+ signaling, has a role in the activation & proliferation of muscle satellite cells (Sakuma et al., 2002). Calpain, another signaling molecule acting down-stream of Ca2+, participates in muscle precursor cell activation (Raynaud et al., 2004). On Ca2+'s role in the skeletal muscular system's development, in Xenopus laevis, Ca2+ is required for myofibril organization & sarcomere assembly (Ferrari et al., 1996). In humans, Ca2+ promotes myoblast differentiation (Konig et al., 2006). In zebrafish, Ca2+ facilitates slow muscle cell myofibrillogenesis & myotomal patterning (Kelu et al., 2017). Other molecules such as IP3R, RyR, TRPC, CaM-dependent MLCK, MAPK & calcineurin (a CaM-dependent phosphatase) also participate in the development process. In mice & frogs, IP3R & RyR, both as Ca2+ transporters, enhance muscle morphogenesis (Ferrari & Spitzer, 1999; Rosemblit et al., 1999). TRPC, functioning as a Ca2+ transporter as well, plays a role in myoblast's differentiation & migration and its fusion into myotube (Louis et al., 2008). In Xenopus, CaM-dependent MLCK, a down-stream signal of Ca2+, is involved in myosin thick filament assembly (Ferrari et al., 1998). MAPK, another down-stream signal of Ca2+, stimulates the proliferation of muscle progenitor (Bennett & Tonks, 1997). In Drosophila, calcineurin participates in flight muscle organization (Gajewski et al., 2003).

Ca2+ is also involved in the vascular system's development, including angiogenesis and vasculogenesis (reviewed in Moccia et al., 2019; Munaron, 2006). Blood vessels are primarily composed of vascular endothelial cells (VEC), vascular smooth muscle cells (VSMC) & fibroblasts. Regarding Ca2+ signaling in angiogenesis, generally, growth factors (GF) & chemokines bind to and activate receptor tyrosine kinases (RTK) & G-protein coupled receptors (GPCR), respectively (Moccia et al., 2019). Subsequently, RTK and GPCR activate phospholipase C (PLC), which catalyzes the hydrolysis of PIP2 (a phospholipid on the membrane) into IP3 and DAG (Moccia et al., 2019). IP3 and DAG then modulate various Ca2+ transporter

proteins (e.g., channels & pumps), generating different types of Ca2+ signals. The Ca2+ signal activates down-stream signaling molecules, ultimately resulting in diverse VEC cellular activities: proliferation, adhesion, migration, sprouting & tube formation, etc (Moccia et al., 2019). GFs & chemokines that are documented to be participatory comprise vascular endothelial growth factor (VEGF) (Matsui et al., 2007; Rozen et al., 2018), angiopoietin (ANG) (Carmeliet & Jain, 2011; Pafumi et al., 2015), epidermal growth factor (EGF) (Gifford et al., 2004; Moccia et al., 2002), fibroblast growth factor 2 (FGF-2) (Maffucci et al., 2009; Mergler et al., 2003), platelet-derived growth factor (PDGF) (Ridefelt et al., 1995) & stromal-derived factor 1α (SDF-1α) (Gupta et al., 1998; Sameermahmood et al., 2008), etc. GPCRs that are reported to be involved include C-X-C chemokine receptor type 4 (CXCR4) (Kuhlmann et al., 2005), sphingosine-1-phosphate receptor 1 (S1R1) (Mehta et al., 2005) & P2Y (Gündüz et al., 2016; Korybalska et al., 2018). Regarding the Ca2+ transporter proteins that are mobilized by IP3 & DAG, different types of VECs recruit distinct Ca2+ transporters in response to different up-stream pro-angiogenic signals. Documented examples include IP3R, RyR, transient receptor potential canonical (TRPC), 2-pore channel (TPC), Orai1 & STIM1 (for SOCE), etc (Moccia et al., 2019). The signaling molecules acting down-stream of Ca2+ signal involve calpain (Zhang et al., 2017), CaMKII (Ashraf et al., 2019), CREB (Chen et al., 2016), ERK1/2 (Inoue & Xiong, 2009), MLCK (Tsai et al., 2014), NFAT(nuclear factor of activated T-cell) (Zhu et al., 2011), NF-κB (Kim et al., 2001; Zhu et al., 2011), eNOS (Brouet et al., 2001; Gélinas et al., 2002), Pyk2 (Avraham et al., 2003), PI3K/AKT (Yu et al., 2016), etc.

Calcium distribution in cells

For calcium distribution in cells, a few points to bear in mind: (1) In the cell, the locations where calcium can be found include the nucleus, endoplasmic reticulum(ER)/sarcoplasmic reticulum(SR, in the muscle cell), mitochondria, cytoplasm, etc. The calcium content percentage of the whole cell at each location is different. Normally, cytoplasm has the lowest percentage (Wen et al., 1989). (2) Calcium can be present in the free state or the bound state. The free state is ionized (Ca2+), and the bound state is non-ionized. Calcium can be bound to phosphate radical, parvalbumin, calsequestrin, calreticulin, etc (Sun et al., 2010). Normally, in each of the afore-mentioned locations, there is much more calcium in the bound state than in the free state (Wen et al., 1989). The ER/SR & mitochondria are referred to as calcium pools when discussing calcium signaling. (3) Only free Ca2+ can act as a signaling molecule.

In the cytoplasm, under normal physiological conditions, when the cell is in the steady state, the [Ca2+] is usually around 10^−7 M, approximately (Berridge et al., 2000). When the cell is in the activated state, the [Ca2+] might rise to 10^−6 M, approximately (Berridge et al., 2000). The cytoplasmic [Ca2+] is low, even in the activated state, considering that the extra-cellular [Ca2+] is usually around 2×10^−3 M (Clapham, 2007). In the cytoplasm, the molecules that bind to calcium and keep them in the bound state include parvalbumin & calreticulin, which can function as a buffer in regulating cytoplasmic [Ca2+] in the context of Ca2+ signaling (Sun et al., 2010).

In the calcium pools (ER/SR & mitochondria), most calcium molecules are sequestered in the bound state, from which free Ca2+ ions can be released and then return to the bound state again to regulate cytoplasmic [Ca2+] in signaling. In the ER lumen, one example of molecules that bind and sequester calcium is calsequestrin (Sun et al., 2010). In the ER, for the sequestered calcium, except for its function as a storage, no other function has been reported (Hancock, 2010). In mitochondria, most Ca2+ ions are immobilized by forming a ‘gel’ by binding to phosphate (Clapham, 1995; Nicholls & Ferguson, 2002). Mitochondria use

calcium to regulate enzyme activity (Clapham, 2007). For example, pyruvate dehydrogenase (PDH), which links between Kreb's cycle & glycolysis and is involved in ATP production, is regulated by Ca2+ (McCormack et al., 1990). In mitochondria, calcium level has been reported to be involved in the pathological process of some degenerative diseases. For example, in neuronal tissue, out-of-range calcium level can cause ATP depletion & subsequent neuronal death (Clapham, 2007). Also, Ca2+ store depletion can affect the cell cycle by arresting cells at the G0/G1 stage (Clapham, 1995).

Ca2+ function as a signaling molecule

For most signaling molecules, they are produced by the cell, perform their function, and then are removed from the system. However, for Ca2+ ions, this is not the case. The Ca2+ ions are not made when needed or destroyed after they have served their role. It is the variation of the free Ca2+ ion concentration in the cytoplasm, [Ca2+]i, that functions as the signal (Hancock, 2010).

As a second messenger, Ca2+ signaling is ubiquitous. It has been found in higher organisms (e.g., mammals & plants) & micro-organisms (e.g., bacteria) (Clapham, 1995; Dominguez, 2004). The study of Ca2+ signaling can often be found in higher animals' neuronal systems (Clapham, 1995). Ca2+ signaling has been reported to be involved in the pathologies of many diseases, including diabetes (Guerrero-Hernandez & Verkhratsky, 2014), hypertension (Pesic et al., 2004), Alzheimer's disease (LaFerla, 2002), Brody's disease (MacLennan, 2000), Down's syndrome (Schuchmann et al., 1998) & cardiac hypertrophy (Wilkins & Molkentin, 2004).

Ca2+ signaling: cytoplasmic [Ca2+]

In order to create variation in [Ca2+]i for signaling, it is important for the cell to be able to: (1) keep a low [Ca2+]i during the resting state, (2) suddenly increase [Ca2+]i when stimuli are received during the excited state, and (3) subsequently decrease [Ca2+]i to return to a low level of [Ca2+]i after signaling.

The source of [Ca2+]i is either the extra-cellular space and/or the intra-cellular calcium pool. Ca2+ can be transported across the cell membrane & the organelle membranes in 2 directions. Both passive & active forms of Ca2+ transportation were involved. Membrane proteins involved in Ca2+ transportation can be channels or pumps, and some of which are also receptors. Energy for active Ca2+ transportation comes from a variety of sources. Trans-cellular transport of Ca2+ can also be involved.

Ca2+ signaling: increasing cytoplasmic [Ca2+]

To increase [Ca2+]i, there are 2 ways to achieve this: (1) Ca2+ is released into the cytoplasm from extra-cellular space through plasma membrane, (2) Ca2+ is released into the cytoplasm from one/a sub-population of the calcium pool whithin the cell.

Ca2+ signaling: increasing cytoplasmic [Ca2+] with plasma membrane (VOC, ROC, MOC, TRP & SOC involved)

When the source of [Ca2+]i in one cell is other cells, Ca2+ ions enter this cell from other cells through gap junctions (Clapham, 2007). This will allow Ca2+ signaling to propagate across a tissue, as this allows Ca2+ ions, as a small molecule, to move from cells with relatively high [Ca2+]i to cells with relatively low [Ca2+]i.

When Ca2+ travels from extra-cellular space into cytoplasm through the plasma membrane, Ca2+ ions can be transported through free diffusion, as well as facilitated diffusion, which is facilitated by the following channels: voltage-operated Ca2+ channels (VOCs), receptor-operated Ca2+ channels (ROCs), mechanically-operated Ca2+ channels (MOCs), transient receptor potential (TRP) channels & store-operated Ca2+ channels (SOCs) (Figure 1-10).

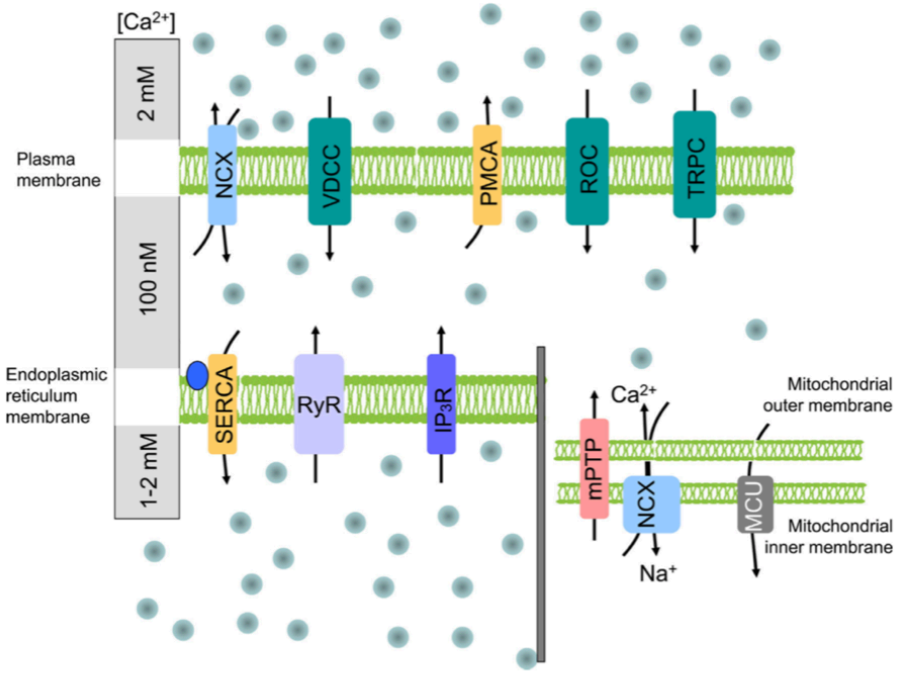

Figure 1-10. Calcium ion transporters located in the plasma membrane, the endoplasmic reticulum membrane and mitochondrial inner membrane. The green boxes represent Ca2+ channels, which transport Ca2+ ions from the extra-cellular space into the cell (cytoplasm) when bound to ligands or upon membrane potential changes. The yellow boxes denote Ca2+ pumps, which transport Ca2+ from the cytoplasm to the extra-cellular space or into the ER, a process requiring energy. NCX belongs to the antiporters, simultaneously transporting Ca2+ while counter-transporting Na+. 2 types of receptors (IP3R & RyR) located on the ER membrane transport Ca2+ from the ER into the cytoplasm. In mitochondria, Ca2+ transport relies on the mitochondrial permeability transition pore & the mitochondrial uniporter, in addition to NCX. Adapted from (Görlach et al., 2015).

VOCs transport Ca2+ ions in a rapid way; therefore, fast entry of Ca2+ ions leads to a swift increase in [Ca2+]i (Clapham, 1995). VOCs, as their name suggests, are sensitive to, and therefore mediated by, voltage changes across the plasma membrane. Within the VOCs, a helix-turn-helix structure exists (Long et al., 2005). This structure functions as the sensor for membrane polarization (Clapham, 1995).

As for ROCs, they can be acted on by many other signaling molecules. Many second messengers that have been reported to act on and induce the opening of ROCs include G proteins, cyclic guanosine monophosphate (cGMP), IP3 & inositol 1,3,4,5-tetrakisphosphate (IP4). However, the precise mechanism between these molecules is still in the dark (Berridge et al., 2000; Clapham, 1995; Kiselyov & Muallem, 1999).

TRP channels are non-selective, and they have 6 transmembrane parts that are organized into a tetrameric structure (Ramsey et al., 2005). In mammals, numerous isoforms of TRP are divided into 6 classes: TRPA,

TRPC, TRPM, TRPP, TRPV & TRPML (Ramsey et al., 2005). TRP channels can be activated by many environmental cues & many signaling molecules. These activating environmental cues include temperature & pH (Ramsey et al., 2005). In mammals, these activating signaling molecules include calmodulin (CaM), phospholipase C (PLC), annexins & S100 protein (Ramsey et al., 2005). TRP channels can be inhibited by environmental cues such as mechanical stress (Ramsey et al., 2005). TRP channels can be inhibited by many signaling molecules, including reactive oxygen species (ROS), diacylglycerol (DAG) & ADP ribose (Ramsey et al., 2005). TRP channels are reported to be involved in the developmental process of many organisms, and their disfunction has been reported in the pathological process of some kidney diseases (Ramsey et al., 2005).

Ca2+ travels into the cytoplasm through SOCs when the intra-cellular calcium pool(s) is/are depleted (Berridge et al., 2000). This type of Ca2+ entry is called capacitative Ca2+ entry (CCE) (Berridge et al., 2000). A mechanism behind CCE has been proposed and is called Ca2+-release-activated current (CRAC) or depletion-activated current (DAC) (Fasolato et al., 1994). The CRAC mechanism was originally reported in studies on mast cells (Hoth & Penner, 1992) & T-lymphocytes (Feske, 2007; Oh-Hora & Rao, 2008). Some proteins involved in CCE have been identified. One involved protein is called STIM1. It has an EF-hand motif and a single transmembrane (ER membrane) region (Roos et al., 2005). STIM1 can act up-stream on Orai1, which is a protein that can form a pore in the plasma membrane (Feske et al., 2006; Zhang et al., 2006). Store depletion in calcium pool activates STIM1, which then acts on the Orai1 pore through which Ca2+ can enter into the cytoplasm (Clapham, 2007). However, the exact mechanism is still in the dark.

Ca2+ signaling: increasing cytoplasmic [Ca2+] with Ca2+ pool (IP3R & RyR involved)
The ER membrane has IP3 receptors (IP3Rs) located on it. IP3R binds to inositol trisphosphate (IP3), which is the product of phosphatidylinositol bisphosphate (PIP2) breakdown and is released from the cell membrane (Berridge & Irvine, 1989). IP3R are also Ca2+ channels, through which free Ca2+ ions can travel from the ER into the cytoplasm. When IP3 binds to IP3Rs, IP3Rs open, allowing rapid release of Ca2+ ions from ER into cytoplasm.

IP3R is tetrameric (Clapham, 1995), and each subunit's molecular weight is 310 kDa (Mikoshiba, 1993). Each subunit has a cationic pore that is not very selective, and Ca2+ ions can travel through these pores (Mikoshiba, 1993). Each subunit also has a lysine- & arginine-rich region, functioning as a ligand (IP3)-binding site that can bind to 1 IP3 molecule (Clapham, 1995). IP3R's C-terminal region spans across the ER membrane (Clapham, 1995). IP3R's N-terminal domain is on the ER membrane's cytoplasmic side and can bind to 1 Ca2+ ion & 2 ATP molecules (Mignery & Sudhof, 1990). IP3R has many isoforms. In mammals, there are at least 4 genes that encode for different homologous IP3Rs (Clapham, 1995). The expression pattern of each homologous IP3R varies in different tissues. IP3R was originally reported in studies on the developmental process in mutant mice as a glyco-phosphoprotein (Mikoshiba, 2007).

Except for IP3, Ca2+ released by IP3R itself can also regulate IP3Rs; in this type of regulation, Ca2+ is called a co-agonist (Sato et al. 2003). If [IP3] is low, low [Ca2+] promotes Ca2+ release from IP3R; high [Ca2+] inhibits Ca2+ release through IP3R (Berridge et al., 2000). A bell-shaped curve can demonstrate the relationship between [Ca2+] and the release of Ca2+ through IP3R (Figure 1-11) (Berridge et al., 2000). Within this curve, the highest Ca2+ concentration released by IP3R is around 0.2-0.3 μM (Bootman & Lipp, 1999). If Ca2+ ions, which are not released from IP3R (e.g., from RyR or mitochondria) arrive near IP3R,

they can also regulate the IP3R in the same way, just like the Ca2+ ions released by IP3R (Hancock, 2010). This Ca2+-induced Ca2+ release (CICR) can turn small changes in [Ca2+] into large changes in [Ca2+] in a rapid way. This CICR phenomenon possessed by IP3R is really important in the formation of local Ca2+ signaling & global Ca2+ signaling (will be mentioned afterward in this section).

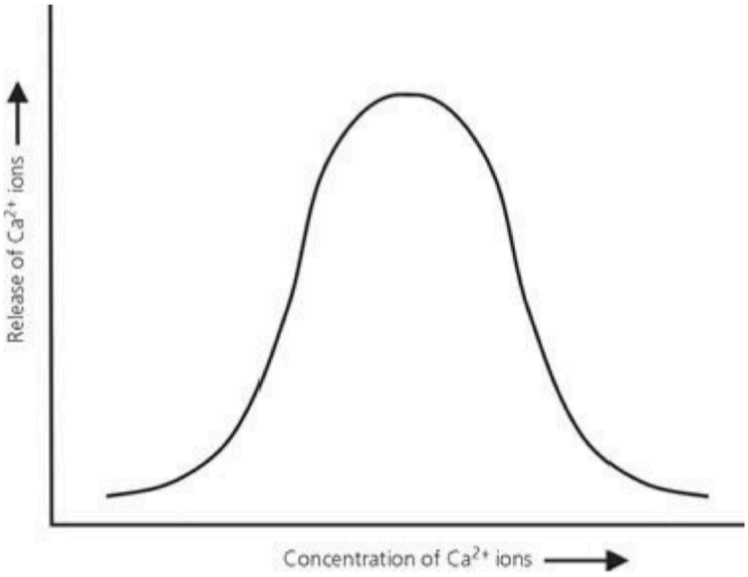

Figure 1-11. IP3R is control by Ca2+ when IP3 concentration is low. This cause CICR from IP3R. Adapted from (Hancock, 2010).

Except for IP3 & Ca2+, IP3R can also be regulated by many other molecules. For example, cAMP-dependent protein kinase can regulate IP3R via phosphorylation (Mikoshiba, 2007). Mg2+ can also modulate IP3R activity (Hancock, 2010).

IP3Rs can regulate the activity of many molecules in different ways, depending on the cell type & tissue type. One example of these molecules is IP3R-binding protein released with IP3 (IRBIT). IRBIT is released when IP3 binds to IP3R (Shirakabe et al., 2006), and can act on downstream signaling targets, such as Na+/ HCO3− co-transporter 1 (NBC1) (Shirakabe et al., 2006).

Ryanodine receptors (RyRs) are another type of Ca2+ channel located on the ER membrane. RyRs bind to Ryanodine, which is an alkaloid derived from plants. Like IP3Rs, RyRs are also Ca2+ channels, through which free Ca2+ ions can travel from the ER into the cytoplasm. At low [Ryanodine], when Ryanodine binds to RyRs, RyRs open, allowing the release of Ca2+ ions from the ER into the cytoplasm (Meissner, 1994). However, at high [Ryanodine] (mM level), the RyRs are closed (Meissner, 1994).

RyRs have 3 isoforms (RyR-1, RyR-2 & RyR-3) encoded by 3 genes (Clapham, 1995). The expression patterns of these isoforms are tissue-specific. RyR-1 is expressed in skeletal muscle, RyR-2 is expressed in cardiac muscle, and RyR-3 is expressed in non-muscle tissue (Clapham, 1995). RyR1 & RyR2 share a high percentage of homologous sequences and have very similar structure, with a molecular weight of about 560 kDa (Clapham, 1995). However, RyR3 is much smaller than RyR1 & RyR2, with the amino acid count less than 650 (Meissner, 1994). RyRs are tetramers (Clapham, 1995). RyR's C-terminal end is located in the ER membrane and has 4 (Takeshima et al., 1989) to 10 (Zorzato et al., 1990) membrane-spanning regions (Meissner, 1994). RyR's N-terminal end is located in the cytosol (Meissner, 1994).

In mammals, due to the fact that Ryanodine is an alkaloid derived from plants, Ryanodine is unlikely to function as a signaling molecule. However, in certain tissues (e.g., striated muscle), the sarcoplasmic reticulum (SR) is physically in close contact with the plasma membrane owing to the fact that there are protein complexes that exist between the SR & plasma membrane and connect the SR membrane & plasma membrane (Meissner, 1994). These protein complexes are called T-tubule feet. T-tubule feet contain RyRs & voltage-sensitive receptors associated with the plasma membrane (Meissner, 1994). Dihydropyridine receptor is an example of these voltage-sensitive receptors (Figure 1-12) (Meissner, 1994). When there is a voltage change across the plasma membrane, the voltage-sensitive receptors detect changes and consequently undergo a conformation change, which is sensed by RyRs (Clapham, 1995). Then RyRs undergo a conformation change, which leads to the opening of RyRs (McPherson & Campbell, 1993). This connection with the plasma membrane possessed by RyRs is really important in the formation of global Ca2+ signaling (will be mentioned afterward in this section).

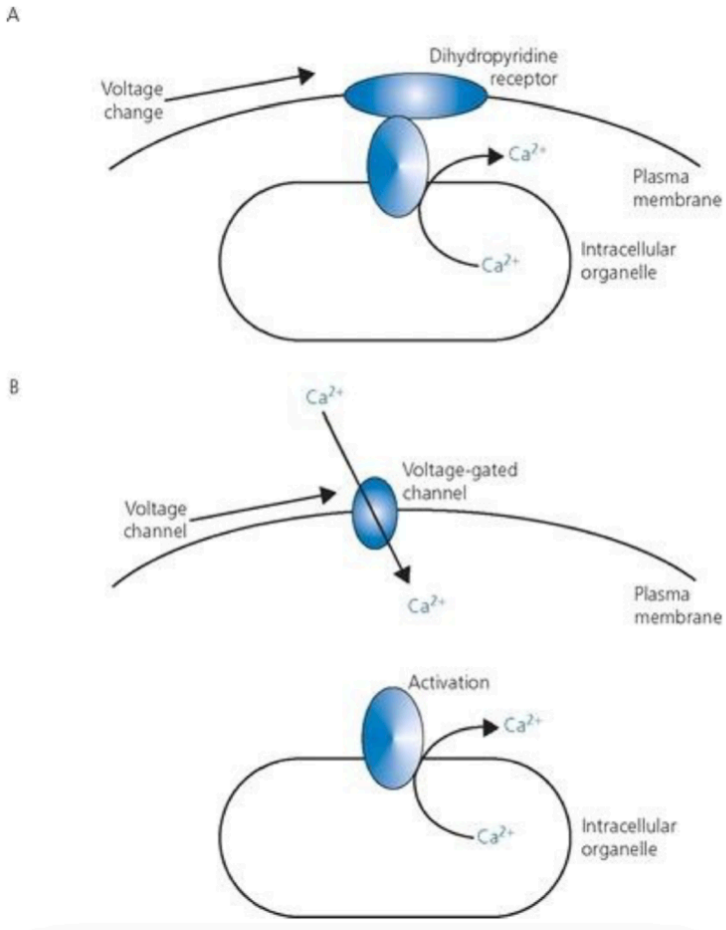

Figure 1-12. The 2 mechanisms for RyRs opening. (A) VOCs on plasma membrane sense its voltage change and undergo conformational change which is relayed to RyRs causing its opening. (B) VOCs import small amounts of Ca2+ into the cytoplasm, which lead to the opening of RyR (CICR). Adapted from (Hancock, 2010).

Like IP3Rs, Ca2+ released by RyR itself can also regulate RyR. Low [Ca2+] promotes Ca2+ release from RyR; high [Ca2+] (in mM level) inhibits Ca2+ release through RyR (Meissner, 1994). A bell-shaped curve can demonstrate the relationship between [Ca2+] and the release of Ca2+ through RyR (Meissner, 1994). If Ca2+ ions, which are not released from RyR (e.g., from a Ca2+ VOC on the plasma membrane), arrive near

RyR, they can also regulate the RyR in the same way, just like the Ca2+ ions released by RyR (Meissner, 1994). Like IP3Rs, this CICR phenomenon possessed by RyR is really important in the formation of local Ca2+ signaling & global Ca2+ signaling (will be mentioned afterward in this section).

Except for Ca2+, RyR can also be regulated by other molecules. For example, cyclic ADP-ribose cADPr (cADPr) can activate RyR. Different isoforms react differently. RyR2 & RyR3 seem to be sensitive to cADPr, whereas RyR1 is not responsive to cADPr molecules (Meissner, 1994).

For mitochondria, Ca2+ ions travel from mitochondria into cytoplasm via Na+/Ca2+ exchangers (NCX) (Berridge et al., 2000). The precise mechanism is still in the dark. It is possible that either 2 Na+ exchange for 1 Ca2+ (without a net charge movement) or 3 Na+ exchange for 1 Ca2+ (with a net charge movement) (Hancock, 2010).

Ca2+ signaling: decreasing cytoplasmic [Ca2+]

In order to decrease the high cytoplasmic [Ca2+] to a low level after signaling, Ca2+ ions in the cytoplasm will be: (1) transported into extra-cellular space, or (2) transported into intra-cellular calcium pool (ER & mitochondria) for storage.

Ca2+ signaling: decreasing cytoplasmic [Ca2+] with plasma membrane (PMCA, NCX & NCKX involved)

Ca2+ can be moved from the cytoplasm into the extracellular space through through Ca2+ pumps. On the plasma membrane, there are 2 types of pumps that can move Ca2+ ions from the cytoplasm into the extracellular space in an active way. They are plasma membrane Ca2+ ATPase (PMCA) pumps & Na+/Ca2+ exchangers. PMCA's energy source is ATP (Hancock, 2010). Na+/Ca2+ exchanger's energy source is the electro-chemical gradient across the plasma membrane (Hancock, 2010).

PMCA pump is a P-type ATPase (Pederson & Carafoli, 1987). For every 1 Ca2+ ion transported out of the cell, it consumes 1 or 2 ATP molecules (Clapham, 1995). PMCA is categorized as a P-type pump due to the fact that during the pumping cycle, a phosphorylated intermediate was involved (Strehler & Treiman, 2004). During the pumping cycle, a phosphoryl group was transiently transferred to an aspartate residue in PMCA (Strehler & Treiman, 2004). This phosphorylation leads to a conformational change, so the PMCA is in a state that allows it to discharge the Ca2+ ions out of the cell across the membrane. With subsequent de-phosphorylation, the PMCA's structure returns to its inactive state so that the Ca2+ cannot travel through, and the PMCA is ready for the next cycle. There are 10 trans-membrane spanning regions in PMCA (Clapham, 1995). In humans, there are several isoforms for PMCA. These isoforms are encoded by 4 genes and are tissue-specific (Clapham, 1995).

For the Na+/Ca2+ exchangers, mainly, there are 2 types of Na+/Ca2+ exchangers: NCX & NCKX. When NCX moves 1 Ca2+ ion out into the extracellular space, it also moves 3 Na+ ions into the cytoplasm (Clapham, 2007). When NCKX moves 1 Ca2+ ion out of the cell, it also moves 1 K+ ion & 4 Na+ ions into the cell (Clapham, 2007).

Comparing PMCA & Na+/Ca2+ exchanger, the PMCA has a higher Ca2+ ion affinity, while the Na+/Ca2+ exchanger has a faster rate in pumping Ca2+ ions out of the cell (Clapham, 2007). Normally, for PMCA

pump, in vitro, it can pump Ca2+ ions at a rate of 30 s^−1, approximately (Hancock, 2010). For the Na+/Ca2+ exchangers, it can pump Ca2+ ions at a rate of 2000 s^−1, approximately (Hancock, 2010). Therefore, in reducing cytoplasmic [Ca2+], Na+/Ca2+ exchangers first decrease the [Ca2+]i very quickly and very dramatically, and then when [Ca2+]i is at a μM level, PMCA continues to decrease the [Ca2+]i in a slower & more subtle way (Hancock, 2010). For the Na+/Ca2+ exchangers, this ability to quickly & dramatically reducing [Ca2+]i is very important for Ca2+ spike maintenance (Hilgemann et al., 2006).

Ca2+ signaling: decreasing cytoplasmic [Ca2+] with Ca2+ pool (SERCA & uniporter involved)
ER uses smooth endoplasmic reticulum Ca2+ ATPase (SERCA) pumps to actively transport Ca2+ ions from the cytoplasm (with low [Ca2+]) into the ER lumen (with high [Ca2+]) across the ER membrane. SERCA uses ATP as its energy source. Like PMCA, SERCAs are also P-type ATPases. For every ATP molecule consumed by SERCA, 2 Ca2+ ions can be taken up by ER (Clapham, 2007). SERCA is categorized as a P-type pump due to the fact that during the pumping cycle, a phosphoryl intermediate was involved (Pederson & Carafoli, 1987). During the pumping cycle, a phosphoryl group was transiently transferred to an aspartate residue in SERCA (Strehler & Treiman, 2004). This phosphorylation leads to a conformational change, so the SERCA is in a state that allows it to transport Ca2+ ions. With subsequent de-phosphorylation, the SERCA's structure returns to its inactive state so that the Ca2+ cannot travel through, and the SERCA is ready for the next cycle of Ca2+ pumping & ATP hydrolysis. The rate of SERCA's Ca2+-pumping is 30 s^−1, approximately (Hancock, 2010).

SERCA has 10 trans-membrane spanning regions (Brini & Carafoli, 2010). SERCA has 3 domains, including 2 bigger main domains & 1 smaller domain (Brini & Carafoli, 2010). 1 of the 2 main domains is embedded in the ER membrane; the other main domain is located on the cytoplasmic side of the ER membrane (Brini & Carafoli, 2010). The smaller domain is located on the lumen side of the ER membrane (Brini & Carafoli, 2010). The embedded main domain functions as a Ca2+ channel by binding Ca2+ ions near the ER membrane center line (Brini & Carafoli, 2010). The other main domain functions as ATPase and therefore is the phosphorylation site (Brini & Carafoli, 2010). SERCA pump's density on the ER membrane is 25,000 per μm^2, approximately (Hancock, 2010). In SR, SERCA is a major component of the SR membrane (Toyoshima et al., 1993).

In mammals, SERCAs have 3 isoforms (SERCA1, SERCA2 & SERCA3) encoded by 3 genes (Clapham, 1995). These isoforms are expressed in a tissue-specific fashion. SERCA1 & SERCA2 are expressed in muscle tissue (different types) (Clapham, 1995). SERCA3 is expressed in non-muscle tissue (Pozzan et al., 1994).

The activity of SERCA can be regulated to achieve that the speed of Ca2+ ion removal from the cytoplasm can be adjusted on demand. It can be quick, or it can be slow if the signaling process needs to be longer. Increased [Ca2+]i promotes SERCA activity (Hancock, 2010). However, increased [Ca2+] inside the ER diminishes SERCA activity. When [Ca2+] inside the ER rises to approximately 300 μM, half of the SERCA activity is lost (Hancock, 2010). Except for Ca2+, SERCAs can also be regulated in a receptor-mediated way (Hancock, 2010).

Mitochondria can also uptake Ca2+ ions to reduce cytoplasmic [Ca2+]. When cytoplasmic [Ca2+] rises, it means that there might be cellular events that need biological energy going on, so Ca2+ ions taken up by

mitochondria can be used to promote mitochondrial activity, leading to a subsequent increase in ATP production (Clapham, 2007). Mitochondria use Ca2+ uniporters to take up Ca2+ ions (Clapham, 1995). Ca2+ uniporters use the proton gradient across the mitochondrial inner membrane as an energy source (Clapham, 2007). This proton gradient is maintained by the respiratory electron transport chain (ETC) (Hancock, 2010). One example of such uniporters is the mitochondrial Ca2+ channel (MiCa) (Kirichok et al., 2004), which has a high Ca2+ affinity (Clapham, 2007).

Ca2+ signaling: cytoplasmic [Ca2+] gradient

Throughout the cytoplasm, the [Ca2+] distribution is not even. [Ca2+] gradient exists from the Ca2+ entry site (Ca2+ channels, e.g., VOC, ROC, MOC, IP3R & RyR, etc). Once free Ca2+ ions enter the cytoplasm, the duration of their free diffusion is about 50 μs, approximately (AIIbritton et al., 1992). The distance they can travel within 50 μs is about 0.1-0.5 μm, approximately (AIIbritton et al., 1992). Why is this ? This is due to the fact that, in the cytoplasm, there are many molecules that can bind to free Ca2+ ions and therefore immobilize Ca2+ ions by keeping them in the bound state (AIIbritton et al., 1992). These buffering molecules' saturation degree & uneven distribution can affect the [Ca2+] gradient (AIIbritton et al., 1992).

There are 2 types of [Ca2+] gradient in the cytoplasm, that is, micro-gradient & nano-gradient. Micro-gradient is caused by free diffusion and can often be observed near the plasma membrane (Hancock, 2010). Micro-gradient occur at a distance of 1-10 μm (micro-meter) from the Ca2+ entry site (Hancock, 2010). In micro-gradient, the highest [Ca2+] is about 1 μM, approximately (Sabatini et al., 2002). Nano-gradient is caused by facilitated diffusion and can often be observed near the plasma membrane & membrane of the calcium pool (e.g., ER) (Hancock, 2010). Nano-gradient occur at a distance of 10 nm (nano-meter) from the Ca2+ entry site (Hancock, 2010). In nano-gradient, the highest [Ca2+] is about 100 μM, approximately (Allbritton & Meyer, 1993). Nano-gradient often lasts less than 1 ms (milli-second) (Long et al., 2005).

Ca2+ signaling: local signal (blip, puff, quark & spark, etc)

Ca2+ signaling has spatio-temporal diversity, and it can be categorized into 2 types: local & global. Local Ca2+ signals include blips, puffs, quarks & sparks, etc. Local Ca2+ signals can be caused by the transient opening of a single or a group of IP3R or RyR channels on the ER membrane, or by Ca2+ channels in the cell membrane.

Blip is caused by the opening of 1 single IP3R. Puff is caused by the opening of 1 group of IP3Rs. A puff can be considered as a bundle of blips. Quark is caused by the opening of 1 single RyR. Spark is caused by the opening of 1 group of RyRs. A spark can be considered as a bundle of quarks. Here are some examples of local signals being reported in various species: sparks reported in cardiac muscle (Cheng et al., 1993), puffs & blips reported in Xenopus oocytes (Yao et al., 1995; Parker & Yao, 1996), quantum emission domains (QED) reported in squid giant synapse (Sugimori et al., 1994) & 'bumps' reported in Drosophila photoreceptors (Hardie, 1991). In the English literature, many other words, such as pulse, pump, burst, transient, etc., have also been used to describe local signals. I think it is important not to spend too much brain power on terminology; instead, focus on the identification & characterization of these local signals.

.

The local Ca2+ signal has a spatial range, meaning that it can only happen in a very limited space that is usually 2 μm (micro-meter) in diameter (Berridge, 1997). Normally, the time course of a local Ca2+ signal is

like the following (Figure 1-13): (1) When the channel opens, [Ca2+] increases rapidly. (2) After the channel closes, [Ca2+] decreases slowly by Ca2+ ions' gradual free diffusion (Berridge, 1997).

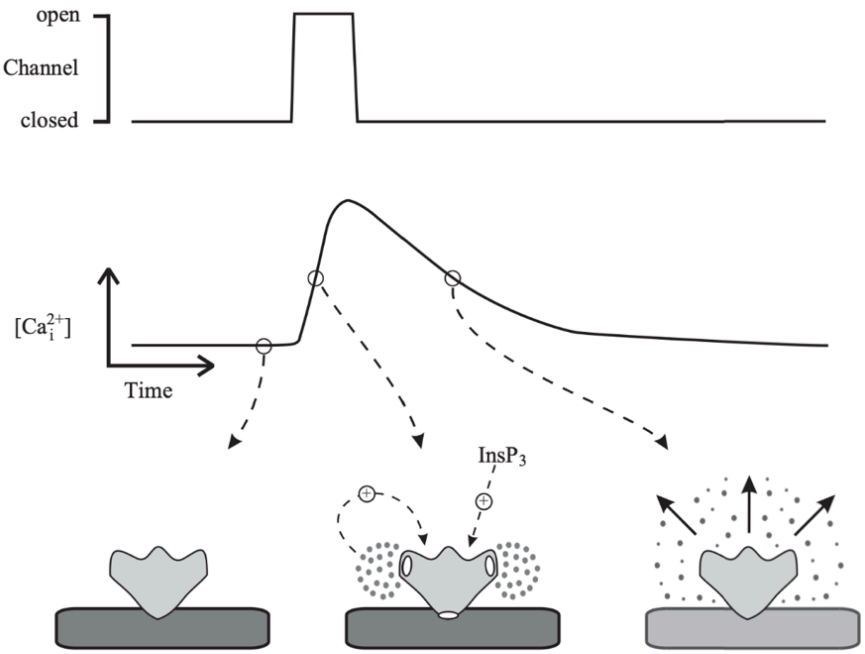

Figure 1-13. Ca2+ local signaling. The brief opening of an IP3R leads to local Ca2+ signaling. This contains a rapid rising stage and a slow recovery stage. Recovery stage happens after the closure of IP3R. The rapidity is caused by CICR. The slowness is caused by Ca2+ passive diffusion. The fore-mentioned mechanism can be transposed onto RYRs. Adapted from (Berridge, 1997).

Local Ca2+ signals have 2 major functions. 1st, they can locally regulate a range of cellular processes (Berridge et al., 1999). 2nd, they enable global Ca2+ signals (e.g., waves & oscillations) to regulate many physiological processes (Berridge et al., 1999). Here are some examples of cellular processes that are directly regulated by local signals: ion channel activation, secretory & synaptic vesicle releasing, and energy metabolism in mitochondria (Berridge et al., 1999).

Compared to global Ca2+ signals, using local Ca2+ signals to regulate these processes has a couple of advantages. 1st, regulation by local Ca2+ signal is highly specific. This is due to the fact that the local Ca2+ signal's spatial range is limited and the fact that [Ca2+] decreases dramatically from the Ca2+ entry site (Berridge et al., 1999). 2nd, regulation by local Ca2+ signals is rapid & relatively low energy-consuming. Here are a couple of examples of rapid regulation by local signals: (1) During synaptic transmission, VOCs in close distances to synaptic vesicles trigger high-intensity Ca2+ signals to induce exocytosis (Berridge et al., 1999). (2) In squid giant synapse, the QEDs happen for about only 1.25 ms (milli-second), while the [Ca2+] can increase to 200-300 μM (Berridge et al., 1999). Due to the fact that the number of Ca2+ ions used in generating a local signal is limited, these Ca2+ ions can be removed more rapidly, consuming less ATP than global signals (Berridge et al., 1999).

Ca2+ signaling: global signal (wave & oscillation)

There are 2 types of global Ca2+ signals: Ca2+ wave & Ca2+ oscillation. Ca2+ concentrations can be measured as waves or oscillations. Ca2+ oscillation can be considered as a bundle of periodically occurring Ca2+ spikes. The Ca2+ wave reflects the spatial nature of Ca2+ signaling, while Ca2+ oscillation reflects the

temporal nature of Ca2+ signaling. In the case of Ca2+ wave, it is the transfer of Ca2+ signal ([Ca2+] elevation) from one location to another and then to the next, propagating. Typically, a Ca2+ wave is first created locally, perhaps on a particular part of the ER/SR, then as the IP3R/RyR activation (release of Ca2+ into the cytoplasm) spreads across the ER/SR membrane, Ca2+ signals propagate through the cytoplasm (will be mentioned afterward in this section). In the case of Ca2+ oscillation, it is a Ca2+ signal that occurs at a relatively fixed location but occurs repeatedly, and each occurrence may be different each time, i.e., each spike may be different (will be mentioned afterward in this section). Not only the amplitude ([Ca2+]) but also the frequency of the Ca2+ oscillation can be used as a signal.

The creation of a wave might use the following mechanism (Figure 1-14) (Figure 1-15). In non-excitable cells, e.g., Xenopus oocytes (Yao et al., 1995; Parker & Yao, 1996), it is achieved through the CICR phenomenon of IP3R/RYR. 1st, in ER, 1 individual IP3R opens randomly, leading to the formation of a blip (Parker & Yao, 1996), which leads to the rapid rising of [Ca2+] in space surrounding IP3R. These Ca2+ ions passively diffuse away. 2nd, rapid rising of [Ca2+] & Ca2+ ion diffusion leads to the activation of IP3Rs near the '1 individual IP3R', leading to a group of IP3Rs releasing Ca2+ ions, leading to blips growing into puffs (Berridge, 1997). 3rd, similarly, this 'a group of IP3Rs' leads to the activation of IP3Rs near them. This goes on, leading to IP3R activation & blips/puffs formation along the ER membrane (Allbritton & Meyer, 1993; Berridge et al., 2000). At the same time, this '1 individual IP3R' is inhibited by increased [Ca2+] in the surrounding space, which also leads to the activation of SERCA near this '1 individual IP3R' (Allbritton & Meyer, 1993; Berridge et al., 2000). SERCA activation reduces [Ca2+] in the space surrounding this '1 individual IP3R' (Allbritton & Meyer, 1993; Berridge et al., 2000). Similarly, 'a group of IP3Rs' are inhibited by increased [Ca2+] in the surrounding space, which also leads to the activation of SERCA near this 'a group of IP3Rs' (Hancock, 2010). SERCA activation reduces [Ca2+] in the space surrounding this 'a group of IP3Rs' (Hancock, 2010). This goes on, leading to IP3R inhibition, SERCA activation & [Ca2+] reduction along the ER membrane (Hancock, 2010).

The wave spread at a speed of approximately 5-100 μm/sec, which is relatively slow (Busa & Nuccitelli, 1985; Dani et al., 1992; Kline et al., 1991; Kubota et al., 1987; Lechleiter et al., 1991; Rooney et al., 1990; Sanderson et al., 1990; Takamatsu & Wier, 1990). It could take approximately 1 second to synchronize Ca2+-releasing to form a global signal like a Ca2+ wave (Berridge et al., 1999).

Waves can travel from one cell to another cell through gap junctions (Robb-Gaspers & Thomas, 1995; Zimmermann, 1999). This phenomenon is important to keep in mind when it comes to apoptosis. If 1 cell will undergo or is undergoing apoptosis, the body might prevent the 'apoptosis signal' from spreading away, during which the spreading of the Ca2+ wave through gap junctions might get prevented as well (Hancock, 2010).

Ca2+ oscillation was first reported in the blowfly's salivary gland. In blow-fly's salivary glands, Ca2+ concentration is demonstrated as a periodic series of spikes (Zimmermann, 1999). There are many factors that could affect the pattern of Ca2+ oscillation, including Ca2+ buffering capacity in the cytoplasm, the type of receptor activated & concentration of agonist, etc (Hancock, 2010). Spikes can be different in many different ways. The frequency might vary. The location in the cytoplasm can be closer or farther (Hancock, 2010). The amplitude can be smaller or greater (Hancock, 2010). The lasting time can be longer or shorter, which means that increased Ca2+ level within the spike may last a longer or shorter period of time (Hancock,

2010). Ca2+ oscillation has been reported to be involved in the process of mitosis initiation & meiosis completion in some cells (Means, 1994).

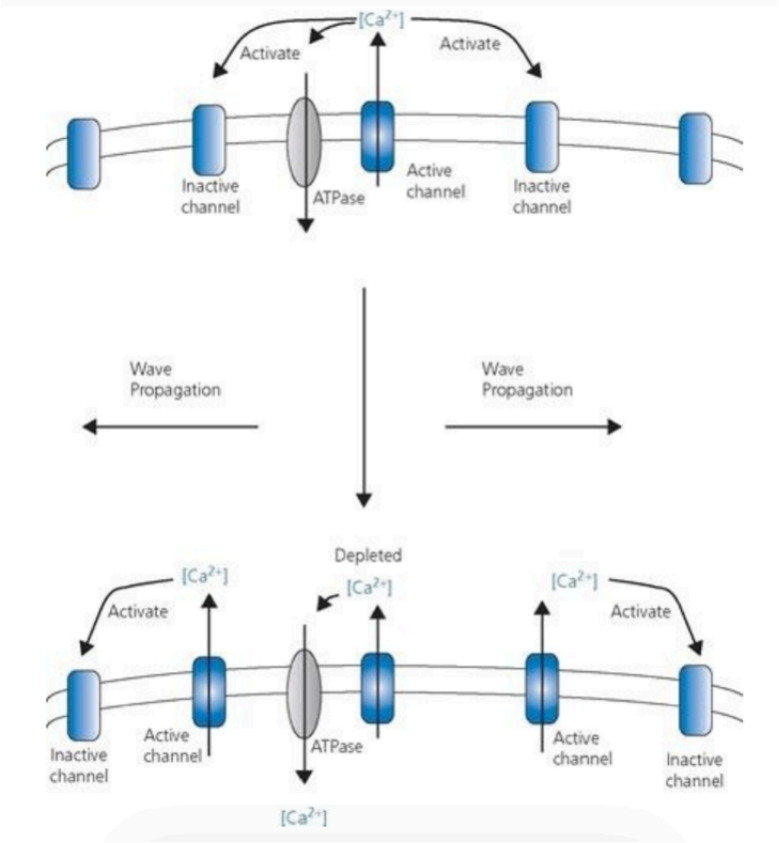

Figure 1-14. A scheme explaining the propagation of Ca2+ waves along the ER membrane. Adapted from (Hancock, 2010).

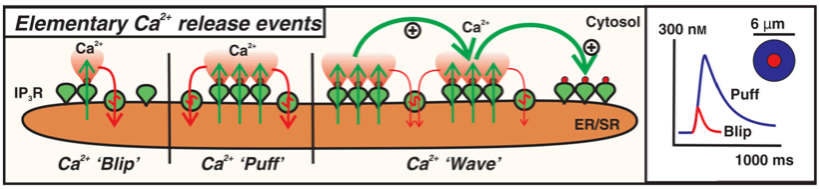

Figure 1-15. Formation of Ca2+ waves from local Ca2+ signal. The diagram is a simplified version by using only IP3Rs for illustration. This mechanism can be transposed onto RYRs as well. Adapted from (Laude & Simpson, 2009).

For the mechanism underlying the formation of Ca2+ oscillation, there are 2 models, which are the one-pool model & the two-pool model. One-pool model means that there is only 1 single Ca2+-pool that Ca2+ ions can be released from (Hancock, 2010). Likewise, the two-pool model means that there are 2 independent Ca2+ pools that Ca2+ ions can be released from (Hancock, 2010). One in 'one-pool' means that there is only 1 type of Ca2+-pool (organelle), meaning that the pool has the same activation kinetics (release & uptake) (Hancock, 2010). Two in 'two-pool' means that there are 2 types of Ca2+-pool (organelle), meaning that the pools have different activation kinetics (release & uptake) (Hancock, 2010). Different activation kinetics (release & uptake) means that the release of Ca2+ ions from 1 pool can happen early to the other pool, or the uptake of Ca2+ ions into 1 pool can happen early to the other pool (Hancock, 2010). In some cells, a 'multiple-pools' situation might exist. Each pool has different activation kinetics and can be regulated by different signaling molecules (Hancock, 2010).

For the one-pool model (Figure 1-16), 1st, Ca2+ ions are released by IP3Rs/RyRs upon channel activation (Atri et al., 1993; Dupont & Goldbeter, 1993). This release is relatively slow. Then, the increased Ca2+ concentration promoted the opening of IP3Rs/RyRs, leading to the accelerated Ca2+ release through IP3Rs/RyRs (Atri et al., 1993; Dupont & Goldbeter, 1993). This leads to a rapid & dramatic increase of Ca2+, which can be considered as a part of a spike (Atri et al., 1993; Dupont & Goldbeter, 1993). Then, with the Ca2+ concentration continuing to increase, even higher concentration of Ca2+ inhibit IP3Rs/RyRs, leading to the closing of channels and the subsequent stopping of Ca2+ concentration increase (Atri et al., 1993; Dupont & Goldbeter, 1993). Then, this 'higher' Ca2+ concentration activates various Ca2+ pumps that remove Ca2+ ions from the cytoplasm & re-sequestered Ca2+ ions in the calcium pool, leading to the decrease in Ca2+ concentration (Atri et al., 1993; Dupont & Goldbeter, 1993).

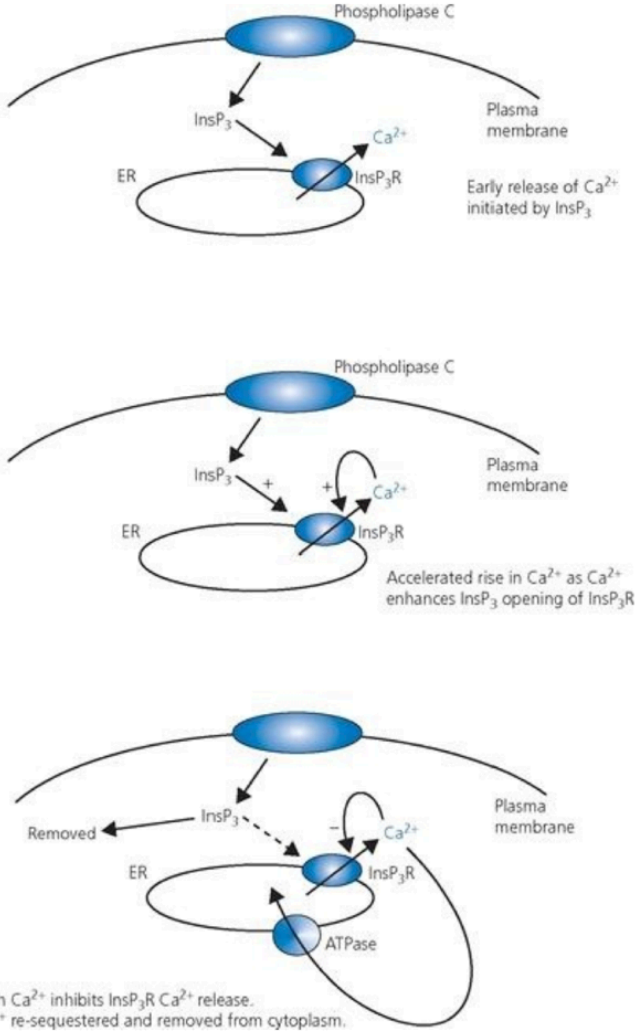

Figure 1-16. One-pool model of Ca2+ oscillation. Adapted from (Hancock, 2010).

CaBP in Ca2+ signaling

Proteins that can bind Ca2+ are Ca2+-binding proteins (CaBP). According to their functions, they can be classified into 3 categories: buffering protein, transporter protein & signaling protein. (1) For the buffering proteins, they can be found in the nucleus, calcium pools & cytoplasm. When they bind to calcium, calcium changes from the ionized free state to the non-ionised bound state, and [Ca2+] decreases. Calcium in a bound state cannot function as a signaling molecule and is held as a storage source (as previously described in this section). Examples of buffering proteins are the following: calbindin, calsequestrin,

calreticulin, parvalbumin, etc. (2) For the transporter protein, they can be found in the cell membrane & calcium pool membrane. They carry Ca2+ ions from the extra-cellular or calcium pools to the cytoplasm or vice versa. Examples of transporter proteins are the following: IP3R, RyR, NCX, NCK. RyR, NCX, NCKX, etc (as previously described in this section). (3) For the signaling proteins, they can be divided into enzymatic ones and non-enzymatic ones. When they bind to calcium, they are activated and undergo an alteration in their conformation, and this conformational change will expose active sites on the protein, activating the next signaling molecule. Examples of signaling proteins are the following: PKC, phospholipase C (PLC), phospholipase A2 (PLA2), calmodulin (CaM), Troponin C (TnC), S100 protein, etc. The most important is CaM (will be mentioned afterward in this section).

In order to bind Ca2+, regarding the structure of CaBPs, the oxygen atom, C2 domain & EF-hand motif are involved.

The oxygen atom is involved in the binding between Ca2+ & CaBPs for the reason that it can provide recognition & physical attraction to Ca2+ (Hancock, 2010). Normally, Ca2+ ion(s) can coordinate 6/7/8 oxygen atoms; therefore, most CaBPs can bind to Ca2+ ion(s) through 6/7/8 oxygen atoms (McPhalen et al., 1991). This number can increase to 12 (McPhalen et al., 1991). Normally, these oxygen atoms are in aspartate or glutamate, due to the fact that these 2 residues are charged at normal physiological pH (Fasman, 1989).

The C2 domain has 120 amino acids, approximately (Cho & Stahelin, 2005). Its structure is an anti-parallel β sheet (Cho & Stahelin, 2005). It contributes to establishing an association between a protein & a membrane (lipid bilayer) (Clapham, 2007). When Ca2+ binds to the C2 domain, it leads to increased affinity between the protein & the membrane (Clapham, 2007). The increased affinity changes the protein's cellular location and makes the protein membrane-associated (Clapham, 2007). Membranes include the cell membrane & mitochondrial membrane. For the cell membrane, it is the inner surface that proteins (e.g., PKC) become associated with (Clapham, 2007). For the mitochondrial membrane, it is the outer surface that proteins become associated with (Clapham, 2007). In humans, the C2 domain might exist in more than 600 proteins (Clapham, 2007).

The EF-hand structure contains 2 α-helices (E&F) that are connected by a loop (Figure 1-17) (Clapham, 1995). It's called EF-hand due to the fact that the α-helice E & α-helice F's position is like a right hand's thumb & forefinger are pointing out (Hancock, 2010). The loop connecting the 2 α-helices is the Ca2+-binding site (Kretsinger, 1980). Aspartate residue & glutamate residue in the loop are responsible for Ca2+-binding (Kretsinger, 1980). Many CaBPs have more than 1 Ca2+-binding site (Clapham, 1995). Some CaBPs don't contain an EF-hand structure.

Lowered calbindin level in the cytoplasm has been reported to be involved in many pathological processes (e.g., Alzheimer's disease) (McLachlan et al., 1987). Calsequestrin's molecular weight is about 44 kDa and is often found in the SR (Wang & Michalak, 2020). It is acidic, due to the fact that more than 1/3 of its amino acids are glutamic/aspartic acid (Wang & Michalak, 2020). 1 molecule of calsequestrin can bind to 43 molecules of Ca2+ (Hancock, 2010).

Troponin has 3 polypeptides, which are TnC (18 kDa), TnI (24 kDa) & TnT (37 kDa) (Sundaralingam et al., 1985). Troponin lies on the muscle fiber's thin filaments, along with tropomyosin (Clapham, 2007). TnC subunit can bind to Ca2+ ions (Sundaralingam et al., 1985). TnC has 2 homologous domains (C-terminal domain & N-terminal domain) (Sundaralingam et al., 1985). Each domain has 2 EF-hand structures for Ca2+-binding (Sundaralingam et al., 1985). The C-terminal domain's EF-hand structures have high affinity for Ca2+, while the N-terminal domain's EF-hand structures have low affinity (Sundaralingam et al., 1985). 2 domains are connected by an α-helix structure (Sundaralingam et al., 1985). TnC's structure is very similar to CaM (Sundaralingam et al., 1985). When the Ca2+ ion binds to EF-hand structures in the TnC subunit, it undergoes a conformational change, which is transmitted to tropomyosin through the other subunits in troponin (Sundaralingam et al., 1985). Then tropomyosin changes its orientation, leading to the relief of steric hindrance caused by the interaction between actin & myosin (Clapham, 2007). This relief promotes muscle functioning (Clapham, 2007).

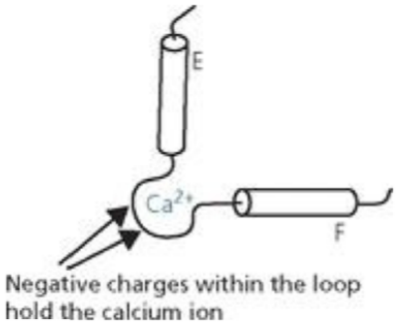

Figure 1-17. EF hand structure: 2 α-helices connected by a loop that function as a Ca2+ binding site. Adapted from (Hancock, 2010).

S100 family proteins contain EF-hand structure. In humans, there are more than 25 genes that encode for this protein (Clapham, 2007). After binding to Ca2+, S100 protein might change its cellular location. Some change its location within the cell, while some change its location from 'within the cell' to 'outside the cell' through secretion (Heizmann, 2002). S100-protein dysfunction has been reported to be involved in the pathological process of many diseases (e.g., cancer & neuro-degenerative disorder) (Heizmann, 2002).

CaM in Ca2+ signaling

CaM is ubiquitous. It is a small acidic protein (Babu et al., 1985). 1 molecule of CaM can bind up to 4 molecules of Ca2+ ions (Babu et al., 1985). CaM's Ca2+ affinity is 10^−6 M, approximately (James et al., 1995). This is lower than [Ca2+]i in the activated cells (10^−5 M) but higher than [Ca2+]i in the resting cell (10^−7 M) (James et al., 1995). CaM's shape is like a dumbbell (Figure 1-18). CaM has 2 globular domains & 1 long flexible α-helix connecting the 2 globular structures (C-terminal & N-terminal) (James et al., 1995). Each globular structure has 2 EF-hand motifs (James et al., 1995). Each EF-hand motif can bind 1 molecule of Ca2+ ion. Within each globular region, the 2 EF-hand motifs are connected by an anti-parallel β-sheet (James et al., 1995). These 2 globular domains' Ca2+ affinities (binding constant) are different. The C-terminal domain's Ca2+ affinity is higher than the N-terminal domain; therefore, it will bind to the Ca2+ ion prior to the N-terminal domain (James et al., 1995). When CaM binds to Ca2+, CaM undergoes a conformational change that reveals 2 hydro-phobic pockets, with 1 in each globular domain (James et al., 1995). These pockets can interact with another molecule/protein. Except for the Ca2+ ion, CaM can bind to other ions, such as Tb3+, Hg2+, Mn2+, etc (Hancock, 2010). In humans, there are 3 CaM-coding genes,

located on chromosome 2, 14 & 19 (Abzhanov et al., 2006). Sometimes, CaM is integrated into another molecule/enzyme. For example, in phosphorylase kinase (PhK), CaM is the δ subunit (Hancock, 2010).

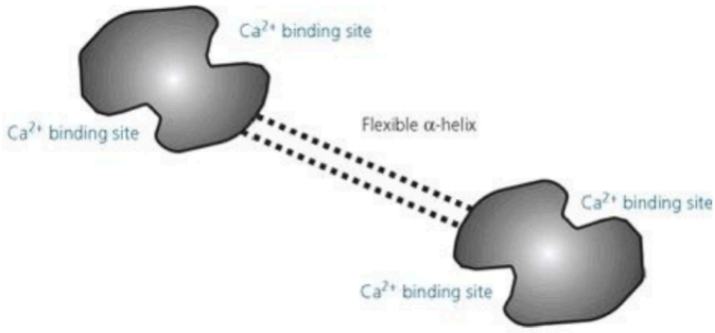

Figure 1-18. Calmodulin domain structure. One CaM contains 4 Ca2+-binding sites. Adapted from (Hancock, 2010).

Except for the Ca2+, CaM can also be regulated through phosphorylation due to the fact that there are phosphorylation sites in the binding regions (Hancock, 2010). It has been reported that CaM itself is phosphorylated in vivo (Hancock, 2010).

Upon binding to Ca2+, CaM is activated to form active Ca2+•CaM compounds. Ca2+•CaM binds to the target enzyme (non-kinase). The target enzyme is activated to form active (Ca2+•CaM)•E compounds (Figure 1-19) (Figure 1-20) (Sun et al., 2010). The activation of Ca2+•CaM on the target enzyme (non-kinase) can be direct or indirect. Indirectly, target enzymes (non-kinases) are activated by activating 'Ca2+ and/or CaM'-dependent protein kinases (Sun et al., 2010). The 'Ca2+ and/or CaM'-dependent protein kinases include CaM-dependent protein kinase (CaMK), Ca2+•CaM-dependent protein kinase (CCaMK), Ca2+-dependent protein kinase (CDPK), and CDPK-related protein kinase (CRK) (Sun et al., 2010). Among them, CaMK is the most important, including CaMK I-V, myosin light chain kinase (MLCK), and PhK (Sun et al., 2010). Target enzymes directly activated by Ca2+•CaM include phospho-diesterase (PDE), adenylyl cyclase (AC), Ca2+-ATPase, etc (Sun et al., 2010). Target enzymes that can be indirectly activated by Ca2+•CaM include glycogen synthase (GS), cAMP-response element binding protein (CREB), IP3R, etc (Sun et al., 2010). Sometimes, in the indirect activation, CaMK activation needs to activate Ca2+•CaM-dependent protein kinase kinase (CaMKK) first (Sun et al., 2010).

$$Ca2+ + CaM \rightleftarrows Ca2+\bullet CaM^*$$
$$(Ca2+\bullet CaM^*) + E \rightleftarrows (Ca2+\bullet CaM^*)\bullet E^*$$

Figure 1-19. Mechanism of Ca2+•CaM in signaling. '*' for activated state. 'E' for enzyme.

CaM can lead to the activation/opening of PMCA & SERCA, which lead to the decrease of [Ca2+]i & the ending of Ca2+ signal (Hancock, 2010). In this case, Ca2+ ions can regulate their own signaling activity through CaM.

Sometimes, in terms of CaM's regulation of other molecules, CaM can have an increasing/activating effect and a decreasing/deactivating effect on 1 molecule at the same time. For example, CaM can increase the level of cAMP by activating adenylyl cyclase (AC), which is the cAMP-producing enzyme (Berridge et al.,

2000). CaM can also decrease the level of cAMP by activating PDE, which is the cAMP-degrading enzyme (Berridge et al., 2000).

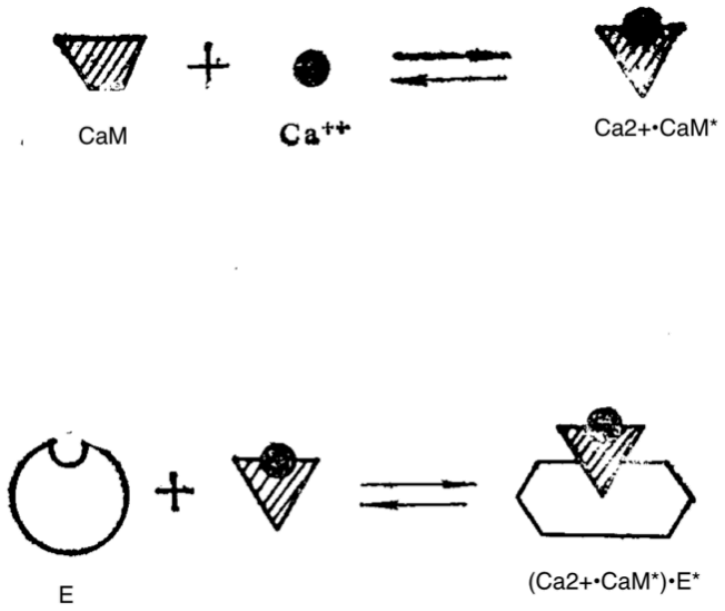

Figure 1-20. Mechanism of Ca2+•CaM in signaling. CaM itself is inactive; upon binding with Ca2+, it undergoes a conformational change to form the active Ca2+•CaM complex. When Ca2+•CaM binds with an inactive target enzyme, the target enzyme undergoes a conformational change to become active, therefore forming the active (Ca2+•CaM)•E complex. '*' for activated state. 'E' for enzyme. Adapted from (Wen et al., 1989).

CaM-like proteins also exist. In Dictyostelium discoideum, more than 60 CaM-like proteins have been reported (Catalano & O'Day, 2007). This kind of protein has a lot of functions and can be found in many different cellular locations (Catalano & O'Day, 2007). In eukaryotes, a similar situation might also exist.

Notes & thoughts

1. Except for IP3Rs in ER membrane, IP3-like receptors have also been reported in the cell membrane of certain cells (Hancock, 2010). However, their precise functions are still in the dark.
2. In many Ca2+-transporter proteins, this 'Thr-X-Cys-Phe-Ile-Cys-Gly' amino acid sequence exists (Hancock, 2010). This sequence is often located in the polypeptide's C-terminal end (Hancock, 2010). This sequence may take part in the Ca2+-channel's opening process (Hancock, 2010). This sequence might be targets of ROS for oxidation due to the fact that cysteine residue's -SH groups might be open to oxidation (Hancock, 2010).
3. Ca2+ can regulate the activation of calcineurin (PP2B) (Catalano & O'Day, 2007) & nitric oxide synthase (Nos) (Clapham, 1995). PP2B is a type of Ca2+-dependent phosphatase. Ca2+ can also regulate the activation of pyruvate dehydrogenase (PDH) (Nicholls & Ferguson, 2002; Rutter et al., 1996).

Ca2+ signaling is quite complex. It is the most complex signaling molecule among all the molecules mentioned in the 'Introduction' chapter. This complexity arises from the involvement of numerous protein molecules, reaching several dozen. When talking about cellular signal transduction, non-protein signaling molecules need to link to protein molecules. Protein molecules involved in Ca2+ signaling and their position

in the transduction pathway (as previously described in this section) are as follows (Figure 1-21): extra-cellular signaling molecules act on (directly/indirectly) CaBPs functioning as Ca2+ transporters (e.g., IP3R, RyR, ROC, VOC, MOC, SOC, SERCA, PMCA, NCX & NCKX, etc), leading to an increase in cytosolic [Ca2+]. Then these Ca2+ ions can either bind to CaBPs functioning as non-enzymatic signaling molecules (e.g., CaM, TnC & S100 protein, etc) or CaBPs functioning as enzymatic signaling molecules (e.g., PKC, PLC & PLA2, etc). Among all these CaBPs, CaM is the most important one, which binds to Ca2+, forming Ca2+•CaM*. Ca2+•CaM* can directly activate target enzyme E (non-kinase) or indirectly activate target enzyme E (non-kinase) through protein kinases that depend on 'Ca2+ and/or CaM' (e.g., CaMK, CCaMK, CDPK & CRK) with CaMK being the most important one. Sometimes, CaMKK can act up-stream on CaMK. CaMK includes CaMK I, CaMK II, CaMK III, CaMK IV, CaMK V, MLCK & PhK, etc. The target enzyme E (non-kinase) includes PDE, AC, SERCA, PMCA, CREB, GS & IP3R, etc. All these dozens of molecules have various sub-types and different tissue-expression patterns.

There are things that make Ca2+ signaling more complex. For example, there is self-activation involved (as previously described in this section): (1) Ca2+ activates IP3R in CICR. (2) Ca2+ activates RyR in CICR. For another example, there are some interactions between the molecules in the signaling pathway mentioned in the last paragraph: (1) In skeletal muscle, DHPR (a VOC on the plasma membrane) can activate RyR. (2) The target enzyme E (non-kinase) of Ca2+•CaM* includes SERCA, PMCA & IP3R. For another example, there are many other ligands that can act on receptors (Ca2+ channels): (1) Mg2+ can activate IP3R. (2) cADPr can activate RyR. (3) IP3/IP4/cGMP/G protein can activate ROC. For another example, there are many other molecules that could be involved (as previously described in this section): (1) ROS can act on CaBPs functioning as Ca2+ transporters. (2) Ca2+ can activate PP2B/Nos/PDH.

There are some Ca2+-related protein molecules that I choose to temporarily set aside when trying to identify the signaling molecules/molecular pathway involved in the notochord bead formation: (1) Molecules involved in Ca2+ metabolism (e.g., calcitonin & PTH, etc). (2) CaBPs functioning as Ca2+ transporters that are located in mitochondria (e.g., mPTP & uniporter). (3) IP3-like receptors. (4) CaM-like proteins. (5) CaBPs functioning as buffers (e.g., parvalbumin, calreticulin & calsequestrin, etc). The reasons are (1) molecules involved in Ca2+ metabolism & CaBPs functioning as buffers seem to show no association with Ca2+ signaling; (2) at present, CaBPs functioning as Ca2+ transporters that are located in mitochondria are less well-characterized and seem to be less important than their counterparts located in the ER due to the fact that IP3Rs & RyRs can form Ca2+ local signals & Ca2+ global signals.

Due to the fact that (1) during the zebrafish larva tail regeneration's early stage, the notochord bead formation was observed along with other morphological features, including trunk contraction; (2) the aim of this project is to identify the signaling molecules/molecular pathway involved in the notochord bead formation mechanism; (3) it is suspected that the notochord bead formation was caused by the trunk's muscle contraction, which is highly related to Ca2+, so the early stage of this project is centered on Ca2+ signaling. A number of Ca2+ signaling-related protein molecules were selected as potential molecules and tested with chemicals (inhibitors & scavengers). Since most of the candidate molecules in my experiment are related to Ca2+ signaling, this 'Ca2+' section is much longer than other sections in the 'introduction' chapter.

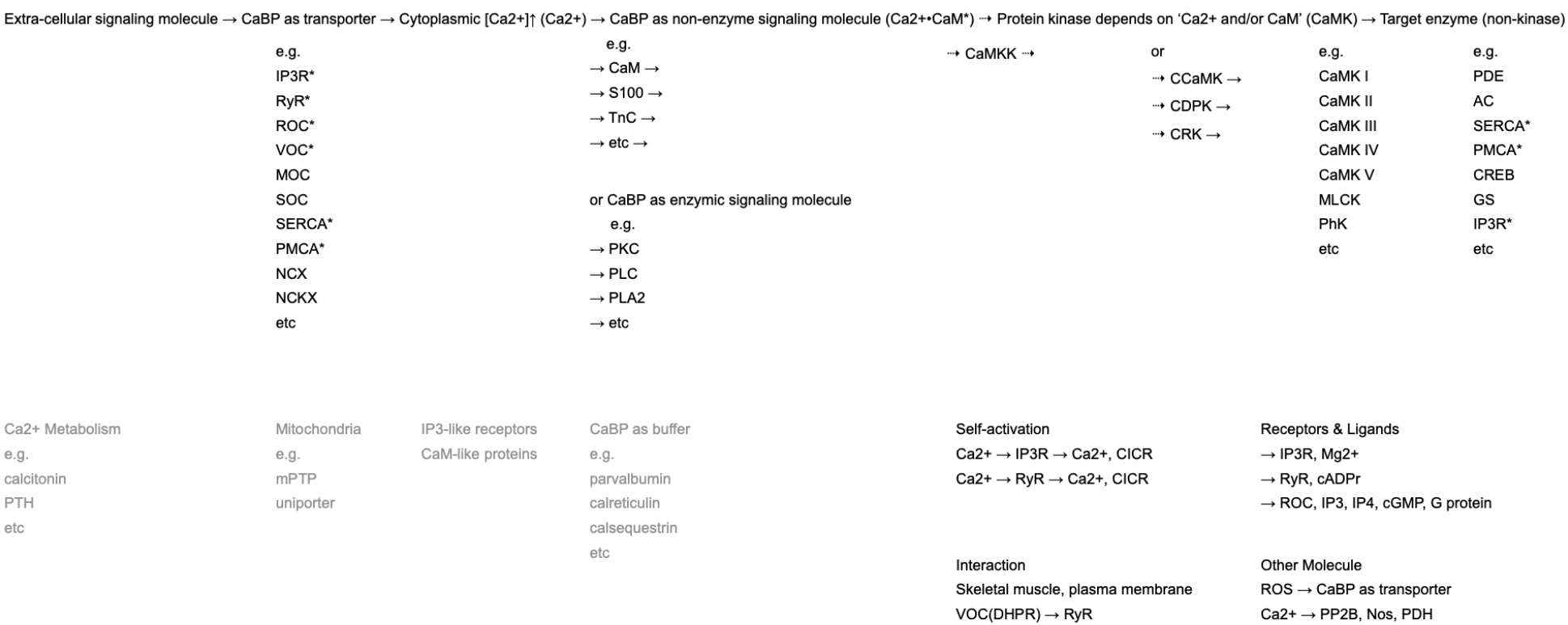

Figure 1-21. Protein molecules involved in Ca2+ signaling cascade. '⇢' dashed arrow means that the pathway is optional. 'Grey colored text' means the protein molecules are temporally not considered. '*' in 'Ca2+•CaM*' means that CaM is activated. '*' in other places could mean that it interact with another molecule (downstream or upstream) in this figure, or it could mean that it, as a receptor, has more ligands, which are mentioned in the lower-right section of this figure.

1.4 H2O2

H2O2 & biological processes related to zebrafish (larva) tail regeneration: a super-mini review

In this review, I shall outline how H2O2 participates in biological processes related to tail regeneration in zebrafish (larva). Given that zebrafish tail regeneration requires the regeneration of muscle, nerve, bone, blood vessels, notochord/spinal cord, skin, connective tissue & pigment cells, and that regeneration sometimes resembles development to some extent, I looked for the following biological processes: (epimorphic) regeneration/morphogenesis of muscle/nerve/bone/blood vessels/notochord/skin, wound healing & inflammation. A relatively large amount of literature has been found for H2O2. Owing to my limited space, I will only select a few (i.e., regeneration & development). Therefore, this review is incomplete, as H2O2 is also involved in other biological processes related to zebrafish tail regeneration.

What will be written and what won't be mentioned is the same as the 'Ca2+' section. Except in point (2) of ‘What will be covered’, replace ‘protein molecules directly involved in Ca2+ signal transduction’ with ‘protein molecules directly involved in H2O2 signal transduction’. Protein molecules directly involved in H2O2 signal transduction: (a) Enzymes associated with H2O2-producing such as NADPH oxidase (Nox) & superoxide dismutase (SOD), etc; (b) Enzymes associated with H2O2-degrading including catalase (CAT), glutathione peroxidase (GPx), peroxiredoxin (PRx), GRx(glutaredoxin) & TRx(thioredoxin), etc; (c) mitochondria-associated molecules.

H2O2 is involved in regeneration in different tissues/organs across various species (reviewed in Deken et al., 2013; Fadilah et al., 2023; Hunt et al., 2024; Meda et al., 2017; Van Der Vliet & Janssen-heininger, 2013). In the literature, the role of H2O2 in regeneration is frequently discussed alongside inflammation and often in conjunction with other active species in ROS. Also, some studies distinguish between wound healing & regeneration, while others do not. In zebrafish (adult), after fin injury caused by exfoliation, H2O2 plays a role in the regeneration of superficial epithelial cells (SEC) (Chen et al., 2016). In SECs, following trauma, H2O2 levels initially rise rapidly, peaking at 12 hours post exfoliation (hpe), before gradually declining and stabilizing by 48 hpe (Chen et al., 2016). In addition, inhibition of H2O2 production and subsequent reduction in H2O2 levels impedes SEC regeneration, while exogenously applied H2O2 promotes SEC regeneration, manifested by an increase in the surface area of SECs (Chen et al., 2016). In Xenopus tadpoles, H2O2 participates in tail regeneration through activating fibroblast growth factor (FGF) and the Wnt/β-catenin pathway (Love et al., 2013). It also inhibits glucose utilization and promotes hydrolysis to activate the expression of specific genes that stimulate tissue growth (Love et al., 2011). Also in Xenopus tail regeneration, H2O2 engages in notochord regeneration through promoting the acetylation of lysine 9 located in histone 3 (H3K9ac), which is a form of epigenetic modification (Suzuki et al., 2016). In gecko tail regeneration (spontaneous), ROS generated by skeletal muscle can regulate skeletal muscle cell autophagy, thereby controlling the regenerative tail’s length (Zhang et al., 2016). In Acomys cahirinus, inhibition of ROS production reduces ROS levels, thereby suppressing regeneration (Simkin et al., 2017). In Hydra, following bi-section, ROS were detected (Vriz et al., 2014). In planarians, after amputation, the generated ROS promote the regeneration of the body, particularly the central nervous system within (Pirotte et al., 2015).

H2O2 is also participated in development in different tissues/organs across various species (reviewed in Berndt & Lillig, 2021; Covarrubias et al., 2008; Rampon et al., 2018; Ufer et al., 2010). In Xenopus mesoderm formation, ROS's engagement is crucial (Han et al., 2018). In zebrafish, the expression of Nox 1 & Nox 5 is high during gastrulation, then returns to baseline levels during morphogenesis (Weaver et al.,

2015). Duox expression increases in the late stage of morphogenesis (Weaver et al., 2015). A graded-distribution of H2O2 level is observed in the embryonic tectum (Gauron et al., 2016). If pan-NOX inhibitors are applied, they disrupt the normal retinotectal projection in the tectum (Gauron et al., 2016). In mice, the expression of superoxide dismutase (SOD), catalase (CAT) & glutathione peroxidase (GPx) increases during the somitogenesis stage (El-hage & Singh, 1990). In zebrafish, peroxiredoxin 1 (PRx1) participates in blood vessel development, as knocking-down PRx1 impairs normal vascular development, resulting in malformations (Huang et al., 2017). In mice, PRx1's involvement in digit development by contributing to inter-digital apoptosis is indicated by proteomic analysis (Shan et al., 2005). In zebrafish, glutaredoxin 2 (GRx2) contributes to embryonic vascular development by playing a role in the de-glutathionylation of Sirtuin-1 (SIRT1, an NAD+-dependent deacetylase) (Bräutigam et al., 2013). Also in zebrafish, GRx3 engages in the formation of red blood cell (RBC), as GRx3 knock-down using morpholino results in reduced erythrocyte counts (Haunhorst et al., 2013). In chicks, thioredoxin 2 (TRx2) knock-down resulted in death of post-mitotic neurons (Pirson et al., 2015). In zebrafish, TRx2 knockdown impairs normal liver development by increasing apoptosis (Zhang et al., 2014).

Reactive oxygen species

Reactive oxygen species (ROS) include a lot of molecules. ROS is a collective term that refers to molecules that are derived from O2. It can be O2-centered radicals, such as the superoxide radical anion (O2•−), the hydroxyl radical (OH•). It can be non-radical derivatives of O2, such as hydrogen peroxide (H2O2), singlet oxygen. It can be charged and uncharged.

ROS can be generated either through electron transfer or by energy transfer reactions (Jacob & Winyard, 2009). Electron transfer refers to the reduction of O2, and energy transfer reactions refer to reactions that are influenced by light in the presence of photosensitizers (Jacob & Winyard, 2009). O2 reduction reactions can reduce either 1-electron, 2-electron or 3-electron from O2, thereby producing the 1-electron reduced forms of O2 (O2•−), 2-electron reduced forms of O2 (H2O2), and 3-electron reduced forms of O2 (OH•) (Figure 1-22) (Jacob & Winyard, 2009). In the human body, O2•−, H2O2 & OH• are commonly formed (Jacob & Winyard, 2009). The O2•− , which is produced from mono-valent reduction of O2 (Figure 1-23), can be considered a parent molecule for a number of other ROS molecules (Figure 1-24) (Jacob & Winyard, 2009).

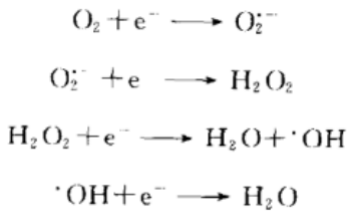

Figure 1-22

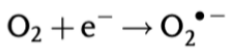

Figure 1-23

O2•−'s production and decomposition in vivo

O2•− can be produced in vitro, as well as in vivo. It can be produced at different locations in the cell, either on the cell membrane or in the organelles. It can be produced enzymatically or non-enzymatically. In vivo, O2•− can be formed in a number of ways. The 2 major types of O2•− production are: (1) produced on the cell membrane by the enzyme called NADPH oxidase (Nox). (2) produced in the mitochondria by the electron transport chain (ETC) (Figure 1-25) (Jacob & Winyard, 2009). In mammals, mitochondrial ETC O2•− production happens when electron leakage happens directly onto O2. This electron leak can happen at 2 places in the ETC: (1) at complex I, where O2•− is produced mainly in the mitochondrial matrix; (2) at

complex III, where O2•− is generated in the mitochondrial matrix and the intermembrane space (Raha & Robinson, 2000; St-Pierre et al., 2002). A number of factors can influence ETC O2•− production. Therefore, O2•− production rate varies among tissues, between organisms, and depending on the conditions (Green et al., 2004; Korshunov et al., 1997; Nicholls, 2003).

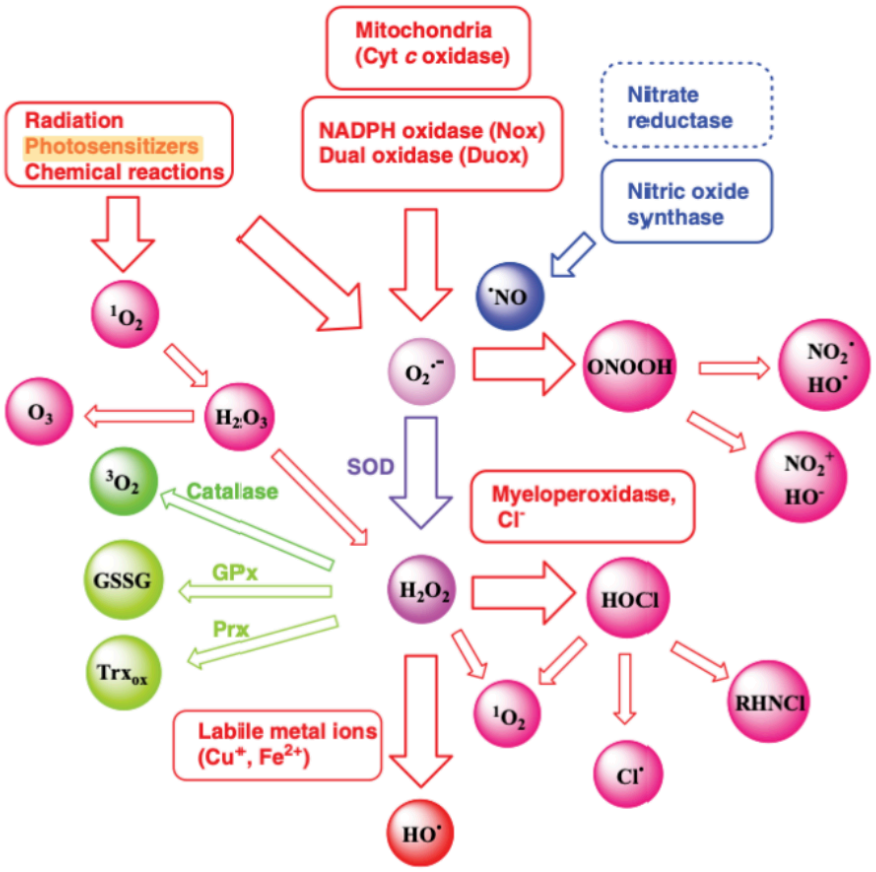

Figure 1-24. A diagram illustrates the chemical transformations between ROS, reactive nitrogen species (RNS) & reactive chlorine species (RCS), along with the enzymes or other catalytic molecules required for these conversions. Blue denotes signalling molecules, pink indicates harmful reactive species, and green represents harmless reactive species. Gradient colors signify harmful reactive species that also function as signalling molecules (e.g., H2O2 & O2•−). Please note that this diagram is incomplete, depicting only a small subset of reactive species involved in redox signal transduction. Adapted from (Jacob & Winyard, 2009).

As for the other numerous ways of O2•− production in vivo, in most circumstances, the O2•− amount generated by these reactions is much less than the O2•− generated by Nox and ETC, due to the fact that these reactions' kinetics are slow (Jacob & Winyard, 2009). As for the enzymatic production of O2•−, there are a number of enzymes that produce O2•− as a by-product of the normal reaction (Jacob & Winyard, 2009). Some examples of these enzymes include peroxidases, xanthine oxidase, cellobiose oxidase, nitric oxide synthase, galactose oxidase, aldehyde oxidase, initropropane dioxygenase, tryptophan dioxygenase and ndoleamine 2,3-dioxygenase (De Groot & Littauer, 1989). As for the non-enzymatic production of O2•−, there are a range of molecules that generate O2•− through auto-oxidizing O2 (Halliwell & Gutteridge, 1999). Some examples of these enzymes include FMNH2, FADH2, glyceraldehyde, certain neurotransmitters and certain hormones (Halliwell & Gutteridge, 1999).

O2•− generated by the fore-mentioned enzymatical or non-enzymatical ways is then dismutated to produce H2O2 (Figure 1-26) (Jacob & Winyard, 2009). The disproportionation of O2•− to H2O2 can occur either non-

enzymatically or enzymatically. It can happen spontaneously or in the presence of superoxide dismutases (SOD), which is copper and zinc- or manganese-dependent (Jacob & Winyard, 2009).

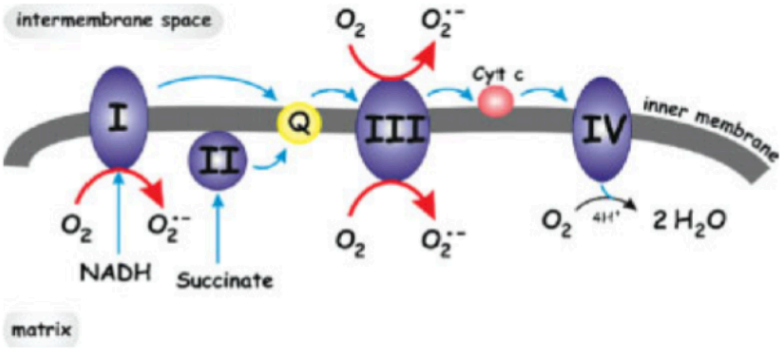

Figure 1-25. Generation of O2•− by the electron transport chain in the mitochondria. The red arrows indicate the generation of O2•−. It can be seen that O2•− is produced by Complex I & Complex III from molecular oxygen by electron leaking. I, II, III & IV stands for complex I, complex II, complex III & complex IV. Q is ubiquinone; Cyt c means cytochrome c. Adapted from (Jacob & Winyard, 2009).

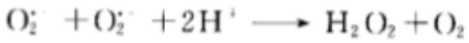

Figure 1-26

H2O2's production and decomposition in vivo

O2•− can be produced in vitro, as well as in vivo. Most H2O2 in vivo is produced through the disproportionation of O2•− which is mainly generated by either Nox enzymes or ETCs (Jacob & Winyard, 2009). The enzyme Noxes, which produces H2O2 in an indirect way, can be regulated by a number of molecules, such as growth factors and cytokines, in a highly site-specific way (Bedard & Krause, 2007). H2O2 can also be produced directly in vivo. H2O2 can be generated directly by a range of enzymes, such as monoamine oxidases A and monoamine oxidases B (Hauptmann et al., 1996; Panfili et al., 1991). H2O2 generated intra-cellularly and extra-cellularly can both function as a redox signaling molecule. For example, H2O2 generated by phagocytes can diffuse into neighboring cells and contribute to signaling (Veal et al., 2007).

Like most ROS molecules, a high concentration of H2O2 is toxic to cells. Therefore, its concentration is strictly regulated in the body. A range of anti-oxidant molecules are present in vivo to remove excess H2O2 and thereby prevent cell tissue damage from H2O2 (Jacob & Winyard, 2009). These molecules thus also limit H2O2 availability in cell signaling (Jacob & Winyard, 2009). Many of these anti-oxidant molecules may also be involved in signal transduction pathways so that the signals transmitted are regulated and controlled (Jacob & Winyard, 2009). The 3 major anti-oxidant proteins are catalases, peroxiredoxins and glutathione peroxidases (Jacob & Winyard, 2009).

H2O2's chemical properties

H2O2 has a long half-life, so it diffuses over long distances in the body (Halliwell & Gutteridge, 2015). H2O2 can be easily mixed with H2O and can diffuse within cells and travel from cell to cell in vivo (Halliwell & Gutteridge, 2015). The diffusion rate is relatively rapid and is influenced by the lipid composition of the cell membrane (Halliwell & Gutteridge, 2015).

H2O2 is a strong oxidizing agent and a mild reducing agent (Halliwell & Gutteridge, 2015). H2O2 is not very reactive with most molecules in the body. When incubating proteins, DNA or lipids with H2O2 at mM levels, no oxidation occurs (Halliwell & Gutteridge, 2015). Even though H2O2 reactivity is not strong, high levels of H2O2 can be cytotoxic to cells and tissues in vivo (Halliwell & Gutteridge, 2015). The H2O2 solution is widely used as a disinfectant in vitro.

H2O2 concentration within cells

The H2O2 concentration within a cell equals its net increase minus its net loss (Jacob & Winyard, 2009). The net increase equals the H2O2 produced within the cell plus the H2O2 influxed from the local environment that is produced by the other cell (Jacob & Winyard, 2009). The net loss equals the H2O2 removed from the cell by the anti-pxident system plus the H2O2 efflux into the local environment (Jacob & Winyard, 2009). Even though H2O2 is a small molecule whose chemical properties are relatively stable and therefore can diffuse relatively freely, biomembranes still limit H2O2 diffusion to some extent (Jacob & Winyard, 2009). Thus, a diffusion gradient exists between the membrane-bound compartments (Antunes & Cadenas, 2000; Seaver & Imlay, 2001). This diffusion rate varies by cell type (Jacob & Winyard, 2009).

H2O2's biological functions

There are 2 major functions of H2O2 in vivo: as a signaling molecule and as a disinfectant. Phagocytes can produce large amounts of H2O2 and release them into the extracellular space (Jacob & Winyard, 2009). These H2O2 molecules are then diffused, reach other neighboring cells, and act on them as part of the immune response to defend the host (Jacob & Winyard, 2009). A small amount of H2O2 produced by cells can function as a secondary messenger in the cell signal transduction pathway (Dröge, 2002; Reth, 2002).

H2O2 functions as a redox signaling molecule mainly through specifically and reversibly modifying the amino acid residues in the target proteins (Jacob & Winyard, 2009). Cysteine residue is the amino acid in the protein that is the main target of H2O2 (Jacob & Winyard, 2009). H2O2 can act on other residues as well (Jacob & Winyard, 2009). This modification can be thiol rotein modifications or non-thiol protein modifications (Jacob & Winyard, 2009). H2O2 can interact either directly or indirectly with protein residues (Jacob & Winyard, 2009). The indirect interaction will require the involvement of other redox couples, such as glutathione couples and thioredoxin couples (Jacob & Winyard, 2009).

As for the upper limit of H2O2 levels in the cells under normal physiological conditions, there is some controversy within the literature. The concentration ranges from 1 μM (reviewed by Stone, 2004) to 15 μM (reviewed by Kregel & Zhang, 2006). It is documented that H2O2 at 1-10 μM is able to promote proliferation in human cells (Saccani et al., 2000). It is also documented that H2O2 levels in plasma at 35 μM can act on cells located in the vasculature (Halliwell et al., 2000). It is also reported that the activated neutrophils are able to produce 1-12 μM H2O2 and release it into the medium (Suematsu et al., 1993; Thomas et al., 1985). It is also reported that the stimulated macrophages can generate 6×10^-14 mol H2O2 h^-1 per cell and release them into extracellular space, and therefore make the H2O2 concentration in the local extracellular space reach 10-100 μM (reviewed by Dröge, 2002).

H2O2 in diseases

High levels of H2O2 have been detected in many diseases, such as cancer (López-Lázaro, 2006), hypertension (1-7 μM in plasma) (Lacy et al., 2000), Alzheimer's disease (Behl, 1994), endstage renal

disease (5-13 μM) (Aslan, 2006), brain ischemia-reperfusion injury (160 μM) (Hyslop et al., 1995). Cancer cells can generate 0.5 nmol H2O2 per 10^4 cells h^-1 (Szatrowski & Nathan, 1991). Increased H2O2 concentrations have also been observed in clinical procedures. For example, during hyperoxic cardiac bypass practice, H2O2 levels in the plasma can be increased by more than 100 times, caused by the inflammatory response in patients (Cavarocchi et al., 1986).

1.5 SFK

SFK & biological processes related to zebrafish (larva) tail regeneration: a super-mini review

In this review, I shall outline how SFK participates in biological processes related to tail regeneration in zebrafish (larva). Given that zebrafish tail regeneration requires the regeneration of muscle, nerve, bone, blood vessels, notochord/spinal cord, skin, connective tissue & pigment cells, and that regeneration sometimes resembles development to some extent, I looked for the following biological processes: (epimorphic) regeneration/morphogenesis of muscle/nerve/bone/blood vessels/notochord/skin, wound healing & inflammation. Unlike Ca2+/H2O2, relatively less literature has been found for SFK. Nevertheless, given my limited space, I will only select a few (i.e., inflammation, nervous system's regeneration and development, skeletal system's development & activation of mast cells and B lymphocytes). Therefore, this review is incomplete, as SFK is also involved in other biological processes related to zebrafish tail regeneration.

What will be written and what won't be mentioned is the same as the 'Ca2+' section.

SFK is involved in inflammation (reviewed in Karin & Clevers, 2016; Pesic & Greten, 2016). It links inflammation with regeneration. In the intestinal mucosa's epithelial regeneration, macrophages and dendritic cells release IL-6, which activates gp130, which then activates SFK, which subsequently activates YAP, and finally YAP activates TEAD (a transcription factor), which promotes cell division and diminishes cell death (Taniguchi et al., 2015).

SFK also participates in the nervous system's regeneration & development through playing a role in axon projection/turning, which is crucial for neural circuits (reviewed in Li et al., 2020; Nicoletti et al., 2022; Paudel et al., 2018; Ye et al., 2019). It fulfills this role through engagement in the regulation of growth cone motility, in which skeletons such as actin filaments and microtubules are also involved (Ye et al., 2019). Other molecules, including DRL (Wouda et al., 2008), Sonic Hedgehog (Shh) (Yam et al., 2009), B-type ephrin (Palmer et al., 2002), UNC5c (a type of netrin receptor) (Poliak et al., 2015), TrkB (Huang & McNamara, 2010), EGFR (Wu et al., 2002) & MMP (Hwang et al., 2007) et a are also involved in the nervous system's regeneration & development and directly interact with SFK. In addition, SFK inhibitors (e.g., PP2) can be used for the treatment of spinal cord injury (reviewed in Miranda et al., 2015).

SFK also plays a role in the skeletal system's development through its association with bone formation and bone matrix homeostasis (reviewed in Kegelman et al., 2020). Other molecules, such as platelet-derived growth factor (PDGF) (Smoot et al., 2017), Yes-associated protein (YAP) (a transcriptional regulator) (Elbediwy et al., 2018; Li et al., 2016; Smoot et al., 2017), paxillin (Martino et al., 2018) & merlin (Sabra et al., 2017) are also participatory in the skeletal system's development and directly act with SFK. However, it has also been reported that SFK has a negative effect on the skeletal system's development. Osteoblast differentiation and the subsequent bone formation are observed to be promoted by lowered expression of c-Src (Marzia et al., 2000).

Also, SFK is assisting mast cell activation (reviewed in Fernández-Guarino & Bacci, 2024). Mast cells are closely associated with inflammation, local immune response, and wound healing. Other molecules comprising PKB, PKC & PI3K directly interplay with SFK and contribute to the degranulation and cytokine production of mast cells (Fernández-Guarino & Bacci, 2024).

In addition, SFK contributes to B lymphocyte development, maturation, activation, proliferation, apoptosis & tolerance (reviewed in Gauld & Cambier, 2004). B lymphocytes, like mast cells, are crucial for inflammation, local immune response, and wound healing. SFK can exert both active and inhibitory effects on B lymphocytes. SFK has several family members, of which the functions may be redundant or unique (Gauld & Cambier, 2004). The contradictory roles of SFK on B lymphocytes may arise from the varied co-expression of different sub-types (Gauld & Cambier, 2004). B cells receive signals primarily via the B cell receptor (BCR), which undergoes aggregation upon antigen binding. Consequently, much research has focused on the relationship between SFK and BCR (Saijo et al., 2003). Among all the SFK family members, Lyn is the most typical example capable of exerting both positive and negative effects on B cells. For the positive effect, Lyn can activate either the MAPK or Ca2+ signaling pathways, both of which subsequently stimulate B cells to proliferate (Gauld & Cambier, 2004). For the negative effect, 2 substrates of Lyn: FcγRIIB & CD22, both of which are inhibitory BCR co-receptors (Nishizumi et al., 1998).

General

The Src-family kinases (SFKs) are non-receptor protein tyrosine kinases (PTKs) that are cytoplasmic proteins associated with the plasma membrane (Bolen et al., 1991; Pawson, 1995). Within the family, there are 10 members: c-Src, Blk, Fgr, Frk, Fyn, Hck, Lck, Lyn, YES, and Yrk (Yeatman, 2004). c-Src (cellular) is the prototype member, which was originally identified as v-Src (viral). Oncogenic v-Src is the mutant form of proto-oncogene c-Src. Other members have structures that are very similar to c-Src, and their amino acid sequences share significant homology (Thomas & Brugge, 1997). Generally speaking, SFK's expression is ubiquitous, and SFK is highly conserved throughout evolution (Stehelin et al., 1976; Brown & Cooper, 1996).

Only c-Src, Fyn & YES's expressions are ubiquitous; the rest 7 members' tissue distribution is rather more restricted (Figure 1-27) (Thomas & Brugge, 1997). For example, Hck & Fgr are expressed predominantly in myeloid leukocytes, Lck is expressed predominantly in T-lymphocytes (Lowell & Soriano, 1996). Frk is found mostly in epithelial-derived cells (Cance et al., 1994). Even though c-Src, Fyn & YES can be found in most tissues, in certain cell types, the expression level of c-Src/Fyn/YES can be much higher (Thomas & Brugge, 1997). For example, in osteoclasts, platelets & neurons, c-Src is expressed at a level that is 5-200 fold higher (Brown & Cooper 1996).

For most cell types, one cell can express multiple members of SFKs & multiple isoforms of each individual member (Engen et al., 2008). In addition, within a cell, SFKs can be found in various distinct sub-cellular locations. For example, c-Src can be found in endosome, caveolae & focal adhesions, and Fgr & Frk can be found in nucleus (Kaplan et al., 1992).

Structure

All members of SFKs have the same structural arrangement of domains (Figure 1-28). From N-terminal (plasma membrane end) to C-terminal (cytoplasm end), each SFK has a Src homology 4 (SH4) domain, a unique domain, a SH3 domain, a SH2 domain, a linker, a SH1 domain & a tail (Cohen et al., 1995; Pawson, 1995). Each member is slightly different.

SH4 is a sequence containing 15 amino acids (Engen et al., 2008). It has a myristoylation signal sequence, and for some members of SFK, it also has a site for palmitoylation (Engen et al., 2008). Glycine (Gly) residue

at position 2 is crucial for myristoylation as it is the site for myristic-acid moiety addition (Thomas & Brugge, 1997). Cysteine (Cys) residue is the site for palmitylation (Resh, 1993). Except c-Src & Blk, the rest of the SFK members all have Cys residues (Resh, 1993). However, even though Cys residues are present in Frk, whether Frk can be palmitylated is not determined (Thomas & Brugge, 1997). The myristoylation site & palmitoylation site can promote interaction between SFK & membrane-bound effectors (Aleshin & Finn, 2010) due to the fact that lipid modification like myristoylation & palmitoylation can promote SFK's membrane localization (Resh, 1994).

Src	Ubiquitous; two neuron-specific isoforms
Fyn	Ubiquitous; T cell-specific isoform (FynT)
Yes	Ubiquitous
Yrk[a]	Ubiquitous
Lyn	Brain, B-cells, myeloid cells; two alternatively spliced forms
Hck	Myeloid cells (two different translational starts)
Fgr	Myeloid cells, B-cells
Blk	B-cells
Lck	T-cells, NK cells, brain
Frk subfamily Frk/Rak Iyk/Bsk	Primarily epithelial cells

[a]Only found in chickens.

Figure 1-27. Expression of SKF. Src, Fyn, Yes & Yrk are ubiquitously expressed. Lyn, Hck, Fgr, Blk & Lck are predominantly expressed in hematopoietic cells, with Lyn & Lck also expressed in brain neurons, both with distinct isoforms present. The Frk subfamily (Frk/Rak & Iyk/Bsk) are expressed primarily in epithelial cells. Adapted from (Thomas & Brugge, 1997).

The unique domain, as its name suggests, is different among SFK members. It is the only non-conserved domain (Engen et al., 2008). It is a sequence containing 50-80 amino acids (Engen et al., 2008). The unique domain promotes interaction between SFKs & molecules that are member-specific (Thomas & Brugge, 1997). For example, Lck's unique domain modulates the interaction between Lck & CD4/CD8, which is a T-cell surface molecule (Rudd et al., 1988; Veillette et al., 1988). c-Src & Lck's unique domains have phosphorylation sites for serine & threonine (Boggon & Eck, 2004). In Lck, serine 42 & serine 59 can be phosphorylated by PKC, leading to the change of Lck's catalytic activity & function (Boggon & Eck, 2004).

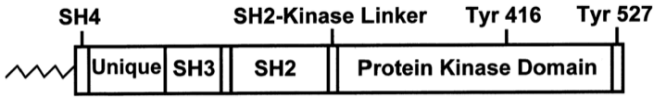

Figure 1-28. SFK structure. From N-terminus to C-terminus, they are SH4 domain (with a myristoyl group), unique domain, SH3 domain, SH2 domain, SH2-Kinase linker, SH1 domain (protein kinase domain) & regulatory segment (tail). This graph is to scale except the myristoyl group. Adapted from (Roskoski, 2004).

SH3 is a sequence containing 60 amino acids (Engen et al., 2008). It modulates interaction between SFKs & other molecules through binding to proline-rich hydrophobic target sequences (Engen et al., 2008). All the ligands of SH3 have this 'P-X-X-P' consensus sequence (Rickles et al., 1995). The 'X' amino acid residues next to the prolines provide affinity & specificity (Rickles et al., 1995). These sequences from SFKs & target molecules normally form a polyproline type II (PPII) helix (Musacchio et al., 1994; Kuriyan & Cowburn, 1997).

The binding between SH3 sequence & ligand sequence can be in either Class I (NH2→COOH) orientation or Class II (COOH→NH2) direction (Yu et al., 1994; Feng et al., 1994). Binding affinity between SH3 sequence & ligand sequence is in the μM (micromolar) range (Thomas & Brugge, 1997). In vivo, this affinity can be strengthened by contacts between the SFK's other domains & target molecule (Thomas & Brugge, 1997). SH3 promotes SFK's conformational changes (Niederhuber et al., 2020), therefore facilitating SFK's substrate recruitment (Weng et al., 1994; Briggs et al., 1995) & kinase activity regulation (Superti-Furga et al., 1993; Murphy et al., 1993; Okada et al., 1993; Briggs et al., 1997). In CNS neurons, c-Src's alternatively spliced forms are expressed (Brugge et al., 1985). In this form, the SH3 domain has a 6/11-amino acid insertion (Brugge et al., 1985). In vitro & in vivo, PI3K & paxillin have been reported to interact with the SH3 domain (Fukui & Hanafusa, 1991).

SH2 normally has an average of 100 amino acid residues in length (Kuriyan & Cowburn, 1997; Waksman, 1993). SH2 has an affinity for and therefore can easily bind to phosphorylated tyrosine residues (Ren et al., 1993); hence, SH2 can promote interaction between SFKs and target proteins that contain phosphotyrosine-peptide sequences (Kuriyan & Cowburn, 1997; Waksman, 1993). Amino acid residues preceding phosphorylated tyrosine residues can affect the binding affinity as well (Bibbins et al., 1993). The SH2 domain's ligand-binding surface is made of 2 'pockets' (Boggon & Eck, 2004). 1 of the 2 pockets binds to the phosphorylated tyrosine; the other pocket binds to the +3 amino acid following the phosphorylated tyrosine (Thomas & Brugge, 1997). For the '+3 amino acid', SFK typically prefers leucine residues (Boggon & Eck, 2004). For the target proteins, this 'pTyr-Glu-Glu-Ile (pYEEI)' peptide motif has a high affinity to bind with SH2 (Engen et al., 2008). The binding between the SH2 domain & the 'pYEEI' is like a 2-holed socket (the SH2 domain) & a 2-pronged plug (the pYEEI peptide motif), with the pTyr residue fitting into the 1st hole while the Ile residue fits into the 2nd hole (Waksman, 1993; Songyang et al., 1993). Within pYEEI, tyrosine's phosphorylation is crucial for the binding, as an unphosphorylated motif can not bind to SH2 (Kuriyan & Cowburn, 1997). SH2 promotes SFK's conformational change (Niederhuber et al., 2020) and is crucial for SFK's kinase activity's down-regulation & SFK's localization. In Frk, its SH2 domain has a nuclear-localization sequence that is responsible for Frk's localization to the nucleus (Cance et al., 1994; Thuveson et al., 1995). In vivo, focal adhesion kinase (Fak) & phosphoinositide 3 kinase (PI3K) have been shown to bind to SH2 (Fukui & Hanafusa, 1991).

The linker connects between the SH2 domain & SH1 domain.

SH1 is the catalytic domain with kinase activity. It contains 2 lobes: a smaller N-terminal one & a larger C-terminal one (Engen et al., 2008). The Tyr-416 (tyrosine), which is an auto-phosphorylation site, in the activation loop (A-loop) is located in the larger C-terminal lobe (Engen et al., 2008).

The tail has a phosphorylation site at Tyr-527 (tyrosine) (Engen et al., 2008).

For all the above-mentioned amino acid residues, their numbering is based on human c-Src's crystal structure.

Auto-inhibition state & activated state

Typically, when unstimulated by upstream signals, SFKs are in an auto-inhibited inactive state. This negatively-regulated conformation is characterized by 4 features: (1) the SH3 domain binds to the linker and

acts on the SH1 domain; (2) the SH2 domain binds to the tail and acts on the SH1 domain; (3) in the tail, Tyr-527 is phosphorylated; (4) in the SH1 domain, Tyr-416 is un-phosphorylated.

When in the inactive state, for the SH3 domain & linker, a PPII helix (left-handed) is formed through this intra-molecular interaction between them (Engen et al., 2008).

When in the inactive state, for the SH2 domain & tail, the phosphorylation of Tyr-527 in the tail promotes the intra-molecular interaction between SH2 & SH1, therefore making the SFKs stay in an inactive conformational structure (Engen et al., 2008). The Tyr-527's phosphorylation is typically carried out by C-terminal Src kinase (Csk) (Nada et al., 1991) & Csk-homologous kinase (Chk) (Chong et al., 2005). Csk has been suspected to be able to regulate all the members of SFKs (Nada et al., 1993; Imamoto & Soriano, 1993). However, there are exceptions. Within some SFK, Tyr-527 is not phosphorylated, but they can stay in the inactive state. For example, in B cells, in Lyn's tail, Tyr-527's phosphorylation is not detectable, but Lyn's catalytic activity is not increased, either (Thomas & Brugge, 1997).

When in the inactive state, for the SH1 domain, there is an αC-helix structure in the N-lobe (Figure 1-29) (Engen et al., 2008); therefore, SH1 is in a conformational structure that is incompatible for substrate-binding & ATP-binding, leading to the inactivity of catalytic activity (Huse & Kuriyan, 2002).

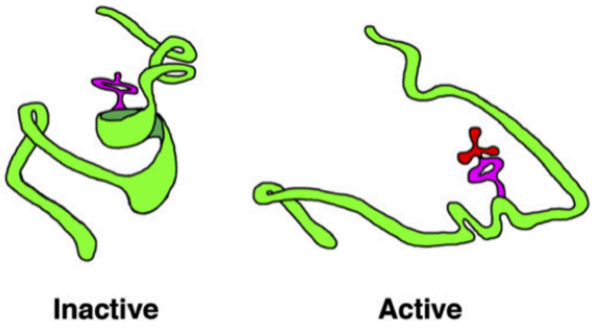

Figure 1-29. A-loop structure comparison between the inactive SFK and active SFK. In inactive SFK's configuration, one α-helix is formed by the A-loop, leading to the blockage of the substrate binding site. In active SFK's structure, the α-helix is not formed due to the phosphorylation status of the A-loop, leading to the opening of the substrate binding site. Adapted from (Ingley, 2008).

When stimulated, SFKs are in an activated state. This up-regulated conformation is characterized by 4 features: (1) The SH3 domain does not bind to the linker and does not act on the SH1 domain; (2) The SH2 domain does not bind to the tail and does not act on the SH1 domain; (3) In the tail, Tyr-527 is un-phosphorylated; (4) In the SH1 domain, Tyr-416 is phosphorylated.

When in the activated state, in the tail, the Tyr-527's dephosphorylation is typically carried out by protein tyrosine phosphatase (PTP) or SH-containing phosphatase (SHP) (Yeatman, 2004; Sen & Johnson, 2011).

When in the activated state, for the SH1 domain, there is no αC-helix structure; therefore, the A-loop is in a conformational structure that is compatible for substrate-binding & ATP-binding (Engen et al., 2008).

Activation & molecule-binding in signaling

By comparing the structures of the auto-inhibited inactive state & activated state (Figure 1-30), it is clear that to activate an SFK, 4 changes are required: (1) The binding of the SH3 domain & the linker must be disrupted; (2) the binding of the SH2 domain & the tail must be disrupted; (3) Tyr-527 in the tail must be de-phosphorylated; (4) Tyr-416 in the SH1 domain must be phosphorylated. (1) & (2) can be achieved by SH3/ SH2 binding to target molecules with a higher affinity. (3) & (4) can be achieved by kinase or phosphatase. For 1 member of SFKs, its activation does not need to fulfill all 4 conditions, due to the fact that 1 individual SFK might be more sensitive to 1 of the 4 requirements (Thomas & Brugge, 1997)., so there are many permutations & combinations.

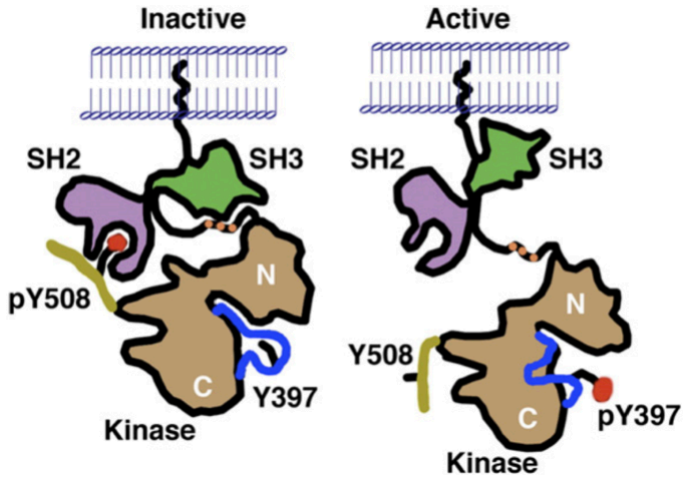

Figure 1-30. Structure comparison between the inactive SFK and active SFK. In inactive SFK's configuration, SH2 binds to the C-terminal region, wherein the tyrosine residue at the C-terminus is phosphorylated (pY508). SH3 interacts with the SH2-kinase linker, forming a PPII helix. Also, the tyrosine residue within the A-loop remains unphosphorylated (Y397), thereby blocking the substrate binding site. In active SFK's structure, SH2 no longer interacts with the C-terminal, wherein the tyrosine is dephosphorylated (Y508). SH3 no longer binds to the SH2-kinase linker. The tyrosine within the A-loop is phosphorylated (pY397), thereby opening the substrate binding site and forming a catalytic cleft comprised of N-lobe & C-lobe. Adapted from (Ingley, 2008).

There are things that could make the activation more complex. SFK activation's temporal aspect could affect SFK activation's biological responses. For example, transient activation or sustained activation of c-Src could lead to different cellular responses following SFK's activation by receptor (Thomas & Brugge, 1997). In PC12 cells, transient SFK activation by MAPK leads to a cell proliferative response, while sustained SFK activation by MAPK leads to a cellular differentiation response (Marshall, 1995).

Molecules related to SFK's activation: (1) Up-stream receptors, e.g., platelet-derived growth factor receptor (PDGFR) (Thomas & Brugge, 1997), signaling lymphocyte activation molecule (SLAM) family receptor (Boggon & Eck, 2004), etc; (2) Down-stream substrates, e.g., PLC (Thomas & Brugge, 1997), PI3K (Ingley, 2008), Fak (Thomas & Brugge, 1997), mitogen-activated protein kinase (MAPK) (Thomas & Brugge, 1997), etc; (3) Kinase/Phosphatase, e.g., Csk, Chk, Ptp, Shp, etc; (4) Adaptor proteins, e.g., Csk-binding protein

(Cbp) (Ingley, 2008), Lck-interacting membrane protein (LIME) (Ingley, 2008), linker for activation of T cells (LAT) (Ingley, 2008), non-T-cell activation linker (NTAL) (Ingley, 2008), SLAM-associated protein (SAP) (Boggon & Eck, 2004), Shc (Thomas & Brugge, 1997), paxillin (Thomas & Brugge, 1997), etc. The above 4 types of molecules can either transiently or sustainedly interact with each other.

Degradation

SFKs that are highly active are marked for degradation, which involves ubiquitination and is mediated by proteasome (Ingley, 2008).

Function

SFKs have been reported to be involved in many cellular activities (e.g., proliferation, differentiation, adhesion, motility and apoptosis) & many physiological processes (e.g., angiogenesis and immunity) (Niederhuber et al., 2020). SFK's misfunction has been reported to be involved in many pathological processes, including cancer (several types) (Ishizawar & Parsons, 2004), neuro-degenerative disease (Chin et al., 2005), HIV/AIDS (Hanna et al., 2001) & epilepsy (Kojima et al., 1998).

1.6 Background

During zebrafish larva tail regeneration, morphological changes were observed

It has been reported by previous members in the Roehl lab that during zebrafish larva tail regeneration, several amputation-induced morphological changes were observed (Romero et al., 2018). Time-lapse videos were taken (Romero et al., 2018). Wild-type fish were used (Romero et al., 2018). The tail was amputated between the pigment gap (Romero et al., 2018). In their experiments, they found out that several morphological features changed during regeneration (Movie 1-1): (1) The formation of notochord bead; (2) Trunk contraction; (3) Change of cell membrane curvature (Romero et al., 2018). Within a few minutes after tail amputation, notochord cells moved out to give rise to the notochord bead (Romero et al., 2018). Trunk contracted along the anterior-posterior axis (Romero et al., 2018). The cell membrane was initially facing towards the anterior (the head) and then changed to face towards the posterior (the tail) (Romero et al., 2018).

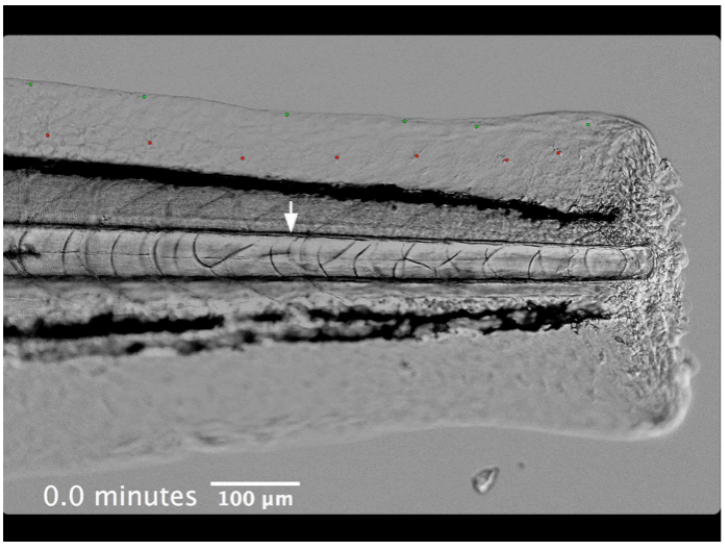

Movie 1-1. Tail regeneration of zebrafish larva after cutting between the pigment gap. 3 major morphological changes observed: notochord bead formation, trunk contraction & cell membrane curvature. Adapted from (Romero et al., 2018).

The notochord bead establishes a Hedgehog signaling center, which is required for the regeneration process to take place (Romero et al., 2018). How is it formed? Trunk contraction might be associated with increased pressure in the notochord. Cell membrane curvature change might be associated with increased pressure in the notochord as well. The muscles in the trunk contract, and the skin moves to cover the injury site, leading to the shortening of the body axis & building-up of pressure in the notochord, contributing to the notochord cell expulsion & notochord bead formation.

During zebrafish larva tail regeneration, Ca2+ was observed

It has been reported by a previous member in the Roehl lab that during zebrafish larva tail regeneration, amputation-induced Ca2+ was observed (Cheung, 2019). Time-lapse videos were taken (Cheung, 2019). Trans-genic fish, Tg(β-actin:Gal4;uas-GCaMP7a), was used to visualize Ca2+ (Cheung, 2019). The tail was amputated between the pigment gap (Cheung, 2019). In her experiments, she found out that from 3 mpa to 60 mpa, Ca2+ level continually increases & accumulates deeper in the amputated tail (Movie 1-2) (Cheung, 2019).

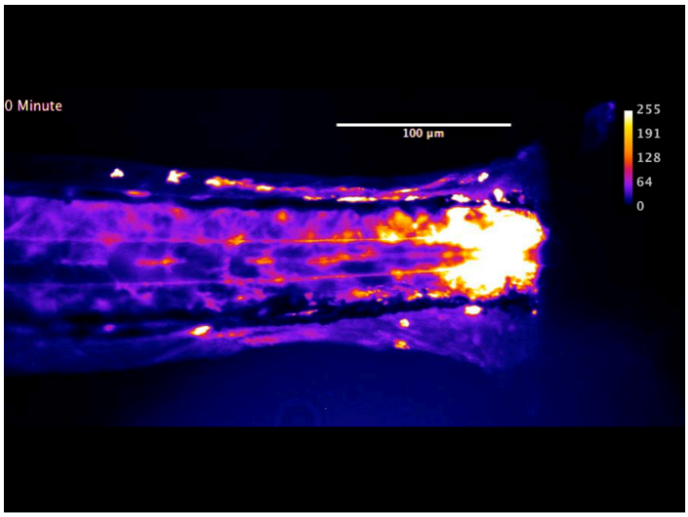

Movie 1-2. Ca2+ visualisation during tail regeneration of zebrafish larva after cutting between the pigment gap. Following tail amputation, from 3 mpa to 60 mpa, the Ca2+ fluorescence intensity gradually increased, spreading from the wound site to encompass nearly the entire body trunk. Video starts at 3 mpa. Scale bar = 100 µm. Adapted from (Cheung, 2019).

During zebrafish larva tail regeneration, H2O2 was observed

It has been reported by a previous member in the Roehl lab that during zebrafish larva tail regeneration, amputation-induced H2O2 was observed (Cheung, 2019). Time-lapse videos were taken (Cheung, 2019). Wild-type fish were used (Cheung, 2019). Fluorescent dye, PFBS-F, was used to visualize H2O2 (Cheung, 2019). The tail was amputated between the pigment gap (Cheung, 2019). From 30 mpa to 180 mpa, the mean PFBS-F fluorescence level was quantified at 30-minute intervals (Cheung, 2019). In her experiments, she found out that H2O2 level continually increases in the wound margin from 10 mpa to 30 mpa and peaks at 30 mpa, then gradually decreases (Movie 1-3) (Figure 1-31) (Cheung, 2019). A 69.22% reduction was observed at 180 mpa compared to 30 mpa (Cheung, 2019).

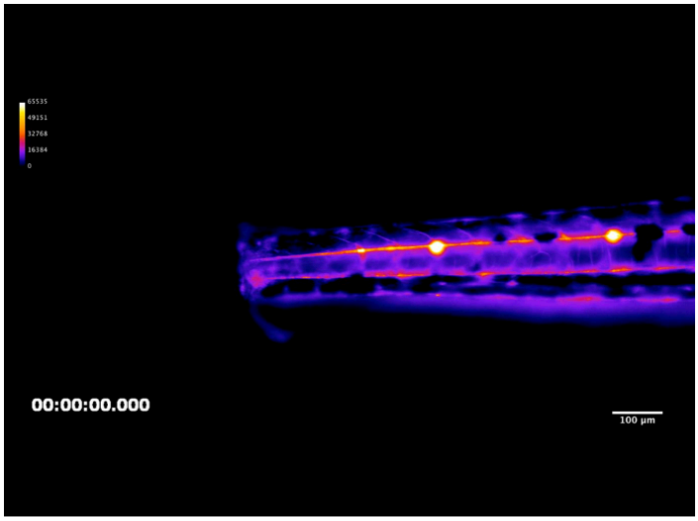

Movie 1-3. H2O2 visualisation during tail regeneration of zebrafish larva after cutting between the pigment gap. After tail excision, from 10 mpa to 30 mpa, H2O2 fluorescence intensity gradually increased, with the signal concentrated near the injury site. The intensity peaked at 30 mpa, then start to decreased. Video starts at 3 mpa. Scale bar = 100 µm. Adapted from (Cheung, 2019).

During zebrafish larva tail regeneration, SFK was observed

It has been reported by a previous member in the Roehl lab that during zebrafish larva tail regeneration, amputation-induced SFK was observed (McCathie, 2018). Wild-type fish were used (McCathie, 2018). Confocal microscopy & immunohistochemistry (IHC) were used for visualization (McCathie, 2018). An anti-phospho-Src (p-Src) antibody that binds to phosphorylated SFKs (activated) was used to visualize p-SFK (McCathie, 2018). An anti-keratan sulphate (KS) antibody was used to visualize notochord cells (McCathie, 2018). The tail was amputated between the pigment gap (McCathie, 2018). In his experiments, he found out that at 1 hpa, p-SFKs seem to be restricted to the wound margin & located in the epithelial cells (Figure 1-32) (McCathie, 2018). No co-localization between p-SFKs & notochord cells was detected (McCathie, 2018). He suspected that notochord cells do not activate SFKs during the tail regeneration (McCathie, 2018).

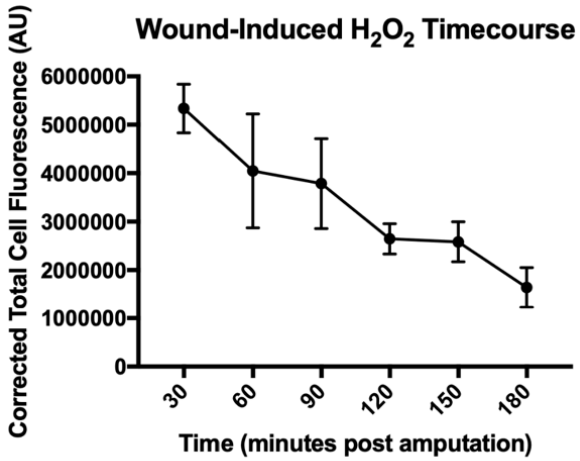

Figure 1-31. H2O2 quantification during tail regeneration of zebrafish larva after cutting between the pigment gap. From 30 mpa to 180 mpa, the H2O2 fluorescence intensity was measured every 30 minutes. The intensity at 180 mpa is 69.22% lower than that at 30 mpa. Adapted from (Cheung, 2019).

Aim of my project: identifying signaling molecules/pathways involved in notochord bead formation in zebrafish (larva) tail regeneration

Among all the aforementioned mechanisms, it is the epimorphic regeneration that caught my attention. Epimorphosis symbolizes a remarkable regenerative process in vertebrates. In some literature, it is portrayed as a nearly ‘perfect’ regeneration, the strongest regeneration. As a result, such regeneration appears as if the damage had never happened. Regeneration inside the human body is considered ‘imperfect’ because regeneration inside the human body is always accompanied by the formation of scars. Even though the scar offers a rapid solution to damage by stabilizing the injured area, it also indicates the presence of substantial inflammation, fibrosis of local tissue, and the permanent partial loss of function.

In order to regrow its amputated tail, the zebrafish has to coordinate the reconstruction of bone, nerves, muscles, blood vessels, skin, notochord/spinal chord, connective tissue & pigment cells, etc. At present, exactly how this epimorphosis regeneration works is unknown. My study will focus on the first stage of the epimorphic regeneration of zebrafish tails. Due to limited time and energy, I will focus on identifying the signaling molecules/pathways involved in notochord bead formation.

To achieve this objective, I conducted chemical screening (Figure 1-33). 4 types of experiments were performed: (1) notochord bead extrusion assay; (2) Ca2+ level assay; (3) H2O2 level assay; (4) pSFK level assay. These were all quite straight-forward and highly repetitive, lacking any sophisticated or subtle design. In essence, these 4 chemical screening experiments' general idea is to use chemicals (primarily inhibitors/ chelators of selected target signaling molecules for negative regulation) to intervene in the tail regeneration in zebrafish (larva), subsequently observing the effects of this chemical intervention on notochord bead extrusion Ca2+ level, H2O2 level & pSFK level. Should a chemical consistently demonstrate statistical significance across multiple replicate experiments (detailed criteria for significance are outlined in the 'Results' section), the selected target signaling molecule is considered a potential signaling molecule involved in zebrafish (larva) tail regeneration.

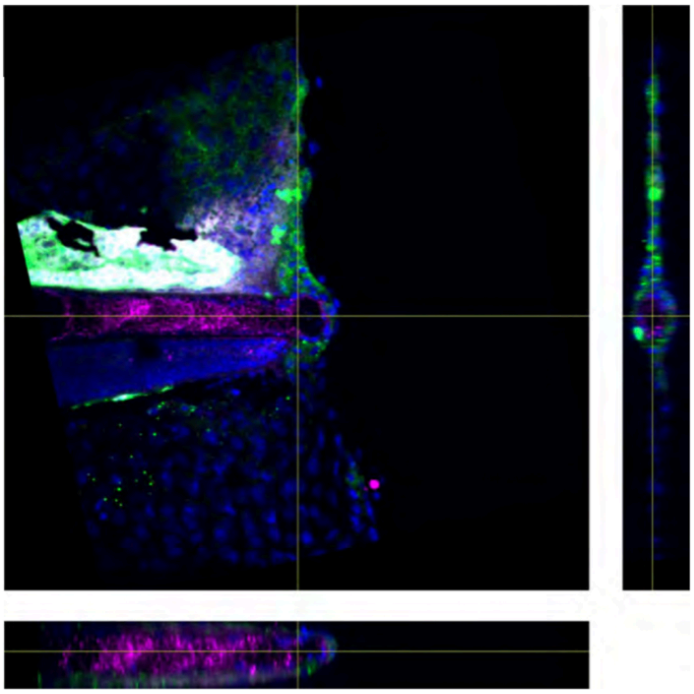

Figure 1-32. SFK visualisation during tail regeneration of zebrafish larva after cutting between the pigment gap. This is a representative photograph taken at 1 hpa. SFK do not overlap with keratan sulphate, but is located mainly in the epithelial cells along the margin. Green: p-SFK; Purple: keratan sulphate (marker for notochord); Blue: DAPI. Adapted from (McCathie, 2018).

The implementation of chemical interventions is straight-forward, simply achieved by adding them to the fish culture medium. For each chemical, the concentration used was determined through a series of preliminary testing experiments in the context of the notochord bead extrusion assay, with this concentration subsequently applied in the Ca2+ level assay, H2O2 level assay & pSFK level assay. Also, for each chemical, the duration/timing of application differed across the 4 types of experiments. The specific duration/ timing is determined by the experimental experience of former Roehl laboratory members and the nature of the experiments themselves. Visualization and quantification of notochord bead extrusion was achieved by measuring the area of notochord bead in photographs taken at a specific time point (6 hpa). In addition, visualization and quantification of Ca2+ level, H2O2 level & pSFK level were done by measuring the fluorescence intensity within a specific defined region (a large area of the body trunk including the wound margin for Ca2+ level assay; the wound margin area for H2O2 level assay and pSFK level assay) within photographs taken at a particular time point (1 hpa for Ca2+ level assay and pSFK level assay; 0.5 hpa for

H2O2 level assay). For the creation of fluorescence, the Ca2+ level assay utilized transgenic fish (GCaMP7a), the H2O2 level assay employed a fluorescent dye (PFBS-F), and the pSFK level assay used antibodies for fluorescent immuno-staining. Details are provided in the ‘Materials & Methods’ section and the ‘Results’ section.

This project is rudimentary and has a lot of limitations. Many necessary and feasible experiments for controlling variables and further validations have not been implemented in the current study, though these may be addressed in future (see ‘Discussion’ section).

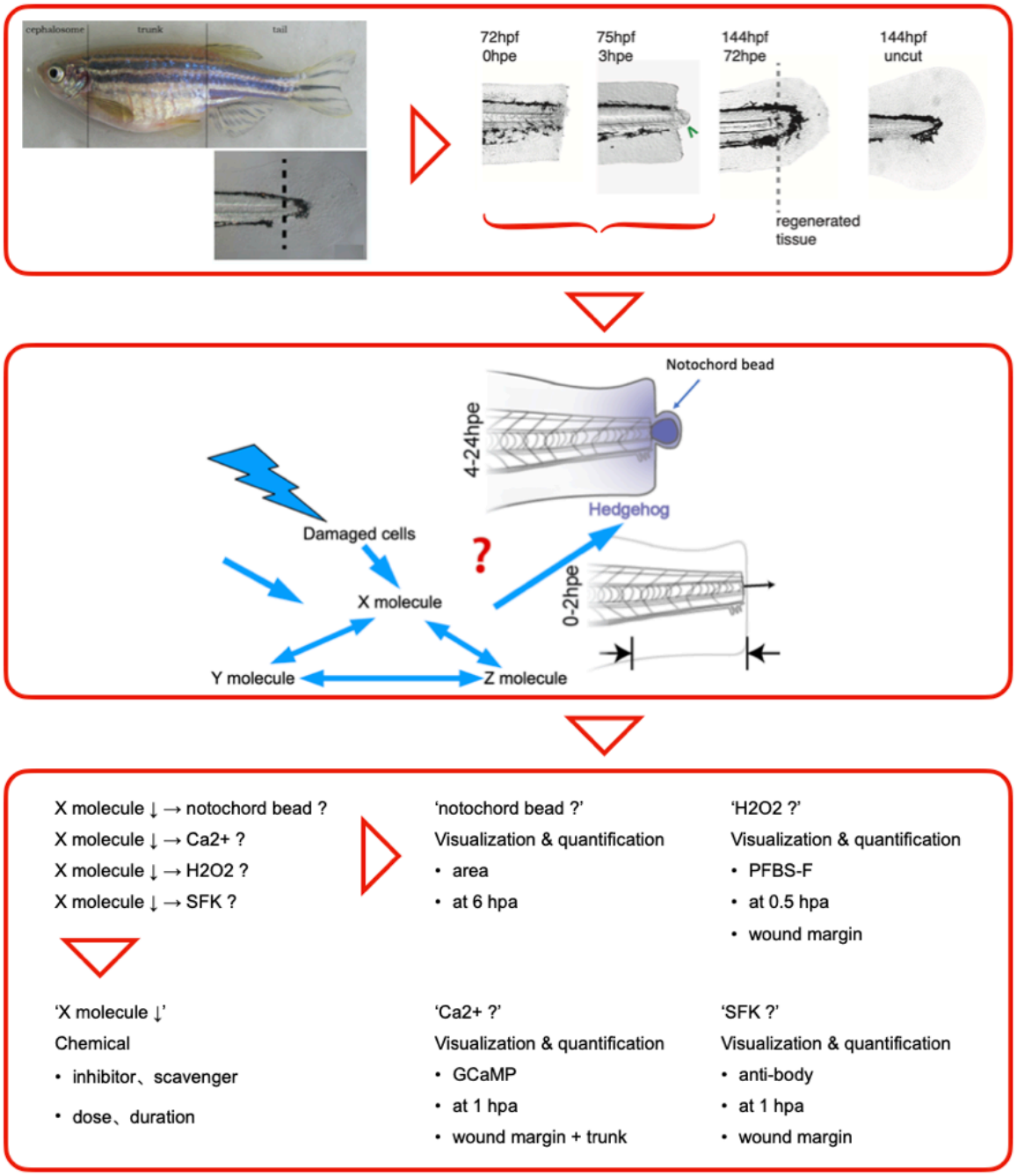

Figure 1-33. This diagram succinctly outlines the objectives, conceptual framework & technical implementation of my project. It employs an informal approach, incorporating bullet points, arrows, etc. Please see the main text for details. Epimorphic regeneration captivated me as a near-perfect form of biological regeneration. Zebrafish tail regeneration exemplifies this process. I sought to identify signalling molecules involved in notochord bead formation, which takes place in the early stage of zebrafish (larval) tail regeneration through chemical screening. 4 experimental approaches were employed: notochord bead extrusion assay, Ca2+ level assay, H2O2 level assay & pSFK level assay. The general idea is to negatively regulate tail regeneration using chemicals, then observe the effects on notochord bead extrusion, Ca2+ levels, H2O2 levels & SFK activity. Please note that the upper left image in the 1st red box depicts an adult fish's body segmentation, whereas my experiment utilized larval fish. In the 1st red box, the upper left picture & the image on the right are adapted from (Lin et al., 2022) & (Romero et al., 2018), respectively.

Chapter 2 Materials & Methods

2.1 General approach

Strain of thoughts for experiment-designing:
after tail amputation
X molecule ↓ → notochord bead ?
X molecule ↓ → Ca2+ ?
X molecule ↓ → H2O2 ?
X molecule ↓ → SFK ?
↑
Techniques/methods used to implement strain of thoughts:
'tail amputation'
between zebrafish (larva) tail's pigment gap.

'X molecule ↓'
Chemical

- inhibitor、scavenger
- dose (optimal)、duration, incline to subjectives
  - Dose (optimal)
    - highest & NO toxicity
    - Notochord bead → Ca2+、H2O2、SFK
    - 1 mM (Max)
  - Duration
    - Notochord bead: -1 hpa to 6 hpa.
    - Ca2+: -1 hpa to 1 hpa.
    - H2O2: -1 hpa to 0.5 hpa.
    - SFK: -1 hpa to 1 hpa.

'Notochord bead ?'

- Visualization
  - bright field microscope
- Quantification
  - Area + Fiji ImageJ
- Timing
  - at 6 hpa

'Ca2+ ?'

- Visualization
  - GCaMP + epi-fluorescent microscope
- Quantification
  - CTCF + Fiji ImageJ
- Timing
  - at 1 hpa
- Space
  - Wound margin + trunk

'H2O2 ?'

- Visualization
  - PFBS-F + epi-fluorescent microscope
- Quantification
  - CTCF + Fiji ImageJ
- Timing
  - at 0.5 hpa (peak)
- Space
  - Wound margin

'SFK ?'

- Visualization
  - A183 antibody + epi-fluorescent microscope
- Quantification
  - CTCF + Fiji ImageJ
- Timing
  - at 1 hpa
- Space
  - Wound margin

Further confirmation

- Chemical
  - Structrally-unrelated analog

Figure 2-1. This is a flowchart-style casual outline of all my experiments in my project. Please see text for details.

The general idea is to cut the tail of 3 or 4 dpf zebrafish larvae, down-regulate target signaling molecules, and observe how it affects the formation of the notochord bead and the level of amputation-induced Ca2+, H2O2 & SFK signaling molecules (Figure 2-1). The down-regulation was achieved by using chemicals, including inhibitors and scavengers. The concentration and length of the chemical treatment were tested before the formal experiment. For the detection of the notochord bead, a brightfield microscope was used. The timepoint, 6 hpa, was picked (Figure 2-2). The area of the bead was measured. For the detection of Ca2+, GCaMP transgenic fish and a fluorescent microscope were used. The timepoint, 1 hpa, was picked. The fluorescent intensity was measured by calculating the CTCF. For the detection of H2O2, a fluorescent dye called PFBS-F was used. The timepoint, 0.5 hpa, was picked. The CTCF was calculated. For the detection of SFK, an anti-phosphoSFK antibody was used for immunostaining. The timepoint, 1 hpa, was picked. CTCF was calculated.

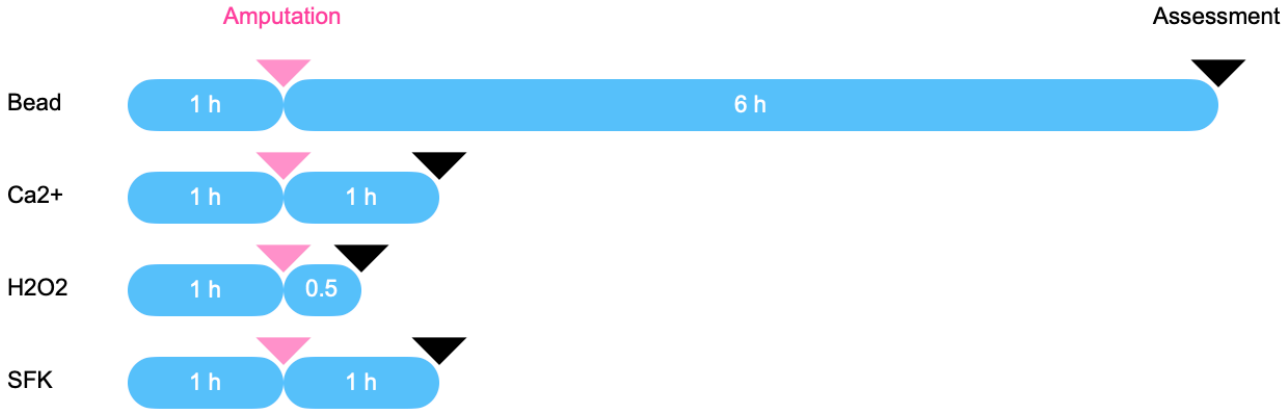

Figure 2-2. A schematic demonstration of the timing of the drug intervention, tail-cutting and assessment of the notochord bead formation, Ca2+ level, H2O2 level and pSFK level. The pink arrow indicates the tail amputation; the black arrow stands for assessment; the blue rectangle refers to the chemical treatment with its duration written in white text. The tail excision happens right after pre-treatment and before treatment, and the assessment takes place immediately after treatment. Please see text for details.

2.2 Tail amputation assay with chemical treatment in zebrafish larva

2.2.1 Notochord bead formation assay

The tail of the fish was amputated using the method described in the 'Tail amputation of zebrafish larva' section. It was cut between the pigment gap. Since there were several groups in one experiment, the watch glass and the scalpel were washed between each group.

For the drug intervention, 3 or 4 dpf wild type fish were used, and they were placed into a glass petri dish for each group. For each experiment, 2 control groups were set up. These include 1 blank control and 1 positive control. DMSO was used as the blank control, and PP2 was used as the positive control. The fish were pre-treated for 1 hour before tail amputation. Then the fish were treated for 6 hours after the tail excision. During the pre-treatment and treatment, the fish were kept in the incubator.

After the 1-hour pre-treatment and 6-hour treatment, the fish were taken out and prepared for photo-taking. They were placed on a glass slide along with a certain amount of drug-containing E3 media. The slide was cleaned with alcohol. The media on the glass slide was stirred with a stainless steel needle. Glass pipettes and tissues were used to remove the extra media. The purpose was to release the surface tension and

create a very thin layer of media over the fish so that the fish could stay moist and lie flat. The smallest amount of media was left with the fish on the glass slide so that it didn't create a thick aqueous surface with curvature that would function like a magnifying lens which could produce an enlarged image of the zebrafish morphology and interfere with the following quantification. A bright-field microscope and a camera were used. A 10 × ocular lens was used. The object lens was set to either 5 × or 10 ×. A software was used to take the photos. The pictures were saved in either JPG/JPEG or TIF format. They were named with the numbers that were assigned by the system by default.

A software programme named Fiji ImageJ was used for the quantification of the notochord bead. The area of the bead was measured.

2.2.2 Ca2+ level assay

The tail of the fish was amputated using the method described in the 'Tail amputation of zebrafish larva' section. It was cut between the pigment gap. The watch glass and the scalpel were washed between each group.

For the drug intervention, 3 or 4 dpf transgenic fish were used, and they were placed into a glass petri dish for each group. GCaMP7a fish were used to visualise Ca2+. DMSO was used as the blank control. The fish were pre-treated for 1 hour before tail amputation. Then the fish were treated for 1 hour after the tail excision. During the pre-treatment and treatment, the fish were kept in the incubator.

After the 1-hour pre-treatment and 1-hour treatment, the fish were taken out and prepared for photo-taking. They were placed on a glass slide along with a certain amount of drug-containing E3 media. The slide was cleaned with alcohol. Glass pipettes and tissues were used to remove the extra media. The purpose was to release the surface tension and create a very thin layer of media over the fish so that the fish could lie flat. The extra media was removed as much as possible. The media left with the fish on the glass slide was less than the media left in the notochord bead formation assay due to the difference in the microscope used. Even a relatively small amount of media would create a hazy image under the fluorescent microscope, but not under the bright-field microscope. The mounting process and the following photo-taking process were fast to keep the fish from drying out. Glass pipettes and tissues were carefully used so that they did not touch the fish; otherwise, it might damage the fish and create an abnormal fluorescence pattern under the microscope, which would make this fish no longer valid for photographing and quantification. The reason behind this is unknown. A fluorescent microscope and a camera were used. A software was used to take the photos. The pictures were saved in CZI format. They were named with the numbers that were assigned by the system by default.

ImageJ was used for the quantification of the fluorescent intensity of the Ca2+ level. The corrected total cell fluorescence (CTCF) was calculated (Figure 2-3).

$$CTCF = integrated\ density - (area \times mean\ fluorescence\ of\ background)$$

Figure 2-3. The formula used to calculate CTCF.

2.2.3 H2O2 level assay

The tail of the fish was amputated using the method described in the ‘Tail amputation of zebrafish larva’ section. It was cut between the pigment gap. The watch glass and the scalpel were washed between each group.

For the drug intervention, 3 or 4 dpf wild type fish were used, and they were placed into a glass petri dish for each group. For each experiment, 2 control groups were set up. These include 1 blank control and 1 positive control. DMSO was used as the blank control, and DPI was used as the positive control. The fluorescent dye PFBS-F was used for visualisation of H2O2. The fish were pre-treated for 1 hour before tail amputation. Then the fish were treated for 0.5 hour after the tail excision. During the pre-treatment and treatment, the fish were kept in the incubator.

After the 1-hour pre-treatment and 0.5-hour treatment, the fish were taken out and prepared for photo-taking. They were mounted in the same way described in the Ca2+ level assay. A fluorescent microscope and a camera were used. A software was used to take the photos. The pictures were saved in CZI format. They were named with the numbers that were assigned by the system by default.

ImageJ was used for the quantification of the fluorescent intensity of the H2O2 level. The corrected total cell fluorescence (CTCF) was calculated.

2.2.4 SFK level assay

The tail of the fish was amputated using the method described in the ‘Tail amputation of zebrafish larva’ section. Pigment gap level amputation and fin-fold only amputation were both performed. The watch glass and the scalpel were washed between each group.

For the drug intervention, 3 or 4 dpf wild type fish were used, and they were placed into a glass petri dish for each group. DMSO was used as the blank control. The fish were pre-treated for 1 hour before tail amputation. Then the fish were treated for 1 hour after the tail excision. During the pre-treatment and treatment, the fish were kept in the incubator. After the 1-hour pre-treatment and 1-hour treatment, the fish were taken out and fixed in fresh 4% paraformaldehyde (PFA) and stored in a 4°C fridge for at least 24 hours. They were then transferred into 100% MeOH by washing them several times with 100% MeOH. The fish were then stored in a -20°C freezer for at least 2 hours, and they were ready for immunostaining. Antibodies were used to visualise SFK by immunostaining the phosphorylated and activated ones.

After the immunostaining, the fish were prepared for photo-taking. They were mounted in the same way described in the Ca2+ level assay. Since the fish were in anti-fade mountant rather than media during the mounting and photo-taking process, the process did not have to be fast. This is due to the fact that anti-fade is not evaporative like the media. A fluorescent microscope and a camera were used. A software was used to take the photos. The pictures were saved in CZI format. They were named with the numbers that were assigned by the system by default.

ImageJ was used for the quantification of the fluorescent intensity of the SFK level. The corrected total cell fluorescence (CTCF) was calculated.

2.3 Preparing zebrafish larva

2.3.1 Zebrafish husbandry

All the zebrafish-related work was performed at The University of Sheffield. The work was regulated by the Animal (Scientific Procedures) Act 1986 and guided by the university's zebrafish facility. A project licence was issued to Dr. Henry Roehl to cover the zebrafish-related work. The licence number is PP3627554. The university's zebrafish facility staff kept the adult zebrafish.

2.3.2 Zebrafish lines

2 lines of zebrafish were used in the experiments. They are the wild-type fish (AB strain) and the transgenic fish Tg(β-actin:Gal4;uas-GCaMP7a). Transgenic zebrafish larvae were identified and sorted by the fluorescent heart and the fluorescent eye. Plasmids containing DNA coding GCaMP7a were used to construct the fish line. 2 promotors were used to account for any potential off-target effects of using only 1 promoter.

2.3.3 Raising zebrafish larva

Clean fish egg-collecting devices were put into the fish tanks in the evening. Gloves were used during the whole process so that the water in the tank was not contaminated by unwanted stuff (e.g., hand cream) on my hands.

The devices were removed from the tanks the next day by noon. The fish normally mate and lay eggs in the morning. The faeces were washed away from the eggs. Then, the eggs were placed into the plastic petri dish, along with the water from the fish tank. Delay in the collection of fish eggs may affect the health of the adult fish in the tank and the normal development of the newly laid eggs. Normally, there are 150-400 eggs for 8 pairs of fish.

The collected eggs were then separated into several plastic petri dishes with about 50 eggs in each dish using a dissection scope and plastic pipette. The map of the zebrafish embryonic development stage was used as a reference during the sorting process. A suitable amount of E3 media was added to the petri dish, then the eggs were placed into the incubator. All eggs were sorted on the same day of collection. Sometimes the eggs were in a very early stage, which made them difficult to sort. In this case, eggs in the fish tank water were put into the incubator for a few hours to develop before sorting.

On the next day of collection, the bad eggs, which had turned into a white color and could be distinguished by the naked eye, were removed.

When using the fish for experiments, fish with abnormal morphology were excluded. These anomalies include an under-developed tail, under-developed pigmentation and an enlarged chest/heart which can all be easily and obviously observed under the dissection scope.

2.4 Tail amputation & chemical treatment

2.4.1 Tail amputation of zebrafish larva

For anaesthesia, tricaine was applied.

The 3 or 4 days post fertilisation (dpf) fish were transferred into a clean watch glass with a suitable amount of E3 media to keep them from drying out. Then the fish were put under the dissection scope. A sharp scalpel

blade was used for excision. The whole amputation process was carried out at a constant room temperature which is about 25°C.

The fish tail was amputated along the dorso-ventral axis in 2 different ways: (1) Pigment gap level amputation. (2) Fin-fold only amputation. In the fin-fold only amputation, only the fin fold of the caudal fin was excised. In the pigment gap level amputation, the pigment gap was used as an indicator (Figure 2-4). Not only the fin fold, but also the muscle, bone, blood vessel, nerve and the notochord were cut.

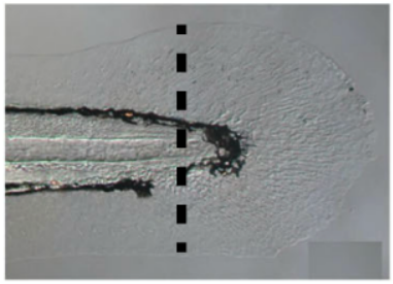

Figure 2-4. Black dotted line indicates the location of tail amputation.

The cutting process was quick and precise to create a clean and neat edge to the wound. The tip of the blade was wetted by dipping into the media, and the media was stirred with the blade right before the cutting so that the blade could go into the media to reach the target cutting site easier and smoothier. The possible reason behind this is that the stirring released the surface tension of the media.

2.4.2 Chemical's optimal concentration testing

For the drug intervention that was involved in the notochord bead formation assay, Ca2+ level assay, H2O2 level assay and SFK level assay. The optimal concentration of each chemical was tested in the notochord bead formation assay and then used for the Ca2+ level assay, H2O2 level assay and SFK level assay.

The optimal concentration is the highest concentration that can be used in the notochord bead formation assay without causing any toxicity to the zebrafish larva. Normally, the higher the concentration, the more toxic it is to the fish. However, exceptions have been observed. Toxicity refers to abnormal morphological features that can be observed with the naked eye under the microscope. Sometimes, these features can be very dramatic, and the fish looked like they were decomposing.

In the 1st round of testing, 3 concentrations were tried: 10 μM, 50 μM & 100 μM. This is based on experience from previous experiments, which involved adding chemicals to zebrafish-containing media, conducted by previous members of the Roehl lab. The reported concentrations, which were used in similar experiments, from published papers were also considered.

The 2nd round of testing was based on the results of the 1st round. There are 4 possible outcomes of the 1st round: (1) Fish treated with 10/50/100 μM chemical showed no toxicity. In this case, higher concentrations (500 μM & 1000 μM) were tested. (2) Fish treated with 10/50/100 μM chemical showed toxicity. In this case, lower concentrations (1 μM & 5 μM) were tested. (3) Fish treated with 10 μM chemical appeared normal, while fish treated with 50/100 μM chemical showed toxicity. In this case, a concentration between 10 μM & 50 μM (25 μM) was tested. (4) Fish treated with 10/50 μM chemical appeared normal, while fish treated with

100 μM chemical showed toxicity. In this case, a concentration between 50 μM & 100 μM (75 μM) was tested.

Concentrations higher than 1000 μM were not tested. For chemicals dissolved in DMSO or other organic solvents, when the concentration was too high (higher than 1 mM), there was precipitate in the media, which is aqueous. These precipitates made the media cloudy and blocked the visual field under the microscope. This made it difficult to carry out the tail amputation, as the pigment gap was barely visible, let alone the transparent fin fold. For chemicals whose solution is coloured, when the concentration was higher than 1 mM, the colour of the media became too dark for tail amputation.

2.5 Preparing chemicals

2.5.1 Chemicals' making, storing & using

All the procedures described below were guided by the safety data sheet (SDS) that came with the chemicals. When the chemical was toxic and hazardous to the human body, gloves were worn and fume cupboards were used.

As for the stability and shelf life of the solids and solutions, related information has rarely been reported, so it was guided by the standard recommendations and instructions provided by the manufacturer.

If the chemical came in solution form, then it was used directly as a stock solution. The solution-making step was skipped. For most of the stock solutions made in the lab, the concentration was set at 10 mM. If the chemical solids came in large amounts and needed to be weighed using the analytical balance, the minimum amount was set at 5 mg. If the amount was too little (less than 5 mg), the measurement error would be too large to be negligible. The error could happen during several rounds of transfers. The chemical solids were dissolved in many different kinds of solvents, which include organic solvents (e.g., DMSO, methanol & ethanol) as well as aqueous solvents (e.g., autoclaved water). Most of the stock solutions were prepared with either DMSO or autoclaved water. Sometimes, for one specific chemical, it can be dissolved in more than one solvent. These different solvents have different maximum solubilities for this specific solid. In most cases, the solvent with higher solubility was chosen. In some circumstances, the solution was difficult to obtain, so the temperature was raised (using a water bath or microwave oven) or the pH was adjusted for the solute to be fully dissolved.

The fully dissolved and well-mixed stock solution was aliquoted for storage. They were aliquoted and tightly sealed into dark-coloured micro-vials, which protect them from light exposure. They were stored at different temperatures (room temperature, 5°C in the fridge, -20°C or -80°C in the freezer), following the storage instructions provided by the manufacturer. When using them for experiments, a 'use how much, take how much' basis was followed so that the thaw-freeze cycle was minimised, chemical decomposition was avoided and accurate concentrations were reached. During experiments, light-sensitive solutions were either wrapped with foil or placed in a stainless steel box.

The unused solids were protected from light exposure and stored at different temperatures, following the storage guidance. When they needed to be taken out of the fridge/freezer to make stock solutions, the cap of the container was not opened immediately. They were placed at room temperature for a while to bring the

temperature of the air and solids inside the container to the same temperature as outside the container. So that the solids did not get damp and the accuracy of the stock solution concentration was not jeopardized.

2.6 Statistical analysis

To compare groups of data for significant differences, suitable statistical tests were selected. For all the datasets that need to be tested in the experiments, they all have only 2 groups of data. These 2 groups are all unrelated. So, for the selection of the statistical test, it depends on whether these groups of data conform to the normal distribution. If they do not conform to the normal distribution, then a non-parametric test called Mann-Whitney U test (two-tailed) was performed. If they conform to the normal distribution, then a parametric test called independent-samples T test (two-tailed) was performed. A normality test was performed to find out if they conform to the normal distribution. In this case, the Shapiro-Wilk test was used. For the 2 groups of data tested with the independent-samples T test, if they do not have the same standard deviation (SD), then the independent-samples T test with Welch's correction (two-tailed) was performed. Homogeneity test was performed to find out if they have the same SD. In this case, the F test was used.

All the tests mentioned above were carried out using the software Prism 9.

Sometimes, within the raw data, there are values that are either abnormally high or low. They are probably the result of some mistakes made during the experiment. They are no longer valid for analysis; hence, these outliners were excluded from the statistical test. For all the tests mentioned above, the confidence level was set to 95%. When the P value is < 0.05, it is considered statistically significant. In the graph, $p > 0.05$ was shown as 'ns', $p < 0.05$ was shown as '*', $p < 0.01$ was shown as '**', $p < 0.001$ was shown as '***' and $p < 0.0001$ was shown as '****'. Scatter plots were created. In each graph, each point represents a fish. The number of points is equal to the number of fish used in the experiment. For the error bar, ‘mean with SEM’ was shown in the graph.

Chapter 3 Results

Molecule	Chemical	Notochord Bead	Ca2+	H2O2	SFK
Ca2+	BAPTA-AM	ns	S(−) N/A	S(−)	ns
SERCA	CPA	ns	ns	ns	N/A
RyR	Dantrolene	ns	ns	ns	N/A
CaV	Flunarizine	ns	ns	N/A	N/A
IP3R	2APB	ns	S(−)	ns	N/A
H2O2	DPI	S(−)	S(−)	S(−) N/A	ns
SFK	KBSRC4	ns	N/A	N/A	N/A
	PP2	S(−)	S(−)	ns	S(−) N/A
	Src inhibitor 1	S(−)	S(+)	ns	S(−) N/A
AMPK	Metformin	ns	S(+)	ns	ns
CREB	666-15	ns	ns	S(−)	ns
EGFR	PD168393	S(−)	S(+)	ns	ns
GP	CP316819	ns	ns	ns	ns
HSD	CBX	ns	S(+)	ns	N/A
LTB4R	U75302	ns	ns	N/A	ns
MAPKK	PD98059	ns	S(+)	ns	N/A
	U0126	ns	S(+)	S(−)	N/A
Microtubule	Nocodazole	S(−)	ns	ns	ns
MLCK	MLCK inhibitor peptide 18	ns	S(+)	ns	N/A
MMP	GM-6001	S(−)	ns	ns	ns
	TAPI-1	S(−)	N/A	ns	N/A
NO•	3-B-7-Nitroindazole	ns	N/A	N/A	N/A
PDE	MMPX	S(−)	S(+)	S(+)	N/A
PI3K	LY294002	ns	ns	ns	ns
	Wortmannin	S(−)	ns	ns	N/A
PKA	KT5720	S(−)	N/A	N/A	ns
PKB	AKT inhibitor IV	ns	ns	S(−)	ns
PKC	Bim-1	S(+)	ns	S(−)	ns
PLA2	ACA	ns	S(+)	ns	N/A
P2R	NF340	ns	N/A	N/A	N/A
	PPADS	ns	ns	ns	ns
	Suramin	ns	N/A	ns	N/A
Rock	Y27632	ns	ns	ns	N/A

Table 3-1. This table summarizes all the experimental results of my project. 'S(−)' indicates being concluded as significant down-regulation (negatively-significant); 'S(+)' indicates being concluded as significant up-regulation (positively-significant); 'ns' denotes being concluded as non-significant; 'N/A' indicates no experiment performed; 'S(−) N/A' indicates a confirmative experiment being concluded as significant down-regulation.

The criteria for determining the significance of a chemical treatment on notochord bead formation/Ca2+ level/ H2O2 level/SFK signaling are: (1) If the treatment consistently significantly impaired notochord bead formation in at least 3 experiments in a row, then it is concluded as S(−) (negatively-significant); (2) If the treatment consistently significantly promoted notochord bead formation in at least 3 experiments in a row, then it is concluded as S(+) (positively-significant); (3) If it is any other situation, then it is concluded as ns (non-significant).

3.1 Molecules involved in notochord bead formation

For all the 'notochord bead extrusion assays', the protocols are as follows, unless otherwise stated. By adding chemicals to the media, I gave the 3 or 4 dpf fish 1 hr of pre-treatment & 6 hrs of treatment, between which the tail was amputated between the pigment gap. For the visualization & quantification of notochord bead formation, I used a bright-field microscope to take photos at 6 hpa, that is, the end of treatment. Then, I measured the area of notochord bead in the photos using Fiji ImageJ.

3.1.1 H2O2 is involved in notochord bead formation

In my experiments, I found out that the lowering of H2O2 level causes impairment of notochord bead formation in zebrafish (larva) tail regeneration. I tried to lower the H2O2 level and then observed how it affected notochord bead formation. For the lowering of H2O2 level, I used a chemical inhibitor called diphenyleneiodonium (DPI) (100 μM) which inhibits the H2O2-producing enzyme called Nox (Morré, 2002). In the DPI-treated fish, a significant decrease (58171.5 ± 26991.9 in control group VS 32337.7 ± 22745.2 in DPI-treated group) in notochord bead area was observed, suggesting that H2O2 is involved in the notochord bead formation (Figure 3-1). Please note that the protocol for this experiment differs from others. The only difference is that the treatment duration is 30 minutes, not 6 hours.

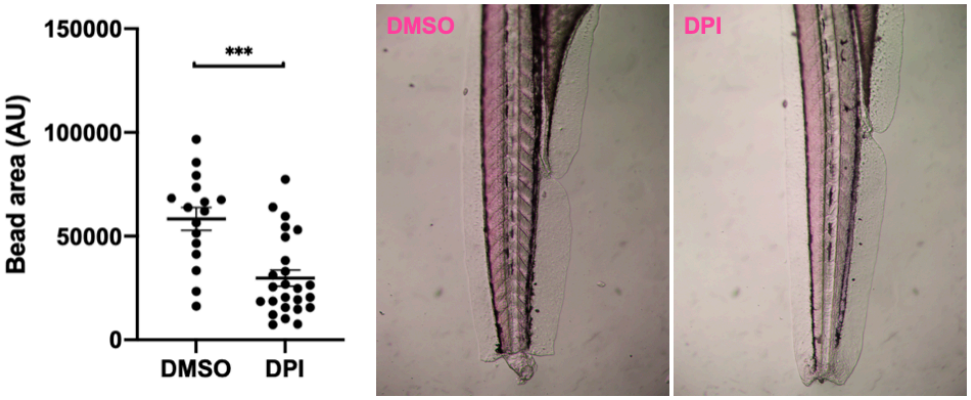

Figure 3-1. Brightfield images, quantification & statistical analysis of the regenerating tails treated with DMSO or DPI (100 μM) following 1 hour pre-treatment, amputation between pigment gap & 6 hours treatment. Data are expressed as mean ± SEM. DMSO: 58171.5 ± 26991.9, DPI: 32337.7 ± 22745.2. Significance was determined using Mann-Whitney test versus DMSO control. no significance (ns), P > 0.05; *, P < 0.05; **, P < 0.01; ***, P < 0.001; ****, P < 0.0001. n = 26 biological replicates. Number of experiments = 3.

3.1.2 SFK is involved in notochord bead formation

In my experiments, I found out that the inhibition of Src family kinase (SFK) activity causes impairment of notochord bead formation. I tried to inhibit SFK activity and then observed how it affected notochord bead

formation. For the inhibition of SFK activity, I used a chemical inhibitor called PP2 (20 μM) (Hanke et al., 1996). In the PP2-treated fish, a significant decrease (204993 ± 92713.9 in control group VS 36199.5 ± 20232.0 in PP2-treated group) in notochord bead area was observed, suggesting that SFK is involved in the notochord bead formation (Figure 3-2). For further confirmation, I used another inhibitor, which is a structure-unrelated analog of PP2, called Src inhibitor 1 (5 μM) (Bain et al., 2007). A significant decrease (74787.3 ± 31528.2 in control group VS 35894.9 ± 12550.9 in Src inhibitor 1-treated group) was also observed (Figure 3-3). I also tried another structure-unrelated analog called KBSRC4 (250 μM) (Brandvold et al., 2012), but its treatment did not have a consistent significance (negative or positive) on notochord bead formation.

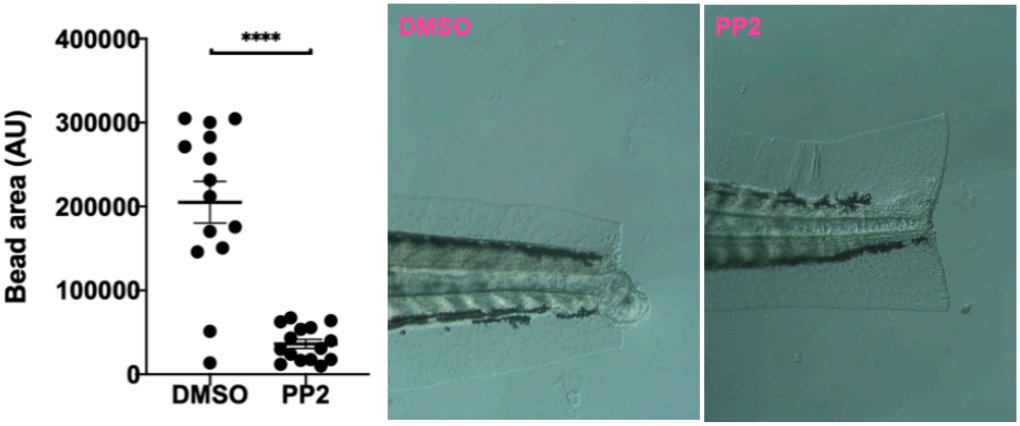

Figure 3-2. Brightfield images, quantification & statistical analysis of the regenerating tails treated with DMSO or PP2 (20 μM) following 1 hour pre-treatment, amputation between pigment gap & 6 hours treatment. Data are expressed as mean ± SEM. DMSO: 204993 ± 92713.9, PP2: 36199.5 ± 20232.0. Significance was determined using Mann-Whitney test versus DMSO control. no significance (ns), P > 0.05; *, P < 0.05; **, P < 0.01; ***, P < 0.001; ****, P < 0.0001. n = 15 biological replicates. Number of experiments = 3.

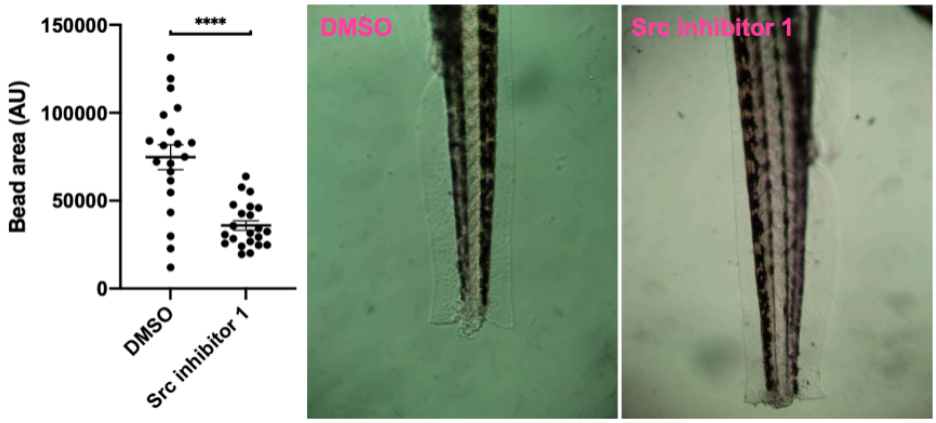

Figure 3-3. Brightfield images, quantification & statistical analysis of the regenerating tails treated with DMSO or Src inhibitor 1 (5 μM) following 1 hour pre-treatment, amputation between pigment gap & 6 hours treatment. Data are expressed as mean ± SEM. DMSO: 74787.3 ± 31528.2, Src inhibitor 1: 35894.9 ± 12550.9. Significance was determined using Mann-Whitney test versus DMSO control. no significance (ns), P > 0.05; *, P < 0.05; **, P < 0.01; ***, P < 0.001; ****, P < 0.0001. n = 15 biological replicates. Number of experiments = 3.

3.1.3 EGFR is involved in notochord bead formation

Since EGFR has been reported to be involved in cricket leg regeneration (Nakamura et al., 2008), planarian regeneration (Fraguas et al., 2011) & rat axon regeneration (Xu et al., 2013), I wonder if it is also involved in

zebrafish tail regeneration. In my experiments, I found out that the inhibition of epidermal growth factor receptor (EGFR) activity causes impairment of notochord bead formation. I tried to inhibit EGFR activity and then observed how it affected notochord bead formation. For the inhibition of EGFR activity, I used a chemical inhibitor called PD168393 (250 μM) (Fry et al., 1998). In the PD168393-treated fish, a significant decrease (63948.8 ± 25736.8 in control group VS 12873.8 ± 4156.8 in PD168393-treated group) in notochord bead area was observed, suggesting that EGFR is involved in the notochord bead formation (Figure 3-4).

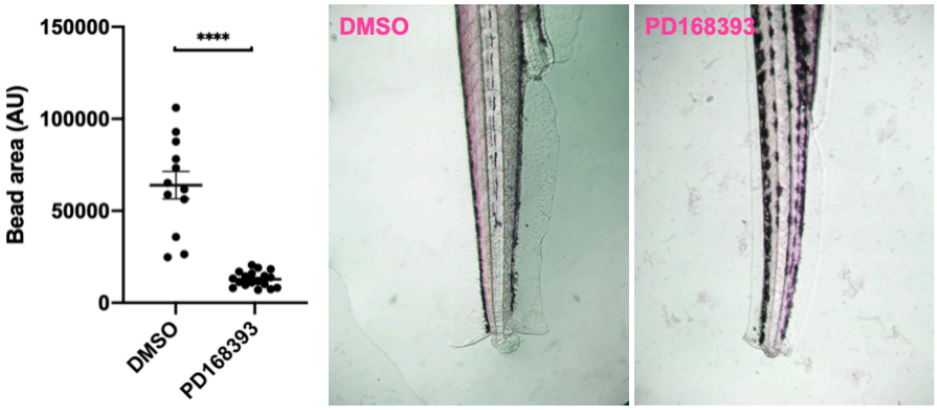

Figure 3-4. Brightfield images, quantification & statistical analysis of the regenerating tails treated with DMSO or PD168393 (250 μM) following 1 hour pre-treatment, amputation between pigment gap & 6 hours treatment. Data are expressed as mean ± SEM. DMSO: 63948.8 ± 25736.8, PD168393: 12873.8 ± 4156.8. Significance was determined using Mann-Whitney test versus DMSO control. no significance (ns), P > 0.05; *, P < 0.05; **, P < 0.01; ***, P < 0.001; ****, P < 0.0001. n = 18 biological replicates. Number of experiments = 3.

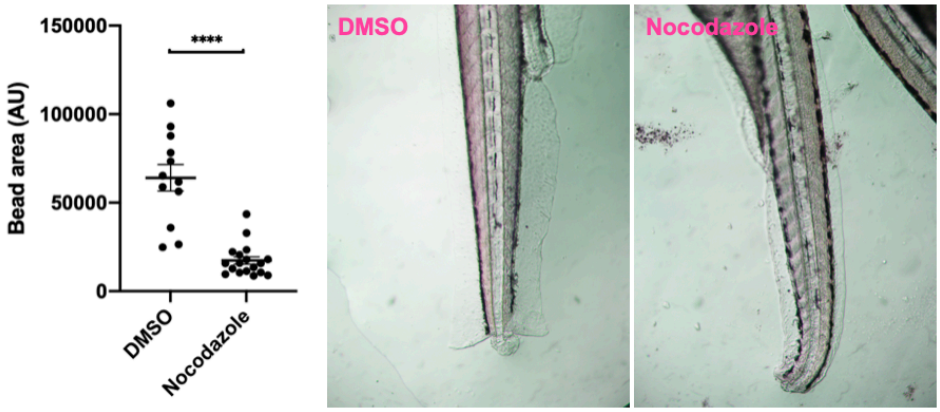

Figure 3-5. Brightfield images, quantification & statistical analysis of the regenerating tails treated with DMSO or Nocodazole (500 μM) following 1 hour pre-treatment, amputation between pigment gap & 6 hours treatment. Data are expressed as mean ± SEM. DMSO: 85395.5 ± 32297.6, Nocodazole: 35438.0 ± 15719.9. Significance was determined using Mann-Whitney test versus DMSO control. no significance (ns), P > 0.05; *, P < 0.05; **, P < 0.01; ***, P < 0.001; ****, P < 0.0001. n = 18 biological replicates. Number of experiments = 3.

3.1.4 Microtubule is involved in notochord bead formation

Due to the fact that microtubules have been reported to participate in rodent axonal regeneration after spine damage (Hellal et al., 2011), I wonder if they are also involved in zebrafish tail regeneration. In my experiments, I found out that the inhibition of microtubule activity causes impairment of notochord bead

formation. I tried to inhibit microtubule activity and then observed how it affected notochord bead formation. For the inhibition of microtubule activity, I used a chemical inhibitor called nocodazole (500 μM) (Vasquez et al., 1997). In the nocodazole-treated fish, a significant decrease (85395.5 ± 32297.6 in control group VS 35438.0 ± 15719.9 in nocodazole-treated group) in the notochord bead area was observed, suggesting that microtubule is involved in the notochord bead formation (Figure 3-5).

3.1.5 MMP is involved in notochord bead formation

Owing to the fact that MMP has been reported to play a role in zebrafish tail development (Wyatt & Crawford, 2021), I wonder if it is also involved in zebrafish tail regeneration. In my experiments, I found out that the inhibition of matrix metalloproteinase (MMP) activity causes impairment of notochord bead formation. I tried to inhibit MMP activity and then observed how it affected notochord bead formation. For the inhibition of MMP activity, I used a chemical inhibitor called GM-6001 (100 μM) (Li et al., 2002). In the GM-6001-treated fish, a significant decrease (110959.1 ± 50587.6 in control group VS 75526.9 ± 41281.5 in GM-6001-treated group) in the notochord bead area was observed, suggesting that MMP is involved in the notochord bead formation (Figure 3-6). For further confirmation, I used another inhibitor, which is a structure-unrelated analog of GM-6001, called TAPI-1 (100 μM) (Crowe et al., 1995). A significant decrease (124411.8 ± 51778.1 in control group VS 51221.4 ± 31763.0 in TAPI-1-treated group) was also observed (Figure 3-7).

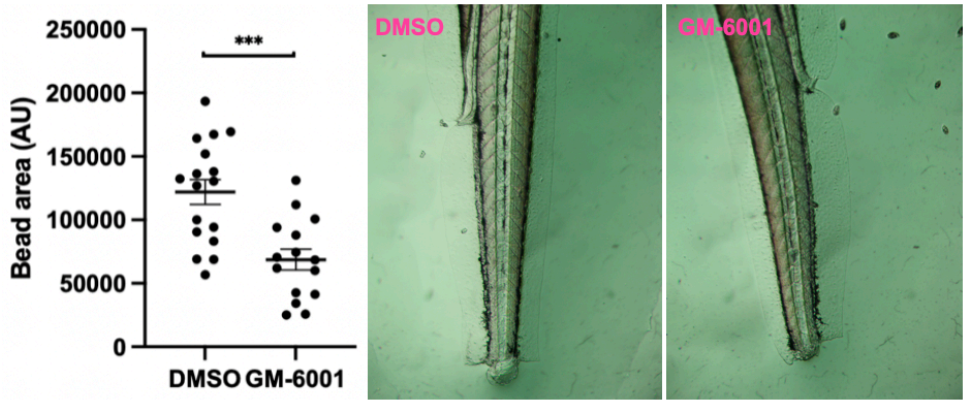

Figure 3-6. Brightfield images, quantification & statistical analysis of the regenerating tails treated with DMSO or GM-6001 (100 μM) following 1 hour pre-treatment, amputation between pigment gap & 6 hours treatment. Data are expressed as mean ± SEM. DMSO: 110959.1 ± 50587.6, GM-6001: 75526.9 ± 41281.5. Significance was determined using Mann-Whitney test versus DMSO control. no significance (ns), $P > 0.05$; *, $P < 0.05$; **, $P < 0.01$; ***, $P < 0.001$; ****, $P < 0.0001$. n = 16 biological replicates. Number of experiments = 3.

3.1.6 PDE is involved in notochord bead formation

Given that PDE has been reported to be engaged in axon regeneration after spine damage (Nikulina et al., 2004), I wonder if it is also involved in zebrafish tail regeneration. In my experiments, I found out that the inhibition of phosphodiesterase (PDE) activity causes impairment of notochord bead formation. I tried to inhibit PDE activity and then observed how it affected notochord bead formation. For the inhibition of PDE activity, I used a chemical inhibitor called MMPX (250 μM) (Wells & Miller, 1988). In the MMPX-treated fish, a significant decrease (139703.6 ± 35933.2 in control group VS 72005.3 ± 38127.0 in MMPX-treated group) in the notochord bead area was observed, suggesting that PDE is involved in the notochord bead formation (Figure 3-8).

3.1.7 PI3K is involved in notochord bead formation

On account of the fact that PI3K has been reported to be associated with rat bone regeneration (Zhang et al., 2016), I wonder if it is also involved in zebrafish tail regeneration. In my experiments, I found out that the inhibition of phosphoinositide-3-kinase (PI3K) activity causes impairment of notochord bead formation. I tried to inhibit PI3K activity and then observed how it affected notochord bead formation. For the inhibition of PI3K activity, I used a chemical inhibitor called Wortmannin (1 μM) (Powis et al., 1994). In the Wortmannin-treated fish, a significant decrease (124411.8 ± 51778.1 in control group VS 23650.7 ± 9839.4 in Wortmannin-treated group) in the notochord bead area was observed, suggesting that PI3K is involved in the notochord bead formation (Figure 3-9). For further confirmation, I used another inhibitor, which is a structure-unrelated analog of Wortmannin, called LY294002 (25 μM) (Vlahos et al., 1994), but its treatment did not have a consistent significance (negative or positive) on notochord bead formation.

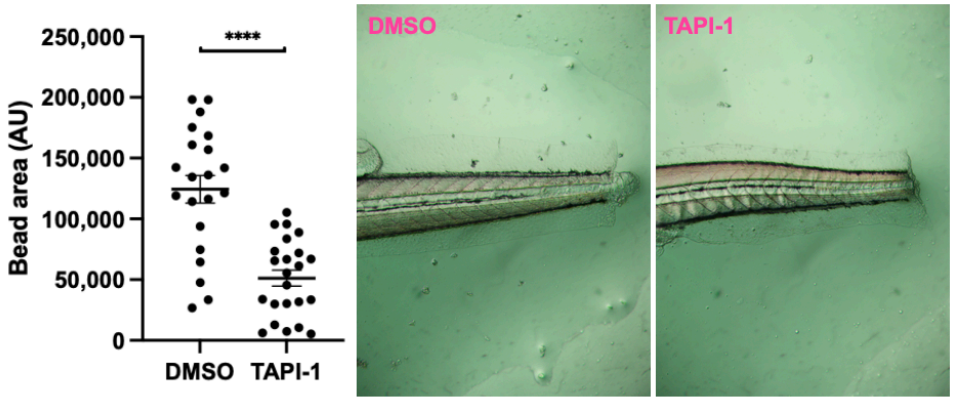

Figure 3-7. Brightfield images, quantification & statistical analysis of the regenerating tails treated with DMSO or TAPI-1 (100 μM) following 1 hour pre-treatment, amputation between pigment gap & 6 hours treatment. Data are expressed as mean ± SEM. DMSO: 124411.8 ± 51778.1, TAPI-1: 51221.4 ± 31763.0. Significance was determined using Mann-Whitney test versus DMSO control. no significance (ns), P > 0.05; *, P < 0.05; **, P < 0.01; ***, P < 0.001; ****, P < 0.0001. n = 23 biological replicates. Number of experiments = 3.

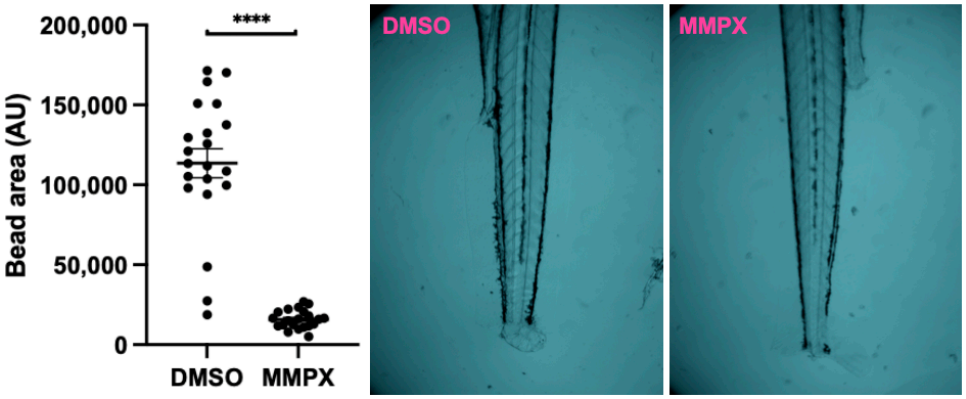

Figure 3-8. Brightfield images, quantification & statistical analysis of the regenerating tails treated with DMSO or MMPX (250 μM) following 1 hour pre-treatment, amputation between pigment gap & 6 hours treatment. Data are expressed as mean ± SEM. DMSO: 139703.6 ± 35933.2, MMPX: 72005.3 ± 38127.0. Significance was determined using Mann-Whitney test versus DMSO control. no significance (ns), P > 0.05; *, P < 0.05; **, P < 0.01; ***, P < 0.001; ****, P < 0.0001. n = 21 biological replicates. Number of experiments = 3.

3.1.8 PKA is involved in notochord bead formation

Since PKA has been reported to be involved in mouse neuro-muscular junction regeneration (Röder et al., 2012), I wonder if it is also involved in zebrafish tail regeneration. In my experiments, I found out that the inhibition of protein kinase A (PKA) activity causes impairment of notochord bead formation. I tried to inhibit

PKA activity and then observed how it affected notochord bead formation. For the inhibition of PKA activity, I used a chemical inhibitor called KT5720 (50 μM) (Kase et al., 1987). In the KT5720-treated fish, a significant decrease (102025.1 ± 48741.1 in control group VS 40252.6 ± 28497.8 in KT5720-treated group) in the notochord bead area was observed, suggesting that PKA is involved in the notochord bead formation (Figure 3-10).

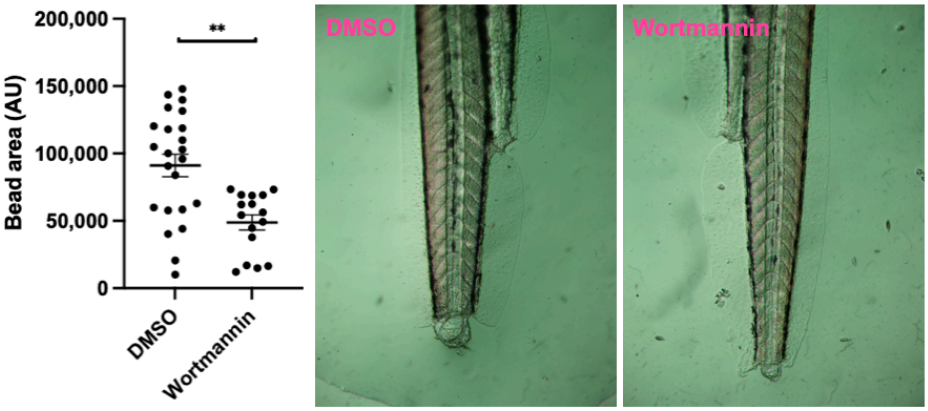

Figure 3-9. Brightfield images, quantification & statistical analysis of the regenerating tails treated with DMSO or Wortmannin (1 μM) following 1 hour pre-treatment, amputation between pigment gap & 6 hours treatment. Data are expressed as mean ± SEM. DMSO: 124411.8 ± 51778.1, KT5720: 23650.7 ± 9839.4. Significance was determined using Mann-Whitney test versus DMSO control. no significance (ns), P > 0.05; *, P < 0.05; **, P < 0.01; ***, P < 0.001; ****, P < 0.0001. n = 16 biological replicates. Number of experiments = 3.

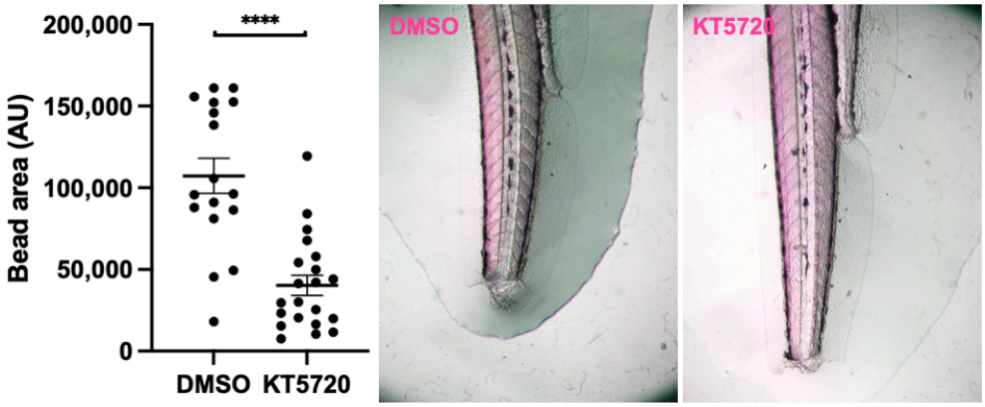

Figure 3-10. Brightfield images, quantification & statistical analysis of the regenerating tails treated with DMSO or KT5720 (50 μM) following 1 hour pre-treatment, amputation between pigment gap & 6 hours treatment. Data are expressed as mean ± SEM. DMSO: 102025.1 ± 48741.1, KT5720: 40252.6 ± 28497.8. Significance was determined using Mann-Whitney test versus DMSO control. no significance (ns), P > 0.05; *, P < 0.05; **, P < 0.01; ***, P < 0.001; ****, P < 0.0001. n = 21 biological replicates. Number of experiments = 3.

3.1.9 Chemical treatments promoted notochord bead formation

PKC, as a CaBP, has been documented in textbooks to be extensively involved in Ca2+ signaling by functioning as an enzymatic signaling molecule; hence, I wonder if it is also involved in zebrafish tail regeneration. In my experiments, I found out that the inhibition of protein kinase C (PKC) activity causes promotion of notochord bead formation. I tried to inhibit PKC activity and then observed how it affected notochord bead formation. For the inhibition of PKC activity, I used a chemical inhibitor called Bisindolylmaleimide (Bim-1) (50 μM) (Toullec et al., 1991). In the Bim-1-treated fish, a significant increase

(139703.6 ± 35933.2 in control group VS 159888.4 ± 46101.6 in Bim-1-treated group) in notochord bead area was observed.

3.1.10 Chemical treatments were concluded as non-significant (ns) on notochord bead formation

In my experiments, I also tried many other chemicals, which are BAPTA-AM (100 μM) (Tymianski et al., 1994), cyclopiazonic acid (CPA) (100 μM) (Seidler et al., 1989), Dantrolene (100 μM) (Kobayashi et al., 2009), Flunarizine (75 μM) (Singh, 1986), 2-aminoethyl diphenylborinate (2APB) (1 μM) (Maruyama et al., 1997), metformin (1 mM) (Shaw et al., 2005), 666-15 (50 μM) (Xie et al., 2015), CP316819 (75 μM) (Yu et al., 2006), CBX (250 μM) (Jellinck et al., 1993), U75302 (10 μM) (Lin et al., 1988), PD98059 (5 μM) (Alessi et al., 1995), U0126 (250 μM) (Favata et al., 1998), MLCK inhibitor peptide 18 (100 μM) (Lukas et al., 1999), 3-B-7-Nitroindazole (100 μM) (Bland-Ward & Moore, 1995), AKT inhibitor IV (2 μM) (Sun et al., 2011), N-(p-amylcinnamoyl) anthranilic acid (ACA) (1 μM) (Harteneck et al., 2007), NF340 (2 mM) (Meis et al., 2009), PPADS (1 mM) (Lambrecht et al., 1992), Suramin (1 mM) (Charlton et al., 1996) & Y27632 (500 μM) (Narumiya et al., 2000) (Table 3-1).

These chemicals are scavenger of Ca2+, inhibitor of sarcoplasmic/endoplasmic reticulum Ca2+ ATPase (SERCA), inhibitor of Ryanodine receptor (RyR), inhibitor of voltage-dependent Ca2+ channel (CaV), inhibitor of inositol 1,4,5-trisphosphate receptor (IP3R), inhibitor of AMP-activated protein kinase (AMPK), inhibitor of cAMP-response element binding protein (CREB), inhibitor of glycogen phosphorylase (GP), inhibitor of hydroxysteroid dehydrogenase (HSD), inhibitor of leukotriene B4 receptor (LTB4R), inhibitor of mitogen-activated protein kinase kinase (MAPKK), inhibitor of MAPKK, inhibitor of myosin light chain kinase (MLCK), inhibitor of a NO•-producing enzyme called neuronal nitric oxide synthase (nNOS), inhibitor of protein kinase B (PKB), inhibitor of phospholipase A2 (PLA2), inhibitor of P2 receptor (P2R), inhibitor of P2R, inhibitor of P2R & inhibitor of Rho-associated protein kinase (Rock), respectively.

The reasons for picking these target molecules for testing in this screening study are: SERCA's engagement with midline signaling during the early stage of zebrafish development (Creton, 2004) and with rat skeletal muscle (soleus) regeneration (Germinario et al., 2002); RyR's role in rat skeletal muscle regeneration (Péréon et al., 1996); L-Type CaV's involvement in neurite regeneration (Kulbatski et al., 2004); IP3R's participation in mouse epithelium regeneration (Jia et al., 2013); RyR's role in rat skeletal muscle regeneration (Péréon et al., 1996); AMPK's association with macrophage activity in muscle regeneration (McArthur et al., 2020); CREB's involvement in muscle regeneration (Stewart et al., 2011); GP's role in regenerating muscle tissue (Gorin et al., 1989) and lizard tail regeneration (Magon, 1977); HSD's engagement with mice angiogenesis (Small et al., 2005); LTB4R's participation in inflammation during cutaneous wound healing (Guimarães et al., 2017), in enhancing epithelial cell proliferation (Matsumoto et al., 2020) and in promotion of macrophage recruitment (Ohkubo et al., 2013); MAPKK's involvement in immune response (reviewed in Zhang & Dong, 2005) and inflammation (reviewed in Moens et al., 2013); MLCK's role in rat muscle regeneration (Libera et al., 1997) and in facilitating mesenchymal stem cell (MSC) migration through PKC signaling (Lin et al., 2015); NO•'s association with rat angiogenesis (Yamamoto et al., 2020) and rat skeletal muscle regeneration (Buono et al., 2011; Sakurai et al., 2013; Yamamoto et al., 2020) through modulating satellite cells (Buono et al., 2011); PKB's engagement in planarian regeneration and tissue maintenance (Peiris et al., 2016) and rat axonal regeneration (Namikawa et al., 2000); PLA2's participation in the early stage of Helisoma trivolvis (a freshwater snail) neural regeneration (Geddis & Rehder, 2003) and mice muscle regeneration through down-regulation of myonecrosis (Xiao et al., 2018);

P2R's role as a pro-angiogenic molecule (Zhou et al., 2016) and its involvement in neuro-genic processes (reviewed in Ribeiro et al., 2018); Rock's association with rat axonal regeneration (Koch et al., 2014) and endothelial tissue regeneration (Okumura et al., 2012), respectively.

These chemical treatments did not have a consistent significance (negative or positive) on notochord bead formation.

3.2 Molecules acting on Ca2+ signaling

For all the 'Ca2+ level assays', the protocols are as follows, unless otherwise stated. By adding chemicals to the media, I gave the 3 or 4 dpf fish 1 hr of pre-treatment & 1 hr of treatment, between which the tail was amputated between the pigment gap. For the visualization & quantification of Ca2+ level, I used a transgenic fish line expressing GCaMP7a (a fluorescent sensor for Ca2+) & an epi-fluorescent microscope to take photos at 1 hpa, that is, the end of treatment. Then, I measured & calculated the fluorescence intensity in the large area of the body trunk (including the wound margin) as CTCF using Fiji ImageJ.

3.2.1 H2O2 promotes Ca2+ signaling

In my experiments, I found out that the lowering of H2O2 level caused the lowering of amputation-induced Ca2+ level in zebrafish (larva) tail regeneration. I tried to lower the H2O2 level and then observed how it affected the amputation-induced Ca2+ level. For the lowering of H2O2 level, I used a Nox (H2O2-producing enzyme) inhibitor called DPI (150 μM). In the DPI-treated group, a significant decrease (2586251.5 ± 875954.9 in control group VS 922193.3 ± 245966.3 in DPI-treated group) in the amputation-induced Ca2+ level was observed, suggesting that H2O2 promotes Ca2+ signaling (Figure 3-11).

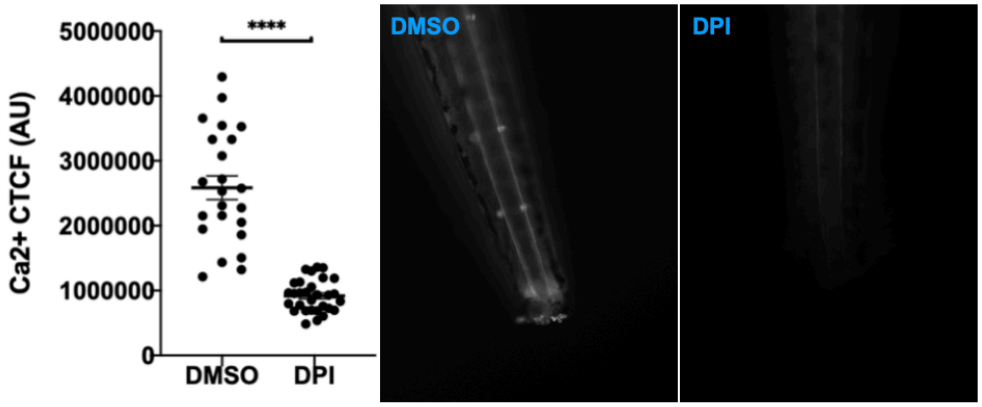

Figure 3-11. Fluorescent images, quantification & statistical analysis of the regenerating tails treated with DMSO or DPI (150 μM) following 1 hour pre-treatment, amputation between pigment gap & 1 hour treatment. Data are expressed as mean ± SEM. DMSO: 2586251.5 ± 875954.9, DPI: 922193.3 ± 245966.3. Significance was determined using Mann-Whitney test versus DMSO control. no significance (ns), $P > 0.05$; *, $P < 0.05$; **, $P < 0.01$; ***, $P < 0.001$; ****, $P < 0.0001$. n = 30 biological replicates. Number of experiments = 3.

3.2.2 SFK promotes Ca2+ signaling

In my experiments, I found out that the inhibition of SFK activity caused the lowering of amputation-induced Ca2+ level. I tried to inhibit SFK activity and then observed how it affected the amputation-induced Ca2+ level. For the inhibition of SFK activity, I used a chemical inhibitor called PP2 (20 μM). In the PP2-treated group, a significant decrease (1562300.0 ± 577982.0 in control group VS 789853.2 ± 283601.7 in PP2-treated group) in the amputation-induced Ca2+ level was observed, suggesting that SFK promotes Ca2+

signaling (Figure 3-12). For further confirmation, I used another inhibitor, which is a structure-unrelated analog of PP2, called Src inhibitor 1 (5 μM). However, a significant increase (2593033.8 ± 1012315.7 in control group VS 4473277.8 ± 839738.4 in Src inhibitor 1-treated group) was observed.

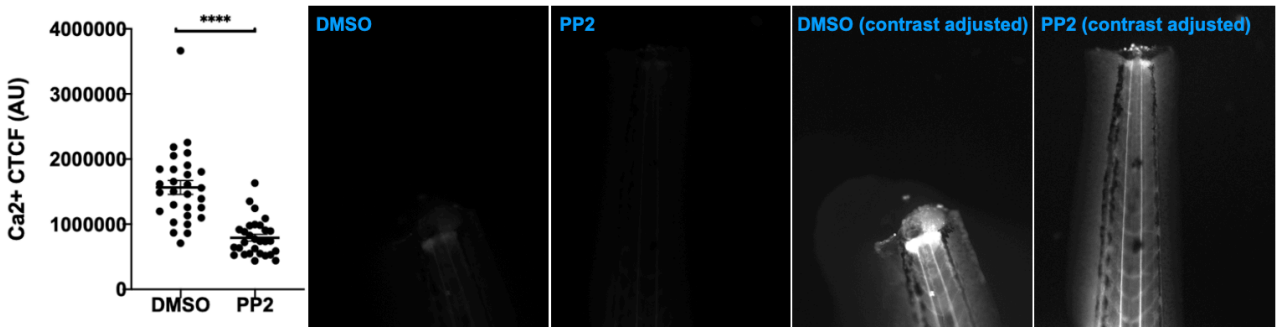

Figure 3-12. Fluorescent images, quantification & statistical analysis of the regenerating tails treated with DMSO or PP2 (20 μM) following 1 hour pre-treatment, amputation between pigment gap & 1 hour treatment. Data are expressed as mean ± SEM. DMSO: 1562300.0 ± 577982.0, PP2: 789853.2 ± 283601.7. Significance was determined using Mann-Whitney test versus DMSO control. no significance (ns), P > 0.05; *, P < 0.05; **, P < 0.01; ***, P < 0.001; ****, P < 0.0001. n = 29 biological replicates. Number of experiments = 3.

3.2.3 Chemical treatments increased Ca2+ level

In my experiments, I also tried many chemicals, which are metformin (1 mM), PD168393 (250 μM), CBX (100 μM), PD98059 (5 μM), U0126 (250 μM), MLCK inhibitor peptide 18 (100 μM), MMPX (500 μM) & ACA (1 μM) (Table 3-1).

These chemicals are inhibitor of AMPK, inhibitor of EGFR, inhibitor of HSD, inhibitor of MAPKK, inhibitor of MAPKK, inhibitor of MLCK, inhibitor of PDE & inhibitor of PLA2, respectively.

These chemical treatments significantly increased the amputation-induced Ca2+ level (4087364.1 ± 1118510.0 in control group VS 8440751.2 ± 1926064.3 in metformin-treated group; 2593033.8 ± 1012315.7 in control group VS 4121983.8 ± 896459.3 in PD168393-treated group; 18776794.1 ± 4036229.7 in control group VS 64266076.0 ± 11409840.1 in CBX-treated group; 2593033.8 ± 1012315.7 in control group VS 8605958.1 ± 1566914.0 in PD98059-treated group; 2056452.7 ± 572070.1 in control group VS 3586982.4 ± 875506.5 in U0126-treated group; 13728631.8 ± 4190730.4 in control group VS 35640024.4 ± 7569846.3 in MLCK inhibitor peptide 18-treated group; 4087364.1 ± 1118610.0 in control group VS 5208914.7 ± 1628310.1 in MMPX-treated group; 13129583.2 ± 3087401.8 in control group VS 21436730.6 ± 4174419.8 in ACA-treated group).

3.2.4 Chemical treatments were concluded as non-significant (ns) on Ca2+ signaling

In my experiments, I also tried many chemicals, which are CPA (100 μM), Dantrolene (100 μM), Flunarizine (75 μM), 666-15 (50 μM), CP316819 (75 μM), U75302 (5 μM), Nocodazole (500 μM), GM-6001 (100 μM), LY294002 (25 μM), Wortmannin (1 μM), AKT inhibitor IV (1 μM), Bim-1 (50 μM), PPADS (1 mM) & Y27632 (10 μM) (Table 3-1).

These chemicals are inhibitor of SERCA, inhibitor of RyR, inhibitor of CaV, inhibitor of CREB, inhibitor of GP, inhibitor of LTB4R, inhibitor of microtubule, inhibitor of MMP, inhibitor of PI3K, inhibitor of PI3K, inhibitor of PKB, inhibitor of PKC, inhibitor of P2R & inhibitor of Rock, respectively.

These chemical treatments did not have a consistent significance (negative or positive) on amputation-induced Ca2+ level.

3.2.5 Confirmative experiments

To verify that Ca2+ level was indeed lowered when using scavengers in the 'notochord bead extrusion assay', 'H2O2 level assay' & 'SFK activity assay', I also tested the Ca2+ scavenger, BAPTA-AM (100 μM), in this Ca2+ level assay. In the BAPTA-AM-treated fish, a significant decrease (486455235.4 ± 184695750.9 in control group VS 365928173.6 ± 258342582.3 in BAPTA-AM-treated group) in Ca2+ level was observed.

3.3 Molecules acting on H2O2 signaling

For all the 'H2O2 level assays', the protocols are as follows, unless otherwise stated. By adding chemicals to the media, I gave the 3 or 4 dpf fish 1 hr of pre-treatment & 0.5 hr of treatment, between which the tail was amputated between the pigment gap. For the visualization & quantification of H2O2 level, I used a fluorescent dye called PFBS-F & an epi-fluorescent microscope to take photos at 0.5 hpa, that is, the end of treatment. Then, I measured & calculated the fluorescence intensity in the wound margin area as CTCF using Fiji ImageJ.

3.3.1 Ca2+ promotes H2O2 signaling

In my experiments, I found out that the lowering of Ca2+ level caused the lowering of amputation-induced H2O2 level in zebrafish (larva) tail regeneration. I tried to lower the Ca2+ level and then observed how it affected the amputation-induced H2O2 level. For the lowering of Ca2+ level, I used a chemical scavenger called BAPTA-AM (100 μM). In the BAPTA-AM-treated group, a significant decrease (4068380.8 ± 1262258.7 in control group VS 2419491.9 ± 698847.4 in BAPTA-AM-treated group) in the amputation-induced H2O2 level was observed, suggesting that Ca2+ promotes H2O2 signaling (Figure 3-13).

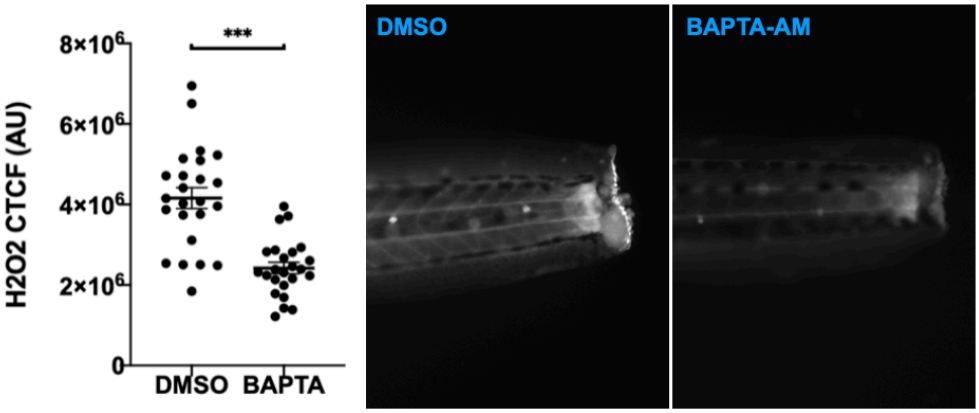

Figure 3-13. Fluorescent images, quantification & statistical analysis of the regenerating tails treated with DMSO or BAPTA-AM (100 μM) following 1 hour pre-treatment, amputation between pigment gap & 0.5 hour treatment. Data are expressed as mean ± SEM. DMSO: 4068380.8 ± 1262258.7, BAPTA-AM: 2419491.9 ± 698847.4. Significance was determined using Mann-Whitney test versus DMSO control. no significance (ns), $P > 0.05$; *, $P < 0.05$; **, $P < 0.01$; ***, $P < 0.001$; ****, $P < 0.0001$. n = 24 biological replicates. Number of experiments = 3.

3.3.2 CREB promotes H2O2 signaling

In my experiments, I found out that the inhibition of CREB activity caused the lowering of amputation-induced H2O2 level. I tried to inhibit CREB activity and then observed how it affected the amputation-induced H2O2 level. For the inhibition of CREB activity, I used a chemical inhibitor called 666-15 (50 μM). In the 666-15-treated group, a significant decrease (198806752.4 ± 39662124.3 in control group VS 32340086.0 ±

8663045.8 in 666-15-treated group) in the amputation-induced H2O2 level was observed, suggesting that CREB promotes H2O2 signaling (Figure 3-14).

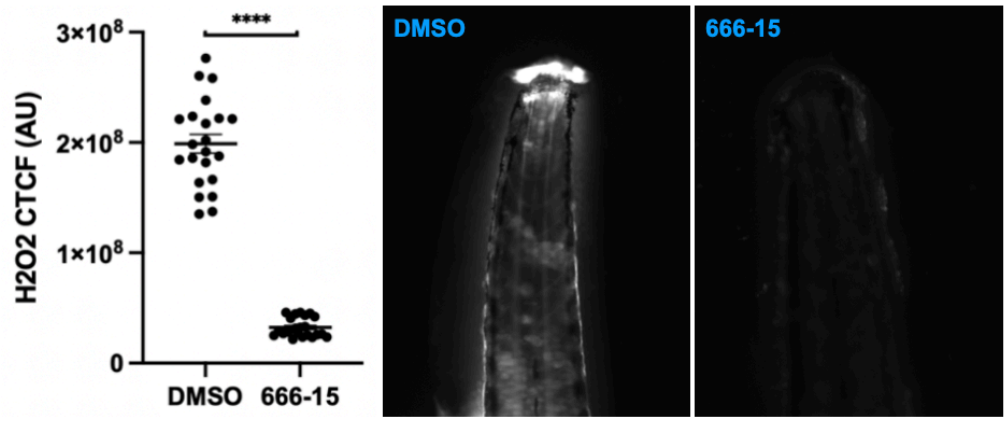

Figure 3-14. Fluorescent images, quantification & statistical analysis of the regenerating tails treated with DMSO or 666-15 (50 μM) following 1 hour pre-treatment, amputation between pigment gap & 0.5 hour treatment. Data are expressed as mean ± SEM. DMSO: 198806752.4 ± 39662124.3, 666-15: 32340086.0 ± 8663045.8. Significance was determined using Mann-Whitney test versus DMSO control. no significance (ns), P > 0.05; *, P < 0.05; **, P < 0.01; ***, P < 0.001; ****, P < 0.0001. n = 22 biological replicates. Number of experiments = 3.

3.3.3 MAPKK promotes H2O2 signaling

In my experiments, I found out that the inhibition of MAPKK activity caused the lowering of amputation-induced H2O2 level. I tried to inhibit MAPKK activity and then observed how it affected the amputation-induced H2O2 level. For the inhibition of MAPKK activity, I used a chemical inhibitor called U0126 (250 μM). In the U0126-treated group, a significant decrease (44511378.3 ± 10859024.8 in control group VS 9940566.4 ± 2861518.2 in U0126-treated group) in the amputation-induced H2O2 level was observed, suggesting that MAPKK promotes H2O2 signaling (Figure 3-15). For further confirmation, I used another inhibitor, which is a structure-unrelated analog of U0126, called PD98059 (5 μM), but its treatment did not have a consistent significance (negative or positive) on amputation-induced H2O2 level.

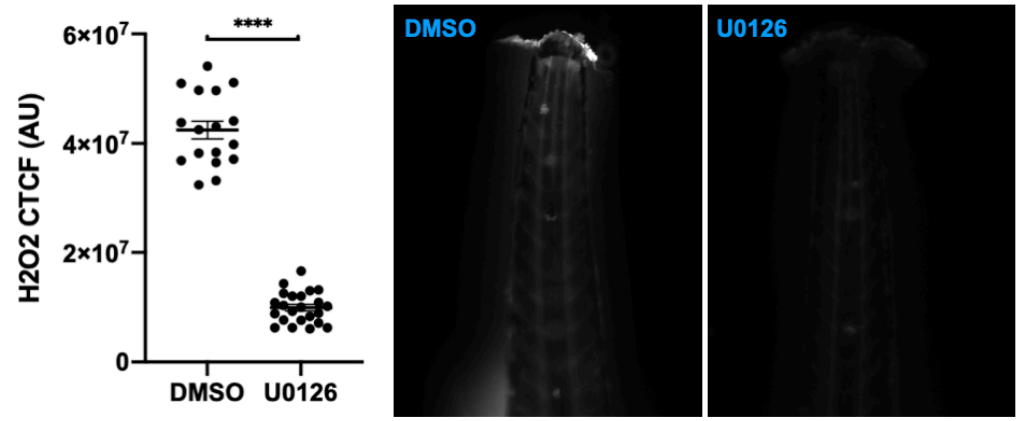

Figure 3-15. Fluorescent images, quantification & statistical analysis of the regenerating tails treated with DMSO or U0126 (250 μM) following 1 hour pre-treatment, amputation between pigment gap & 0.5 hour treatment. Data are expressed as mean ± SEM. DMSO: 44511378.3 ± 10859024.8, U0126: 9940566.4 ± 2861518.2. Significance was determined using Mann-Whitney test versus DMSO control. no significance (ns), P > 0.05; *, P < 0.05; **, P < 0.01; ***, P < 0.001; ****, P < 0.0001. n = 23 biological replicates. Number of experiments = 3.

3.3.4 PKB promotes H2O2 signaling

In my experiments, I found out that the inhibition of PKB activity caused the lowering of amputation-induced H2O2 level. I tried to inhibit PKB activity and then observed how it affected the amputation-induced H2O2 level. For the inhibition of PKB activity, I used a chemical inhibitor called AKT inhibitor IV (1 μM). In the AKT inhibitor IV-treated group, a significant decrease (34920691.1 ± 5927333.4 in control group VS 14657379.6 ± 2639567.1 in AKT inhibitor IV-treated group) in the amputation-induced H2O2 level was observed, suggesting that PKB promotes H2O2 signaling (Figure 3-16).

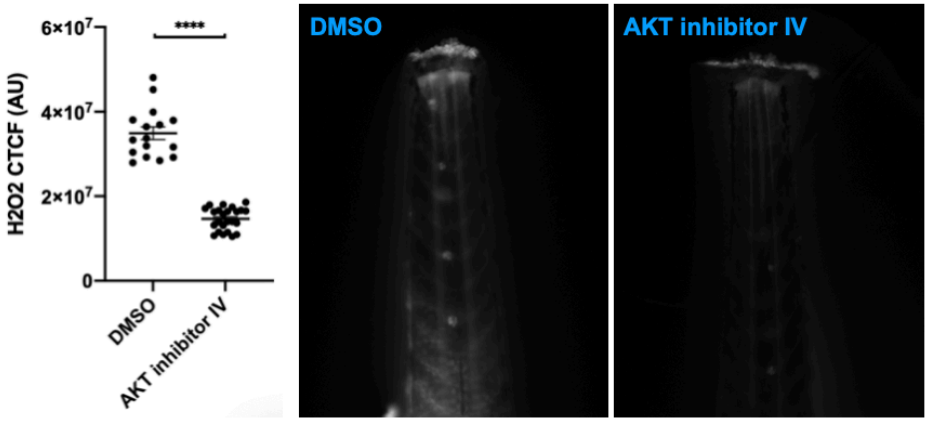

Figure 3-16. Fluorescent images, quantification & statistical analysis of the regenerating tails treated with DMSO or AKT inhibitor IV (1 μM) following 1 hour pre-treatment, amputation between pigment gap & 0.5 hour treatment. Data are expressed as mean ± SEM. DMSO: 34920691.1 ± 5927333.4, AKT inhibitor IV: 14657379.6 ± 2639567.1. Significance was determined using Mann-Whitney test versus DMSO control. no significance (ns), P > 0.05; *, P < 0.05; **, P < 0.01; ***, P < 0.001; ****, P < 0.0001. n = 24 biological replicates. Number of experiments = 3.

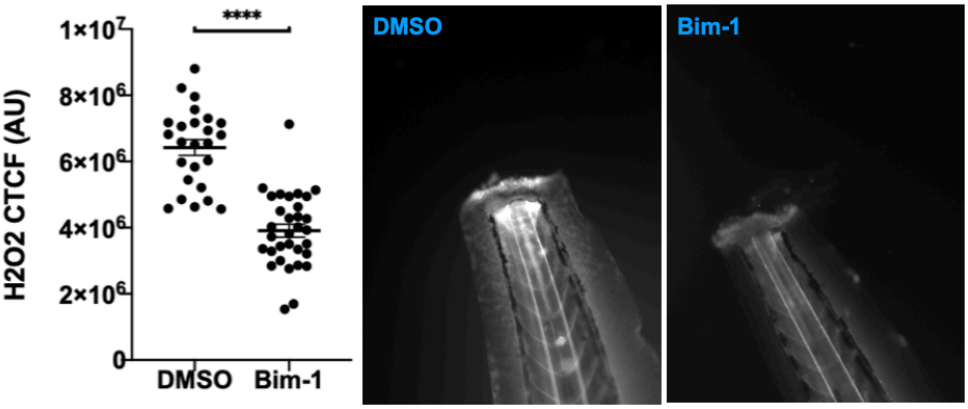

Figure 3-17. Fluorescent images, quantification & statistical analysis of the regenerating tails treated with DMSO or Bim-1 (50 μM) following 1 hour pre-treatment, amputation between pigment gap & 0.5 hour treatment. Data are expressed as mean ± SEM. DMSO: 6416211.2 ± 1196214.6, Bim-1: 3900671.2 ± 1117727.2. Significance was determined using Mann-Whitney test versus DMSO control. no significance (ns), P > 0.05; *, P < 0.05; **, P < 0.01; ***, P < 0.001; ****, P < 0.0001. n = 32 biological replicates. Number of experiments = 3.

3.3.5 PKC promotes H2O2 signaling

In my experiments, I found out that the inhibition of PKC activity caused the lowering of amputation-induced H2O2 level. I tried to inhibit PKC activity and then observed how it affected the amputation-induced H2O2 level. For the inhibition of PKC activity, I used a chemical inhibitor called Bim-1 (50 μM). In the Bim-1-treated group, a significant decrease (6416211.2 ± 1196214.6 in control group VS 3900671.2 ± 1117727.2 in Bim-1-treated group) in the amputation-induced H2O2 level was observed, suggesting that PKC promotes H2O2 signaling (Figure 3-17).

3.3.6 Chemical treatments increased H2O2 level

In my experiments, I found out that the inhibition of PDE activity caused the increase of amputation-induced H2O2 level. I tried to inhibit PDE activity and then observed how it affected the amputation-induced H2O2 level. For the inhibition of PDE activity, I used a chemical inhibitor called MMPX (100 μM). In the MMPX-treated group, a significant increase (36375381.0 ± 7685515.5 in control group VS 58416090.0 ± 15532158.6 in MMPX-treated group) in the amputation-induced H2O2 level was observed.

3.3.7 Chemical treatments were concluded as non-significant (ns) on H2O2 signaling

In my experiments, I also tried many chemicals, which are CPA (100 μM), Dantrolene (100 μM), 2APB (1 μM), PP2 (20 μM), Src inhibitor 1 (5 μM), metformin (1 mM), PD168393 (250 μM), CP316819 (75 μM), CBX (100 μM), Nocodazole (500 μM), MLCK inhibitor peptide 18 (100 μM), GM-6001 (100 μM), TAPI-1 (100 μM), LY294002 (25 μM), Wortmannin (0.5 μM), ACA (1 μM), PPADS (1 mM), Suramin (1 mM) & Y27632 (10 μM) (Table 3-1).

These chemicals are inhibitor of SERCA, inhibitor of RyR, inhibitor of IP3R, inhibitor of SFK, inhibitor of SFK, inhibitor of AMPK, inhibitor of EGFR, inhibitor of GP, inhibitor of HSD, inhibitor of microtubule, inhibitor of MLCK, inhibitor of MMP, inhibitor of MMP, inhibitor of PI3K, inhibitor of PI3K, inhibitor of PLA2, inhibitor of P2R, inhibitor of P2R & inhibitor of Rock, respectively.

These chemical treatments did not have a consistent significance (negative or positive) on amputation-induced H2O2 level.

3.3.8 Confirmative experiments

To verify that H2O2 level was indeed lowered when using inhibitor in the ‘notochord bead extrusion assay’, ‘Ca2+ level assay’ & ‘SFK activity assay’, I also tested the Nox inhibitor, DPI (150 μM), in this H2O2 level assay. In the DPI-treated fish, a significant decrease (67360207.8 ± in 14512287.3 control group VS 22594445.4 ± 8656928.2 in DPI-treated group) in H2O2 level was observed.

3.4 Molecules acting on SFK signaling

For all the ‘SFK activity assays’, the protocols are as follows, unless otherwise stated. By adding chemicals to the media, I gave the 3 or 4 dpf fish 1 hr of pre-treatment & 1 hr of treatment, between which the tail was amputated between the pigment gap. For the visualization & quantification of SFK activity, I used an anti-phosphoSFK antibody for immuno-staining & an epi-fluorescent microscope to take photos at 1 hpa, that is, the end of treatment. Then, I measured & calculated the fluorescence intensity in the wound margin area as corrected total cell fluorescence (CTCF) using Fiji ImageJ.

3.4.1 Chemical treatments were concluded as non-significant (ns) on SFK signaling

In my experiments, I tried many chemicals, which are BAPTA-AM (100 μM), DPI (100 μM), metformin (1 mM), 666-15 (50 μM), PD168393 (250 μM), CP316819 (75 μM), U75302 (5 μM), nocodazole (500 μM), GM-6001 (100 μM), LY294002 (25 μM), KT5720 (50 μM), AKT inhibitor IV (2.5 μM), Bim-1 (50 μM) & PPADS (1 mM) (Table 3-1).

These chemicals are scavenger of Ca2+, inhibitor of Nox, inhibitor of AMPK, inhibitor of CREB, inhibitor of EGFR, inhibitor of GP, inhibitor of LTB4R, inhibitor of microtubule, inhibitor of MMP, inhibitor of PI3K, inhibitor of PKA, inhibitor of PKB, inhibitor of PKC & inhibitor of P2R, respectively.

These chemical treatments did not have a consistent significance (negative or positive) on amputation-induced SFK activity in the epimorphic regeneration process that happens in zebrafish (larva) tail.

3.4.2 Confirmative experiments

To verify that SFK activity was indeed inhibited when using inhibitors in the 'notochord bead extrusion assay', 'Ca2+ level assay' & 'H2O2 level assay', I also tested these SFK inhibitors, PP2 (20 μM) & Src inhibitor 1 (5 μM), in this SFK activity assay. In the PP2-treated fish, a significant decrease (524886.2 ± 338690.0 in control group VS 128138.9 ± 74748.6 in PP2-treated group) in pSFK level was observed. In the Src inhibitor 1-treated fish, a significant decrease (3228984.1 ± 891868.0 in control group VS 1482557.3 ± 428664.7 in Src inhibitor 1-treated group) was also observed.

3.5 Summary

Here I have summarized all the results from all my experiments (Table 3-1), and all the S(−) (significant down-regulation) experimental results from my project (Figure 3-18).

H2O2 → Bead	H2O2 → Ca2+	Ca2+ → H2O2
SFK → Bead	SFK → Ca2+	CREB → H2O2
EGFR → Bead		MAPKK → H2O2
Microtubule → Bead		PKB → H2O2
MMP → Bead		PKC → H2O2
PDE → Bead		
PI3K → Bead		
PKA → Bead		

Figure 3-18. A summary of all the S(−) experimental results of my project.

Chapter 4 Discussion

4.1 Chemical screening in zebrafish larva VS my experiments

In my project (4 types of experiments), I only tried a few dozen chemicals, in small quantities, slowly and laboriously. I have noticed that in other people's chemical screening projects in zebrafish (egg, larva & adult), they can test a lot of chemicals very fast. Typically, hundreds, thousands, or even over 10,000 chemicals can be tested in such projects (Figure 4-1). For the chemical screening in zebrafish eggs, if the embryos used are wild-type ones, the screening rate is 500-1000 chemicals per week with 2 or 3 operators working simultaneously (Kaufman et al., 2009). If the embryos are mutant ones, more embryos are required, thus demanding greater time and effort (Kaufman et al., 2009). It's orders-of-magnitude different from my few dozen. I wonder how they do it and if it was possible for me to try more chemicals faster as well. So, I picked 3 chemical screening projects in zebrafish larva's regeneration process as examples: (1) Nerve regeneration induced by fin-fold damage by tweezer (Bremer et al., 2017). They tried 480 chemicals and found 21 inhibitors. (2) Hair cell regeneration induced by chemical treatment (neomycin) (Namdaran et al., 2012). They tried 1680 chemicals and found 8 molecules, of which 6 were inhibitors & 2 were enhancers. (3) Fin-fold regeneration induced by amputation by a blade (Mathew et al., 2007). They tried 2000 chemicals and found 17 inhibitors.

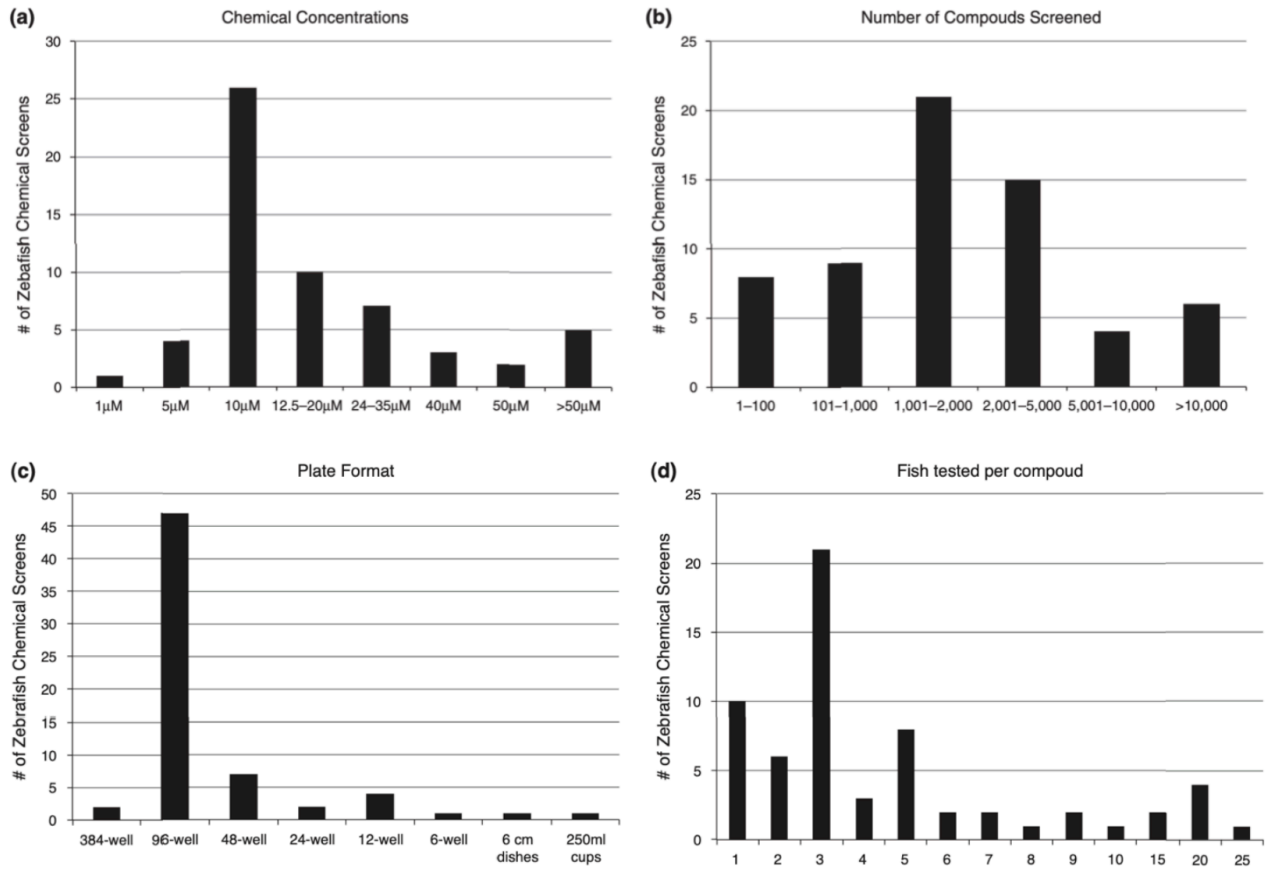

Figure 4-1. 15 years of chemical screening in zebrafish (embryo, larva & adult). 66 studies using screening by the numbers. (A) Concentration of chemicals used for screening. (B) Number of chemicals screened. (C) Type of plate used. (D) Number of zebrafish used for each chemical. Adapted from (Rennekamp & Peterson, 2014).

In the 1st project, they used the ICCB Known Bioactives Library (Enzo), which has 480 small-molecule compounds with known targets (Figure 4-2)(Figure 4-3) (Bremer et al., 2017). In the 1st round, they screened the chemicals for toxicity, and 134 chemicals were excluded for being able to affect the overall health of fish (Bremer et al., 2017). Each chemical was tested individually with n = 3 fish (Bremer et al.,

2017). They uniformly diluted the stock solution from the library 1000 times before treating the fish (Bremer et al., 2017). Due to the variation in stock solution concentration, the treating concentration of each chemical is either 1 μM or 5 μg/mL (Bremer et al., 2017). The criteria for toxicity include: morphological change, cardiac arrest, tissue necrosis & decreased responsiveness to environmental stimulus after 12/24/48 hours of treatment (Bremer et al., 2017). In the 2nd round, they put the remaining 346 chemicals into 69 pools with 4/5 chemicals in each pool (Bremer et al., 2017). 4 fish were put in each pool (Bremer et al., 2017). The fish fin-fold was damaged by a tweezer to induce nerve regeneration; 24 hours of chemical treatment (1:1000 dilution of stock solution) started immediately after damage, and assessment by microscopical-imaging was made immediately after treatment (Bremer et al., 2017). 15 out of 69 pools showed significant results, as the fish failed to form a ring-like axon network (Bremer et al., 2017). The criteria for the significance of each pool is that 2 out of 4 fish failed (Bremer et al., 2017). In the 3rd round, for the chemicals in these 15 pools, the highest concentration without causing toxicity for each chemical was tested (Bremer et al., 2017). For this, 1:1000 to 1:100 dilutions of stock solutions were tested on fish (Bremer et al., 2017). After this, they put 1 chemical in 1 well in the 96-well plates (Bremer et al., 2017). 4 fish were put in each well. The fish fin-fold was damaged by a tweezer to induce nerve regeneration; 24 hours of chemical treatment started immediately after damage, and assessment by microscopical-imaging was made immediately after treatment. 21 chemicals showed significance, as the fish failed to form a ring-like axon network (Bremer et al., 2017). The criteria for the significance of each well is that 2 out of 4 fish failed.

By comparison, I noticed the following (Table 4-1): (1) Multi-well plate VS Glass petri dish, n = 2/3/4 VS n = 15/20, Pooling VS Not Pooling. Most chemical screening projects in zebrafish used multi-well plates, mostly 96-well plates. All 3 example projects used 48/96-well plates. I used a glass Petri dish. For most chemical screening, n = 3. For the 3 examples, n = 2/3/4. In my project, n = 15/20. Some chemical screening used pooling. 1 out of the 3 examples used pooling. In my project, I did not use pooling. These differences mean that: (a) In 1 experiment, I can only do 3/4/5 experiment groups, and therefore could test 3/4/5 chemicals (except for SFK experiments, where the assessment used fixed fish rather than live fish; will be mentioned afterward in this section), while they can do at least 40/90 experiment groups. When an entire library of chemicals needs to be screened, chemicals are sometimes pooled together to save time and effort by reducing the number of duplicate experiments (Stern et al., 2005). However, this practice may lead to unknown interactions occurring between chemicals within a single pool (Kaufman et al., 2009). (b) My ’n’ is bigger, therefore more time-consuming. These 2 factors keep me from testing chemicals in a high/fast-throughput way. Based on my situation, my experimental design can't be further improved to test more chemicals in a faster and less laborious way. (2) [ ] & Toxicity. For most chemical screenings in zebrafish, the screening usually takes several rounds. In different projects with different experimental designs, the same chemical, in different rounds, may be in different concentrations. In the 1st project of the 3 examples, in round 1, each chemical was diluted 1:1000, excluding chemicals with toxicity (Bremer et al., 2017). In round 2, each chemical was still diluted 1:1000 (Bremer et al., 2017). In round 3, the optimum concentration of each chemical was measured first (Bremer et al., 2017). Each chemical was diluted from 1:1000 to 1:100 (Bremer et al., 2017). Then the optimum concentration was used in screening (Bremer et al., 2017). In the 2nd project of the 3 examples, in round 1, each chemical was diluted 1:1000, and they identified 176 chemicals as possible inhibitors & 115 compounds as potential activators, with another 243 drugs showed toxicity (Namdaran et al., 2012). For these 243 drugs, they did not test for lower concentrations to determine whether they could interfere hair cell regeneration while still ensuring animal health (Namdaran et al., 2012). This round was expected to have a few false-negatives and numerous false-positives (Namdaran et al.,

2012). In round 2 & round 3, each chemical was also diluted 1:1000 (Namdaran et al., 2012). To eliminate false-positives, chemicals that were consistent across 3 screenings were considered as ‘hits’ (Namdaran et al., 2012). They confirmed 40 inhibitors of hair cell regeneration & 10 enhancers (Namdaran et al., 2012). In round 4, each chemical’s optimal concentration, which is the lowest concentration with the strongest inhibitory/positive effect, is determined using a dose-response function obtained using a range of doses (from 0.1 μM to 100 μM) (Namdaran et al., 2012). Eventually, they identified 6 inhibitors & 2 activators (Namdaran et al., 2012). I measured the optimal concentration (highest without causing toxicity) of each chemical in the notochord bead extrusion assay and then used it in the Ca2+ level assay, H2O2 level assay & SFK level assay. (3) Assessment (live VS Fix). In my notochord bead extrusion assay, Ca2+ level assay & H2O2 level assay, the assessment was done live. In the SFK level assay, the assessment was done using fixed fish. For the notochord bead extrusion assay, I tried fixing the fish a few times and noticed that fixing made the notochordal beads shrink slightly, which is visible to the naked eye, so I choose to do it live. For the Ca2+ level assay & H2O2 level assay, it can only be done in live due to the nature of the experiments themselves. For the SFK level assay, it can only be done using fixed fish. Therefore, in 1 SFK experiment, I can do 10/11/12 experiment groups and therefore test 10/11/12 chemicals, while in the notochord bead extrusion assay, Ca2+ level assay & H2O2 level assay, I can only do 3/4/5 experiment groups and therefore test 3/4/5 chemicals (as previously described in this section). Based on my situation, my experimental design, these choices cannot be changed to do more or faster. Based on my situation, my experimental design can't be further improved to test more chemicals in a faster and less laborious way. (4) Automation. Some chemical screenings in zebrafish have automation. Counting fish and pipetting the appropriate number into the wells consumes both time and effort (Rennekamp & Peterson, 2014). Currently, several automated systems are under development, with 2 primarily designed for Caenorhabditis elegans and later adapted for zebrafish and 2 designed specifically for zebrafish embryos (Graf et al., 2011; Mandrell et al., 2012). One automation system for zebrafish embryo placement is already in practical use for chemical screening (Truong et al., 2013). None of the 3 examples mentioned automation. In my experiments, I do not have automation. In my experiments, counting & separating fish is the least time-consuming. The most time-consuming steps are tail cutting, mounting & photographing. When it comes to tail-cutting, it has to be cut in a specific position (pigment gap), rather than random damage. I can only do 1 fish at a time, rather than multiple fish at one cut. Based on my situation, my experimental design can't be further improved to test more chemicals in a faster and less laborious way, and I could not find an existing machine/robot to help me at the moment.

480 chemicals [ICCB Known Bioactives library (Enzo)], with 134 chemicals excluding for toxicity
↓
346 chemicals remaining
↓
69 pools × 4/5 chemicals/pool, n = 4 fish/pool
↓
15 pools significant, with 3 pools failed to identify a singly effective chemical
↓
12 pools remaining, with 1/2/3 chemicals/pool identified
↓
21 chemicals identified

Figure 4-3. A flowchart-style casual outline of the experiment from (Bremer et al., 2017). Please be noted that the experiment for further validation and/or variable controlling might have been omitted.

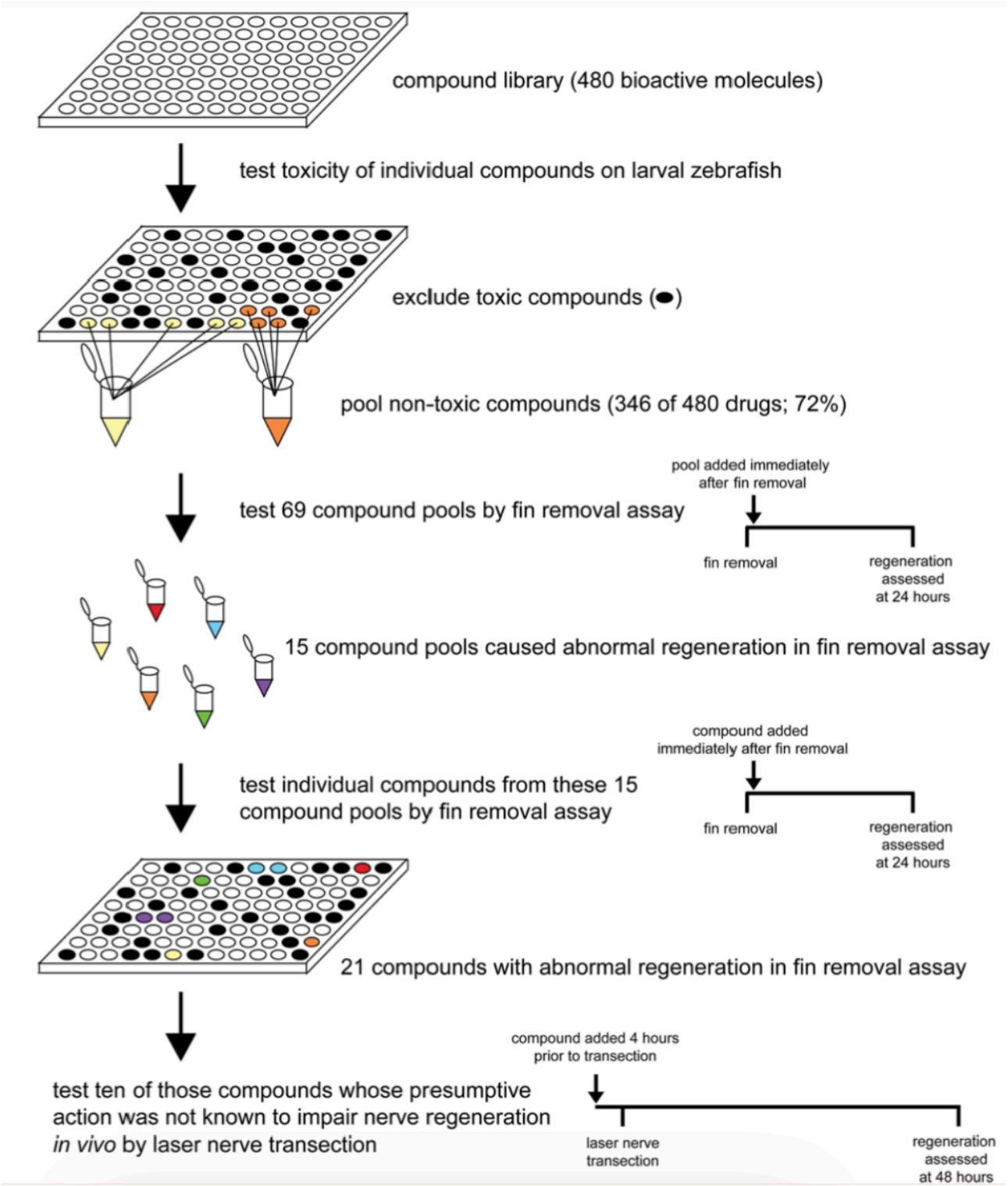

Figure 4-2. The workflow for small-molecule screening. Adapted from (Bremer et al., 2017).

In addition to chemical screening, I have noticed that there are other experiments that can analyze many molecules at the same time, such as gene expression analysis, proteome analysis, etc. In gene expression analysis, a few time points are selected for tissue collection, RNA extraction/isolation & sample preparation, and then micro-array analysis (GeneChip) can analyze about 15,000 genes/transcripts simultaneously and then identify & annotate about 250/500/750 down/up-regulated genes/transcripts using databases (Figure

4-4). In proteomic analysis, the process is similar, but various mass spectrometry analyzes are used to identify hundreds of proteins.

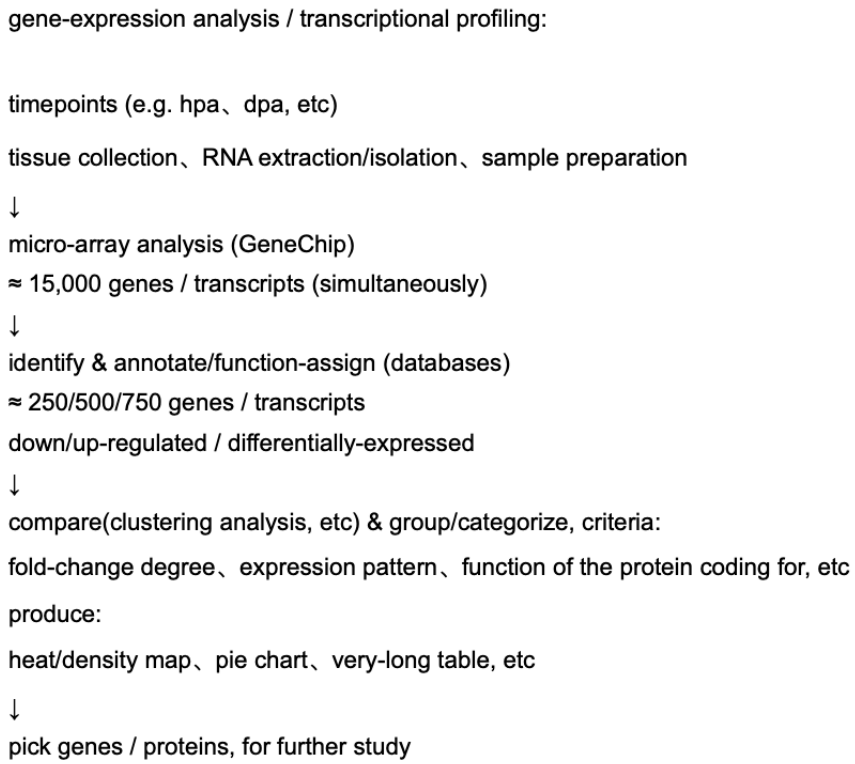

Figure 4-4. A flowchart-style casual outline of ‘gene-expression analysis’ experiments.

For non-protein, non-central dogma (transcription & translation)-related signaling molecules like Ca2+ & H2O2, whose assessment can only be done live, when trying to figure out their roles in the molecular signaling pathway of a physiological/pathological process using the method of exclusion, there doesn't seem to be a relatively quick and easy way. Ca2+ and H2O2 are important signaling molecules that cannot and shouldn’t be dodged. As for a solution for this? I could not provide one.

	(Bremer et al., 2017)	(Namdaran et al., 2012)	(Mathew et al., 2007)
# of chemical screened	480	1680	2000
# of chemical identified	21 (inhibitors)	8 (6 inhibitors + 2 enhancers)	17 (inhibitors)
Multi-well plate type	96-well plate	48-well plate	96-well plate
# of chemical in each well	4/5 chemical/well	1 chemical/well	1 chemical/well
# of fish/chemical/round	4 fish/well	3 fish/well	2 fish/well
[ ] of chemical	1 µM or 5 µg/mL	10 µM or 4 µg/mL	25 µM
Duration of chemical treatment	24 hours.	48 hours.	3 days.
Regeneration type	Nerve regeneration induced by fin-fold damage by tweezer.	Hair cell regeneration induced by chemical treatment (neomycin).	Fin-fold regeneration induced by amputation by blade.
Assessment after treatment	Microscopically imaged.	Microscopically imaged.	Microscopically imaged.
Automation involved ?	Not mentioned.	Not mentioned.	Not mentioned.

Table 4-1. Small-molecule compounds screening in zebrafish larva regeneration from (Bremer et al., 2017), (Namdaran et al., 2012) & (Mathew et al., 2007).

4.2 Notes on my experiments' protocols (designing timetable)

In my project (4 types of experiments), I only tried a few dozen chemicals, in small quantities, slowly and laboriously. Based on my situation, my experimental design cannot be changed to do more and faster. It was already the best it could be. Here, I'll use the H2O2 experiment (ΔF/F0), which is the slowest & most laborious one, as an example to briefly illustrate how I designed my timetable (Figure 4-5).

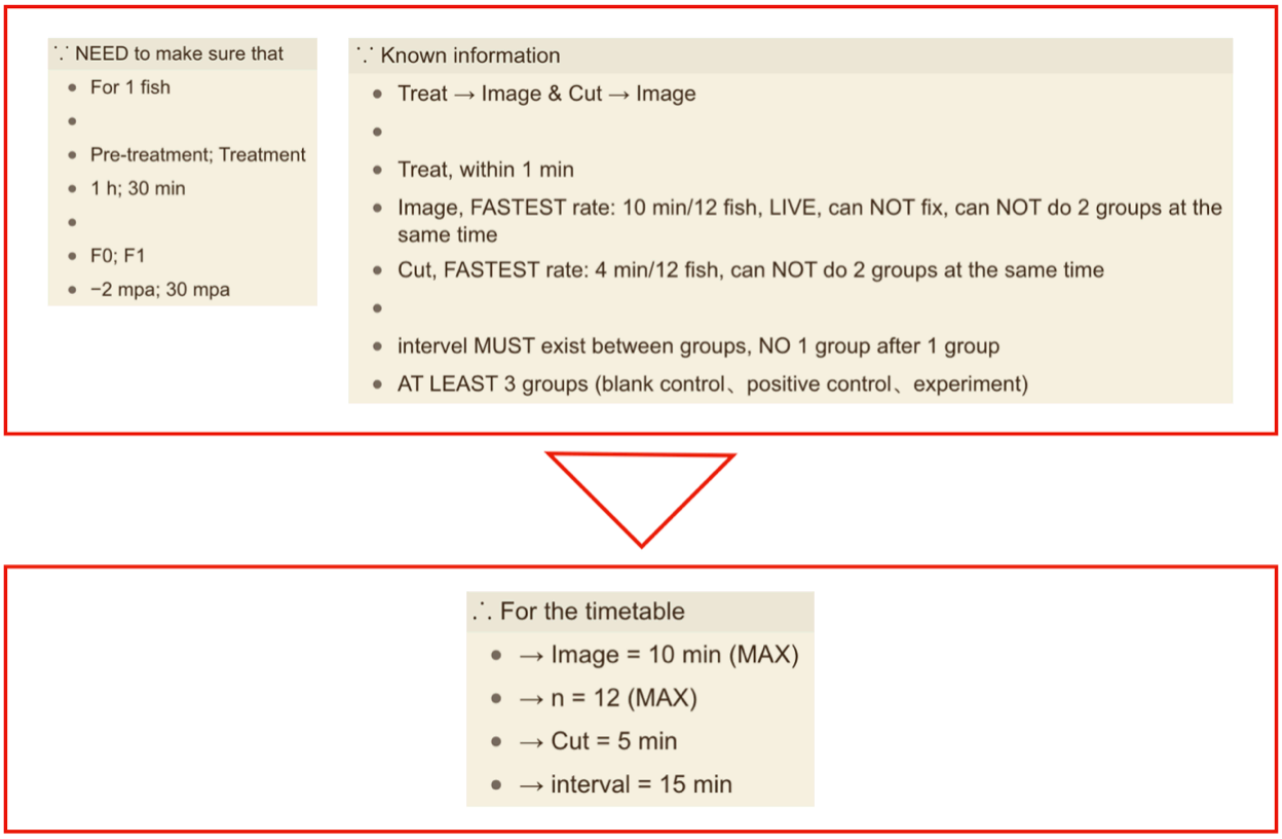

Figure 4-5. Working out the timetable for H2O2 level experiment using the ΔF/F0 method.

For each fish in 1 experiment (several groups), I have to make sure that: (1) The pre-treatment is 1 h; (2) The treatment is 30 min; (3) 1 F0 photo should be taken at -2 mpa; (4) 1 F1 photo should be taken at 30 mpa; (5) 2 photos (F0 & F1) should match, meaning that they should correspond to the same fish.

For each fish, the protocol is: 'Treat → Image & Cut → Image'. It is known/defined that: (1) 'Treat'. It happens very fast, and it cannot be slowed down; (2) 'Image'. Its maximum rate is 10 min for every 12 fish, and it can be slowed down; (3) 'Cut'. Its maximum rate is 4 min for every 12 fish, and it can be slowed down. 'Image' is the most time-consuming one; therefore, it is the rate-limiting step.

For the design of 1 experiment, it is known/defined that: (1) Intervals must exist between each group due to the fact that: (a) 'Image'. Fish can not be fixed. 'Image' can only be done lively, 1 fish after 1 fish; therefore, it is time-consuming, and I can't do 2 groups at once; (b) 'Cut'. It can only be done 1 fish after 1 fish; therefore, it is time-consuming, and I can't do 2 groups at the same time; (c) 'Treat'. I can do at least 2 groups at the same time. Also, the intervals shouldn't be too long to avoid the situation of 1 group starting after 1 group from happening; (2) At least 3 groups (1 blank control group, 1 positive control group, 1 experiment group).

Therefore, all in all, the timetable should be: (1) ‘Image’ = 10 min (maximum); (2) n = 12 (maximum); (3) ‘Cut’ = 5 min; (4) interval = 15 min. However, in the actual experiments, for each fish, the ‘Pre-Treatment’ duration ranged from 1 h to 1 h 5 min, the ‘Treatment’ duration ranged from 33 min to 35 min, the timepoints for F0 photo-taking ranged from -7 mpa to -5 mpa, and the timepoints for F1 photo-taking ranged from 33 mpa to 35 mpa (Table 4-2)(Table 4-3).

Group	Treat (0:00)	Image (0:50); Cut (1:00) 10 min; 5 min	Image (1:30) 10 min
1	0:00	0:50-1:00-1:05	1:30-1:40 ←
2	0:15	1:05-1:15-1:20	1:45-1:55
3	0:30	1:20-1:30-1:35 →	2:00-2:10

Table 4-2. The timetable for 1 H_2O_2 level experiment using the ΔF/F0 method, with the maximum of 3 groups (control + experiment) of fish. Group 1, treat at 0:00; the 10 min imaging (F0) process starts at 0:50 & ends at 1:00; the 5 min tail-cutting process starts at 1:00 & ends at 1:05; the 10 min imaging (F1) process starts at 1:30 & ends at 1:40. Similar interpretation of this table for Group 2 & 3. ‘→’ & ‘←‘ mean that there are some overlaps.

Fish (n)	Treat (0:00)	Image (0:50) 10 min	Cut (1:00) 5 min	Image (1:30) 10 min	Pre-treatment; Treatment	F0; F1
1	0:00	0:53-	1:00-	1:33-	1 h; 33 min	−7 mpa; 33 mpa
2	0:00	0:53-	1:00-	1:33-	1 h; 33 min	−7 mpa; 33 mpa
3	0:00	0:54-	1:01-	1:34-	1 h 1 min; 33 min	−7 mpa; 33 mpa
4	0:00	0:54-	1:01-	1:34-	1 h 1 min; 33 min	−7 mpa; 33 mpa
5	0:00	0:55	1:02-	1:35	1 h 2 min; 33 min	−7 mpa; 33 mpa
6	0:00	0:55	1:02-	1:35	1 h 2 min; 33 min	−7 mpa; 33 mpa
7	0:00	0:58-	1:03-	1:38-	1 h 3 min; 35 min	−5 mpa; 35 mpa
8	0:00	0:58-	1:03-	1:38-	1 h 3 min; 35 min	−5 mpa; 35 mpa
9	0:00	0:59-	1:04-	1:39-	1 h 4 min; 35 min	−5 mpa; 35 mpa
10	0:00	0:59-	1:04-	1:39-	1 h 4 min; 35 min	−5 mpa; 35 mpa
11	0:00	1:00	1:05	1:40	1 h 5 min; 35 min	−5 mpa; 35 mpa
12	0:00	1:00	1:05	1:40	1 h 5 min; 35 min	−5 mpa; 35 mpa

Table 4-3. The timetable for the fish in 1 group (control or experiment) in 1 H_2O_2 level experiment using the F/F0 method, with the maximum of 12 fish in 1 group. For fish #1, treat at 0:00; image (F0) taken at around 0:53; cut at around 1:00; image (F1) taken at 1:33. The duration for pre-treatment is 1 h. The duration for treatment is 33 min. F0 image is taken at −7 mpa. F1 image is taken at 33 mpa. Similar interpretation of this table for the rest of the fish (fish #2 to fish #12).

4.3 Notes on Ca2+ visualization & quantification in my experiments

Currently, in calcium visualization and quantification, the measured calcium can be: (1) free/ionized calcium; (2) bound calcium; (3) total calcium. The measured calcium can be located in: (1) cytoplasm/cytosol. Some literature also uses “intracellular calcium” to denote this; (2) organelle/pool/store. This can be classical sites such as ER/SR and mitochondria, or other sites including Golgi apparatus (GA), etc; (3) nucleus. The essence of measuring calcium signaling is measuring concentration. Calcium signals can be: (1) elementary/ local ones such as blips, puffs, quarks & sparks; (2) global ones containing waves and oscillations, with amplitude and frequency often being measured parameters. Some literature also describes calcium signals as single action-potential (AP)-, single channel-, or IP3-associated.

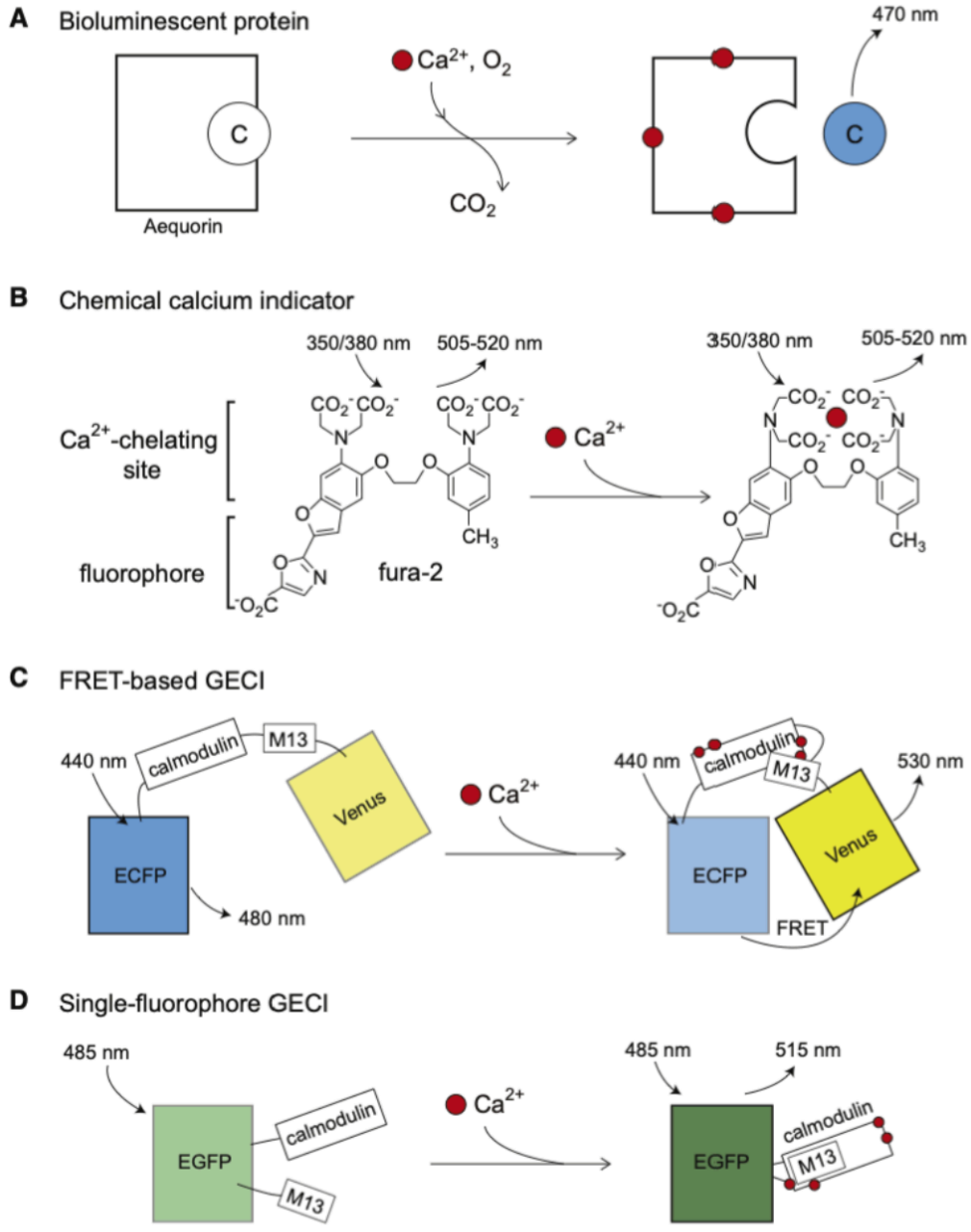

Figure 4-6. Calcium Indicators. (A) Bioluminescent protein. (B) Chemical calcium indicator. (C) FRET-based GECI. (D) Single-fluorophore GECI. Adapted from (Grienberger & Konnerth, 2012).

At present, visualization and quantification of calcium can be performed: (1) in vivo, within living and intact organisms; (2) in vitro, in isolated cell cultures/slices. From a spatial resolution perspective, calcium

measurement can be achieved at: (1) organelle/sub-compartment/sub-cellular level, either in vivo or in vitro; (2) single/multi-cellular level (i.e., ≈ 100/1000 cells), achievable in vivo or in vitro; (3) bulk-tissue level, available in vivo or in vitro as well.

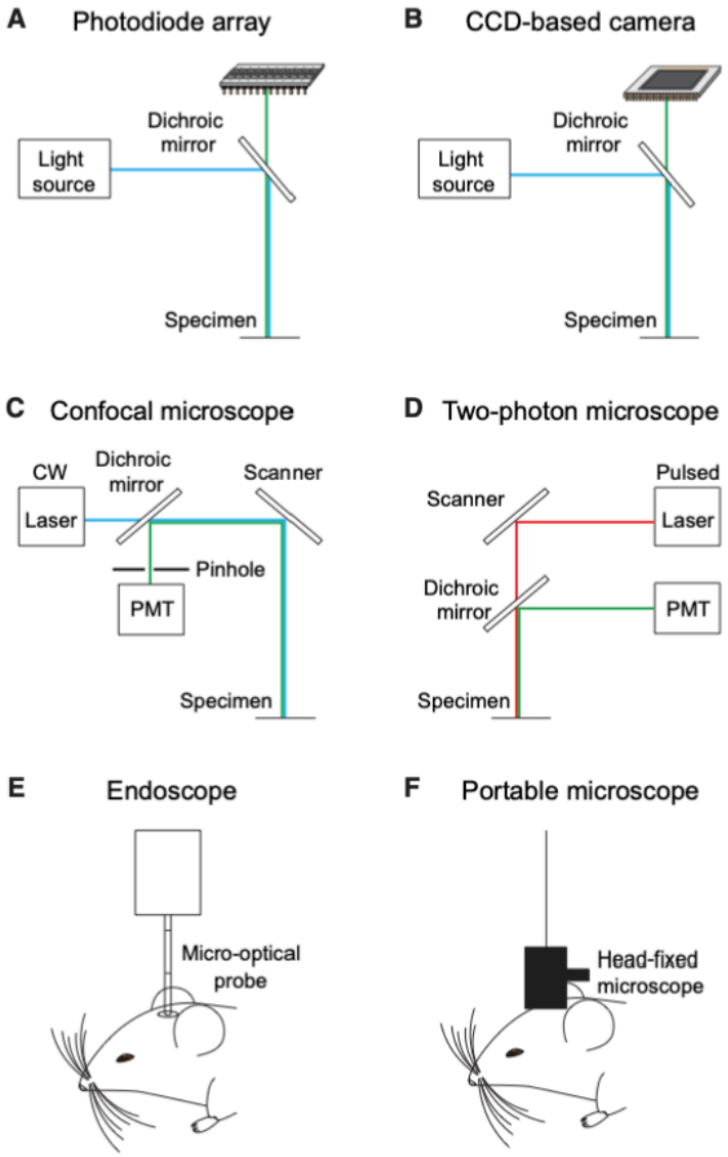

Figure 4-7. Imaging techniques. (A) Wide-field microcope with a photodiode array. (B) Wide-field microcope with a CCD-based camera. (C) Confocal laser scanning microcope. (D) Two-photon laser scanning microcope. (E) Endoscope for non-head-fixed animal. (F) Portable head-fixed microscope. Adapted from (Grienberger & Konnerth, 2012).

The development and current status of Ca2+ visualization and quantification techniques are reviewed in detail in (Grienberger & Konnerth, 2012; Russell, 2010). Here, I'll summarize very roughly the different types of Ca2+ bio-indicators with their delivery technique & matching imaging technique (i.e., the microscope). The major types of Ca2+ bio-indicators, listed chronologically by invention date, are: (1) aequorin; (2) dye; (3) fluorescent protein-based Ca2+ indicator (FPI) / genetically encoded calcium indicator (GECI), etc (Figure 4-6). (1) Aequorin is rarely used nowadays. It is a bio-luminescent protein with a delivery technique that is achievable at the single-cell level, the multi-cell level, or through transgenic organisms. (2) Dyes are fluorescent non-protein organic chemicals that are normally synthetic through chemical-engineering. They can be either single-wavelength ones or dual-wavelength ones, based on their mechanism. Some classic

examples include Arsenazo, Fluo, Fura & Oregon Green, etc. The delivering technique for them could be achieved at either the single-cell level (i.e., an individual cell) or the multi-cell level (i.e., a population of cells with a diameter of approximately 300-500 μm). Single-cell level loading could be implemented through micro-electrode impalement (Jaffe et al., 1992; Svoboda et al., 1997), whole-cell patch-clamp (Eilers & Konnerth, 2009; Margrie et al., 2002), single-cell electroporation (Judkewitz et al., 2009; Kitamura et al., 2008; Nevian & Helmchen, 2007) & single-cell bolus loading (Helmchen et al., 1996), etc. Multi-cell level delivery could be made possible by acetoxymethyl (AM) ester loading (Grynkiewicz et al., 1985), dextran-conjugated loading (Gelperin & Flores, 1997) & bulk electroporation (Nagayama et al., 2007), etc. The imaging techniques for dyes are the same as those of GECIs. (3) GECIs are fluorescent proteins, and their delivery technique is through transgenic organisms. They can be either single-wavelength ones or dual-wavelength ones as well, based on their mechanism. Some common examples include Chameleon, Camgaroo & GCaMP, etc. Imaging techniques for them include standard wide-field epi-fluorescent microscopes, confocal laser-scanning fluorescent microscopes & 2/multi-photon laser-scanning fluorescent microscopes (Figure 4-7). Also, wide-field epi-fluorescent microscopes can be coupled with photodiode arrays, charge-coupled devices (CCDs) or complementary metal-oxide-semiconductor (CMOS) cameras. The light-scattering phenomenon in thick tissue limits the penetration depth of microscopy. For epi-fluorescent microscopy & confocal microscopy, their penetration depth is about 20 μm (Russell, 2010). While for photon microscopy, penetration depth can reach approximately 100 μm. Therefore, the former microscopes are likely used in in vitro studies, whereas the latter one is more suitable for in vivo experiments. In addition, fiber-optic-based micro-endoscopes can provide a certain level of assistance in terms of deeper visualization.

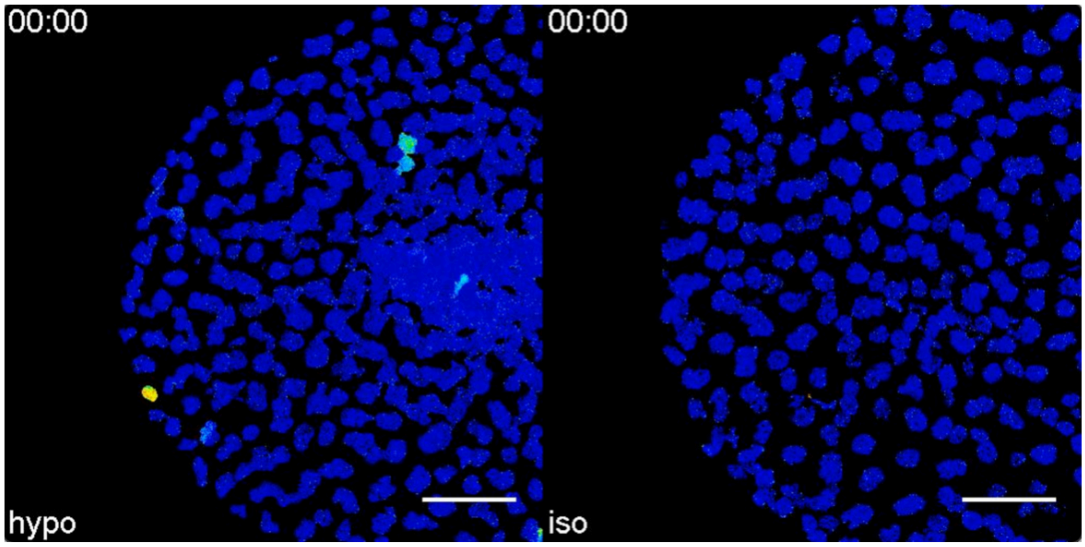

Movie 4-1. Left: Zebrafish's nuclear Ca2+ signal at caudal fin casued by UV-laser damaging in hypotonic solution. Right: Zebrafish's nuclear Ca2+ signal at caudal fin casued by UV-laser damaging in isotonic solution. UV-laser damaging at 60 s. Scale bar: 50 μm. Adapted from (Enyedi et al., 2016).

After visualizing and quantifying calcium, the most basic/typical resulting graph features time on the horizontal axis and fluorescence intensity or [Ca2+] on the vertical axis. Occasionally, the vertical axis displays frequency, and the unit of time can be ms/s/min/h. Direct use of fluorescence intensity represents a qualitative approach, whereas converting fluorescence intensity to [Ca2+] represents a quantitative approach. Semi-quantitative methods are also sometimes employed. Fluorescence intensity is frequently expressed as ΔF/F0 or F/F0, where ΔF denotes relative change and F0 represents the baseline/initial level. Typically, ΔF/F0 ranges between 1% and 20% (Carter et al., 2022). Sometimes, fluorescence intensity is chosen over [Ca2+] because it is more suitable in specific contexts, or conversion to [Ca2+] is unnecessary,

e.g., when using non-ratiometric Ca2+ indicators, which are difficult in terms of calibration (Whitaker, 2010). GCaMP belongs to this category.

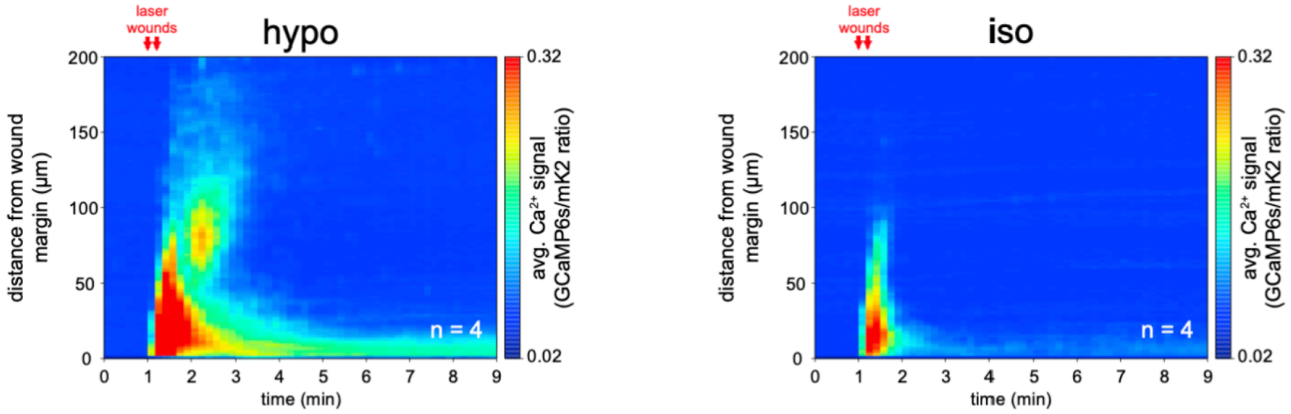

Figure 4-9. Left: transgenic zebrafish Tg(hsp70l: GCaMP6s-NLS-P2A-mK2-NLS)'s spatio-temporal nuclear Ca2+ profile after being wounded in hypotonic medium. Right: transgenic zebrafish Tg(hsp70l: GCaMP6s-NLS-P2A-mK2-NLS)'s spatio-temporal Ca2+ profile after being wounded in isotonic medium. Adapted from (Enyedi et al., 2016).

In my experiment, I used Tg(β-actin:Gal4;uas-GCaMP7a) as the calcium indicator and epi-fluorescent microscopy as the imaging technique to measure free/ionized Ca2+ level in the cytoplasm, with the spatial resolution at the bulk tissue level. Also, the Y axis of my quantification graph is fluorescence intensity (AU).

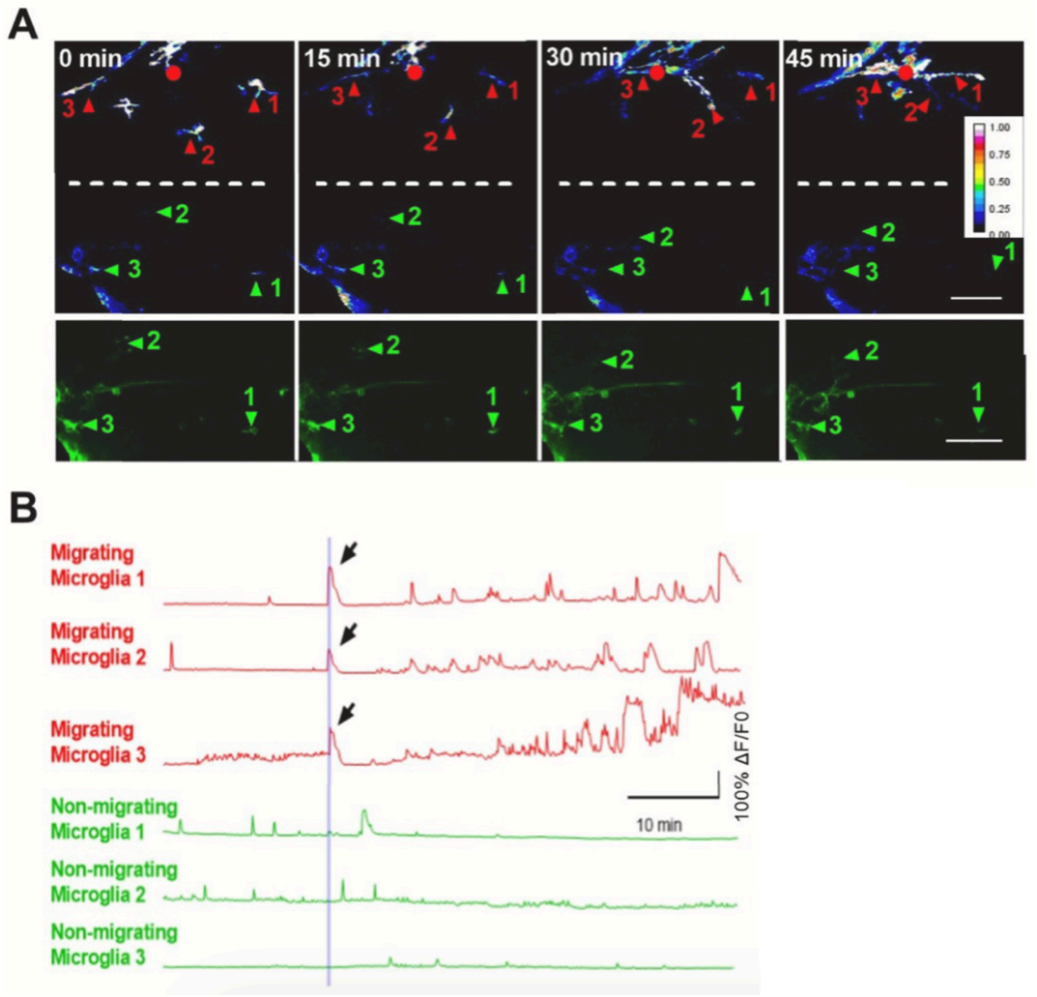

Figure 4-8. (A) Up, microglia's Ca2+ activity & its migration induced by injury. Red dot: laser-induced local brain injury. Red numbers & arrowheads: microglias that are responsive to injury. Green numbers & arrowheads: microglias that are non-responsive to injury. Dashed white line: mid-line between hemispheres. Down, non-responsive microglias in contralateral hemisphere. (B) Microglia's Ca2+ activity in (A). Vertical line: local brain injury. Arrow: injury-induced Ca2+ transient. Adapted from (Du et al., 2022).

I have concerns about the visualization & quantification of Ca2+ level in my experiments, so I found 3 in vivo experiments that used GCaMP to study zebrafish regeneration to compare with my project (Table 4-4). In the 1st study, they focused on local brain injury-induced microglia migration (Figure 4-8) (Du et al., 2022). They used GCaMP5 (expressed in microglia) as the calcium indicator and 2-photon laser-scanning fluorescent microscope as the imaging technique to measure free/ionized Ca2+ level in the cytoplasm, with the spatial resolution at the single/multi-cellular level (Du et al., 2022). Also, the Y axis of their quantification graph is fluorescence intensity (ΔF/F0), and the words 'Ca2+ burst' and 'Ca2+ transient' were used in their report to describe the Ca2+ signal they measured (Du et al., 2022). In the 2nd study, their research is about caudal fin-fold wounding caused by laser (Movie 4-1)(Figure 4-9) (Enyedi et al., 2016). They used nuclear-targeted GCaMP6s as the calcium indicator and confocal laser-scanning fluorescent microscope with spinning disk as the imaging technique to measure free/ionized Ca2+ level in the nucleus, with the spatial resolution at the single/multi-cellular level (Enyedi et al., 2016). Also, the Y axis of their quantification graph is fluorescence intensity (GCaMP6s/mK2 ratio), and the words 'Ca2+ oscillation', 'Ca2+ transient' and 'Ca2+ wave' were used in their report to describe the Ca2+ signal they measured (Enyedi et al., 2016). In the 3rd study, they investigated caudal fin fold wounding-induced macrophage recruitment & activation (Movie 4-2)(Figure 4-10) (Sipka et al., 2021). They used GCaMP6s as the calcium indicator and confocal laser-scanning fluorescent microscope with spinning disk as the imaging technique to measure free/ionized Ca2+ level in the cytoplasm, with the spatial resolution at the single/multi-cellular level (Sipka et al., 2021). Also, the Y axis of their quantification graph is fluorescence intensity (mean gray value), and the words 'Ca2+ oscillation' and 'Ca2+ wave' were used in their report to describe the Ca2+ signal they measured (Sipka et al., 2021).

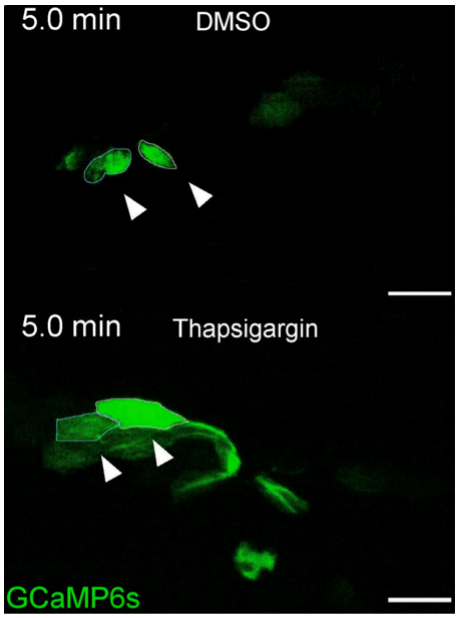

Movie 4-2. Up: GCaMP6s fluorescence in epithelial cell (fin fold) after injury in fish treated with DMSO. Down: GCaMP6s fluorescence in epithelial cell (fin fold) after injury in fish treated with Thapsigargin. Arrowhead: cells picked for quantification. Adapted from (Sipka et al., 2021).

My concern comes mainly from the experiment results of a former member of Roehl's lab. When she applied thapsigargin (a non-competitive SERCA inhibitor) in the Ca2+ level assay using the same transgenic fish line

I utilized, she found that it did not have a consistent effect on Ca2+ levels, and then concluded as ns. However, thapsigargin's use is frequently mentioned in the protocol literature, and it has been reported to be effective in research papers on zebrafish (larva) fin regeneration (Sipka et al., 2021; Yoo et al., 2012). Secondly, the former Roehl lab member who made the Ca2+ time-lapse video mentioned in her Master's thesis that the Ca2+ level condition shown in the video is not quite reproducible (Cheung, 2019). She said that sometimes the fluorescence fades 5 minutes into the time-lapse video and then never appears again (Cheung, 2019). She suspects this may be due to fluorescent bleaching and is concerned that the increase in Ca2+ fluorescence demonstrated in the movie may be due to continued over-exposure (Cheung, 2019).

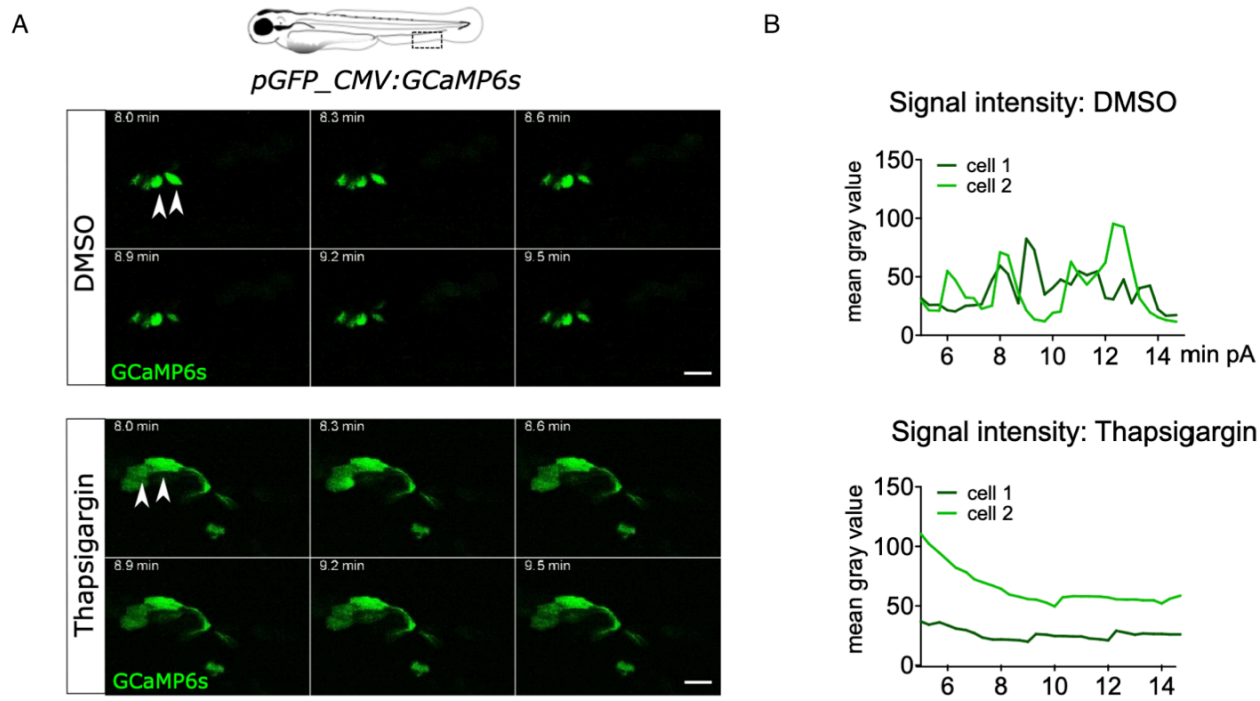

Figure 4-10. (A) Up: Frames from a video showing GCaMP6s fluorescence in epithelial cell (fin fold) in fish treated with DMSO after injury. Down: Frames from a video showing GCaMP6s fluorescence in epithelial cell (fin fold) in fish treated with Thapsigargin after injury. (B) Up: quantification of GCaMP6s fluorescence intensity in fish treated with DMSO. Down: quantification of GCaMP6s fluorescence intensity in fish treated with Thapsigargin. Adapted from (Sipka et al., 2021).

	My project	(Du et al., 2022)	(Enyedi et al., 2016)	(Sipka et al., 2021)
Model animal	zebrafish (larva)	zebrafish (larva)	zebrafish (larva)	zebrafish (larva)
Biological process	tail regeneration by amputaion between the pigment gap	local brain injury-induced microglia migration	caudal fin-fold wounding caused by laser	caudal fin fold wounding-induced macrophage recruitment & activation
Experiment type	in vivo	in vivo	in vivo	in vivo
Calcium indicator used	GCaMP7	GCaMP5 (expressed in microglia)	GCaMP6s (nuclear-targeted)	GCaMP6s
Microscope used	epi-fluorescent microscope	2-photon laser-scanning fluorescent microscope	confocal laser-scanning fluorescent microscope with spinning disk	confocal laser-scanning fluorescent microscope with spinning disk
Calcium type measured	free / ionized Ca2+	free / ionized Ca2+	free / ionized Ca2+	free / ionized Ca2+
Calcium location measured	cytoplasm (presumed)	cytoplasm (presumed)	nucleus	cytoplasm
Spatial resolution	bulk tissue	single/multi-cellular	single/multi-cellular	single/multi-cellular
Terminology used to describe the Calcium signal measured	N/A	Ca2+ burst、Ca2+ transient	Ca2+ oscillation、Ca2+ transient、Ca2+ wave	Ca2+ oscillation、Ca2+ wave
Y axis of Calcium quantification graph	fluorescence intensity (AU)	fluorescence intensity (ΔF/F0)	fluorescence intensity (GCaMP6s/mK2 ratio)	fluorescence intensity (mean gray value)

Table 4-4. In vivo experiments using GCaMP in zebrafish in the context of regeneration from my study, (Du et al., 2022), (Enyedi et al., 2016) & (Sipka et al., 2021).

4.4 Current study's limitations & future work

Molecule	Chemical	Notochord Bead	Ca2+	H2O2	SFK
Ca2+	BAPTA-AM	ns	S(−) N/A	S(−)	ns
SERCA	CPA	ns	ns	ns	N/A
RyR	Dantrolene	ns	ns	ns	N/A
CaV	Flunarizine	ns	ns	N/A	N/A
IP3R	2APB	ns	S(−)	ns	N/A
H2O2	DPI	S(−)	S(−)	S(−) N/A	ns
SFK	KBSRC4	ns	N/A	N/A	N/A
	PP2	S(−)	S(−)	ns	S(−) N/A
	Src inhibitor 1	S(−)	S(+)	ns	S(−) N/A
AMPK	Metformin	ns	S(+)	ns	ns
CREB	666-15	ns	ns	S(−)	ns
EGFR	PD168393	S(−)	S(+)	ns	ns
GP	CP316819	ns	ns	ns	ns
HSD	CBX	ns	S(+)	ns	N/A
LTB4R	U75302	ns	ns	N/A	ns
MAPKK	PD98059	ns	S(+)	ns	N/A
	U0126	ns	S(+)	S(−)	N/A
Microtubule	Nocodazole	S(−)	ns	ns	ns
MLCK	MLCK inhibitor peptide 18	ns	S(+)	ns	N/A
MMP	GM-6001	S(−)	ns	ns	ns
	TAPI-1	S(−)	N/A	ns	N/A
NO•	3-B-7-Nitroindazole	ns	N/A	N/A	N/A
PDE	MMPX	S(−)	S(+)	S(+)	N/A
PI3K	LY294002	ns	ns	ns	ns
	Wortmannin	S(−)	ns	ns	N/A
PKA	KT5720	S(−)	N/A	N/A	ns
PKB	AKT inhibitor IV	ns	ns	S(−)	ns
PKC	Bim-1	S(+)	ns	S(−)	ns
PLA2	ACA	ns	S(+)	ns	N/A
P2R	NF340	ns	N/A	N/A	N/A
	PPADS	ns	ns	ns	ns
	Suramin	ns	N/A	ns	N/A
Rock	Y27632	ns	ns	ns	N/A

Table 4-5. This table summarizes all the experimental results of my project. Please note that this table is identical to the one in the 'Results' chapter, except it has some red boxes created using red borders. Red boxes highlight some of the self-contradictory or noteworthy parts of the results.

My experimental results exhibit some contradictions or noteworthy aspects (Table 4-5)(Table 4-6). 1st, when using structurally-unrelated analogues for the same target molecule, the outcomes are sometimes inconsistent. Examples are: (1) in the notochord bead extrusion assay targeting SFK, its inhibitors KBSRC4, PP2 and Src inhibitor 1 showed different results, with KBSRC4 treatment concluded as ns, while PP2 and Src inhibitor 1 treatment showed significant reduction. A possible reason is that KBSRC4 does not affect fish because it fails to reach the target site, and it only affects mammals because drug development utilized mammalian cell cultures. Also, for experiments aimed at PI3K, its inhibitors LY294002 and Wortmannin exhibited the same problem, with LY294002 treatment being non-significant, whereas Wortmannin treatment was inhibitory. The same possible explanation applies; (2) in the Ca2+ level assay targeting SFK, its inhibitors PP2 and Src inhibitor 1 showed contradictory outcomes, with PP2 treatment presenting significant down-regulation and Src inhibitor 1 treatment presenting significant up-regulation. Unfortunately, I could not offer a reasonable explanation for this; (3) In the H2O2 level assay targeting MAPKK, its inhibitor PD98059 didn't significantly alter the amputation-induced H2O2 level, while U0126 treatment significantly diminished the H2O2 level. Possible explanations are as stated above. 2ndly, in the Ca2+ level assay designed for the Ca2+ transporters (i.e., SERCA, RyR, CaV and IP3R) including channels as well as pumps located on the membrane, most of the inhibitor treatments were concluded as ns (i.e., CPA, Dantrolene & Flunarizine). Only 2APB significantly reduced the tail amputation-induced cytoplasmic Ca2+ level. What I gleaned from this phenomenon is that it is difficult to alter Ca2+ concentration in the cytoplasm simply by using chemicals targeting one individual type of transporter. Therefore, if the goal is to alter cytoplasmic Ca2+ concentration to observe its effect on another factor, using chelating agents is a more direct approach. If the objective is to investigate the role of a specific type of Ca2+ transporter within a signaling pathway/network, relying solely on inhibitors is largely ineffective. 3rd, in the Ca2+ level assay & H2O2 level assay studying IP3R, inhibitor 2APB's treatment significantly decreased amputation-induced cytoplasmic Ca2+ concentration but didn't alter the H2O2 level. Since treatment with BAPTA, which is the Ca2+ scavenger reducing Ca2+ level, decreases the H2O2 level, shouldn't 2APB also reduce the H2O2 level? But that's not the case. Yet, I cannot offer the slightest explanation.

4th, regarding all the S(+) results in my experiments (i.e., notochord bead extrusion assay, Ca2+ level assay and H2O2 level assay), particularly in the Ca2+ experiments where there are numerous S(+) instances, I cannot think of any possible explanation. 5th, in the notochord bead extrusion assay investigating Ca2+, MAPKK, PKB and CREB, all the inhibitor treatments (i.e., BAPTA, U0126, AKT inhibitor IV & 666-15) showed no significance. Shouldn't they show a significant decrease in the notochord bead area, just like the DPI treatment? Due to the fact that these treatments decreased H2O2 level, and the DPI treatment, which reduces H2O2 level, down-regulated the notochord bead, suggesting that H2O2 was involved in notochord bead formation. However, no clear explanation can be offered. 6th, Ca2+ continues to increase after 30 mpa, when the H2O2 starts to decrease. My results suggest that H2O2 promotes Ca2+ signaling, and Ca2+ up-regulates H2O2 signaling as well. So why does the H2O2 level decrease after 30 mpa when Ca2+ increases H2O2 and Ca2+ level continues to increase ? No reasonable explanation can be provided. 7th, my results have suggested that CREB promotes H2O2 signaling. However, CREB is a transcription factor, and gene expression is rather slow. Hence, how does CREB regulate H2O2 level ? One possible scenario is that the 1-hour pre-treatment and 0.5-hour treatment might allow the Duox's expression to be inhibited by CREB. This speculation could be approved or disapproved by measuring the mRNA level of Duox.

Molecule	Chemical	Notochord Bead	H2O2	Ca2+
Ca2+	BAPTA-AM	ns	S(−)	S(−) N/A
H2O2	DPI	S(−)	S(−) N/A	S(−)
SFK	PP2	S(−)	ns	S(−)
	Src inhibitor 1	S(−)	ns	N/A
EGFR	PD168393	S(−)	ns	N/A
MAPKK	U0126	ns	S(−)	N/A
MMP	GM-6001	S(−)	ns	ns
	TAPI-1	S(−)	ns	N/A
PDE	MMPX	S(−)	N/A	N/A
PI3K	Wortmannin	S(−)	ns	ns
PKA	KT5720	S(−)	N/A	N/A
PKB	AKT inhibitor IV	ns	S(−)	ns
PKC	Bim-1	N/A	S(−)	ns
CREB	666-15	ns	S(−)	ns
Microtubule	Nocodazole	S(−)	ns	ns

Table 4-6. This table presents a part of the experimental results of my project, and it is placed here to facilitate demonstrating the self-contradictory or noteworthy parts of the results that could not be highlighted using red boxes. For clear demonstration, several displays have changed compared to the full table of my results: (1) S(+) changed to N/A; (2) Ca2+ column switched with H2O2 column; (3) CREB & Microtubule row moved to the bottom; (4) S(−) box filled with pink.

8th, my results have suggested that microtubule was involved in the notochord bead formation, but in which cells? Some molecules studied in my project (e.g., SFK) have been reported to be involved in immune cell activity, and these molecules have been indicated in my study to be involved in notochord bead formation as well. For example, it has been reported that SFK was involved in neutrophil adhesion and extravasation in the inflammation process that happens in mice (Figure 4-11)(Figure 4-12)(Rohwedder et al., 2019). In their experiments, they found out that the lowering of SFK levels caused impairment of neutrophil adhesion and extravasation (Rohwedder et al., 2019). They tried to lower the SFK level and then observed how it affected neutrophil adhesion and extravasation. For the inflammation induction, they used tumor necrosis factor-α (TNF) injection (Rohwedder et al., 2019). For the lowering of SFK levels, they generated Hck, Fgr & Lyn triple-deficient mice (Rohwedder et al., 2019). For the assessment of neutrophil adhesion and extravasation, they used intravital microscopy, counted the number of neutrophils and calculated the neutrophil adhesion efficiency and extravasation efficiency in the cremaster muscle postcapillary venule and peritoneal cavity (Rohwedder et al., 2019). For the adhesion efficiency in the cremaster muscle postcapillary venule, a significant reduction was observed in SFK-KO mice compared to wild type mice (Rohwedder et al., 2019). For the extravasation efficiency in the cremaster muscle, a significant reduction was observed in SFK-deficient mice compared to control (Rohwedder et al., 2019). For another example, it has been reported that SFK was involved in B cell development in mice (Figure 4-13)(Figure 4-14)(Saijo et al., 2003). In their experiments, they found out that the lowering of SFK levels caused impairment of B cell development (Saijo et al., 2003). They tried to lower SFK level and then observed how it affected B cell development. For the

lowering of SFK levels, they generated Blk, Fyn & Lyn triple-deficient & various double-deficient mice by breeding the Blk, Fyn & Lyn single-deficient mice (Saijo et al., 2003). For the assessment of B cell development, they analyzed B lineage cells in the bone marrow, spleen, lymph nodes and peritoneal cavity using fluorescence-activated cell sorting (FACS) analysis & Topro-3/CaspaTag staining, which stains apoptotic cells (Saijo et al., 2003). B lineage cells include pro-B cells, pre-B cells, immature B cells, recirculating B cells & mature B cells (Saijo et al., 2003). For the B lineage cells in the bone marrow, a significant decrease in viable cell number was observed in the pre-B cells, immature B cells and recirculating B cells in the SFK-deficient mice compared to the wild-type mice (Saijo et al., 2003). For the B lineage cells in the spleen, lymph nodes and peritoneal cavity, a significant reduction was also observed in the SFK-deficient mice compared to the wild-type controls (Saijo et al., 2003). Also, for the pro-B & pre-B cells, a significantly increased number of apoptotic cells was detected in the SFK-deficient mice compared to the control (Saijo et al., 2003). The relationship between these molecules and these immune cells could be explored.

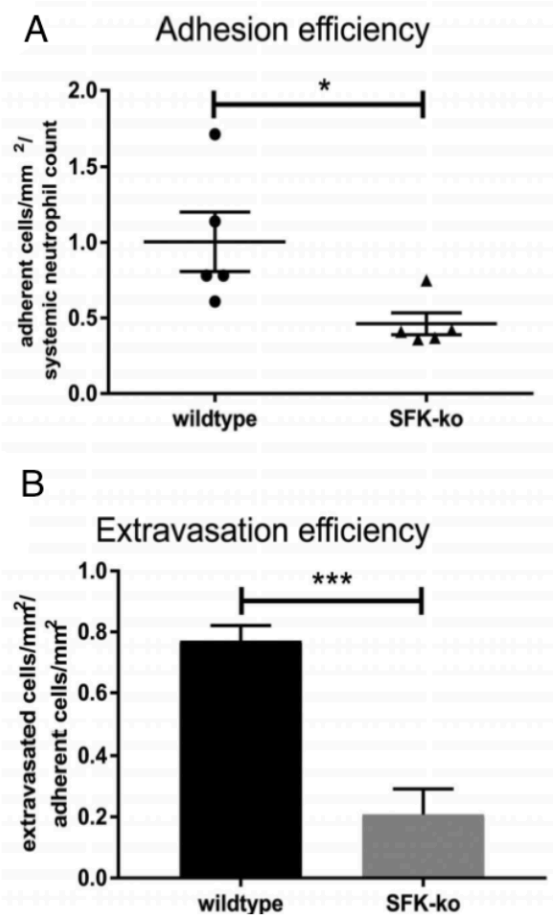

Figure 4-11. (A) Adhesion efficiency from wildtype or SFK-knockout (ko) mice. (B) Extravasation efficiency from wildtype or SFK-ko mice. Adapted from (Rohwedder et al., 2019).

Conclusion:
SFK involved in neutrophil adhesion.
SFK involved in neutrophil extravasation.
↑
Results:
SFK ↓ → neutrophil adhesion ↓
SFK ↓ → neutrophil extravasation ↓
↑
Strain of thoughts for experiment-designing:
SFK ↓ → neutrophil adhesion ?
SFK ↓ → neutrophil extravasation ?
↑
Techniques/methods used to implement strain of thoughts:
'inflammation'
TNF-α injection

'SFK ↓'
gene knockout of Hck、Fgr、Lyn

'neutrophil ?'
intravital microscopy

number
adhesion efficiency
extravasation efficiency

cremaster muscle postcapillary venule
peritoneal cavity

Figure 4-12. A flowchart-style casual outline of the experiment from (Rohwedder et al., 2019). Please be noted that the experiment for further validation and/or variable controlling might have been omitted.

It is very difficult to put all the results into a possible model of a signaling network. Much more reliable data is needed to decipher the mechanism. There are too many molecules involved and a little bit of data for each of

the molecules. The limitations in the experiment design, which will be discussed below, make the results valid but with low confidence (Figure 4-15)(Figure 4-16). Hence, the results should be interpreted with utmost caution.

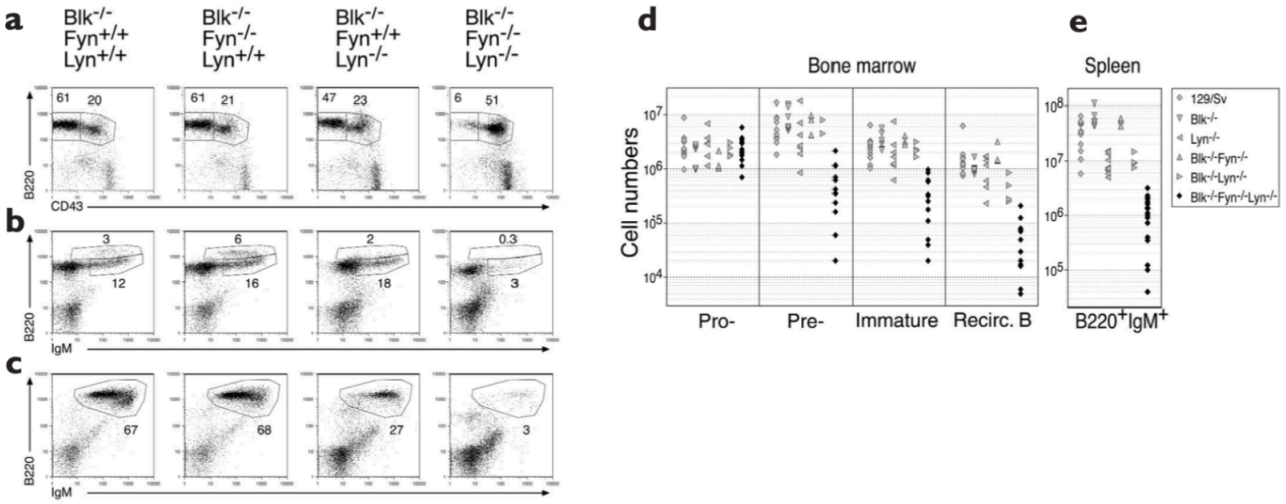

Figure 4-13. (A-C) FACS analysis of B cells in bone marrow (a,b) & spleen (c) in various SFK-deficient mice. (D-E) Numbers of B cells in wild-type & SFK-deficient mice. Adapted from (Saijo et al., 2003).

Conclusion:
SFK involved in B cell development.
↑
Results:
SFK ↓ → B cell ↓
↑
Strain of thoughts for experiment-designing:
SFK ↓ → B cell ?
↑
Techniques/methods used to implement strain of thoughts:
'SFK ↓'
various(single/double/triple) Blk/Fyn/Lyn-deficient mice

'B cell ?'
FACS(fluorescence-activated cell sorting) analysis
Topro-3、CaspaTag staining

pro-B
pre-B
immature B
recirculating B
mature B

bone marrow
spleen
lymph node
peritoneal cavity

number
viable
apoptotic

Figure 4-14. A flowchart-style casual outline of the experiment from (Saijo et al., 2003). Please be noted that the experiment for further validation and/or variable controlling might have been omitted.

Strain of thoughts for experiment-designing:

after tail amputation

X molecule ↓ → notochord bead ?

X molecule ↓ → Ca2+ ?

X molecule ↓ → H2O2 ?

X molecule ↓ → SFK ?

↑

Techniques/methods used to implement strain of thoughts:

'tail amputation'

between zebrafish (larva) tail's pigment gap.

'X molecule ↓'

Chemical

- inhibitor、scavenger
- dose (optimal)、duration, incline to subjectives
  - Dose (optimal)
    - highest & NO toxicity
    - Notochord bead → Ca2+、H2O2、SFK
    - 1 mM (Max)
  - Duration
    - Notochord bead: -1 hpa to 6 hpa.
    - Ca2+: -1 hpa to 1 hpa.
    - H2O2: -1 hpa to 0.5 hpa.
    - SFK: -1 hpa to 1 hpa.

'Notochord bead ?'

- Visualization
  - bright field microscope
- Quantification
  - Area + Fiji ImageJ
- Timing
  - at 6 hpa

'Ca2+ ?'

- Visualization
  - GCaMP + epi-fluorescent microscope
- Quantification
  - CTCF + Fiji ImageJ
- Timing
  - at 1 hpa
- Space
  - Wound margin + trunk

'H2O2 ?'

- Visualization
  - PFBS-F + epi-fluorescent microscope
- Quantification
  - CTCF + Fiji ImageJ
- Timing
  - at 0.5 hpa (peak)
- Space
  - Wound margin

'SFK ?'

- Visualization
  - A183 antibody + epi-fluorescent microscope
- Quantification
  - CTCF + Fiji ImageJ
- Timing
  - at 1 hpa
- Space
  - Wound margin

Further confirmation

- Chemical
  - Structrally-unrelated analog

Limitations & future work:

'X molecule ↓'

Chemical

- Duration
  - after amputation, e.g., 3 hpa to 5 hpa

Gene knock-down / knock-out

- CRISPR-Cas、MO、siRNA, etc
- side effect / redundancy

'Notochord bead ?'

- Quantification
  - volume
- Timing
  - continuous dynamics

'Ca2+ ?'

- Visualization
  - GCaMP using different promotor
  - 2nd method, R-GECO, etc
- Timing
  - continuous dynamics
- Space
    - which cells (cellular level)

'H2O2 ?'

- Visualization
  - 2nd method, HyPer 3, etc
- Timing
  - continuous dynamics
- Space
    - which cells (cellular level)

'SFK ?'

- Visualization / Quantification
  - Western blot、RT-PCR, etc
- Timing
  - continuous dynamics
- Space
    - which cells (cellular level)
- Sub-type
  - expression pattern
  - database(EST analysis) / literature

Further confirmation

- more structrally-unrelated analogs
- rescue experiment, activator、CaCl2 solution、H2O2 solution

Controlling the variables

- no amputation (control group)
- increased tissue volume
- pH change (probe BCECF-AM)

Figure 4-15. The left panel is a flowchart-style casual outline of all my experiments in my project. The right panel is a casual outline of my current project's limitations and some possible future work. Please see text for details. Also, the left panel is identical to the figure in the 'Materials & Methods' chapter.

In the current study, when using chemical treatment to lower the level or inhibit the activity of molecules of interest, the methodology might be problematic. 1st, the concentration for the Ca2+/H2O2/SFK level assay was determined in the notochord bead formation assay. While the treatment time for the notochord bead formation assay was 6 hrs, the treatment time for the Ca2+/H2O2/SFK level assay was 1/0.5/1 hr, which is much less than 6 hrs. The concentration for the Ca2+/H2O2/SFK level assay could be higher due to the fact that their treatment time is shorter and the fish may be more tolerable for higher concentrations. False non-significance might be caused by a potential low concentration. 2nd, when determining the optimal concentration in the notochord bead formation assay, the standard is that the optimal concentration is the highest one that does not cause any observable toxicity. This is determined by observing the fish with naked eyes or under a bright-field microscope and judging from common sense and experience, to see if this fish looks sick or not. In this case, toxicity is a rather vague concept due to the fact that no measurement of any quantitative variables was made. The concentration might be too high for the fish, but it was not noticed. False significant reduction might be caused by the potential high concentration. 3rd, the selection of chemical treatment's parameter combinations (i.e., concentration & duration) is prone to subjective influence (Figure 4-17). Here I use the cases in the notochord bead formation assay as examples, and this also applies to the other 3 assays. When designing the experiments for the notochord bead formation assay, I intended to use the same pre-treatment and treatment duration (i.e., from −1 hpa to 6 hpa) for all chemicals. I am aware that DPI has been used by former Roehl lab members in notochord bead extrusion assays before. Therefore, instead of testing for the optimal concentration like I did with all the other chemicals, I took a glance at their paper, noticed the number 150 μM and used it in my experiment. However, fish dosed with 150 μM DPI for 1 hour of pre-treatment and 6 hours of treatment showed toxicity. Naturally, I tried a lower concentration and found out that 1 hour pre-treatment and 6 hours treatment of 50 μM DPI did not have a significant impact (ns) on notochord bead extrusion. Thus, I went back and carefully reviewed the paper, noticing that their treatment duration is 1 hour. In their assay, 1 hour pre-treatment and 1 hour of treatment with 150 μM DPI significantly decrease the notochord bead area at 6 hpa. As can be seen above, different combinations of concentration and duration yield entirely different outcomes for the same chemical (DPI). This phenomenon indicates that it is possible to achieve one's desired outcome [i.e., ns, S(+) or S(−)] through a certain combination of dose and duration selected under the influence of subjectives. I believe the best way to minimize/avoid this situation is by maintaining consistency throughout the entire notochord bead extrusion assay through using the same timepoints for all the chemicals. My experiments were conducted this way, but other Roehl lab members' are not. In their notochord bead assays, different time points were used for each chemical, with DPI treatment from -1 hpa to 1 hpa, MCI186 (a ROS scavenger) treatment from 0 hpa to 3 hpa, PP2 treatment from -1 hpa to 6 hpa, and Nocodazole treatment from 0 hpa to 6 hpa (Romero et al., 2018).

In the current study, when using chemical treatment for intervention, there is another type of design for duration (Figure 4-18). In my current project, chemical treatments' durations all include pre-treatment, but it is also worth trying to omit the pre-treatment, meaning administering the drug after tail amputation, even though not necessarily right after. These 2 different designs have been reported to yield different results in zebrafish tail regeneration studies, though what they assessed are regenerate length and neutrophils at the amputation site (Yoo et al., 2012). If I try to adapt this new design to my project, the notochord bead assay is more suitable/adaptable, while the other 3 assays seem less feasible due to the fact that their timepoints for assessment were set too close to the amputation. For example, I could set the treatment from 2 hpa to 6 hpa

for the notochord bead assay, rather than from -1 hpa to 6 hpa. Also, could this 'different outcomes by different durations' case be another example of the 'influence by subjectives' I described above?

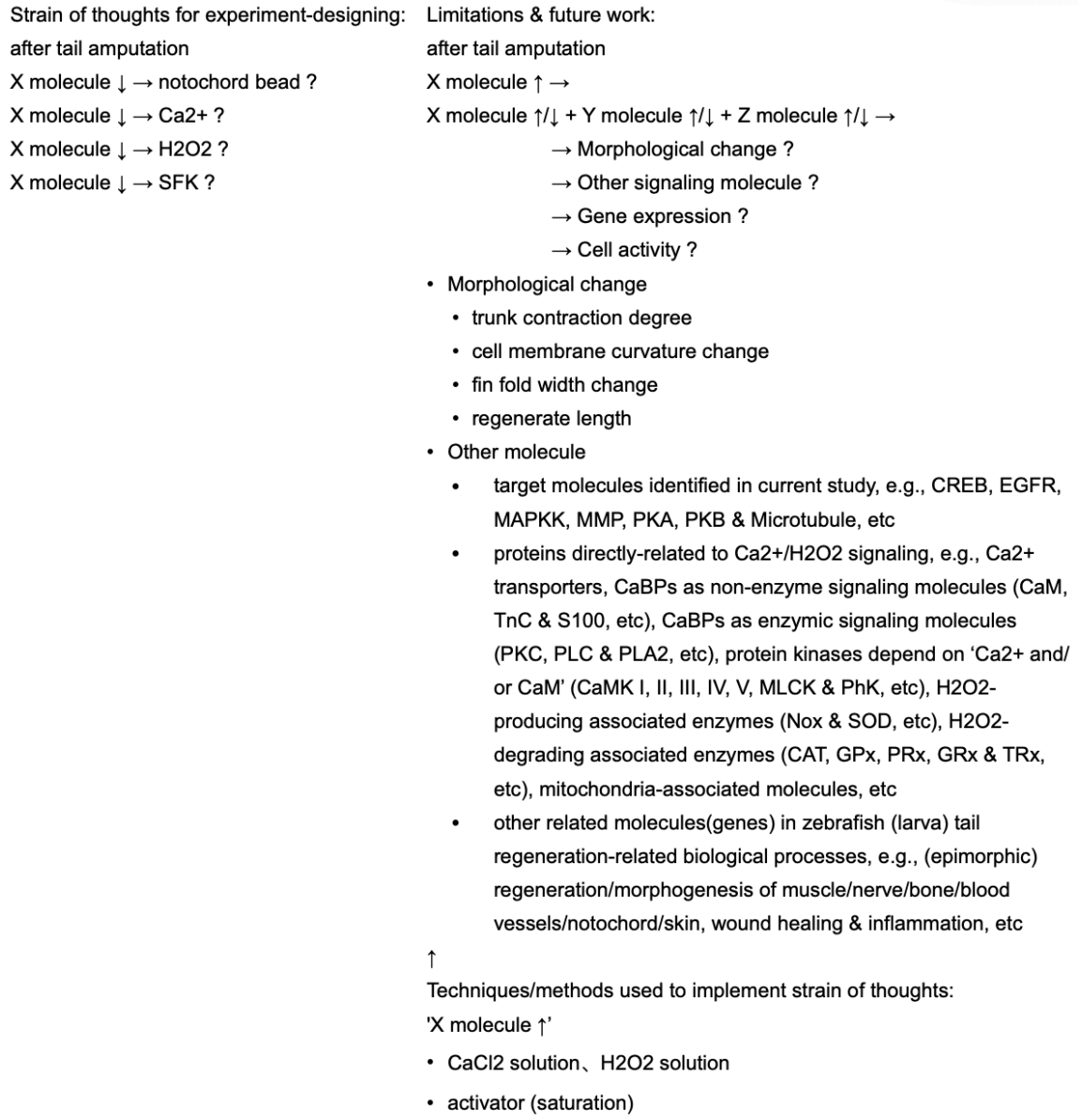

Figure 4-16. The right panel is a flowchart-style casual outline of my current project's limitations and some possible future work. Please see text for details.

In the current study, for lowering the level or inhibiting the activity of certain molecules of interest, I only used one method, that is, chemical treatment. Experiments that use other methods to lower the level or inhibit the activity of these molecules could be performed. For example, gene knock-out or knock-down of the H2O2-producing enzyme, SFK or other protein molecules targeted in this study using CRISPR-Cas, morpholino (MO) or small interfering RNA (siRNA), could be performed. However, gene knock-out/knock-down may cause side effects that compromise the survival of the zebrafish. Furthermore, healthy zebrafish with successful gene knock-out/knock-down may inherently possess redundancy, rendering gene manipulation ineffective, meaning that the level of targeted molecule remains unaltered.

In the current study, for the assessment of notochord bead formation, it is the area of the notochord bead in the photo that was measured. It would be ideal to measure the volume of the notochord bead instead of the area.

In the current study, for the visualization and/or quantification of the amputation-induced Ca2+/H2O2/SFK signaling, I only used one method for each molecule, which is GCaMP7a (a genetically-encoded fluorescent indicator), PFBS-F (a fluorescent dye) and A183 immuno-staining antibody for Ca2+/H2O2/pSFK, respectively. Experiments that use other methods, such as GCaMP using a different promoter and R-GECO (a genetically encoded fluorescent probe) for Ca2+, HyPer 3 (a genetically-encoded fluorescent indicator) for H2O2, Western blot (WB) and RT-PCR for pSFK, could be carried out.

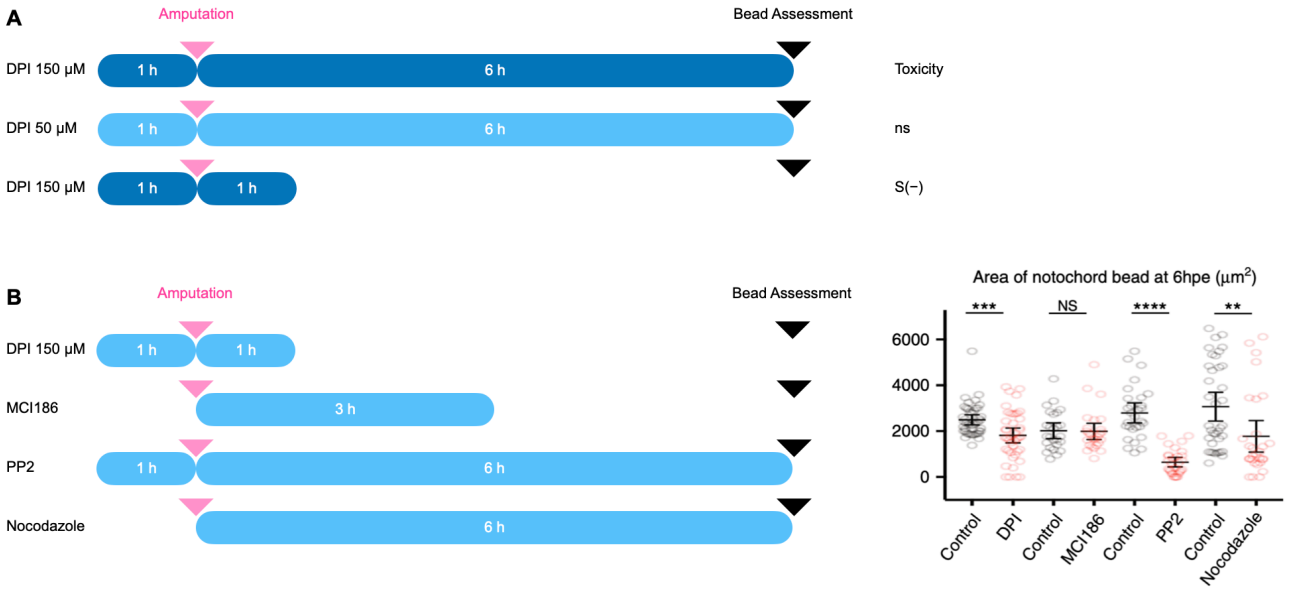

Figure 4-17. A schematic demonstration of the timing of the drug intervention, tail-cutting and assessment of the notochord bead formation. The pink arrow indicates the tail amputation between the pigment gap; the black arrow stands for bead assessment; the blue rectangle refers to the chemical treatment, with its duration written in white text, and deeper blue indicates higher concentration; ns stands for non-significant; S(−) stands for significant decrease. The tail excision happens right after pre-treatment and before treatment, and the assessment takes place immediately after treatment. Please see text for details. (A) The upper 2 rectangles are made to illustrate the experiments from my project, while the 3rd rectangle is made by me with information from (Romero et al., 2018). (B) The left figure is made using the parameters from (Romero et al., 2018). The right graph is adapted from (Romero et al., 2018).

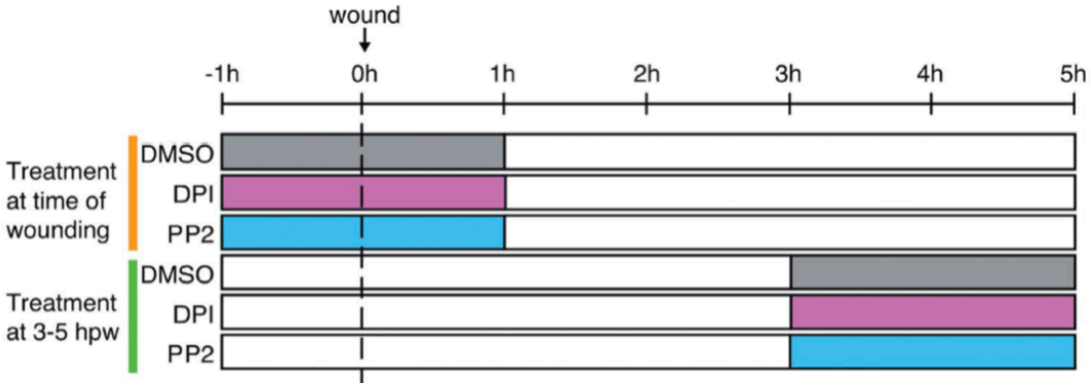

Figure 4-18. A schematic demonstration of the timing of the drug intervention, tail-cutting. The upper 3 rectangles marked in yellow represent the type of design for chemical intervention's duration that I used in my project, i.e., the ones that include pre-treatment. The lower 3 rectangles marked in green represent another type of design that I could have tried in my experiments but did not, i.e., the ones that do not include pre-treatment. Adapted from (Yoo et al., 2012).

In the current study, for the visualization and quantification of the level/activity of amputation-induced Ca2+, H2O2 & SFK, only the level/activity at one timepoint was assessed. The time point for Ca2+/H2O2/pSFK level was picked at 1 hpa, 0.5 hpa & 1 hpa, respectively. 0.5 hpa is the peak time of H2O2 level determined by previous members of the Roehl lab. Whereas 1 hpa is not necessarily the peaking point for Ca2+/pSFK level, as former members of the Roehl lab only visualized it upon 1 hpa and demonstrated that Ca2+/pSFK level continues to increase until 1 hpa, which is worrisome. Therefore, it is worthwhile to conduct

experiments that visualize and quantify Ca2+ and pSFK levels beyond 1 hpa and determine their peaking point. Moreover, it would be ideal to carry out continuous visualization and quantification of the level of Ca2+, H2O2 & pSFK instead of just one time point, due to the fact that maybe it is the dynamics of the level of these molecules that matters. For example, after the drug intervention, the H2O2 level could increase at a slower rate, so that the slope of the curve is not as steep as in the control group. The peak time could be later than 30 mpa. The level of H2O2 at the peak time is not necessarily lower than that of the control group. Even, it could be higher. Just measuring the H2O2 level at 30 mpa could lead to a wrong result and conclusion that the H2O2 level was decreased. Not to mention the fact that Ca2+ continued to increase after 30 mpa, when the H2O2 started to decrease. Despite that, my results suggest that H2O2 promoted Ca2+ signaling. Since my results also suggest that SFK promoted Ca2+ signaling, could the increase in Ca2+ level between 30 mpa and 1 hpa have something to do with SFK? However, the level of SFK was only measured at 1 hpa. The data obtained by measuring the level at only one time point seems to be far from sufficient to elucidate the mechanism.

Conclusion:
Duox 1 produced H2O2.
↑
Results:
Nox 1 ↓ → H2O2 =
Nox 2 ↓ → H2O2 =
Nox 4 ↓ → H2O2 =
tail fin → Nox 5 not expressed
tail fin → Duox 1 expressed
Duox 1 ↓ → H2O2 ↓
↑
Strain of thoughts for experiment-designing:
Nox 1 ↓ → H2O2 ?
Nox 2 ↓ → H2O2 ?
Nox 4 ↓ → H2O2 ?
Tail fin → Nox 5 ?
Tail fin → Duox 1 ?
Duox 1 ↓ → H2O2 ?
(knowing there are Nox 1、Nox 2、Nox 4、Nox 5、Duox 1)
↑
Techniques/methods used to implement strain of thoughts:
'Nox 1 ↓'
'Nox 2 ↓'
'Nox 4 ↓'
MO for gene expression silencing (targeting P22phox/cyba subunit)

'Nox 5 ?'
'Duox 1 ?'
semi-quantitative PCR

'Duox 1 ↓'
MO for gene expression silencing

Figure 4-19. A flowchart-style casual outline of the experiment from (Niethammer et al., 2009). Please be noted that the experiment for further validation and/or variable controlling might have been omitted.

In the current study, the cellular source of these amputation-induced Ca2+, H2O2 & SFK was not specified. I basically just measured the fluorescence density in the trunk area. For the Ca2+ level, the measurement covered the majority of the trunk area, including the wound margin. For the H2O2 level, a smaller area was covered, with the measurement was made only along the edge of the cutting site. For the SFK level, the same measuring area for H2O2 level, which is the wound margin, was utilized. Experiments to determine the source of Ca2+, H2O2 & SFK could be carried out. Moreover, certain areas or structures were sometimes observed to be very bright with a high level of fluorescent density. For the Ca2+ level, the lateral line sensory system was sometimes very bright. For the H2O2 level, some very bright dots around the wounding site were sometimes observed. They seem to be the epithelial cells covering the cutting site. However, no formal further investigation was performed.

All SFK members
↓ (EST analysis)
Src、Fyna、Fynb、Yes、Yrk
↓ (RT-PCR)
Fynb & Yes
↓ (MO gene knock-down)
Fynb involved in regeneration

Figure 4-20. A flowchart-style casual outline of the experiment from (Yoo et al., 2012). Please be noted that the experiment for further validation and/or variable controlling might have been omitted.

In the current study, for all the protein molecules studied (e.g., SFK), exactly which subtypes were involved in the notchord bead formation or interacted with other signaling molecules was not specified. These protein signaling molecules all have many subtypes; these subtypes have different expression patterns in different species and in different cell types. Some of the pattern information may be found in the database or literature to help identify the specific subtypes involving. For example, It has been reported that H2O2 was produced by Duox 1 in the regeneration process that happens in zebrafish's tail fin (Figure 4-19)(Niethammer et al., 2009). From the literature, they know that the types of Nox that are encoded by the zebrafish genome are Nox 1, Nox 2, Nox 4, Nox 5 & Duox 1 (Oktyabrsky & Smirnova, 2007). First, they tried to lower the level of Nox 1, Nox 2 and Nox 4 and then observed how it affected the H2O2 level (Niethammer et al., 2009). Also from the literature, they know that Nox 1, Nox 2 and Nox 4 all have a subunit called P22phox (cyba) (Bedard & Krause, 2007). So for the lowering of Nox 1, Nox 2 & Nox 4 level, they tried to interfere with the P22phox pre-mRNA splicing process (Niethammer et al., 2009). They used anti-sense morpholino (MO), the gene expression silencing tool, to target the pre-mRNA splice sites of the P22phox subunit of Nox 1, Nox 2 and Nox 4 (Niethammer et al., 2009). No significant change in the H2O2 level was observed, so this ruled out Nox 1, Nox 2 and Nox 4 (Niethammer et al., 2009). Now the candidate molecules are Nox 5 & Duox 1. Then, they performed semi-quantitative PCR for Nox 5 & Duox 1 and found out that Nox 5 is not expressed in the tail fin, but Duox 1 is expressed (Niethammer et al., 2009). Finally, they used MO for Duox 1 as well (Niethammer et al., 2009). The lowering of the Duox 1 level significantly decreased the H2O2 level (Niethammer et al., 2009). Therefore, Duox 1 is the Nox enzyme that produced the wound-induced H2O2. For another example, It has been reported that fynb is the SFK that is involved in the zebrafish's tail fin fold regeneration (Figure 4-20)(Yoo et al., 2012). First, they analyzed the expressed sequence tag (EST) profiles in the NCBI UniGene database and found that among all SFK members, Src, Fyna, Fynb, Yes & Yrk are

likely to be expressed in the fin fold (Yoo et al., 2012). Then, they performed RT-PCR and detected Fynb & Yes in the caudal fin and epithelial cells after purifying the mRNA from the tip of the tail fin and using fluorescence-activated cell sorting (FACS) to sort the green fluorescent protein (GFP)-positive epithelial cells in the transgenic zebrafish tg(krt4-GFP) (Figure 4-21)(Yoo et al., 2012). Hence, it's the Fynb & Yes that are likely expressed in the caudal fin fold's epithelial cells. Finally, they performed Fynb and/or Yes knock-down with MO, which inhibits the pre-mRNA transcripts' splicing through targeting the splice sites (Yoo et al., 2012). They made 2 Fynb single-mutants, 1 Yes single-mutant and 1 Fynb & Yes double-mutant (Figure 4-22)(Yoo et al., 2012). They found that both the 2 Fynb single-mutants and the Fynb & Yes double-mutant reduced the regenerate length at 3 dpw (Yoo et al., 2012). Therefore, it is Fynb that is involved in caudal fin fold regeneration. Furthermore, they carried out in situ hybridization for confirmation and detected Fynb's mRNA in the caudal fin fold (Figure 4-23)(Yoo et al., 2012).

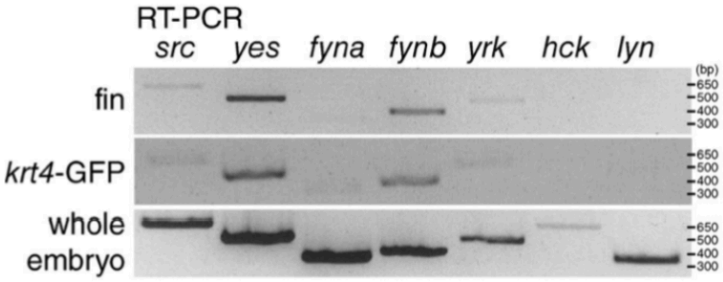

Figure 4-21 RT-PCR of various members of SFK. hck & lyn are negative controls, as they are hematopoiesis specific. Adapted from (Yoo et al., 2012).

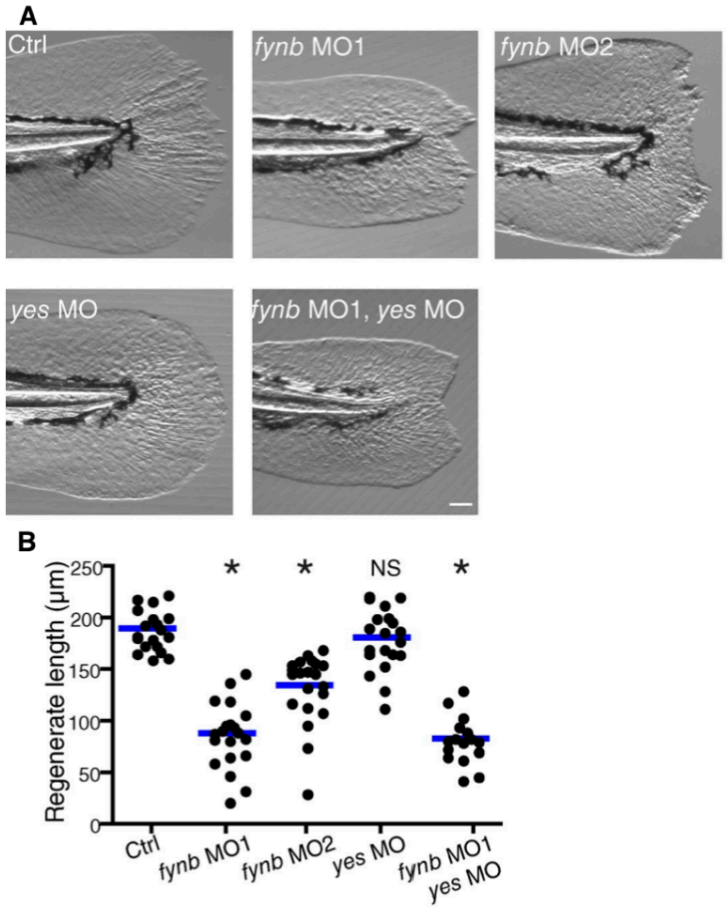

Figure 4-22. (A) Representative photos of regenerate length at 3 dpw (days post wounding). (B) Quantification of the tail fin egenerate length at 3 dpw. Adapted from (Yoo et al., 2012).

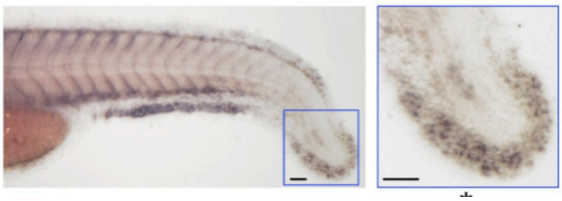

Figure 4-23. Fynb mRNA's in situ hybridization. The tail fin fold emphasized with the blue box is magnified. Adapted from (Yoo et al., 2012).

In the current study, for further confirmation of the results, a structure-unrelated analog of the inhibitor was only used for a couple of target molecules. For all the targeted molecules treated with inhibitors or scavengers, experiments using structurally unrelated analogs could be carried out. Also, rescue experiments using chemical activators, CaCl2 solution and H2O2 solution for targeted molecules were not performed and could be carried out.

In the current study, for controlling variables, I did not rule out the possibility that the increase in fluorescent density was caused by increased tissue volume. The tail trunk is a very thick tissue, and when the truck contracts during the notochord bead formation, the tissue structure might get thicker, which could contribute to the increase in fluorescence intensity. Also, I did not rule out the possibility that the significant changes in the level of targeted molecules were caused by the change of pH in the environment. Enzyme activity is very sensitive to pH change, which could be caused by changes in the local environment caused by tail amputation. This possibility can be ruled out by using a pH probe, e.g., 3'-O-Acetyl-2',7'-bis(carboxyethyl)-4 or 5-carboxyfluorescein diacetoxymethyl ester (BCECF-AM). In addition, a control group with no amputation could be set up for each experiment.

In the current study, I only tried to lower the level or inhibit the activity of certain molecules of interest and see how it affected the notochord bead formation and the level of amputation-induced Ca2+, H2O2 & SFK. Experiments that increase the level or promote the activity of these molecules and see how it affects notochord bead formation and the level of Ca2+, H2O2 & SFK could be performed. For example, CaCl2 solution could be used to increase the Ca2+ level, H2O2 solution could be used to increase the H2O2 level, and activators could be used to enhance other target molecules' activity. When using an activator, be mindful of the saturation of the target molecule. When applying exogenous H2O2, there are a few things to keep in mind. The effects of H2O2 produced endogenously, either by the cell itself or other neighboring cells, can be mimicked by H2O2 added exogenously. When applying exogenously H2O2 to cells or tissues, in order to mimic or produce a normal physiological effect within the cell cytosol, the appropriate concentration of the added exogenous H2O2 is thought to range from approximately 10 μM to 1000 μM (Jacob & Winyard, 2009). This number has taken dilution effects into account (Jacob & Winyard, 2009). However, other factors can affect the final concentration that reaches the cells or the concentration in the cell cytosol. They are: (1) The H2O2 effluxed. This is normally done through passive diffusion. (2) The H2O2 scavenged. (3) H2O2's local distribution (Jacob & Winyard, 2009). H2O2's distribution within the cell can be influenced by the scavenger's distribution. For example, catalase is usually present in the peroxisome (Jacob & Winyard, 2009). Also, H2O2 is more likely to be stable in an oxidizing environment than in a reducing atmosphere. The oxidizing environment includes the extra-cellular space or certain intra-cellular compartments such as the endoplasmic reticulum and the Golgi apparatus (Jacob & Winyard, 2009). The reducing atmosphere includes the cytosol and the nucleus (Jacob & Winyard, 2009). The exposure time should be considered as well when

considering the fore-mentioned factors. Taken together, the final concentration of H2O2 in the cytosol is difficult to estimate and therefore should be measured (Jacob & Winyard, 2009). In addition to using chemicals to target a single molecule of interest through either up-regulation or down-regulation in one experiment, experiments that utilize chemicals to target 2 or more molecules could also be conducted. For in vivo experiments like those in my current project, targeting 3 or more molecules with activators or inhibitors in a single experiment is relatively uncommon. Nevertheless, this type of experiment is more frequently seen in in vitro experiments.

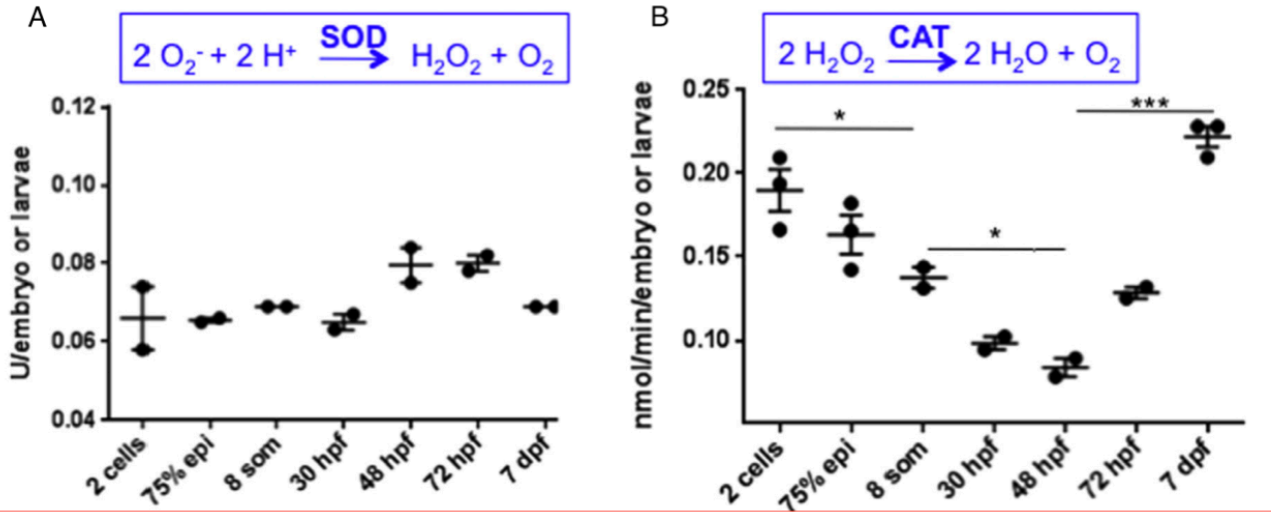

Figure 4-24. (A) SOD activity during development. (B) CAT activity during development. Adapted from (Gauron et al., 2016).

Conclusion:
H2O2 level controlled through CAT (degradation).
↑
Results:
development → CAT ↓
development → SOD =
(H2O2↑ coincide with CAT↓)
↑
Strain of thoughts for experiment-designing:
development → CAT ?
development → SOD ?

Figure 4-25. A flowchart-style casual outline of the experiment from (Gauron et al., 2016). Please be noted that the experiment for further validation and/or variable controlling might have been omitted.

In the current study, I only assessed notochord bead formation, the level of amputation-induced Ca2+/H2O2 and the activity of amputation-induced SFK. Experiments that assess the morphological changes that happen along the notochord bead formation (e.g., the change of fin fold width, the contraction degree of the trunk & the change of the cell membrane Menger curvature) and the regenerate's length after the completion of tail regeneration could be performed. Moreover, experiments that assess other molecules could be performed. These molecules could include: (1) candidates identified in current study, e.g., CREB, EGFR, MAPKK, MMP, PKA, PKB & Microtubule, etc; (2) proteins directly-related to Ca2+/H2O2 signaling, e.g., Ca2+ transporters, CaBPs as non-enzyme signaling molecules (CaM, TnC & S100, etc), CaBPs as enzymatic signaling molecules (PKC, PLC & PLA2, etc), protein kinases that depend on 'Ca2+ and/or CaM' (CaMK I, II, III, IV, V, MLCK & PhK, etc), H2O2-producing associated enzymes (Nox & SOD, etc), H2O2-degrading associated enzymes (CAT, GPx, PRx, GRx & TRx, etc), mitochondria-associated molecules, etc;

(3) other related molecules (genes) in zebrafish (larva) tail regeneration-related biological processes, e.g., (epimorphic) regeneration/morphogenesis of muscle/nerve/bone/blood vessels/notochord/skin, wound healing & inflammation, etc. In addition, experiments that assess cell activities that are involved in the afore-mentioned biological processes could be carried out. For example, as for how H2O2 level was regulated during notochord bead formation, besides Nox, the H2O2-producing enzyme, H2O2-removing enzymes such as CAT & SOD are also worth digging around, due to the fact that It has been reported that the H2O2 level was likely to be regulated through its degradation during zebrafish embryonic development due to the experimental results that the increased level of H2O2 during development was associated with an reduced CAT activity (Figure 4-24)(Figure 4-25)(Gauron et al., 2016). In their experiments, they found out that throughout development, the detected SOD's activity level was very stable (Gauron et al., 2016). As for the CAT, its activity decreased at one point (Gauron et al., 2016). They tried to measure the activity level of 2 enzymes called superoxide dismutase (SOD) and catalase (CAT) during development. SOD is responsible for the production of H2O2 inside the biological system, and CAT is the major enzyme involved in H2O2 degradation. Together, they control the H2O2 level to ensure normal homeostasis. At the point at which the significantly decreased CAT activity was detected, a significant increase in the level of H2O2 was observed (Gauron et al., 2016). Therefore, the relationship between H2O2 levels and CAT activity was an inverse correlation (Gauron et al., 2016).

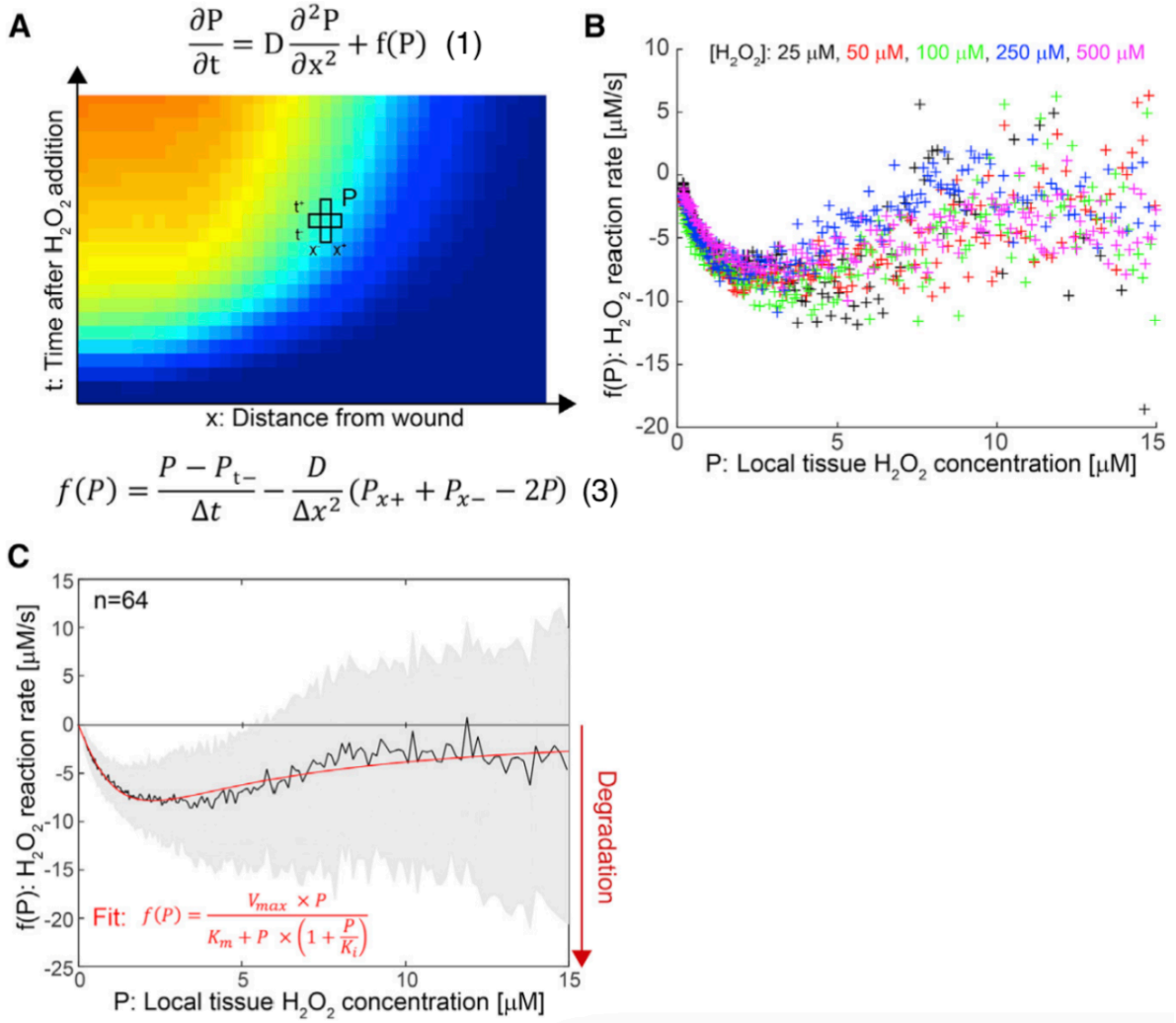

Figure 4-26. Calculating f(P) (local H2O2 net reaction rate) from time-lapse H2O2 images. (A) f(P) calculation equation & data obtaining process from time-lapse H2O2 image. (B) f(P) is calculated from 25/50/100/250/500 μM H2O2 experiments. (C) Pooled data from 25/50/100/250/500 μM H2O2 experiments. Red fitted line & red equation is the substrate-inhibition model. Adapted from (Jelcic et al., 2017).

Last but not least, for H2O2 signaling, it should be kept in mind the limitation of the distance that H2O2 can travel, as it has been reported that H2O2 signal can relay only up to 30 μm from the injury site in zebrafish fin fold regeneration (Jelcic et al., 2017). Their study took place in roughly 2 steps. First, they used exogenous H2O2 solutions to figure out the relationship between f(P) and P (Figure 4-26), and then they focused on endogenous H2O2 (i.e., the amputation-induced) to determine the distance over which the H2O2 signal can be transmitted (Figure 4-27). 1st, in order to calculate f(P) (local H2O2 net reaction rate), they obtained many time-lapse H2O2 movies/images & worked out the f(P) calculation equation. For obtaining time-lapse H2O2 movies, zebrafish larva tail fin is amputated, then certain concentration (25, 50, 100, 250, 500 μM) of exogenous H2O2 is added into media at 1 hpa (Jelcic et al., 2017). At this timepoint, the endogenous (amputation-induced) H2O2 should have decayed (Jelcic et al., 2017). Then they imaged the fish for 1 h until 2 hpa (Jelcic et al., 2017). H2O2 is visualized by HyPer, which is a genetically-coded sensor (Jelcic et al., 2017). For working-out the f(P) calculation equation (Figure 4-28)(Figure 4-29), the whole calculation process is based on 2 assumptions: (1) Considering that the zebrafish larva tail fin is flat, the H2O2 diffusion process through tissue is a reaction-diffusion process that happens in 1-dimension. (2) Fickian diffusion (Jelcic et al., 2017). For equation (1), local [H2O2] change is a function of H2O2 diffusion & H2O2 reaction (Jelcic et al., 2017). In this continuous equation of the H2O2 reaction-diffusion, t = time, x = distance to the amputation site, D = H2O2 diffusivity, P = local [H2O2], and f(P) = local H2O2 net reaction rate (Jelcic et al., 2017). For equation (2), this is the discretized equation of equation (1). In this discrete equation of the H2O2 reaction-diffusion, Δt = 1 min (time-lapse acquisition's temporal resolution), Δx = 2.6 μm (pixel size), D = 1000 μm^2/s (Vestergaard et al., 2012), ΔP = $P - P_{t^-}$, and $\Delta^2 P = P_{x^+} + P_{x^-} - 2P$ (Jelcic et al., 2017). For equation (3), this is the f(P) calculation equation solved from equation (2). They calculated f(P) using the data from time-lapse H2O2 movies/images from 25/50/100/250/500 μM H2O2 experiments. They found out that even though exogenous [H2O2], penetration depth & H2O2 gradient are different, the relationship between f(P) & P from all the data seems to follow the same kinetics; that is, when local [H2O2] (i.e., P) < 2 μM, H2O2's degradation rate increases with [H2O2] (Jelcic et al., 2017). When local [H2O2] > 2 μM, the H2O2's degradation rate stops to increase but starts to decrease (Jelcic et al., 2017). When local [H2O2] = 8-10 μM, the H2O2 degradation rate decreased to 0 (Jelcic et al., 2017). This means that H2O2 inhibits H2O2-degradation at high [H2O2], which could fit into a substrate-inhibition model (Jelcic et al., 2017). This also means that: (1) When [H2O2] is high, the anti-oxidant system becomes overwhelmed; H2O2 signaling can break the anti-oxidant barrier to directly act on the downstream signaling target. (2) When [H2O2] is low, H2O2 signaling can not break the anti-oxidant barrier to directly act on the downstream signaling target (Jelcic et al., 2017). They proposed 2 possible mechanisms: (1) Peroxiredoxin (Prx) over-oxidation (Wood et al., 2003), (2) NADPH depletion (Jelcic et al., 2017). Prx is an H2O2-degradation enzyme and is a part of the Prx-Trx anti-oxidant chain. Therefore, they tried auranofin (Aur) treatment in the 25 μM H2O2 experiments (Jelcic et al., 2017). Aur is a chemical inhibitor of thioredoxin (Trx) which is involved in H2O2-degradation by being a part of the Prx-Trx anti-oxidant chain. In their experiments, they found out that when local [H2O2] (P) is low, treatment (500 nM & 1 μM) showed dose-dependent H2O2-degradation inhibition (Jelcic et al., 2017). 2nd, they also tried to obtain time-lapse H2O2 movies under other conditions. This time, the zebrafish larva tail fin is amputated in hypotonic (normal) media or isotonic media, without adding any exogenous H2O2 (Jelcic et al., 2017). In isotonic media, the wound closure process is inhibited, therefore slower. In hypotonic (normal) media, the wound closure process is rather faster (Gault et al., 2014). In their experiments, they found out that: (1) Generally, amputation-induced (endogenous) H2O2 gradient's highest concentration does not exceed 5 μM. (2) Normally, this high concentration of H2O2 exists only within 30 μm from the amputation

site (Jelcic et al., 2017). Due to the fact that in their experiments in the 1st step, they found out that only when [H2O2] is high (> 2 μM), H2O2 signaling can break the anti-oxidant barrier to directly act on the downstream signaling target, therefore they conclude that even though the H2O2 gradient exists farther away from the amputation site, the H2O2 signaling can only happen in places highly restricted (< 30 μm) to the amputation site (Jelcic et al., 2017). Considering the fact that (1) in their previous study, they found out that H2O2 promotes the migration of leukocytes that are located near the blood vessel, which is 100-300 μm away from the amputation site before zebrafish larva fin-fold amputation (Niethammer et al., 2009); (2) the consensus way of H2O2 signaling is through redox-sensitive cysteine residue, therefore they concluded that (1) H2O2 is unlikely to directly act on leukocytes; (2) there are other spatial-relay mechanisms for H2O2-regulated leukocyte migration (Jelcic et al., 2017).

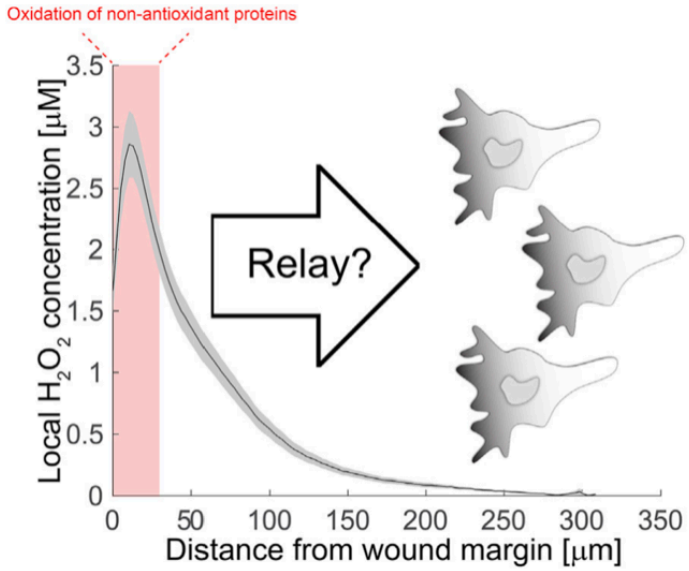

Figure 4-27. The amputation-induced (endogenous) H2O2 signaling might only happen in the place close to amputation site. The curve is the average profile of H2O2 gradient at 20 mpa. Red-shaded rectangle is the place ([H2O2] > 2 μM) where anti-oxidant barrier is broken. Adapted from (Jelcic et al., 2017).

local [H2O2] change diffusion reaction

$$\frac{\partial P}{\partial t} = D\frac{\partial^2 P}{\partial x^2} + f(P). \qquad (1)$$

$$\frac{\Delta P}{\Delta t} \approx D\frac{\Delta^2 P}{\Delta x^2} + f(P). \qquad (2)$$

$$f(P) = \frac{P - P_{t^-}}{\Delta t} - \frac{D}{\Delta x^2}(P_{x^+} + P_{x^-} - 2P). \qquad (3)$$

Figure 4-28. Calculating f(P) (local H2O2 net reaction rate) from time-lapse H2O2 images. (1) The continuous reaction-diffusion equation. Local [H2O2] change is a function of H2O2 diffusion & H2O2 reaction. (2) The discrete reaction-diffusion equation. (3) f(P) calculation equation solved from 'equation (2)'. Adapted from (Jelcic et al., 2017).

Calculate f(P) ← Time-lapse H2O2 movies/images + f(P) calculation equation:

For equation (1) (2) (3):
t = time.
x = distance to the amputation site.
D = H2O2 diffusivity through tissue.
P = local [H2O2].
f(P) = local H2O2 net reaction rate.
↓
For equation (2) (3):
Δt = 1 min (time-lapse acquisition), from data (movies/images).
Δx = 2.6 μm (pixel size), from data (movies/images).
D = 1000 μm^2/s, from literature.
P ≈ HyPer signal.
ΔP = $P - P_{t-}$, from data (movies/images).
$\Delta^2 P = P_{x+} + P_{x-} - 2P$, from data (movies/images).
↓
f(P) = ?

Figure 4-29. A flowchart-style casual outline of the f(P) calculating process from (Jelcic et al., 2017).

References

Abzhanov, A., Kuo, W.P., Hartmann, C., Grant, B.R., Grant, P.R., and Tabin, C.J. (2006) The calmodulin pathway and evolution of elongated beak morphology in Darwin's finches. Nature 442: 563–567 https://doi.org/10.1038/nature04843.

Addis, T., and Lew, W. (1940) THE RESTORATION OF LOST ORGAN TISSUE. The Journal of Experimental Medicine 71: 325–333 https://doi.org/10.1084/jem.71.3.325.

Akimenko, M., Marí-Beffa, M., Becerra, J., and Géraudie, J. (2003) Old questions, new tools, and some answers to the mystery of fin regeneration. Developmental Dynamics 226: 190–201 https://doi.org/10.1002/dvdy.10248.

Aleshin, A., and Finn, R.S. (2010) SRC: A Century of Science Brought to the Clinic. Neoplasia 12: 599–607 https://doi.org/10.1593/neo.10328.

Alessi, D.R., Cuenda, A., Cohen, P., Dudley, D.T., and Saltiel, A.R. (1995) PD 098059 is a specific inhibitor of the activation of mitogen-activated protein kinase kinase in vitro and in vivo. Journal of Biological Chemistry 270: 27489–27494 https://doi.org/10.1074/jbc.270.46.27489.

Allbritton, N.L., and Meyer, T. (1993) Localized calcium spikes and propagating calcium waves. Cell Calcium 14: 691–697 https://doi.org/10.1016/0143-4160(93)90095-n.

Allbritton, N.L., Meyer, T., and Stryer, L. (1992) Range of messenger action of calcium ion and inositol 1,4,5-Trisphosphate. Science 258: 1812–1815 https://doi.org/10.1126/science.1465619.

Alvarado, A.S. (2000) Regeneration in the metazoans: why does it happen? BioEssays 22: 578–590 https://doi.org/10.1002/(sici)1521-1878(200006)22:6<578::aid-bies11>3.0.co;2-#.

Al-Shanti, N., and Stewart, C.E. (2009) Ca2+/calmodulin-dependent transcriptional pathways: potential mediators of skeletal muscle growth and development. Biological Reviews/Biological Reviews of the Cambridge Philosophical Society 84: 637–652 https://doi.org/10.1111/j.1469-185x.2009.00090.x.

Antigny, F., Konig, S., Bernheim, L., and Frieden, M. (2014) Inositol 1,4,5 trisphosphate receptor 1 is a key player of human myoblast differentiation. Cell Calcium 56: 513–521 https://pubmed.ncbi.nlm.nih.gov/25468730/.

Antunes, F., and Cadenas, E. (2000) Estimation of H2O2 gradients across biomembranes. FEBS Letters 475: 121–126 https://doi.org/10.1016/s0014-5793(00)01638-0.

Ashraf, S., Bell, S., O'Leary, C., Canning, P., Micu, I., Fernandez, J.A., et al. (2019) CAMKII as a therapeutic target for growth factor-induced retinal and choroidal neovascularisation. JCI Insight https://doi.org/10.1172/jci.insight.122442.

Aslan, M. (2006) Insulin resistance inH pyloriinfection and its association with oxidative stress. World Journal of Gastroenterology 12: 6865 https://doi.org/10.3748/wjg.v12.i42.6865.

Atri, A., Amundson, J., Clapham, D., and Sneyd, J. (1993) A single-pool model for intracellular calcium oscillations and waves in the Xenopus laevis oocyte. Biophysical Journal 65: 1727–1739 https://doi.org/10.1016/s0006-3495(93)81191-3.

Avraham, H.K., Lee, T.H., Koh, Y., Kim, T.A., Jiang, S., Sussman, M., et al. (2003) Vascular Endothelial Growth Factor Regulates Focal Adhesion Assembly in Human Brain Microvascular Endothelial Cells through Activation of the Focal Adhesion Kinase and Related Adhesion Focal Tyrosine Kinase. Journal of Biological Chemistry 278: 36661–36668 https://doi.org/10.1074/jbc.m301253200.

Babu, Y.S., Sack, J.S., Greenhough, T.J., Bugg, C.E., Means, A.R., and Cook, W.J. (1985) Three-dimensional structure of calmodulin. Nature 315: 37–40 https://doi.org/10.1038/315037a0.

Bain, J., Plater, L., Elliott, M., Shpiro, N., Hastie, C.J., Mclauchlan, H., et al. (2007) The selectivity of protein kinase inhibitors: a further update. Biochemical Journal 408: 297–315 https://doi.org/10.1042/bj20070797.

Bedard, K., and Krause, K.-H. (2007) The NOX family of ROS-Generating NADPH Oxidases: Physiology and Pathophysiology. Physiological Reviews 87: 245–313 https://doi.org/10.1152/physrev.00044.2005.

Behl, C. (1994) Hydrogen peroxide mediates amyloid β protein toxicity. Cell 77: 817–827 https://doi.org/10.1016/0092-8674(94)90131-7.

Bennett, A.M., and Tonks, N.K. (1997) Regulation of distinct stages of skeletal muscle differentiation by Mitogen-Activated Protein kinases. Science 278: 1288–1291 https://pubmed.ncbi.nlm.nih.gov/9360925/.

Berndt, C., and Lillig, C. (2021) Redox Regulation of Differentiation and De-differentiation. 1st ed., CRC Press, Boca Raton.

Berridge, M., Lipp, P., and Bootman, M. (1999) Calcium signalling. Current Biology 9: R157–R159.

Berridge, M.J. (1997) Elementary and Global Aspects of Calcium Signalling. Journal of Experimental Biology 200: 315–319.

Berridge, M.J., and Irvine, R.F. (1989) Inositol phosphates and cell signalling. Nature 341: 197–205 https://doi.org/10.1038/341197a0.

Berridge, M.J., Lipp, P., and Bootman, M.D. (2000) The versatility and universality of calcium signalling. Nature Reviews Molecular Cell Biology 1: 11–21 https://www.nature.com/articles/35036035.

Bibbins, K.B., Boeuf, H., and Varmus, H.E. (1993) Binding of the Src SH2 domain to phosphopeptides is determined by residues in both the SH2 domain and the phosphopeptides. Molecular and Cellular Biology 13: 7278–7287 https://doi.org/10.1128/mcb.13.12.7278.

Bland-Ward, P.A., and Moore, P.K. (1995) 7-Nitro indazole Derivatives are potent inhibitors of brain, endothelium and inducible isoforms of nitric oxide synthase. Life Sciences 57: PL131–PL135 https://doi.org/10.1016/0024-3205(95)02046-l.

Bolen, J.B., Thompson, P.A., Eiseman, E., and Horak, I.D. (1991) Expression and Interactions of the Src Family of Tyrosine Protein Kinases in T Lymphocytes. Advances in Cancer Research 103–149 https://doi.org/10.1016/s0065-230x(08)60997-5.

Bootman, M.D., and Lipp, P. (1999) Calcium signalling: Ringing changes to the 'bell-shaped curve.' Current Biology 9: R876–R878 https://doi.org/10.1016/s0960-9822(00)80072-x.

Brandvold, K.R., Steffey, M.E., Fox, C.C., and Soellner, M.B. (2012) Development of a highly selective C-SRC kinase inhibitor. ACS Chemical Biology 7: 1393–1398 https://doi.org/10.1021/cb300172e.

Bremer, J., Skinner, J., and Granato, M. (2017) A small molecule screen identifies in vivo modulators of peripheral nerve regeneration in zebrafish. PLoS ONE 12: e0178854 https://doi.org/10.1371/journal.pone.0178854.

Briggs, S.D., Bryant, S.S., Jove, R., Sanderson, S.D., and Smithgall, T.E. (1995) The Ras GTPase-activating Protein (GAP) Is an SH3 Domain-binding Protein and Substrate for the Src-related Tyrosine Kinase, Hck. Journal of Biological Chemistry 270: 14718–14724 https://doi.org/10.1074/jbc.270.24.14718.

Briggs, S.D., Sharkey, M., Stevenson, M., and Smithgall, T.E. (1997) SH3-mediated Hck Tyrosine Kinase Activation and Fibroblast Transformation by the Nef Protein of HIV-1. Journal of Biological Chemistry 272: 17899–17902 https://doi.org/10.1074/jbc.272.29.17899.

Brini, M., and Carafoli, E. (2010) The plasma membrane CA2+ ATPASE and the plasma membrane sodium calcium exchanger cooperate in the regulation of cell calcium. Cold Spring Harbor Perspectives in Biology 3: a004168 https://doi.org/10.1101/cshperspect.a004168.

Brouet, A., Sonveaux, P., Dessy, C., Balligand, J.L., and Feron, O. (2001) Hsp90 Ensures the Transition from the Early Ca2+-dependent to the Late Phosphorylation-dependent Activation of the Endothelial Nitric-oxide Synthase in Vascular Endothelial Growth Factor-exposed Endothelial Cells. Journal of Biological Chemistry 276: 32663–32669 https://doi.org/10.1074/jbc.m101371200.

Brown, M.T., and Cooper, J.A. (1996) Regulation, substrates and functions of src. Biochimica Et Biophysica Acta (BBA) - Reviews on Cancer 1287: 121–149 https://doi.org/10.1016/0304-419x(96)00003-0.

Brugge, J.S., Cotton, P.C., Queral, A.E., Barrett, J.N., Nonner, D., and Keane, R.W. (1985) Neurones express high levels of a structurally modified, activated form of pp60c-src. Nature 316: 554–557 https://doi.org/10.1038/316554a0.

Bräutigam, L., Jensen, L.D.E., Poschmann, G., Nyström, S., Bannenberg, S., Dreij, K., et al. (2013) Glutaredoxin regulates vascular development by reversible glutathionylation of sirtuin 1. Proceedings of the National Academy of Sciences 110: 20057–20062 https://doi.org/10.1073/pnas.1313753110.

Buono, R., Vantaggiato, C., Pisa, V., Azzoni, E., Bassi, M.T., Brunelli, S., et al. (2011) Nitric oxide sustains Long-Term skeletal muscle regeneration by regulating fate of satellite cells via signaling pathways requiring VANGL2 and cyclic GMP. Stem Cells 30: 197–209 https://doi.org/10.1002/stem.783.

Busa, W.B., and Nuccitelli, R. (1985) An elevated free cytosolic Ca2+ wave follows fertilization in eggs of the frog, Xenopus laevis. The Journal of Cell Biology 100: 1325–1329 https://doi.org/10.1083/jcb.100.4.1325.

Cance, W.G., Craven, R.J., Bergman, M., Xu, L., Alitalo, K., and Liu, E.T. (1994) Rak, a novel nuclear tyrosine kinase expressed in epithelial cells. PubMed 5: 1347–55 https://pubmed.ncbi.nlm.nih.gov/7696183.

Carlson, B.M. (2007) Principles of regenerative biology. Elsevier/Academic Press, Amsterdam ; Burlington, Mass.

Carmeliet, P., and Jain, R.K. (2011) Molecular mechanisms and clinical applications of angiogenesis. Nature 473: 298–307 https://doi.org/10.1038/nature10144.

Carter, M., Essner, R., Goldstein, N., and Iyer, M. (2022) Guide to Research Techniques in Neuroscience. Academic Press, Oxford.

Catalano, A., and O'Day, D.H. (2007) Calmodulin-binding proteins in the model organism Dictyostelium: A complete & critical review. Cellular Signalling 20: 277–291 https://doi.org/10.1016/j.cellsig.2007.08.017.

Cavarocchi, N.C., England, M.D., Schaff, H.V., Russo, P., Orszulak, T.A., Schnell, W.A., et al. (1986) Oxygen free radical generation during cardiopulmonary bypass: correlation with complement activation. Circulation 74: III130-3 https://pubmed.ncbi.nlm.nih.gov/3769186/.

Chan, C.M., Aw, J.T.M., Webb, S.E., and Miller, A.L. (2016) SOCE proteins, STIM1 and Orai1, are localized to the cleavage furrow during cytokinesis of the first and second cell division cycles in zebrafish embryos. Zygote 24: 880–889 https://pubmed.ncbi.nlm.nih.gov/27702423/.

Chan, C.M., Chen, Y., Hung, T.S., Miller, A.L., Shipley, A.M., and Webb, S.E. (2015) Inhibition of SOCE disrupts cytokinesis in zebrafish embryos via inhibition of cleavage furrow deepening. The International Journal of Developmental Biology 59: 289–301 https://pubmed.ncbi.nlm.nih.gov/26679947/.

Charlton, S.J., Brown, C.A., Weisman, G.A., Turner, J.T., Erb, L., and Boarder, M.R. (1996) PPADS and suramin as antagonists at cloned P2Y- and P2U-purinoceptors. British Journal of Pharmacology 118: 704–710 https://doi.org/10.1111/j.1476-5381.1996.tb15457.x.

Chen, C.H., Puliafito, A., Cox, B.T., Primo, L., Fang, Y., Stefano Di Talia, and Poss, K.D. (2016) Multicolor Cell Barcoding Technology for Long-Term Surveillance of Epithelial Regeneration in Zebrafish. Developmental Cell 36: 668–680.

Chen, F., Zhu, L., Cai, L., Zhang, J., Zeng, X., Li, J., et al. (2016) A stromal interaction molecule 1 variant up-regulates matrix metalloproteinase-2 expression by strengthening nucleoplasmic Ca2+ signaling. Biochimica Et Biophysica Acta (BBA) - Molecular Cell Research 1863: 617–629 https://doi.org/10.1016/j.bbamcr.2016.01.007.

Chen, J., Xia, L., Bruchas, M.R., and Solnica-Krezel, L. (2017) Imaging early embryonic calcium activity with GCaMP6s transgenic zebrafish. Developmental Biology 430: 385–396 https://pubmed.ncbi.nlm.nih.gov/28322738/.

Chen, M., Huang, R.-C., Yang, L.-Q., Ren, D.-L., and Hu, B. (2019) In vivo imaging of evoked calcium responses indicates the intrinsic axonal regenerative capacity of zebrafish. The FASEB Journal 33: 7721–7733 http://dx.doi.org/10.1096/fj.201802649r.

Cheng, H., Lederer, W.J., and Cannell, M.B. (1993) Calcium Sparks: Elementary Events Underlying Excitation-Contraction Coupling in Heart Muscle. Science 262: 740–744 https://doi.org/10.1126/science.8235594.

Cheung, K. (2019). Understanding the Role of Wound-Induced Calcium and Reactive Oxygen Species During Zebrafish Larval Tail Regeneration. Master. The University of Sheffield.

Chin, J., Palop, J.J., Puoliväli, J., Massaro, C., Bien-Ly, N., Gerstein, H., et al. (2005) Fyn Kinase Induces Synaptic and Cognitive Impairments in a Transgenic Mouse Model of Alzheimer's Disease. Journal of Neuroscience 25: 9694–9703 https://doi.org/10.1523/jneurosci.2980-05.2005.

Cho, A., Tang, Y., Davila, J., Deng, S., Chen, L., Miller, E., et al. (2014) Calcineurin Signaling Regulates Neural Induction through Antagonizing the BMP Pathway. Neuron 82: 109–124 https://doi.org/10.1016/j.neuron.2014.02.015.

Cho, W., and Stahelin, R.V. (2005) Membrane-Protein interactions in cell signaling and membrane trafficking. Annual Review of Biophysics and Biomolecular Structure 34: 119–151 https://doi.org/10.1146/annurev.biophys.33.110502.133337.

Chong, Y.-P., Ia, K.K., Mulhern, T.D., and Cheng, H.-C. (2005) Endogenous and synthetic inhibitors of the Src-family protein tyrosine kinases. Biochimica Et Biophysica Acta (BBA) - Proteins and Proteomics 1754: 210–220 https://doi.org/10.1016/j.bbapap.2005.07.027.

Clapham, D.E. (1995) Calcium signaling. Cell 80: 259–268 https://doi.org/10.1016/0092-8674(95)90408-5.

Clapham, D.E. (2007) Calcium signaling. Cell 131: 1047–1058 https://doi.org/10.1016/j.cell.2007.11.028.

Cohen, G.B., Ren, R., and Baltimore, D. (1995) Modular binding domains in signal transduction proteins. Cell 80: 237–248 https://doi.org/10.1016/0092-8674(95)90406-9.

Covarrubias, L., Hernández-García, D., Schnabel, D., Salas-Vidal, E., and Castro-Obregón, S. (2008) Function of reactive oxygen species during animal development: Passive or active? Developmental Biology 320: 1–11 https://doi.org/10.1016/j.ydbio.2008.04.041.

Creton, R. (2004) The calcium pump of the endoplasmic reticulum plays a role in midline signaling during early zebrafish development. Developmental Brain Research 151: 33–41 https://doi.org/10.1016/j.devbrainres.2004.03.016.

Crowe, P.D., Walter, B.N., Mohler, K.M., Otten-Evans, C., Black, R.A., and Ware, C.F. (1995) A metalloprotease inhibitor blocks shedding of the 80-kD TNF receptor and TNF processing in T lymphocytes. The Journal of Experimental Medicine 181: 1205–1210 https://doi.org/10.1084/jem.181.3.1205.

Dani, J.W., Chernjavsky, A., and Smith, S.J. (1992) Neuronal activity triggers calcium waves in hippocampal astrocyte networks. Neuron 8: 429–440 https://doi.org/10.1016/0896-6273(92)90271-e.

De Deken, X., Corvilain, B., Dumont, J.E., and Miot, F. (2013) Roles of DUOX-Mediated Hydrogen Peroxide in metabolism, host defense, and signaling. Antioxidants and Redox Signaling 20: 2776–2793 https://doi.org/10.1089/ars.2013.5602.

De Groot, H., and Littauer, A. (1989) Hypoxia, reactive oxygen, and cell injury. Free Radical Biology and Medicine 6: 541–551 https://doi.org/10.1016/0891-5849(89)90047-6.

Dominguez, D.C. (2004) Calcium signalling in bacteria. Molecular Microbiology 54: 291–297 https://doi.org/10.1111/j.1365-2958.2004.04276.x.

Dröge, W. (2002) Free radicals in the physiological control of cell function. Physiological Reviews 82: 47–95 https://doi.org/10.1152/physrev.00018.2001.

Du, T., Zhou, X., Zhang, R.D.Y., and Du, X.-F. (2022) Roles of Ca2+ activity in injury-induced migration of microglia in zebrafish in vivo. Biochemistry and Biophysics Reports 32: 101340 http://dx.doi.org/10.1016/j.bbrep.2022.101340.

Dupont, G., and Goldbeter, A. (1993) One-pool model for Ca2+ oscillations involving Ca2+ and inositol 1,4,5-trisphosphate as co-agonists for Ca2+ release. Cell Calcium 14: 311–322 https://doi.org/10.1016/0143-4160(93)90052-8.

Eilers, J., and Konnerth, A. (2009) Dye Loading with Patch Pipettes. Cold Spring Harbor Protocols 2009: pdb.prot5201 https://doi.org/10.1101/pdb.prot5201.

Elbediwy, A., Vanyai, H., Diaz-De-La-Loza, M.D.C., Frith, D., Snijders, A.P., and Thompson, B.J. (2018) Enigma proteins regulate YAP mechanotransduction. Journal of Cell Science 131 https://doi.org/10.1242/jcs.221788.

El-hage, S., and Singh, S.M. (1990) Temporal expression of genes encoding free radical–metabolizing enzymes is associated with higher mRNA levels during in utero development in mice. Developmental Genetics 11: 149–159 https://doi.org/10.1002/dvg.1020110205.

Enyedi, B., Jelcic, M., and Niethammer, P. (2016) The Cell Nucleus Serves as a Mechanotransducer of Tissue Damage-Induced Inflammation. Cell 165: 1160–1170.

Fadilah, N.I.M., Phang, S.J., Kamaruzaman, N., Salleh, A., Zawani, M., Sanyal, A., et al. (2023) Antioxidant biomaterials in cutaneous wound Healing and Tissue Regeneration: A Critical review. Antioxidants 12: 787 https://doi.org/10.3390/antiox12040787.

Fasman, G.D. (1989) Prediction of protein structure and the principles of protein conformation. https://doi.org/10.1007/978-1-4613-1571-1.

Fasolato, C., Innocenti, B., and Pozzan, T. (1994) Receptor-activated Ca2+ influx: how many mechanisms for how many channels? Trends in Pharmacological Sciences 15: 77–83 https://doi.org/10.1016/0165-6147(94)90282-8.

Favata, M.F., Horiuchi, K.Y., Manos, E.J., Daulerio, A.J., Stradley, D.A., Feeser, W.S., et al. (1998) Identification of a novel inhibitor of mitogen-activated protein kinase kinase. Journal of Biological Chemistry 273: 18623–18632 https://doi.org/10.1074/jbc.273.29.18623.

Feng, S., Chen, J.K., Yu, H., Simon, J.A., and Schreiber, S.L. (1994) Two Binding Orientations for Peptides to the Src SH3 Domain: Development of a General Model for SH3-Ligand Interactions. Science 266: 1241–1247 https://doi.org/10.1126/science.7526465.

Fernández-Guarino, M., and Bacci, S. (2024) Mast cells and wound healing: Still an open question. PubMed 18757 https://pubmed.ncbi.nlm.nih.gov/38742450.

Ferrari, M.B., and Spitzer, N.C. (1999) Calcium signaling in the developing xenopus myotome. Developmental Biology 213: 269–282 https://pubmed.ncbi.nlm.nih.gov/10479447/.

Ferrari, M.B., Ribbeck, K., Hagler, D.J., and Spitzer, N.C. (1998) A calcium signaling cascade essential for myosin thick filament assembly in xenopus myocytes. The Journal of Cell Biology 141: 1349–1356 https://pubmed.ncbi.nlm.nih.gov/9628891/.

Ferrari, M.B., Rohrbough, J., and Spitzer, N.C. (1996) Spontaneous calcium transients regulate myofibrillogenesis in EmbryonicXenopusMyocytes. Developmental Biology 178: 484–497 https://pubmed.ncbi.nlm.nih.gov/8812144/.

Ferrer-Buitrago, M., Dhaenens, L., Lu, Y., Bonte, D., Vanden Meerschaut, F., De Sutter, P., et al. (2017) Human oocyte calcium analysis predicts the response to assisted oocyte activation in patients experiencing fertilization failure after ICSI. Human Reproduction 33: 416–425 https://doi.org/10.1093/humrep/dex376.

Ferretti, P., and Géraudie, J. (1998) Cellular and Molecular Basis of Regeneration. Wiley & Sons Ltd, New York.

Feske, S. (2007) Calcium signalling in lymphocyte activation and disease. Nature Reviews Immunology 7: 690–702 https://doi.org/10.1038/nri2152.

Feske, S., Gwack, Y., Prakriya, M., Srikanth, S., Puppel, S.-H., Tanasa, B., et al. (2006) A mutation in Orai1 causes immune deficiency by abrogating CRAC channel function. Nature 441: 179–185 https://doi.org/10.1038/nature04702.

Fraguas, S., Barberán, S., and Cebrià, F. (2011) EGFR signaling regulates cell proliferation, differentiation and morphogenesis during planarian regeneration and homeostasis. Developmental Biology 354: 87–101 https://doi.org/10.1016/j.ydbio.2011.03.023.

Fry, D.W., Bridges, A.J., Denny, W.A., Doherty, A., Greis, K.D., Hicks, J.L., et al. (1998) Specific, irreversible inactivation of the epidermal growth factor receptor and erbB2, by a new class of tyrosine kinase inhibitor. Proceedings of the National Academy of Sciences 95: 12022–12027 https://doi.org/10.1073/pnas.95.20.12022.

Fuchs, E., and Segre, J.A. (2000) Stem cells: a new lease on life. Cell 100: 143–155 http://dx.doi.org/10.1016/s0092-8674(00)81691-8.

Fukui, Y., and Hanafusa, H. (1991) Requirement of phosphatidylinositol-3 kinase modification for its association with p60src. Molecular and Cellular Biology 11: 1972–1979 https://doi.org/10.1128/mcb.11.4.1972.

Gajewski, K., Wang, J., Molkentin, J.D., Chen, E.H., Olson, E.N., and Schulz, R.A. (2003) Requirement of the calcineurin subunit gene canB2 for indirect flight muscle formation in Drosophila. Proceedings of the National Academy of Sciences 100: 1040–1045 https://pubmed.ncbi.nlm.nih.gov/12538857/.

Gauld, S.B., and Cambier, J.C. (2004) Src-family kinases in B-cell development and signaling. Oncogene 23: 8001–8006 https://www.nature.com/articles/1208075.

Gault, W.J., Enyedi, B., and Niethammer, P. (2014) Osmotic surveillance mediates rapid wound closure through nucleotide release. The Journal of Cell Biology 207: 767–782 https://doi.org/10.1083/jcb.201408049.

Gauron, C., Meda, F., Dupont, E., Albadri, S., Quenech'Du, N., Ipendey, E., et al. (2016) Hydrogen peroxide (H2O2) controls axon pathfinding during zebrafish development. Developmental Biology 414: 133–141 https://doi.org/10.1016/j.ydbio.2016.05.004.

Geddis, M.S., and Rehder, V. (2003) Initial stages of neural regeneration in Helisoma trivolvis are dependent upon PLA2 activity. Journal of Neurobiology 54: 555–565 https://doi.org/10.1002/neu.10183.

Gelperin, A., and Flores, J. (1997) Vital staining from dye-coated microprobes identifies new olfactory interneurons for optical and electrical recording. Journal of Neuroscience Methods 72: 97–108 https://doi.org/10.1016/s0165-0270(96)02169-3.

Germinario, E., Esposito, A., Midrio, M., Betto, R., and Danieli-Betto, D. (2002) Expression of Sarco(endo)Plasmic Reticulum Ca2+-Atpase Slow (SERCA2) Isoform in Regenerating Rat Soleus Skeletal Muscle Depends on Nerve Impulses. Experimental Physiology 87: 575–583 https://www.cambridge.org/core/journals/experimental-physiology/article/abs/expression-of-sarcoendoplasmic-reticulum-ca2atpase-slow-serca2-isoform-in-regenerating-rat-soleus-skeletal-muscle-depends-on-nerve-impulses/0E9BE6C382EE26C79426F66462E38F24.

Gifford, S., Grummer, M., Pierre, S., Austin, J., Zheng, J., and Bird, I. (2004) Functional characterization of HUVEC-CS: Ca2+ signaling, ERK 1/2 activation, mitogenesis and vasodilator production. Journal of Endocrinology 182: 485–499 https://doi.org/10.1677/joe.0.1820485.

Gorin, F., Ignacio, P., Gelinas, R., and Carlsen, R. (1989) Abnormal expression of glycogen phosphorylase genes in regenerated muscle. AJP Cell Physiology 257: C495–C503 https://doi.org/10.1152/ajpcell.1989.257.3.c495.

Graf, S.F., Hötzel, S., Liebel, U., Stemmer, A., and Knapp, H.F. (2011) Image-Based Fluidic Sorting System for Automated Zebrafish Egg Sorting into Multiwell Plates. JALA Journal of the Association for Laboratory Automation 16: 105–111 https://doi.org/10.1016/j.jala.2010.11.002.

Green, K., Brand, M.D., and Murphy, M.P. (2004) Prevention of mitochondrial oxidative damage as a therapeutic strategy in diabetes. Diabetes 53: S110–S118 https://doi.org/10.2337/diabetes.53.2007.s110.
Grienberger, C., and Konnerth, A. (2012) Imaging calcium in neurons. Neuron 73: 862–885 https://doi.org/10.1016/j.neuron.2012.02.011.

Grynkiewicz, G., Poenie, M., and Tsien, R.Y. (1985) A new generation of Ca2+ indicators with greatly improved fluorescence properties. Journal of Biological Chemistry 260: 3440–3450 https://doi.org/10.1016/s0021-9258(19)83641-4.

Guerrero-Hernandez, A., and Verkhratsky, A. (2014) Calcium signalling in diabetes. Cell Calcium 56: 297–301 https://doi.org/10.1016/j.ceca.2014.08.009.

Guimarães, F.R., Sales-Campos, H., Nardini, V., Da Costa, T.A., Fonseca, M.T.C., Júnior, V.R., et al. (2017) The inhibition of 5-Lipoxygenase (5-LO) products leukotriene B4 (LTB 4) and cysteinyl leukotrienes (cysLTs) modulates the inflammatory response and improves cutaneous wound healing. Clinical Immunology 190: 74–83 https://doi.org/10.1016/j.clim.2017.08.022.

Gupta, S.K., Lysko, P.G., Pillarisetti, K., Ohlstein, E., and Stadel, J.M. (1998) Chemokine receptors in human endothelial cells. Journal of Biological Chemistry 273: 4282–4287 https://doi.org/10.1074/jbc.273.7.4282.

Gélinas, D.S., Bernatchez, P.N., Rollin, S., Bazan, N.G., and Sirois, M.G. (2002) Immediate and delayed VEGF-mediated NO synthesis in endothelial cells: Role of PI3K, PKC and PLC pathways. British Journal of Pharmacology 137: 1021–1030 https://doi.org/10.1038/sj.bjp.0704956.

Görlach, A., Bertram, K., Hudecova, S., and Krizanova, O. (2015) Calcium and ROS: A mutual interplay. Redox Biology 6: 260–271 http://dx.doi.org/10.1016/j.redox.2015.08.010.

Gündüz, D., Tanislav, C., Schlüter, K.D., Schulz, R., Hamm, C., and Aslam, M. (2016) Effect of ticagrelor on endothelial calcium signalling and barrier function. Thrombosis and Haemostasis 117: 371–381 https://doi.org/10.1160/th16-04-0273.

Halliwell, B., and Gutteridge, J.M.C. (1999) Free radicals in biology and medicine. 3rd ed., Clarendon Press ; New York, Oxford.

Halliwell, B., and Gutteridge, J.M.C. (2015) Free radicals in biology and medicine. 5th ed., Oxford University Press, Oxford.

Halliwell, B., Clement, M.V., and Long, L.H. (2000) Hydrogen peroxide in the human body. FEBS Letters 486: 10–13 https://doi.org/10.1016/s0014-5793(00)02197-9.

Han, Y., Ishibashi, S., Iglesias-Gonzalez, J., Chen, Y., Love, N.R., and Amaya, E. (2018) CA2+-Induced mitochondrial ROS regulate the early embryonic cell cycle. Cell Reports 22: 218–231 https://doi.org/10.1016/j.celrep.2017.12.042.

Hancock, J.T. (2010) Cell signalling. 3rd ed., Oxford Univ. Press, Oxford ; New York.

Hanke, J.H., Gardner, J.P., Dow, R.L., Changelian, P.S., Brissette, W.H., Weringer, E.J., et al. (1996) Discovery of a novel, potent, and SRC family-selective tyrosine kinase inhibitor. Journal of Biological Chemistry 271: 695–701 https://doi.org/10.1074/jbc.271.2.695.

Hanna, Z., Weng, X., Kay, D.G., Poudrier, J., Lowell, C., and Jolicoeur, P. (2001) The Pathogenicity of Human Immunodeficiency Virus (HIV) Type 1 Nef in CD4C/HIV Transgenic Mice Is Abolished by Mutation of Its SH3-Binding Domain, and Disease Development Is Delayed in the Absence of Hck. Journal of Virology 75: 9378–9392 https://doi.org/10.1128/jvi.75.19.9378-9392.2001.

Hara, Y., Nagayama, K., Yamamoto, T.S., Matsumoto, T., Suzuki, M., and Ueno, N. (2013) Directional migration of leading-edge mesoderm generates physical forces: Implication in Xenopus notochord formation during gastrulation. Developmental Biology 382: 482–495 https://pubmed.ncbi.nlm.nih.gov/23933171/.

Hardie, R.C. (1991) Whole-cell recordings of the light induced current in dissociated Drosophila photoreceptors: evidence for feedback by calcium permeating the light-sensitive channels. Proceedings of the Royal Society B Biological Sciences 245: 203–210 https://doi.org/10.1098/rspb.1991.0110.

Harteneck, C., Frenzel, H., and Kraft, R. (2007) N-(p-Amylcinnamoyl)anthranilic Acid (ACA): A Phospholipase A2 Inhibitor and TRP Channel Blocker. Cardiovascular Drug Reviews 25: 61–75 https://doi.org/10.1111/j.1527-3466.2007.00005.x.

Harty, M., Neff, A.W., King, M.W., and Mescher, A.L. (2003) Regeneration or scarring: An immunologic perspective. Developmental Dynamics 226: 268–279 https://pubmed.ncbi.nlm.nih.gov/12557205/.

Haunhorst, P., Hanschmann, E.-M., Bräutigam, L., Stehling, O., Hoffmann, B., Mühlenhoff, U., et al. (2013) Crucial function of vertebrate glutaredoxin 3 (PICOT) in iron homeostasis and hemoglobin maturation. Molecular Biology of the Cell 24: 1895–1903 https://doi.org/10.1091/mbc.e12-09-0648.

Hauptmann, N., Grimsby, J., Shih, J.C., and Cadenas, E. (1996) The metabolism of tyramine by monoamine oxidase A/B causes oxidative damage to mitochondrial DNA. Archives of Biochemistry and Biophysics 335: 295–304 https://doi.org/10.1006/abbi.1996.0510.

Hayashi, K., Yamamoto, T.S., and Ueno, N. (2018) Intracellular calcium signal at the leading edge regulates mesodermal sheet migration during Xenopus gastrulation. Scientific Reports 8 https://doi.org/10.1038/s41598-018-20747-w.

Heizmann, C.W. (2002) S100 proteins: structure functions and pathology. Frontiers in Bioscience 7: d1356-1368 https://doi.org/10.2741/a846.

Hellal, F., Hurtado, A., Ruschel, J., Flynn, K.C., Laskowski, C.J., Umlauf, M., et al. (2011) Microtubule stabilization reduces scarring and causes axon regeneration after spinal cord injury. Science 331: 928–931 https://doi.org/10.1126/science.1201148.

Helmchen, F., Imoto, K., and Sakmann, B. (1996) Ca2+ buffering and action potential-evoked Ca2+ signaling in dendrites of pyramidal neurons. Biophysical Journal 70: 1069–1081 https://doi.org/10.1016/s0006-3495(96)79653-4.

Higgins, G.M., and Anderson, R.M. (1931) Experimental pathology of the liver: restoration of the liver of the white rat following partial surgical removal. Arch Pathol 12: 186–202 https://ci.nii.ac.jp/naid/10010034415.
Hilgemann, D.W., Yaradanakul, A., Wang, Y., and Fuster, D. (2006) Molecular control of cardiac sodium homeostasis in health and Disease. Journal of Cardiovascular Electrophysiology 17 https://doi.org/10.1111/j.1540-8167.2006.00383.x.

Hoth, M., and Penner, R. (1992) Depletion of intracellular calcium stores activates a calcium current in mast cells. Nature 355: 353–356 https://doi.org/10.1038/355353a0.

Huang, P., Chiu, C., Chang, H., Wang, Y., Syue, H., Song, Y., et al. (2017) Prdx1-encoded peroxiredoxin is important for vascular development in zebrafish. FEBS Letters 591: 889–902 https://doi.org/10.1002/1873-3468.12604.

Huang, Y.Z., and McNamara, J.O. (2010) Mutual regulation of SRC family kinases and the neurotrophin receptor TRKB. Journal of Biological Chemistry 285: 8207–8217 https://pubmed.ncbi.nlm.nih.gov/20064930/.

Hunt, M., Torres, M., Bachar-Wikstrom, E., and Wikstrom, J.D. (2024) Cellular and molecular roles of reactive oxygen species in wound healing. Communications Biology 7 https://doi.org/10.1038/s42003-024-07219-w.

Huse, M., and Kuriyan, J. (2002) The conformational plasticity of protein kinases. Cell 109: 275–282 https://doi.org/10.1016/s0092-8674(02)00741-9.

Hwang, J.J., Park, M., and Koh, J. (2007) Copper activates TrkB in cortical neurons in a metalloproteinase-dependent manner. Journal of Neuroscience Research 85: 2160–2166 https://pubmed.ncbi.nlm.nih.gov/17520746/.

Hyslop, P.A., Zhang, Z., Pearson, D.V., and Phebus, L.A. (1995) Measurement of striatal H2O2 by microdialysis following global forebrain ischemia and reperfusion in the rat: correlation with the cytotoxic potential of H2O2 in vitro. Brain Research 671: 181–186 https://doi.org/10.1016/0006-8993(94)01291-o.

Imamoto, A., and Soriano, P. (1993) Disruption of the csk gene, encoding a negative regulator of Src family tyrosine kinases, leads to neural tube defects and embryonic lethality in mice. Cell 73: 1117–1124 https://doi.org/10.1016/0092-8674(93)90641-3.

Inoue, K., and Xiong, Z.G. (2009) Silencing TRPM7 promotes growth/proliferation and nitric oxide production of vascular endothelial cells via the ERK pathway. Cardiovascular Research 83: 547–557 https://doi.org/10.1093/cvr/cvp153.

Iovine, M.K. (2007) Conserved mechanisms regulate outgrowth in zebrafish fins. Nature Chemical Biology 3: 613–618 https://www.nature.com/articles/nchembio.2007.36.

Ishizawar, R., and Parsons, S.J. (2004) c-Src and cooperating partners in human cancer. Cancer Cell 6: 209–214 https://doi.org/10.1016/j.ccr.2004.09.001.

Jaffe, D.B., Johnston, D., Lasser-Ross, N., Lisman, J.E., Miyakawa, H., and Ross, W.N. (1992) The spread of Na+ spikes determines the pattern of dendritic Ca2+ entry into hippocampal neurons. Nature 357: 244–246 https://doi.org/10.1038/357244a0.

James, P., Vorherr, T., and Carafoli, E. (1995) Calmodulin-binding domains: just two faced or multi-faceted? Trends in Biochemical Sciences 20: 38–42 https://doi.org/10.1016/s0968-0004(00)88949-5.

Jelcic, M., Enyedi, B., Xavier, J.B., and Niethammer, P. (2017) Image-Based Measurement of H2O2 Reaction-Diffusion in Wounded Zebrafish Larvae. Biophysical Journal 112: 2011–2018 https://doi.org/10.1016/j.bpj.2017.03.021.

Jellinck, P.H., Monder, C., McEwen, B.S., and Sakai, R.R. (1993) Differential inhibition of 11β-hydroxysteroid dehydrogenase by carbenoxolone in rat brain regions and peripheral tissues. The Journal of Steroid Biochemistry and Molecular Biology 46: 209–213 https://doi.org/10.1016/0960-0760(93)90296-9.

Jia, C., Hayoz, S., Hutch, C.R., Iqbal, T.R., Pooley, A.E., and Hegg, C.C. (2013) An IP3R3- and NPY-Expressing microvillous cell mediates tissue homeostasis and regeneration in the mouse olfactory epithelium. PLoS ONE 8: e58668 https://doi.org/10.1371/journal.pone.0058668.

Judkewitz, B., Rizzi, M., Kitamura, K., and Häusser, M. (2009) Targeted single-cell electroporation of mammalian neurons in vivo. Nature Protocols 4: 862–869 https://doi.org/10.1038/nprot.2009.56.

Kaplan, K.B., Swedlow, J.R., Varmus, H.E., and Morgan, D.O. (1992) Association of p60c-src with endosomal membranes in mammalian fibroblasts. The Journal of Cell Biology 118: 321–333 https://pmc.ncbi.nlm.nih.gov/articles/PMC2290043/.

Karin, M., and Clevers, H. (2016) Reparative inflammation takes charge of tissue regeneration. Nature 529: 307–315.

Kase, H., Iwahashi, K., Nakanishi, S., Matsuda, Y., Yamada, K., Takahashi, M., et al. (1987) K-252 compounds, novel and potent inhibitors of protein kinase C and cyclic nucleotide-dependent protein kinases. Biochemical and Biophysical Research Communications 142: 436–440 https://doi.org/10.1016/0006-291x(87)90293-2.

Kashir, J., Deguchi, R., Jones, C., Coward, K., and Stricker, S.A. (2013) Comparative biology of sperm factors and fertilization-induced calcium signals across the animal kingdom. Molecular Reproduction and Development 80: 787–815 https://pubmed.ncbi.nlm.nih.gov/23900730/.

Kaufman, C.K., White, R.M., and Zon, L. (2009) Chemical genetic screening in the zebrafish embryo. Nature Protocols 4: 1422–1432 https://doi.org/10.1038/nprot.2009.144.

Kawakami, A., Fukazawa, T., and Takeda, H. (2004) Early fin primordia of zebrafish larvae regenerate by a similar growth control mechanism with adult regeneration. Developmental Dynamics 231: 693–699 https://doi.org/10.1002/dvdy.20181.

Kegelman, C.D., Collins, J.M., Nijsure, M.P., Eastburn, E.A., and Boerckel, J.D. (2020) Gone caving: Roles of the Transcriptional Regulators YAP and TAZ in skeletal Development. Current Osteoporosis Reports 18: 526–540 https://doi.org/10.1007/s11914-020-00605-3.

Kelu, J.J., Webb, S.E., Parrington, J., Galione, A., and Miller, A.L. (2017) Ca 2+ release via two-pore channel type 2 (TPC2) is required for slow muscle cell myofibrillogenesis and myotomal patterning in intact zebrafish embryos. Developmental Biology 425: 109–129 https://pubmed.ncbi.nlm.nih.gov/28390800/.

Kim, I., Moon, S.O., Kim, S.H., Kim, H.J., Koh, Y.S., and Koh, G.Y. (2001) Vascular Endothelial Growth Factor Expression of Intercellular Adhesion Molecule 1 (ICAM-1), Vascular Cell Adhesion Molecule 1 (VCAM-1), and E-selectin through Nuclear Factor-κB Activation in Endothelial Cells. Journal of Biological Chemistry 276: 7614–7620 https://doi.org/10.1074/jbc.m009705200.

Kirichok, Y., Krapivinsky, G., and Clapham, D.E. (2004) The mitochondrial calcium uniporter is a highly selective ion channel. Nature 427: 360–364 https://doi.org/10.1038/nature02246.

Kiselyov, K., and Muallem, S. (1999) Fatty acids, diacylglycerol, Ins(1,4,5)P3 receptors and Ca2+ influx. Trends in Neurosciences 22: 334–337 https://doi.org/10.1016/s0166-2236(99)01426-5.

Kitamura, K., Judkewitz, B., Kano, M., Denk, W., and Häusser, M. (2007) Targeted patch-clamp recordings and single-cell electroporation of unlabeled neurons in vivo. Nature Methods 5: 61–67 https://doi.org/10.1038/nmeth1150.

Kline, D., Kopf, G.S., Muncy, L.F., and Jaffe, L.A. (1991) Evidence for the involvement of a pertussis toxin-insensitive G-protein in egg activation of the frog, Xenopus laevis. Developmental Biology 143: 218–229 https://doi.org/10.1016/0012-1606(91)90072-b.

Kobayashi, S., Yano, M., Suetomi, T., Ono, M., Tateishi, H., Mochizuki, M., et al. (2009) Dantrolene, a therapeutic agent for malignant hyperthermia, markedly improves the function of failing cardiomyocytes by stabilizing interdomain interactions within the ryanodine receptor. Journal of the American College of Cardiology 53: 1993–2005 https://doi.org/10.1016/j.jacc.2009.01.065.

Koch, J.C., Tönges, L., Barski, E., Michel, U., Bähr, M., and Lingor, P. (2014) ROCK2 is a major regulator of axonal degeneration, neuronal death and axonal regeneration in the CNS. Cell Death and Disease 5: e1225 https://doi.org/10.1038/cddis.2014.191.

Kojima, N., Ishibashi, H., Obata, K., and Kandel, E.R. (1998) Higher Seizure Susceptibility and Enhanced Tyrosine Phosphorylation of N-Methyl-d-Aspartate Receptor Subunit 2B in fyn Transgenic Mice. Learning & Memory 5: 429–445 https://doi.org/10.1101/lm.5.6.429.

Konig, S., BéGuet, A., Bader, C.R., and Bernheim, L. (2006) The calcineurin pathway links hyperpolarization (Kir2.1)-induced Ca2+ signals to human myoblast differentiation and fusion. Development 133: 3107–3114 https://pubmed.ncbi.nlm.nih.gov/16831831/.

Korshunov, S.S., Skulachev, V.P., and Starkov, A.A. (1997) High protonic potential actuates a mechanism of production of reactive oxygen species in mitochondria. FEBS Letters 416: 15–18 https://doi.org/10.1016/s0014-5793(97)01159-9.

Korybalska, K., Rutkowski, R., Luczak, J., Czepulis, N., Karpinski, K., and Witowski, J. (2018) The role of purinergic P2Y12 receptor blockers on the angiogenic properties of endothelial cells: an in vitro study. PubMed 69 https://pubmed.ncbi.nlm.nih.gov/30415240.

Kregel, K.C., and Zhang, H.J. (2006) An integrated view of oxidative stress in aging: basic mechanisms, functional effects, and pathological considerations. AJP Regulatory Integrative and Comparative Physiology 292: R18–R36 https://doi.org/10.1152/ajpregu.00327.2006.

Kretsinger, R.H. (1980) Structure and evolution of Calcium-Modulated Protein. Critical Reviews in Biochemistry 8: 119–174 https://doi.org/10.3109/10409238009105467.

Kubota, H.Y., Yoshimoto, Y., Yoneda, M., and Hiramoto, Y. (1987) Free calcium wave upon activation in Xenopus eggs. Developmental Biology 119: 129–136 https://doi.org/10.1016/0012-1606(87)90214-4.

Kuhlmann, C.R.W., Schaefer, C.A., Reinhold, L., Tillmanns, H., and Erdogan, A. (2005) Signalling mechanisms of SDF-induced endothelial cell proliferation and migration. Biochemical and Biophysical Research Communications 335: 1107–1114 https://doi.org/10.1016/j.bbrc.2005.08.006.

Kulbatski, I., Cook, D.J., and Tator, C.H. (2004) Calcium Entry through L-Type Calcium Channels Is Essential for Neurite Regeneration in Cultured Sympathetic Neurons. Journal of Neurotrauma 21: 357–374 https://doi.org/10.1089/089771504322972130.

Kuriyan, J., and Cowburn, D. (1997) MODULAR PEPTIDE RECOGNITION DOMAINS IN EUKARYOTIC SIGNALING. Annual Review of Biophysics and Biomolecular Structure 26: 259–288 https://doi.org/10.1146/annurev.biophys.26.1.259.

Lacy, F., Kailasam, M.T., O'Connor, D.T., Schmid-SchöNbein, G.W., and Parmer, R.J. (2000) Plasma hydrogen peroxide production in human essential hypertension. Hypertension 36: 878–884 https://doi.org/10.1161/01.hyp.36.5.878.

LaFerla, F.M. (2002) Calcium dyshomeostasis and intracellular signalling in Alzheimer's disease. Nature Reviews Neuroscience 3: 862–872 https://doi.org/10.1038/nrn960.

Lambrecht, G., Friebe, T., Grimm, U., Windscheif, U., Bungardt, E., Hildebrandt, C., et al. (1992) PPADS, a novel functionally selective antagonist of P2 purinoceptor-mediated responses. European Journal of Pharmacology 217: 217–219 https://doi.org/10.1016/0014-2999(92)90877-7.

Laude, A.J., and Simpson, A.W.M. (2009) Compartmentalized signalling: Ca2+ compartments, microdomains and the many facets of Ca2+ signalling. FEBS Journal 276: 1800–1816 https://doi.org/10.1111/j.1742-4658.2009.06927.x.

Lechleiter, J., Girard, S., Peralta, E., and Clapham, D. (1991) Spiral Calcium Wave Propagation and Annihilation in Xenopus laevis Oocytes. Science 252: 123–126 https://doi.org/10.1126/science.2011747.

Leclerc, C., Webb, S.E., Daguzan, C., Moreau, M., and Miller, A.L. (2000) Imaging patterns of calcium transients during neural induction in Xenopus laevis embryos. Journal of Cell Science 113: 3519–3529 https://pubmed.ncbi.nlm.nih.gov/10984442/.

Li, C., Cantor, W.J., Nili, N., Robinson, R., Fenkell, L., Tran, Y.L.E., et al. (2002) Arterial repair after stenting and the effects of gm6001, a matrix metalloproteinase inhibitor. Journal of the American College of Cardiology 39: 1852–1858 https://doi.org/10.1016/s0735-1097(02)01873-9.

Li, P., Silvis, M.R., Honaker, Y., Lien, W.H., Arron, S.T., and Vasioukhin, V. (2016) αE-catenin inhibits a Src–YAP1 oncogenic module that couples tyrosine kinases and the effector of Hippo signaling pathway. Genes & Development 30: 798–811 https://genesdev.cshlp.org/content/30/7/798.

Li, X., Li, Y., Li, S., Li, H., Yang, C., and Lin, J. (2020) The role of Shh signalling pathway in central nervous system development and related diseases. Cell Biochemistry and Function 39: 180–189 https://doi.org/10.1002/cbf.3582.

Libera, L.D., Podhorska-Okolow, M., Martin, B., Massimino, M.L., Brugnolo, R., and Cantini, M. (1997) Smooth muscle myosin light chain kinase is transiently expressed in skeletal muscle during embryogenesis and muscle regeneration both in vivo and in vitro. Journal of Muscle Research and Cell Motility 18: 295–303 https://doi.org/10.1023/a:1018618008483.

Lin, A.H., Morris, J., Wishka, D.G., and Gorman, R.R. (1988) Novel molecules that antagonize leukotriene B4 binding to neutrophils. Annals of the New York Academy of Sciences 524: 196–200 https://doi.org/10.1111/j.1749-6632.1988.tb38542.x.

Lin, C.Y., Zu, C.H., Yang, C.C., Tsai, P.J., Shyu, J.F., Chen, C.P., et al. (2015) IL-1B-Induced mesenchymal stem cell migration involves MLCK activation via PKC signaling. Cell Transplantation 24: 2011–2028 https://doi.org/10.3727/096368914x685258.

Liu, Y., and Schneider, M.F. (2014) FGF2 activates TRPC and Ca2+ signaling leading to satellite cell activation. Frontiers in Physiology 5 https://pubmed.ncbi.nlm.nih.gov/24575047/.

Long, S.B., Campbell, E.B., and MacKinnon, R. (2005) Voltage sensor of KV1.2: Structural basis of electromechanical coupling. Science 309: 903–908 https://doi.org/10.1126/science.1116270.

Louis, M., Zanou, N., Van Schoor, M., and Gailly, P. (2008) TRPC1 regulates skeletal myoblast migration and differentiation. Journal of Cell Science 121: 3951–3959 https://pubmed.ncbi.nlm.nih.gov/19001499/.

Love, N.R., Chen, Y., Bonev, B., Gilchrist, M.J., Fairclough, L., Lea, R., et al. (2011) Genome-wide analysis of gene expression during Xenopus tropicalis tadpole tail regeneration. BMC Developmental Biology 11 https://doi.org/10.1186/1471-213x-11-70.

Love, N.R., Chen, Y., Ishibashi, S., Kritsiligkou, P., Lea, R., Koh, Y., et al. (2013) Amputation-induced reactive oxygen species are required for successful Xenopus tadpole tail regeneration. Nature Cell Biology 15: 222–228 https://doi.org/10.1038/ncb2659.

Lowell, C.A., and Soriano, P. (1996) Knockouts of Src-family kinases: stiff bones, wimpy T cells, and bad memories. Genes & Development 10: 1845–1857 https://doi.org/10.1101/gad.10.15.1845.

Lukas, T.J., Mirzoeva, S., Slomczynska, U., and Watterson, D.M. (1999) Identification of novel classes of protein kinase inhibitors using combinatorial peptide chemistry based on functional genomics knowledge. Journal of Medicinal Chemistry 42: 910–919 https://doi.org/10.1021/jm980573a.

López-Lázaro, M. (2006) Dual role of hydrogen peroxide in cancer: Possible relevance to cancer chemoprevention and therapy. Cancer Letters 252: 1–8 https://doi.org/10.1016/j.canlet.2006.10.029.

Ma, L.H., Webb, S.E., Chan, C.M., Zhang, J., and Miller, A.L. (2008) Establishment of a transitory dorsal-biased window of localized Ca2+ signaling in the superficial epithelium following the mid-blastula transition in zebrafish embryos. Developmental Biology 327: 143–157 https://doi.org/10.1016/j.ydbio.2008.12.015.

MacLennan, D.H. (2000) Ca2+ signalling and muscle disease. European Journal of Biochemistry 267: 5291–5297 https://doi.org/10.1046/j.1432-1327.2000.01566.x.

Maffucci, T., Raimondi, C., Abu Hayyeh, S., Dominguez, V., Sala, G., Zachary, I., and Falasca, M. (2009) A phosphoinositide 3-Kinase/Phospholipase CGAMMA1 pathway regulates fibroblast growth Factor-Induced capillary tube formation. PLoS ONE 4: e8285 https://doi.org/10.1371/journal.pone.0008285.

Magon, D.K. (1977) Glucose metabolism in the regenerating tail of the Scincid lizard,Mabuya striata. Journal of Natural History 11: 121–126 https://doi.org/10.1080/00222937700770091.

Mandrell, D., Truong, L., Jephson, C., Sarker, M.R., Moore, A., Lang, C., et al. (2012) Automated zebrafish chorion removal and single embryo placement: Optimizing throughput of zebrafish developmental toxicity screens. SLAS TECHNOLOGY 17: 66–74 https://doi.org/10.1177/2211068211432197.

Margrie, T., Brecht, M., and Sakmann, B. (2002) In vivo, low-resistance, whole-cell recordings from neurons in the anaesthetized and awake mammalian brain. Pflügers Archiv - European Journal of Physiology 444: 491–498 https://doi.org/10.1007/s00424-002-0831-z.

Marshall, C.J. (1995) Specificity of receptor tyrosine kinase signaling: Transient versus sustained extracellular signal-regulated kinase activation. Cell 80: 179–185 https://doi.org/10.1016/0092-8674(95)90401-8.

Martino, F., Perestrelo, A.R., Vinarský, V., Pagliari, S., and Forte, G. (2018) Cellular mechanotransduction: from tension to function. Frontiers in Physiology 9 https://doi.org/10.3389/fphys.2018.00824.

Maruyama, T., Kanaji, T., Nakade, S., Kanno, T., and Mikoshiba, K. (1997) 2APB, 2-Aminoethoxydiphenyl borate, a Membrane-Penetrable Modulator of INS(1,4,5)P3-Induced CA2+ release. The Journal of Biochemistry 122: 498–505 https://doi.org/10.1093/oxfordjournals.jbchem.a021780.

Marzia, M., Sims, N.A., Voit, S., Migliaccio, S., Taranta, A., Bernardini, S., et al. (2000) Decreased C-SRC expression enhances osteoblast differentiation and bone formation. The Journal of Cell Biology 151: 311–320 https://doi.org/10.1083/jcb.151.2.311.

Mathew, L.K., Sengupta, S., Kawakami, A., Andreasen, E.A., Löhr, C.V., Loynes, C.A., et al. (2007) Unraveling Tissue Regeneration Pathways Using Chemical Genetics. Journal of Biological Chemistry 282: 35202–35210 https://doi.org/10.1074/jbc.m706640200.

Matsui, A., Okigaki, M., Amano, K., Adachi, Y., Jin, D., Takai, S., et al. (2007) Central role of Calcium-Dependent tyrosine kinase PYK2 in endothelial nitric oxide Synthase–Mediated angiogenic response and vascular function. Circulation 116: 1041–1051 https://doi.org/10.1161/circulationaha.106.645416.

Matsumoto, Y., Matsuya, Y., Nagai, K., Amagase, K., Saeki, K., Matsumoto, K., et al. (2020) Leukotriene B4 receptor type 2 accelerates the healing of intestinal lesions by promoting epithelial cell proliferation. Journal of Pharmacology and Experimental Therapeutics 373: 1–9 https://doi.org/10.1124/jpet.119.263145.

McArthur, S., Juban, G., Gobbetti, T., Desgeorges, T., Theret, M., Gondin, J., et al. (2020) Annexin A1 drives macrophage skewing to accelerate muscle regeneration through AMPK activation. Journal of Clinical Investigation 130: 1156–1167 https://doi.org/10.1172/jci124635.

McCathie, G. (2018). The Molecular & Cellular Interactions of Wound-Induced Hydrogen Peroxide in the Regenerating Larval Zebrafish Tail. Ph.D. The University of Sheffield.

McCormack, J.G., Halestrap, A.P., and Denton, R.M. (1990) Role of calcium ions in regulation of mammalian intramitochondrial metabolism. Physiological Reviews 70: 391–425 https://doi.org/10.1152/physrev.1990.70.2.391.

McLachlan, D.R.C., Wong, L., Bergeron, C., and Baimbridge, K.G. (1987) Calmodulin and calbindin D28K in Alzheimer disease. Alzheimer Disease & Associated Disorders 1: 171–179 https://doi.org/10.1097/00002093-198701030-00009.

McPhalen, C.A., Strynadka, N.C.J., and James, M.N.G. (1991) Calcium-Binding Sites in Proteins: A Structural Perspective. Advances in Protein Chemistry 77–144 https://doi.org/10.1016/s0065-3233(08)60535-5.

McPherson, P.S., and Campbell, K.P. (1993) The ryanodine receptor/Ca2+ release channel. Journal of Biological Chemistry 268: 13765–13768 https://doi.org/10.1016/s0021-9258(19)85166-9.
Means, A.R. (1994) Calcium, calmodulin and cell cycle regulation. FEBS Letters 347: 1–4 https://doi.org/10.1016/0014-5793(94)00492-7.

Meda, F., Rampon, C., Dupont, E., Gauron, C., Mourton, A., Queguiner, I., et al. (2017) Nerves, H2O2 and Shh: Three players in the game of regeneration. Seminars in Cell and Developmental Biology 80: 65–73 https://doi.org/10.1016/j.semcdb.2017.08.015.

Mehta, D., Konstantoulaki, M., Ahmmed, G.U., and Malik, A.B. (2005) Sphingosine 1-Phosphate-induced mobilization of intracellular CA2+ mediates RAC activation and adherens junction assembly in endothelial cells. Journal of Biological Chemistry 280: 17320–17328 https://doi.org/10.1074/jbc.m411674200.

Meis, S., Hamacher, A., Hongwiset, D., Marzian, C., Wiese, M., Eckstein, N., et al. (2009) NF546 [4,4′-(Carbonylbis(imino-3,1-phenylene-carbonylimino-3,1-(4-methyl-phenylene)-carbonylimino))-bis(1,3-xylene-α,α′-diphosphonic Acid) Tetrasodium Salt] Is a Non-Nucleotide P2Y11 Agonist and Stimulates Release of Interleukin-8 from Human Monocyte-Derived Dendritic Cells. Journal of Pharmacology and Experimental Therapeutics 332: 238–247 https://doi.org/10.1124/jpet.109.157750.

Meissner, G. (1994) Ryanodine Receptor/Ca2+ release channels and their regulation by endogenous Effectors. Annual Review of Physiology 56: 485–508 https://doi.org/10.1146/annurev.ph.56.030194.002413.

Mergler, S., Dannowski, H., Bednarz, J., Engelmann, K., Hartmann, C., and Pleyer, U. (2003) Calcium influx induced by activation of receptor tyrosine kinases in SV40-transfected human corneal endothelial cells. Experimental Eye Research 77: 485–495 https://doi.org/10.1016/s0014-4835(03)00154-4.

Mignery, G.A., and Südhof, T.C. (1990) The ligand binding site and transduction mechanism in the inositol-1,4,5-triphosphate receptor. The EMBO Journal 9: 3893–3898 https://doi.org/10.1002/j.1460-2075.1990.tb07609.x.

Mikoshiba, K. (1993) Inositol 1,4,5-trisphosphate receptor. Trends in Pharmacological Sciences 14: 86–89 https://doi.org/10.1016/0165-6147(93)90069-v.

Mikoshiba, K. (2007) IP3 receptor/Ca2+ channel: from discovery to new signaling concepts. Journal of Neurochemistry 102: 1426–1446 https://doi.org/10.1111/j.1471-4159.2007.04825.x.

Miranda, J., Salgado, I., Torrado, A., and Santiago, J. (2015) Tamoxifen and Src kinase inhibitors as neuroprotective/neuroregenerative drugs after spinal cord injury. Neural Regeneration Research 10: 385 https://doi.org/10.4103/1673-5374.153685.

Mizuno, H., Sassa, T., Higashijima, S.-I., Okamoto, H., and Miyawaki, A. (2013) Transgenic zebrafish for ratiometric imaging of cytosolic and mitochondrial Ca2+ response in teleost embryo. Cell Calcium 54: 236–245 https://pubmed.ncbi.nlm.nih.gov/23906585/.

Moccia, F., Berra-Romani, R., Tritto, S., Signorelli, S., Taglietti, V., and Tanzi, F. (2002) Epidermal growth factor induces intracellular Ca2+ oscillations in microvascular endothelial cells. Journal of Cellular Physiology 194: 139–150 https://doi.org/10.1002/jcp.10198.

Moccia, F., Negri, S., Shekha, M., Faris, P., and Guerra, G. (2019) Endothelial CA2+ signaling, angiogenesis and vasculogenesis: just what it takes to make a blood vessel. International Journal of Molecular Sciences 20: 3962 https://doi.org/10.3390/ijms20163962.

Moens, U., Kostenko, S., and Sveinbjørnsson, B. (2013) The role of Mitogen-Activated Protein Kinase-Activated Protein Kinases (MAPKAPKs) in inflammation. Genes 4: 101–133 https://doi.org/10.3390/genes4020101.

Morgan, T.H. (1901) Regeneration. Macmillan & co., ltd., New York.

Morré, D.J. (2002) Preferential Inhibition of the Plasma Membrane NADH Oxidase (NOX) Activity by Diphenyleneiodonium Chloride with NADPH as Donor. Antioxidants and Redox Signaling 4: 207–212 https://doi.org/10.1089/152308602753625960.

Munaron, L. (2006) Intracellular calcium, endothelial cells and angiogenesis. Recent Patents on Anti-Cancer Drug Discovery 1: 105–119 https://pubmed.ncbi.nlm.nih.gov/18221030/.

Murphy, S.M., Bergman, M., and Morgan, D.O. (1993) Suppression of c-Src activity by C-terminal Src kinase involves the c-Src SH2 and SH3 domains: analysis with Saccharomyces cerevisiae. Molecular and Cellular Biology 13: 5290–5300 https://doi.org/10.1128/mcb.13.9.5290.

Musacchio, A., Saraste, M., and Wilmanns, M. (1994) High-resolution crystal structures of tyrosine kinase SH3 domains complexed with proline-rich peptides. Nature Structural & Molecular Biology 1: 546–551 https://doi.org/10.1038/nsb0894-546.

Nada, S., Okada, M., MacAuley, A., Cooper, J.A., and Nakagawa, H. (1991) Cloning of a complementary DNA for a protein-tyrosine kinase that specifically phosphorylates a negative regulatory site of p60c-src. Nature 351: 69–72 https://doi.org/10.1038/351069a0.

Nada, S., Yagi, T., Takeda, H., Tokunaga, T., Nakagawa, H., Ikawa, Y., et al. (1993) Constitutive activation of Src family kinases in mouse embryos that lack Csk. Cell 73: 1125–1135 https://doi.org/10.1016/0092-8674(93)90642-4.

Nagayama, S., Zeng, S., Xiong, W., Fletcher, M.L., Masurkar, A.V., Davis, D.J., et al. (2007) In vivo simultaneous tracing and CA2+ imaging of local neuronal circuits. Neuron 53: 789–803 https://doi.org/10.1016/j.neuron.2007.02.018.

Nakamura, T., Mito, T., Miyawaki, K., Ohuchi, H., and Noji, S. (2008) EGFR signaling is required for re-establishing the proximodistal axis during distal leg regeneration in the cricket Gryllus bimaculatus nymph. Developmental Biology 319: 46–55 https://doi.org/10.1016/j.ydbio.2008.04.002.

Nakatani, Y., Kawakami, A., and Kudo, A. (2007) Cellular and molecular processes of regeneration, with special emphasis on fish fins. Development Growth & Differentiation 49: 145–154 https://doi.org/10.1111/j.1440-169x.2007.00917.x.

Namdaran, P., Reinhart, K.E., Owens, K.N., Raible, D.W., and Rubel, E.W. (2012) Identification of Modulators of Hair Cell Regeneration in the Zebrafish Lateral Line. Journal of Neuroscience 32: 3516–3528 https://doi.org/10.1523/jneurosci.3905-11.2012.

Namikawa, K., Honma, M., Abe, K., Takeda, M., Mansur, K., Obata, T., et al. (2000) AKT/Protein kinase B prevents Injury-Induced motoneuron death and accelerates axonal regeneration. Journal of Neuroscience 20: 2875–2886 https://doi.org/10.1523/jneurosci.20-08-02875.2000.

Narumiya, S., Ishizaki, T., and Ufhata, M. (2000) Use and properties of ROCK-specific inhibitor Y-27632. Methods in Enzymology on CD-ROM/Methods in Enzymology 273–284 https://doi.org/10.1016/s0076-6879(00)25449-9.

Nechiporuk, A., and Keating, M.T. (2002) A proliferation gradient between proximal andmsxb-expressing distal blastema directs zebrafish fin regeneration. Development 129: 2607–2617 https://doi.org/10.1242/dev.129.11.2607.

Nevian, T., and Helmchen, F. (2007) Calcium indicator loading of neurons using single-cell electroporation. Pflügers Archiv - European Journal of Physiology 454: 675–688 https://doi.org/10.1007/s00424-007-0234-2.
Nicholls, D.G. (2003) Mitochondrial membrane potential and aging. Aging Cell 3: 35–40 https://doi.org/10.1111/j.1474-9728.2003.00079.x.

Nicholls, D.G., and Ferguson, S.J. (2002) Bioenergetics 3. 3rd ed., Academic Press, San Diego, Calif.
Nicoletti, V.G., Pajer, K., Calcagno, D., Pajenda, G., and Nógrádi, A. (2022) The role of metals in the neuroregenerative action of BDNF, GDNF, NGF and other neurotrophic factors. Biomolecules 12: 1015 https://doi.org/10.3390/biom12081015.

Niethammer, P., Grabher, C., Look, A.T., and Mitchison, T.J. (2009) A tissue-scale gradient of hydrogen peroxide mediates rapid wound detection in zebrafish. Nature 459: 996–999 http://dx.doi.org/10.1038/nature08119.

Nikulina, E., Tidwell, J.L., Dai, H.N., Bregman, B.S., and Filbin, M.T. (2004) The phosphodiesterase inhibitor rolipram delivered after a spinal cord lesion promotes axonal regeneration and functional recovery. Proceedings of the National Academy of Sciences 101: 8786–8790 https://doi.org/10.1073/pnas.0402595101.

Nishizumi, H., Horikawa, K., Mlinaric-Rascan, I., and Yamamoto, T. (1998) A Double-Edged Kinase LYN: a positive and negative regulator for antigen receptor–mediated signals. The Journal of Experimental Medicine 187: 1343–1348 https://pubmed.ncbi.nlm.nih.gov/9547345/.

Oh-Hora, M., and Rao, A. (2008) Calcium signaling in lymphocytes. Current Opinion in Immunology 20: 250–258 https://doi.org/10.1016/j.coi.2008.04.004.

Ohkubo, H., Ito, Y., Minamino, T., Mishima, T., Hirata, M., Hosono, K., et al. (2013) Leukotriene B4type-1 receptor signaling promotes liver repair after hepatic ischemia/reperfusion injury through the enhancement of macrophage recruitment. The FASEB Journal 27: 3132–3143 https://doi.org/10.1096/fj.13-227421.

Okada, M., Howell, B.W., Broome, M.A., and Cooper, J.A. (1993) Deletion of the SH3 domain of Src interferes with regulation by the phosphorylated carboxyl-terminal tyrosine. Journal of Biological Chemistry 268: 18070–18075 https://doi.org/10.1016/s0021-9258(17)46812-8.

Oktyabrsky, O.N., and Smirnova, G.V. (2007) Redox regulation of cellular functions. Biochemistry (Moscow) 72: 132–145 http://dx.doi.org/10.1134/s0006297907020022.

Okumura, N., Koizumi, N., Ueno, M., Sakamoto, Y., Takahashi, H., Tsuchiya, H., et al. (2012) ROCK Inhibitor Converts Corneal Endothelial Cells into a Phenotype Capable of Regenerating In Vivo Endothelial Tissue. American Journal of Pathology 181: 268–277 https://doi.org/10.1016/j.ajpath.2012.03.033.

Pafumi, I., Favia, A., Gambara, G., Papacci, F., Ziparo, E., Palombi, F., and Filippini, A. (2015) Regulation of Angiogenic Functions by Angiopoietins through Calcium-Dependent Signaling Pathways. BioMed Research International 2015: 1–14 https://doi.org/10.1155/2015/965271.

Palmer, A., Zimmer, M., Erdmann, K.S., Eulenburg, V., Porthin, A., Heumann, R., et al. (2002) EphrinB phosphorylation and reverse signaling: regulation by Src kinases and PTP-BL phosphatase. Molecular Cell 9: 725–737 https://pubmed.ncbi.nlm.nih.gov/11983165/.

Panfili, E., Sandri, G., and Ernster, L. (1991) Distribution of glutathione peroxidases glutathione reductase in rat brain mitochondria. FEBS Letters 290: 35–37 https://doi.org/10.1016/0014-5793(91)81219-x.

Parker, I., and Yao, Y. (1996) Ca2+ transients associated with openings of inositol trisphosphate-gated channels in Xenopus oocytes. The Journal of Physiology 491: 663–668 https://doi.org/10.1113/jphysiol.1996.sp021247.

Paudel, S., Sindelar, R., and Saha, M. (2018) Calcium Signaling in Vertebrate Development and Its Role in Disease. International Journal of Molecular Sciences 19: 3390.

Pawson, T. (1995) Protein modules and signalling networks. Nature 373: 573–580 https://doi.org/10.1038/373573a0.

Pedersen, P.L., and Carafoli, E. (1987) Ion motive ATPases. I. Ubiquity, properties, and significance to cell function. Trends in Biochemical Sciences 12: 146–150 https://doi.org/10.1016/0968-0004(87)90071-5.
Peiris, T.H., Ramirez, D., Barghouth, P.G., and Oviedo, N.J. (2016) The Akt signaling pathway is required for tissue maintenance and regeneration in planarians. BMC Developmental Biology 16 https://doi.org/10.1186/s12861-016-0107-z.

Pesic, A., Madden, J.A., Pesic, M., and Rusch, N.J. (2004) High blood pressure upregulates arterial L-Type Ca2+ channels. Circulation Research 94 https://doi.org/10.1161/01.res.0000131495.93500.3c.

Pesic, M., and Greten, F.R. (2016) Inflammation and cancer: tissue regeneration gone awry. Current Opinion in Cell Biology 43: 55–61 https://doi.org/10.1016/j.ceb.2016.07.010.

Pfefferli, C., and Jaźwińska, A. (2015) The art of fin regeneration in zebrafish. Regeneration 2: 72–83 https://doi.org/10.1002/reg2.33.

Pirotte, N., Stevens, A.S., Fraguas, S., Plusquin, M., Van Roten, A., Van Belleghem, F., et al. (2015) Reactive oxygen species in planarian regeneration: an upstream necessity for correct patterning and brain formation. Oxidative Medicine and Cellular Longevity 2015: 1–19 https://doi.org/10.1155/2015/392476.

Pirson, M., Debrulle, S., Clippe, A., Clotman, F., and Knoops, B. (2015) Thioredoxin-2 modulates neuronal programmed cell death in the embryonic chick spinal cord in basal and Target-Deprived conditions. PLoS ONE 10: e0142280 https://doi.org/10.1371/journal.pone.0142280.

Poliak, S., Morales, D., Croteau, L.P., Krawchuk, D., Palmesino, E., Morton, S., et al. (2015) Synergistic integration of Netrin and ephrin axon guidance signals by spinal motor neurons. eLife 4 https://pmc.ncbi.nlm.nih.gov/articles/PMC4764565/.

Poss, K.D., Keating, M.T., and Nechiporuk, A. (2003) Tales of regeneration in zebrafish. Developmental Dynamics 226: 202–210 https://doi.org/10.1002/dvdy.10220.

Powis, G., Bonjouklian, R., Berggren, M.M., Gallegos, A., Abraham, R., Ashendel, C., et al. (1994) Wortmannin, a potent and selective inhibitor of phosphatidylinositol-3-kinase. PubMed 54: 2419–23 https://pubmed.ncbi.nlm.nih.gov/8162590.

Pozzan, T., Rizzuto, R., Volpe, P., and Meldolesi, J. (1994) Molecular and cellular physiology of intracellular calcium stores. Physiological Reviews 74: 595–636 https://doi.org/10.1152/physrev.1994.74.3.595.
Péréon, Y., Navarro, J., Sorrentino, V., Louboutin, J.-P., Noireaud, J., and Palade, P. (1996) Regulation of dihydropyridine receptor and ryanodine receptor gene expression in regenerating skeletal muscle. Pflügers Archiv - European Journal of Physiology 433: 221–229 https://doi.org/10.1007/s004240050271.

Raha, S., and Robinson, B.H. (2000) Mitochondria, oxygen free radicals, disease and ageing. Trends in Biochemical Sciences 25: 502–508 https://doi.org/10.1016/s0968-0004(00)01674-1.

Rampon, C., Volovitch, M., Joliot, A., and Vriz, S. (2018) Hydrogen peroxide and redox regulation of developments. Antioxidants 7: 159 https://doi.org/10.3390/antiox7110159.

Ramsey, I.S., Delling, M., and Clapham, D.E. (2005) AN INTRODUCTION TO TRP CHANNELS. Annual Review of Physiology 68: 619–647 https://doi.org/10.1146/annurev.physiol.68.040204.100431.
Raynaud, F., Carnac, G., Marcilhac, A., and Benyamin, Y. (2004) m-Calpain implication in cell cycle during muscle precursor cell activation. Experimental Cell Research 298: 48–57 https://pubmed.ncbi.nlm.nih.gov/15242761/.

Ren, R., Mayer, B.J., Cicchetti, P., and Baltimore, D. (1993) Identification of a Ten-Amino Acid Proline-Rich SH3 Binding Site. Science 259: 1157–1161 https://doi.org/10.1126/science.8438166.

Rennekamp, A.J., and Peterson, R.T. (2014) 15 years of zebrafish chemical screening. Current Opinion in Chemical Biology 24: 58–70 https://doi.org/10.1016/j.cbpa.2014.10.025.

Resh, M. (1993) Interaction of tyrosine kinase oncoproteins with cellular membranes. Biochimica Et Biophysica Acta (BBA) - Reviews on Cancer 1155: 307–322 https://doi.org/10.1016/0304-419x(93)90012-2.

Resh, M.D. (1994) Myristylation and palmitylation of Src family members: The fats of the matter. Cell 76: 411–413 https://doi.org/10.1016/0092-8674(94)90104-x.

Reth, M. (2002) Hydrogen peroxide as second messenger in lymphocyte activation. Nature Immunology 3: 1129–1134 https://www.nature.com/articles/ni1202-1129.

Ribeiro, D.E., Glaser, T., Oliveira-Giacomelli, Á., and Ulrich, H. (2018) Purinergic receptors in neurogenic processes. Brain Research Bulletin 151: 3–11 https://doi.org/10.1016/j.brainresbull.2018.12.013.

Rickles, R.J., Botfield, M.C., Zhou, X.M., Henry, P.A., Brugge, J.S., and Zoller, M.J. (1995) Phage display selection of ligand residues important for Src homology 3 domain binding specificity. Proceedings of the National Academy of Sciences 92: 10909–10913 https://doi.org/10.1073/pnas.92.24.10909.

Ridefelt, P., Yokote, K., Claesson-Welsh, L., and Siegbahn, A. (1995) Pdgf-BB Triggered Cytoplasmic Calcium Responses in Cells with Endogenous or Stably Transfected PDGF β-Receptors. Growth Factors 12: 191–201 https://doi.org/10.3109/08977199509036879.

Robb-Gaspers, L.D., and Thomas, A.P. (1995) Coordination of Ca2+ signaling by intercellular propagation of Ca2+ waves in the intact liver. Journal of Biological Chemistry 270: 8102–8107 https://doi.org/10.1074/jbc.270.14.8102.

Rohwedder, I., Kurz, A.R.M., Pruenster, M., Immler, R., Pick, R., Eggersmann, T., et al. (2019) Src family kinase-mediated vesicle trafficking is critical for neutrophil basement membrane penetration. Haematologica 105: 1845–1856 http://dx.doi.org/10.3324/haematol.2019.225722.

Romero, M.M.G., McCathie, G., Jankun, P., and Roehl, H.H. (2018) Damage-induced reactive oxygen species enable zebrafish tail regeneration by repositioning of Hedgehog expressing cells. Nature Communications 9 http://dx.doi.org/10.1038/s41467-018-06460-2.

Rondeau, V., Jain, A., Truong, V., and Srivastava, A.K. (2019) Involvement of the Akt-dependent CREB signaling pathway in hydrogen-peroxide-induced early growth response protein-1 expression in rat vascular smooth muscle cells. Canadian Journal of Physiology and Pharmacology 97: 885–892 https://doi.org/10.1139/cjpp-2019-0061.

Rooney, T.A., Sass, E.J., and Thomas, A.P. (1990) Agonist-induced cytosolic calcium oscillations originate from a specific locus in single hepatocytes. Journal of Biological Chemistry 265: 10792–10796 https://doi.org/10.1016/s0021-9258(18)87017-x.

Roos, J., DiGregorio, P.J., Yeromin, A.V., Ohlsen, K., Lioudyno, M., Zhang, S., et al. (2005) STIM1, an essential and conserved component of store-operated Ca2+ channel function. The Journal of Cell Biology 169: 435–445 https://doi.org/10.1083/jcb.200502019.

Rosemblit, N., Moschella, M.C., S, E.O., Gutstein, D.E., S, K.O., and Marks, A.R. (1999) Intracellular Calcium Release Channel Expression during Embryogenesis. Developmental Biology 206: 163–177 https://doi.org/10.1006/dbio.1998.9120.

Rozen, E.J., Roewenstrunk, J., Barallobre, M.J., Di Vona, C., Jung, C., Figueiredo, A.F., et al. (2018) DYRK1A kinase positively regulates angiogenic responses in endothelial cells. Cell Reports 23: 1867–1878 https://doi.org/10.1016/j.celrep.2018.04.008.

Rudd, C.E., Trevillyan, J.M., Dasgupta, J.D., Wong, L.L., and Schlossman, S.F. (1988) The CD4 receptor is complexed in detergent lysates to a protein-tyrosine kinase (pp58) from human T lymphocytes. Proceedings of the National Academy of Sciences 85: 5190–5194 https://doi.org/10.1073/pnas.85.14.5190.

Russell, J.T. (2010) Imaging calcium signals in vivo: a powerful tool in physiology and pharmacology. British Journal of Pharmacology 163: 1605–1625 https://doi.org/10.1111/j.1476-5381.2010.00988.x.

Rutter, G.A., Burnett, P., Rizzuto, R., Brini, M., Murgia, M., Pozzan, T., et al. (1996) Subcellular imaging of intramitochondrial Ca2+ with recombinant targeted aequorin: significance for the regulation of pyruvate dehydrogenase activity. Proceedings of the National Academy of Sciences 93: 5489–5494 https://doi.org/10.1073/pnas.93.11.5489.

Röder, I.V., Strack, S., Reischl, M., Dahley, O., Khan, M.M., Kassel, O., et al. (2012) Participation of Myosin VA and PKA Type I in the regeneration of neuromuscular junctions. PLoS ONE 7: e40860 https://doi.org/10.1371/journal.pone.0040860.

Sabatini, B.L., Oertner, T.G., and Svoboda, K. (2002) The life cycle of Ca2+ ions in dendritic spines. Neuron 33: 439–452 https://doi.org/10.1016/s0896-6273(02)00573-1.

Sabra, H., Brunner, M., Mandati, V., Wehrle-Haller, B., Lallemand, D., Ribba, A.S., et al. (2017) β1 integrin–dependent Rac/group I PAK signaling mediates YAP activation of Yes-associated protein 1 (YAP1) via NF2/merlin. Journal of Biological Chemistry 292: 19179–19197 https://doi.org/10.1074/jbc.m117.808063.

Saccani, A., Saccani, S., Orlando, S., Sironi, M., Bernasconi, S., Ghezzi, P., et al. (2000) Redox regulation of chemokine receptor expression. Proceedings of the National Academy of Sciences 97: 2761–2766 https://doi.org/10.1073/pnas.97.6.2761.

Saijo, K., Schmedt, C., Su, I.H., Karasuyama, H., Lowell, C.A., Reth, M., et al. (2003) Essential role of Src-family protein tyrosine kinases in NF-κB activation during B cell development. Nature Immunology 4: 274–279 https://pubmed.ncbi.nlm.nih.gov/12563261/.

Sakuma, K., Nishikawa, J., Nakao, R., Watanabe, K., Totsuka, T., Nakano, H., et al. (2002) Calcineurin is a potent regulator for skeletal muscle regeneration by association with NFATc1 and GATA-2. Acta Neuropathologica 105: 271–280 https://pubmed.ncbi.nlm.nih.gov/12557015/.

Sakurai, T., Kashimura, O., Kano, Y., Ohno, H., Ji, L.L., Izawa, T., and Best, T.M. (2013) Role of nitric oxide in muscle regeneration following eccentric muscle contractions in rat skeletal muscle. The Journal of Physiological Sciences 63: 263–270 https://doi.org/10.1007/s12576-013-0262-y.

Sameermahmood, Z., Balasubramanyam, M., Saravanan, T., and Rema, M. (2008) Curcumin modulates SDF-1A/CXCR4–Induced migration of human retinal endothelial cells (HRECs). Investigative Ophthalmology & Visual Science 49: 3305 https://doi.org/10.1167/iovs.07-0456.

Sanderson, M.J., Charles, A.C., and Dirksen, E.R. (1990) Mechanical stimulation and intercellular communication increases intracellular Ca2+ in epithelial cells. Cell Regulation 1: 585–596 https://doi.org/10.1091/mbc.1.8.585.

Sato, C., Hamada, K., Ogura, T., Miyazawa, A., Iwasaki, K., Hiroaki, Y., et al. (2003) Inositol 1,4,5-trisphosphate receptor contains multiple cavities and L-shaped ligand-binding domains. Journal of Molecular Biology 336: 155–164 https://doi.org/10.1016/j.jmb.2003.11.024.

Schuchmann, S., Müller, W., and Heinemann, U. (1998) Altered Ca2+Signaling and mitochondrial deficiencies in hippocampal neurons of trisomy 16 mice: a model of Down's Syndrome. Journal of Neuroscience 18: 7216–7231 https://doi.org/10.1523/jneurosci.18-18-07216.1998.

Seaver, L.C., and Imlay, J.A. (2001) Alkyl Hydroperoxide Reductase Is the Primary Scavenger of Endogenous Hydrogen Peroxide in Escherichia coli. Journal of Bacteriology 183: 7173–7181 https://doi.org/10.1128/jb.183.24.7173-7181.2001.

Seidler, N.W., Jona, I., Vegh, M., and Martonosi, A. (1989) Cyclopiazonic Acid is a Specific Inhibitor of the Ca2+-ATPase of Sarcoplasmic Reticulum. Journal of Biological Chemistry 264: 17816–17823.
Sen, B., and Johnson, F.M. (2011) Regulation of Src Family Kinases in Human Cancers. Journal of Signal Transduction 2011: 1–14 https://doi.org/10.1155/2011/865819.

Shan, S.W., Tang, M.K., Cai, D.Q., Chui, Y.L., Chow, P.H., Grotewold, L., and Lee, K.K.H. (2005) Comparative proteomic analysis identifies protein disulfide isomerase and peroxiredoxin 1 as new players involved in embryonic interdigital cell death. Developmental Dynamics 233: 266–281 https://doi.org/10.1002/dvdy.20404.

Shaw, R.J., Lamia, K.A., Vasquez, D., Koo, S.-H., Bardeesy, N., DePinho, R.A., et al. (2005) The kinase LKB1 mediates glucose homeostasis in liver and therapeutic effects of metformin. Science 310: 1642–1646 https://doi.org/10.1126/science.1120781.

Shi, W., Fang, Z., Li, L., and Luo, L. (2015) Using zebrafish as the model organism to understand organ regeneration. Science China Life Sciences 58: 343–351 http://dx.doi.org/10.1007/s11427-015-4838-z.

Shindo, A., Hara, Y., Yamamoto, T.S., Ohkura, M., Nakai, J., and Ueno, N. (2010) Tissue-Tissue Interaction-Triggered Calcium Elevation Is Required for Cell Polarization during Xenopus Gastrulation. PLoS ONE 5: e8897 https://pubmed.ncbi.nlm.nih.gov/20126393/.

Shirakabe, K., Priori, G., Yamada, H., Ando, H., Horita, S., Fujita, T., et al. (2006) IRBIT, an inositol 1,4,5-trisphosphate receptor-binding protein, specifically binds to and activates pancreas-type Na+/HCO3-cotransporter 1 (pNBC1). Proceedings of the National Academy of Sciences 103: 9542–9547 https://doi.org/10.1073/pnas.0602250103.

Shumilina, E., Huber, S.M., and Lang, F. (2011) Ca2+ signaling in the regulation of dendritic cell functions. AJP Cell Physiology 300: C1205–C1214 https://doi.org/10.1152/ajpcell.00039.2011.

Simkin, J., Gawriluk, T.R., Gensel, J.C., and Seifert, A.W. (2017) Macrophages are necessary for epimorphic regeneration in African spiny mice. eLife 6 https://doi.org/10.7554/elife.24623.

Singh, B. (1986) The mechanism of action of calcium antagonists relative to their clinical applications. British Journal of Clinical Pharmacology 21 https://doi.org/10.1111/j.1365-2125.1986.tb02860.x.

Sinha, S., Elbaz-Alon, Y., and Avinoam, O. (2022) Ca2+ as a coordinator of skeletal muscle differentiation, fusion and contraction. FEBS Journal 289: 6531–6542 https://doi.org/10.1111/febs.16552.

Sipka, T., Peroceschi, R., Hassan-Abdi, R., Groß, M., Ellett, F., Begon-Pescia, C., et al. (2021) Damage-Induced Calcium Signaling and Reactive Oxygen Species Mediate Macrophage Activation in Zebrafish. Frontiers in Immunology 12 http://dx.doi.org/10.3389/fimmu.2021.636585.

Small, G.R., Hadoke, P.W.F., Sharif, I., Dover, A.R., Armour, D., Kenyon, C.J., et al. (2005) Preventing local regeneration of glucocorticoids by 11β-hydroxysteroid dehydrogenase type 1 enhances angiogenesis. Proceedings of the National Academy of Sciences 102: 12165–12170 https://doi.org/10.1073/pnas.0500641102.

Smoot, R.L., Werneburg, N.W., Sugihara, T., Hernandez, M.C., Yang, L., Mehner, C., et al. (2017) Platelet-derived growth factor regulates YAP transcriptional activity via Src family kinase dependent tyrosine phosphorylation. Journal of Cellular Biochemistry 119: 824–836 https://doi.org/10.1002/jcb.26246.

Songyang, Z., Shoelson, S.E., Chaudhuri, M., Gish, G., Pawson, T., Haser, W.G., et al. (1993) SH2 domains recognize specific phosphopeptide sequences. Cell 72: 767–778 https://doi.org/10.1016/0092-8674(93)90404-e.

St-Pierre, J., Buckingham, J.A., Roebuck, S.J., and Brand, M.D. (2002) Topology of Superoxide Production from Different Sites in the Mitochondrial Electron Transport Chain. Journal of Biological Chemistry 277: 44784–44790 https://doi.org/10.1074/jbc.m207217200.

Stehelin, D., Varmus, H.E., Bishop, J.M., and Vogt, P.K. (1976) DNA related to the transforming gene(s) of avian sarcoma viruses is present in normal avian DNA. Nature 260: 170–173 https://doi.org/10.1038/260170a0.

Stern, H.M., Murphey, R.D., Shepard, J.L., Amatruda, J.F., Straub, C.T., Pfaff, K.L., et al. (2005) Small molecules that delay S phase suppress a zebrafish bmyb mutant. Nature Chemical Biology 1: 366–370 https://doi.org/10.1038/nchembio749.

Steward, F.C., Mapes, M.O., Kent, A.E., and Holsten, R.D. (1964) Growth and Development of Cultured Plant Cells. Science 143: 20–27 https://doi.org/10.1126/science.143.3601.20.

Stewart, R., Flechner, L., Montminy, M., and Berdeaux, R. (2011) CREB is activated by muscle injury and promotes muscle regeneration. PLoS ONE 6: e24714 https://doi.org/10.1371/journal.pone.0024714.

Stone, J.R. (2004) An assessment of proposed mechanisms for sensing hydrogen peroxide in mammalian systems. Archives of Biochemistry and Biophysics 422: 119–124 https://doi.org/10.1016/j.abb.2003.12.029.

Strehler, E., and Treiman, M. (2004) Calcium pumps of plasma membrane and cell interior. Current Molecular Medicine 4: 323–335 https://doi.org/10.2174/1566524043360735.

Suematsu, M., Schmid-Schonbein, G.W., Chavez-Chavez, R.H., Yee, T.T., Tamatani, T., Miyasaka, M., et al. (1993) In vivo visualization of oxidative changes in microvessels during neutrophil activation. AJP Heart and Circulatory Physiology 264: H881–H891 https://doi.org/10.1152/ajpheart.1993.264.3.h881.

Sugimori, M., Lang, E.J., Silver, R.B., and Llinás, R. (1994) High-Resolution Measurement of the Time Course of Calcium-Concentration Microdomains at Squid Presynaptic Terminals. Biological Bulletin 187: 300–303 https://pubmed.ncbi.nlm.nih.gov/7841233/.

Sun, D., Cui, S., and Sun, Y. (2010) Cell Signal Transduction. 4th ed., China Science Publishing & Media, Beijing.

Sun, Q., Wu, R., Cai, S., Lin, Y., Sellers, L., Sakamoto, K., et al. (2011) Synthesis and biological evaluation of analogues of AKT (Protein kinase B) Inhibitor-IV. Journal of Medicinal Chemistry 54: 1126–1139 https://doi.org/10.1021/jm100912b.

Sundaralingam, M., Bergstrom, R., Strasburg, G., Rao, S.T., Roychowdhury, P., Greaser, M., and Wang, B.C. (1985) Molecular Structure of Troponin C from Chicken Skeletal Muscle at 3-Angstrom Resolution. Science 227: 945–948 https://doi.org/10.1126/science.3969570.

Superti-Furga, G., Fumagalli, S., Koegl, M., Courtneidge, S.A., and Draetta, G. (1993) Csk inhibition of c-Src activity requires both the SH2 and SH3 domains of Src. The EMBO Journal 12: 2625–2634 https://doi.org/10.1002/j.1460-2075.1993.tb05923.x.

Suzuki, M., Takagi, C., Miura, S., Sakane, Y., Suzuki, M., Sakuma, T., et al. (2016) In vivo tracking of histone H3 lysine 9 acetylation in Xenopus laevis during tail regeneration. Genes to Cells 21: 358–369 https://doi.org/10.1111/gtc.12349.

Svoboda, K., Denk, W., Kleinfeld, D., and Tank, D.W. (1997) In vivo dendritic calcium dynamics in neocortical pyramidal neurons. Nature 385: 161–165 https://doi.org/10.1038/385161a0.

Szatrowski, T.P., and Nathan, C.F. (1991) Production of large amounts of hydrogen peroxide by human tumor cells. PubMed 51: 794–8 https://pubmed.ncbi.nlm.nih.gov/1846317.

Takamatsu, T., and Wier, W.G. (1990) Calcium waves in mammalian heart: quantification of origin, magnitude, waveform, and velocity. The FASEB Journal 4: 1519–1525 https://doi.org/10.1096/fasebj.4.5.2307330.

Takeshima, H., Nishimura, S., Matsumoto, T., Ishida, H., Kangawa, K., Minamino, N., et al. (1989) Primary structure and expression from complementary DNA of skeletal muscle ryanodine receptor. Nature 339: 439–445 https://doi.org/10.1038/339439a0.

Tal, T.L., Franzosa, J.A., and Tanguay, R.L. (2009) Molecular Signaling networks that choreograph epimorphic Fin Regeneration in Zebrafish – A Mini-Review. Gerontology 56: 231–240 https://doi.org/10.1159/000259327.

Taniguchi, K., Wu, L.-W., Grivennikov, S.I., De Jong, P.R., Lian, I., Yu, F.-X., et al. (2015) A gp130–Src–YAP module links inflammation to epithelial regeneration. Nature 519: 57–62 https://www.nature.com/articles/nature14228.

Thomas, E.L., Grisham, M.B., Melton, D.F., and Jefferson, M.M. (1985) Evidence for a role of taurine in the in vitro oxidative toxicity of neutrophils toward erythrocytes. Journal of Biological Chemistry 260: 3321–3329 https://doi.org/10.1016/s0021-9258(19)83623-2.

Thomas, S.M., and Brugge, J.S. (1997) CELLULAR FUNCTIONS REGULATED BY SRC FAMILY KINASES. Annual Review of Cell and Developmental Biology 13: 513–609 https://doi.org/10.1146/annurev.cellbio.13.1.513.

Thuveson, M., Albrecht, D., Zurcher, G., Andres, A.C., and Ziemiecki, A. (1995) IYK, a novel intracellular protein tyrosine kinase differentially expressed in the mouse mammary gland and intestine. Biochemical and Biophysical Research Communications 209: 582–589 https://doi.org/10.1006/bbrc.1995.1540.

Toullec, D., Pianetti, P., Coste, H., Bellevergue, P., Grand-Perret, T., Ajakane, M., et al. (1991) The bisindolylmaleimide GF 109203X is a potent and selective inhibitor of protein kinase C. Journal of Biological Chemistry 266: 15771–15781 https://doi.org/10.1016/s0021-9258(18)98476-0.

Toyoshima, C., Sasabe, H., and Stokes, D.L. (1993) Three-dimensional cryo-electron microscopy of the calcium ion pump in the sarcoplasmic reticulum membrane. Nature 362: 469–471 https://doi.org/10.1038/362469a0.

Trembley, J.H., and Steer, C.J. (1998) Perspectives on liver regeneration. Journal of the Minnesota Academy of Science 63: 37–46 https://digitalcommons.morris.umn.edu/jmas/vol63/iss2/4.

Truong, L., Reif, D.M., St Mary, L., Geier, M.C., Truong, H.D., and Tanguay, R.L. (2013) Multidimensional in vivo hazard assessment using zebrafish. Toxicological Sciences 137: 212–233 https://doi.org/10.1093/toxsci/kft235.

Tsai, F.C., Seki, A., Yang, H.W., Hayer, A., Carrasco, S., Malmersjö, S., and Meyer, T. (2014) A polarized Ca2+, diacylglycerol and STIM1 signalling system regulates directed cell migration. Nature Cell Biology 16: 133–144 https://doi.org/10.1038/ncb2906.

Tu, M.K., and Borodinsky, L.N. (2014) Spontaneous calcium transients manifest in the regenerating muscle and are necessary for skeletal muscle replenishment. Cell Calcium 56: 34–41 https://pubmed.ncbi.nlm.nih.gov/24854233/.

Tu, M.K., Levin, J.B., Hamilton, A.M., and Borodinsky, L.N. (2016) Calcium signaling in skeletal muscle development, maintenance and regeneration. Cell Calcium 59: 91–97 https://doi.org/10.1016/j.ceca.2016.02.005.

Tymianski, M., Spigelman, I., Zhang, L., Carlen, P.L., Tator, C.H., Charlton, M.P., and Wallace, M.C. (1994) Mechanism of action and persistence of neuroprotection by Cell-Permeant CA2+Chelators. Journal of Cerebral Blood Flow & Metabolism 14: 911–923 https://doi.org/10.1038/jcbfm.1994.122.

Ufer, C., Wang, C.C., Borchert, A., Heydeck, D., and Kuhn, H. (2010) Redox control in mammalian embryo development. Antioxidants and Redox Signaling 13: 833–875 https://doi.org/10.1089/ars.2009.3044.

Van Der Vliet, A., and Janssen-Heininger, Y.M.W. (2013) Hydrogen peroxide as a damage signal in tissue injury and inflammation: murderer, mediator, or messenger? Journal of Cellular Biochemistry 115: 427–435 https://doi.org/10.1002/jcb.24683.

Vasquez, R.J., Howell, B., Yvon, A.M., Wadsworth, P., and Cassimeris, L. (1997) Nanomolar concentrations of nocodazole alter microtubule dynamic instability in vivo and in vitro. Molecular Biology of the Cell 8: 973–985 https://pmc.ncbi.nlm.nih.gov/articles/PMC305707/.

Veal, E.A., Day, A.M., and Morgan, B.A. (2007) Hydrogen peroxide sensing and signaling. Molecular Cell 26: 1–14 https://doi.org/10.1016/j.molcel.2007.03.016.

Veillette, A., Bookman, M.A., Horak, E.M., and Bolen, J.B. (1988) The CD4 and CD8 T cell surface antigens are associated with the internal membrane tyrosine-protein kinase p56lck. Cell 55: 301–308 https://doi.org/10.1016/0092-8674(88)90053-0.

Vestergaard, C.L., Flyvbjerg, H., and Møller, I.M. (2012) Intracellular Signaling by Diffusion: Can Waves of Hydrogen Peroxide Transmit Intracellular Information in Plant Cells? Frontiers in Plant Science 3 https://doi.org/10.3389/fpls.2012.00295.

Vlahos, C.J., Matter, W.F., Hui, K.Y., and Brown, R.F. (1994) A specific inhibitor of phosphatidylinositol 3-kinase, 2-(4-morpholinyl)-8-phenyl-4H-1-benzopyran-4-one (LY294002). Journal of Biological Chemistry 269: 5241–5248 https://doi.org/10.1016/s0021-9258(17)37680-9.

Vriz, S., Reiter, S., and Galliot, B. (2014) Cell death: a program to regenerate. Current Topics in Developmental Biology/Current Topics in Developmental Biology 121–151 https://doi.org/10.1016/b978-0-12-391498-9.00002-4.

Waksman, G. (1993) Binding of a high affinity phosphotyrosyl peptide to the Src SH2 domain: Crystal structures of the complexed and peptide-free forms. Cell 72: 779–790 https://doi.org/10.1016/0092-8674(93)90405-f.

Wang, Q., and Michalak, M. (2020) Calsequestrin. Structure, function, and evolution. Cell Calcium 90: 102242 https://doi.org/10.1016/j.ceca.2020.102242.

Weaver, C.J., Leung, Y.F., and Suter, D.M. (2015) Expression dynamics of NADPH oxidases during early zebrafish development. The Journal of Comparative Neurology 524: 2130–2141 https://doi.org/10.1002/cne.23938.

Webb, S.E., and Miller, A.L. (2006) Ca2+ signaling and early embryonic patterning during the Blastula and Gastrula Periods of Zebrafish and Xenopus development. Biochimica Et Biophysica Acta (BBA) - Molecular Cell Research 1763: 1192–1208 https://pubmed.ncbi.nlm.nih.gov/16962186/.

Weissman, I.L. (2000) Stem cells: units of development, units of regeneration, and units in evolution. Cell 100: 157–168 http://dx.doi.org/10.1016/s0092-8674(00)81692-x.

Wells, J.N., and Miller, J.R. (1988) [46] Methylxanthine inhibitors of phosphodiesterases. Methods in Enzymology on CD-ROM/Methods in Enzymology 489–496 https://doi.org/10.1016/0076-6879(88)59048-1.

Wen, Y., Zhang, Z., and Hu, B. (1989) Calcium and Calmodulin. 1st ed., Chemical Industry Press, Beijing.

Weng, Z., Thomas, S.M., Rickles, R.J., Taylor, J.A., Brauer, A.W., Seidel-Dugan, C., et al. (1994) Identification of Src, Fyn, and Lyn SH3-binding proteins: implications for a function of SH3 domains. Molecular and Cellular Biology 14: 4509–4521 https://doi.org/10.1128/mcb.14.7.4509.

Whitaker, M. (2005) Calcium at fertilization and in early development. Physiological Reviews 86: 25–88 https://pubmed.ncbi.nlm.nih.gov/16371595/.

Whitaker, M. (2010) Calcium in Living Cells. 1st ed., Academic Press, Oxford.

Wilkins, B.J., and Molkentin, J.D. (2004) Calcium–calcineurin signaling in the regulation of cardiac hypertrophy. Biochemical and Biophysical Research Communications 322: 1178–1191 https://doi.org/10.1016/j.bbrc.2004.07.121.

Wood, Z.A., Poole, L.B., and Karplus, P.A. (2003) Peroxiredoxin Evolution and the Regulation of Hydrogen Peroxide Signaling. Science 300: 650–653 https://doi.org/10.1126/science.1080405.

Wouda, R.R., Bansraj, M.R.K.S., De Jong, A.W.M., Noordermeer, J.N., and Fradkin, L.G. (2008) Src family kinases are required for WNT5 signaling through the Derailed/RYK receptor in theDrosophilaembryonic central nervous system. Development 135: 2277–2287 https://doi.org/10.1242/dev.017319.

Wu, W., Graves, L.M., Gill, G.N., Parsons, S.J., and Samet, J.M. (2002) SRC-dependent phosphorylation of the epidermal growth factor receptor on tyrosine 845 is required for zinc-induced RAS activation. Journal of Biological Chemistry 277: 24252–24257 https://pubmed.ncbi.nlm.nih.gov/11983694/.

Wyatt, R.A., and Crawford, B.D. (2021) Post-translational activation of Mmp2 correlates with patterns of active collagen degradation during the development of the zebrafish tail. Developmental Biology 477: 155–163 https://doi.org/10.1016/j.ydbio.2021.05.016.

Xiao, H., Li, H., Zhang, D., Li, Y., Sun, S., and Huang, C. (2018) Inactivation of venom PLA2 alleviates myonecrosis and facilitates muscle regeneration in envenomed mice: a time course observation. Molecules 23: 1911 https://doi.org/10.3390/molecules23081911.

Xie, F., Li, B.X., Kassenbrock, A., Xue, C., Wang, X., Qian, D.Z., et al. (2015) Identification of a Potent Inhibitor of CREB-Mediated Gene Transcription with Efficacious in Vivo Anticancer Activity. Journal of Medicinal Chemistry 58: 5075–5087 https://doi.org/10.1021/acs.jmedchem.5b00468.

Xu, M., Zhou, H., Hu, C., Liang, Y., Hu, L., and Chen, D. (2013) The mechanisms of EGFR in the regulation of axon regeneration. Cell Biochemistry and Function 32: 101–105 https://doi.org/10.1002/cbf.2977.

Yam, P.T., Langlois, S.D., Morin, S., and Charron, F. (2009) Sonic Hedgehog Guides Axons through a Noncanonical, Src-Family-Kinase-Dependent Signaling Pathway. Neuron 62: 349–362 https://doi.org/10.1016/j.neuron.2009.03.022.

Yamamoto, N., Oyaizu, T., Enomoto, M., Horie, M., Yuasa, M., Okawa, A., and Yagishita, K. (2020) VEGF and bFGF induction by nitric oxide is associated with hyperbaric oxygen-induced angiogenesis and muscle regeneration. Scientific Reports 10 https://doi.org/10.1038/s41598-020-59615-x.

Yao, Y., Choi, J., and Parker, I. (1995) Quantal puffs of intracellular Ca2+ evoked by inositol trisphosphate in Xenopus oocytes. The Journal of Physiology 482: 533–553 https://doi.org/10.1113/jphysiol.1995.sp020538.

Ye, X., Qiu, Y., Gao, Y., Wan, D., and Zhu, H. (2019) A Subtle Network Mediating Axon Guidance: Intrinsic Dynamic Structure of Growth Cone, Attractive and Repulsive Molecular Cues, and the Intermediate Role of Signaling Pathways. Neural Plasticity 2019: 1–26.

Yeatman, T.J. (2004) A renaissance for SRC. Nature Reviews Cancer 4: 470–480 https://doi.org/10.1038/nrc1366.

Yoo, S.K., Freisinger, C.M., LeBert, D.C., and Huttenlocher, A. (2012) Early redox, Src family kinase, and calcium signaling integrate wound responses and tissue regeneration in zebrafish. Journal of Cell Biology 199: 225–234 http://dx.doi.org/10.1083/jcb.201203154.

Yoshinari, N., Ishida, T., Kudo, A., and Kawakami, A. (2008) Gene expression and functional analysis of zebrafish larval fin fold regeneration. Developmental Biology 325: 71–81 https://doi.org/10.1016/j.ydbio.2008.09.028.

Yu, H., Chen, J.K., Feng, S., Dalgarno, D.C., Brauer, A.W., and Schrelber, S.L. (1994) Structural basis for the binding of proline-rich peptides to SH3 domains. Cell 76: 933–945 https://doi.org/10.1016/0092-8674(94)90367-0.

Yu, L.J., Chen, Y., Treadway, J.L., McPherson, R.K., McCoid, S.C., Gibbs, E.M., and Hoover, D.J. (2006) Establishment of Correlation between in Vitro Enzyme Binding Potency and in Vivo Pharmacological Activity: Application to Liver Glycogen Phosphorylase a Inhibitors. Journal of Pharmacology and Experimental Therapeutics 317: 1230–1237 https://doi.org/10.1124/jpet.105.100545.

Yu, Y. b., Su, K. h., Kou, Y.R., Guo, B. c., Lee, K. i., Wei, J., and Lee, T. s. (2016) Role of transient receptor potential vanilloid 1 in regulating erythropoietin-induced activation of endothelial nitric oxide synthase. Acta Physiologica 219: 465–477 https://doi.org/10.1111/apha.12723.

Zhang, J., Cui, X., Wang, L., Liu, F., Jiang, T., Li, C., et al. (2014) The Mitochondrial Thioredoxin is Required for Liver Development in Zebrafish. Current Molecular Medicine 14: 772–782 https://doi.org/10.2174/1566524014666140724103927.

Zhang, J., Liu, X., Li, H., Chen, C., Hu, B., Niu, X., et al. (2016) Exosomes/tricalcium phosphate combination scaffolds can enhance bone regeneration by activating the PI3K/Akt signaling pathway. Stem Cell Research & Therapy 7.

Zhang, Q., Wang, Y., Man, L., Zhu, Z., Bai, X., Wei, S., et al. (2016) Reactive oxygen species generated from skeletal muscles are required for gecko tail regeneration. Scientific Reports 6 https://doi.org/10.1038/srep20752.

Zhang, S.L., Yeromin, A.V., Zhang, X.H. -f., Yu, Y., Safrina, O., Penna, A., et al. (2006) Genome-wide RNAI screen of Ca2+ influx identifies genes that regulate Ca2+ release-activated Ca2+ channel activity. Proceedings of the National Academy of Sciences 103: 9357–9362 https://doi.org/10.1073/pnas.0603161103.

Zhang, Y., Liu, N.M., Wang, Y., Youn, J.Y., and Cai, H. (2017) Endothelial cell calpain as a critical modulator of angiogenesis. Biochimica Et Biophysica Acta (BBA) - Molecular Basis of Disease 1863: 1326–1335 https://doi.org/10.1016/j.bbadis.2017.03.021.

Zhang, Y.L., and Dong, C. (2005) MAP kinases in immune responses. Cellular & Molecular Immunology 2(1): 20–27 https://pubmed.ncbi.nlm.nih.gov/16212907.

Zhou, Z., Chrifi, I., Xu, Y., Pernow, J., Duncker, D.J., Merkus, D., and Cheng, C. (2016) Uridine adenosine tetraphosphate acts as a proangiogenic factor in vitro through purinergic P2Y receptors. AJP Heart and Circulatory Physiology 311: H299–H309 https://doi.org/10.1152/ajpheart.00578.2015.

Zhu, L., Song, S., Pi, Y., Yu, Y., She, W., Ye, H., et al. (2011) Cumulated Ca2+ spike duration underlies Ca2+ oscillation frequency-regulated NFκB transcriptional activity. Journal of Cell Science 124: 2591–2601 https://doi.org/10.1242/jcs.082727.

Zimmermann, B. (1999) The mechanism mediating regenerative intercellular Ca2+ waves in the blowfly salivary gland. The EMBO Journal 18: 3222–3231 https://doi.org/10.1093/emboj/18.12.3222.

Zorzato, F., Fujii, J., Otsu, K., Phillips, M., Green, N.M., Lai, F.A., et al. (1990) Molecular cloning of cDNA encoding human and rabbit forms of the Ca2+ release channel (ryanodine receptor) of skeletal muscle sarcoplasmic reticulum. Journal of Biological Chemistry 265: 2244–2256 https://doi.org/10.1016/s0021-9258(19)39968-5.